UNIVERSIDAD DE CÓRDOBA

Programa de Doctorado en Biociencias y Ciencias Agroalimentarias

Departamento de Ingeniería Forestal
Área de Ingeniería Agroforestal

Patrón espacial de variables bióticas y abióticas implicadas en la mortalidad por podredumbre radical en *Quercus ilex* L. subsp. *ballota* (Desf.) Samp. en el suroeste de la Península Ibérica

Spatial pattern of biotic and abiotic variables involved in root rot mortality in *Quercus ilex* L. subsp. *ballota* (Desf.) Samp. in south-western Iberian Peninsula

Directores – Tutor*:

Dr. Rafael María Navarro Cerrillo* (Catedrático de Universidad-UCO)
Dra. Rocío Hernández Clemente (Contrato Ramón y Cajal-UCO)
Dr. Francisco José Ruiz Gómez (Contrato post doctoral-UCO)

Tesis Doctoral presentada por

Rafael Sánchez De la Cuesta

para la obtención del título de

Doctor Ingeniero de Montes por la Universidad de Córdoba

Córdoba, febrero de 2022

TITULO: *PATRÓN ESPACIAL DE VARIABLES BIÓTICAS Y ABIÓTICAS IMPLICADAS EN LA MORTALIDAD POR PODREDUMBRE RADICAL EN QUERCUS ILEX SUBSP. BALLOTA (DESF.) SAMP. EN EL SUROESTE DE LA PENÍNSULA IBÉRICA*

AUTOR: *Rafael Sánchez de la Cuesta*

© Edita: UCOPress. 2022
Campus de Rabanales
Ctra. Nacional IV, Km. 396 A
14071 Córdoba

https://www.uco.es/ucopress/index.php/es/
ucopress@uco.es

TÍTULO DE LA TESIS: Patrón espacial de variables bióticas y abióticas implicadas en la mortalidad por podredumbre radical en *Quercus ilex* L. subsp. *ballota* (Desf.) Samp. en el suroeste de la Península Ibérica

DOCTORANDO: Rafael Sánchez De la Cuesta

INFORME RAZONADO DE LOS DIRECTORES DE LA TESIS

El doctorando presenta y desarrolla un amplio estudio experimental sobre el decaimiento de la encina (*Quercus ilex* L.) en las dehesas de Andalucía, a partir de datos a diferentes escalas temporales y espaciales. La metodología empleada es correcta e incorpora técnicas novedosas de análisis estadístico y analítico, en particular orientadas al estudio de procesos de decaimiento y mortalidad en sistemas adehesados. La tesis amplía el conocimiento relacionado con esta interacción de oomicetos patógenos de podredumbre radicular, principalmente a *Phytophthora cinnamomi* Rands.

El resultado es original en el contexto de los estudios relacionados con la evaluación de la estructura y funcionalidad de las comunidades de hongos y oomicetos presentes en las dehesas afectadas por procesos de decaimiento en Andalucía. La Tesis Doctoral se presenta con estructura de **Capítulos**, habiendo derivado de ellos dos artículos científicos que han sido publicados en revistas científicas de impacto, indexadas en el Journal Citation Reports (JCR):

- **Cap.2. Sánchez-Cuesta, R.**, Navarro-Cerrillo, R. M., Quero, J. L., & Ruiz-Gómez, F. J. **2020**. Small-Scale Abiotic Factors Influencing the Spatial Distribution of *Phytophthora cinnamomi* under Declining *Quercus ilex* Trees. *Forests*, 11(4), 375. (ISSN 1999-4907)
  https://doi.org/10.3390/f11040375 (Open Access)
  - Este artículo aparece como portada de la revista *Forests*: "Volume 11, Issue. 4. April 2020"
  - Este artículo se ha publicado como capítulo de libro, del número especial de la revista *Forests* "Phytophthora Infestations in Forest Ecosystems" (ISBN 978-3-0365-0801-6 pdf)

  Índice de Impacto (JCR): **2.633**. **Q1** *Forestry*, posición 13/67 (2020).

- **Cap. 4. Sánchez-Cuesta, R.**, Ruiz-Gómez, F. J., Duque-Lazo, J., González-Moreno, P., & Navarro-Cerrillo, R. M. **2021**. The environmental drivers influencing spatio-temporal dynamics of oak defoliation and mortality in dehesas of Southern Spain. *Forest Ecology and Management*, 485, 118946. (ISSN 0378-1127)
  https://doi.org/10.1016/j.foreco.2021.118946 (Open Access)
  Índice de Impacto (JCR): **3.558**. **Q1** *Forestry*, posición 7/67 (2020).

Por otro lado, en el periodo de formación predoctoral, Rafael Sánchez de la Cuesta, ha participado en varios proyectos científico-técnicos y líneas de investigación del Departamento de Ingeniería Forestal y del Grupo de Investigación ERSAF "Evaluación y Restauración de Sistemas Agrícolas y Forestales" (RNM-360), miembro en este último desde el año 2007. De estos trabajos se relacionan, a continuación, las publicaciones en revistas JCR y las comunicaciones (oral/póster) en los que ha participado:

Artículos científicos relacionados con la línea de investigación:

- Hornero, A., Zarco-Tejada, P. J., Quero, J. L., North, P. R. J., Ruiz-Gómez, F. J., **Sánchez-Cuesta, R.**, & Hernandez-Clemente, R. **2021**. Modelling hyperspectral-and thermal-based plant traits for the early detection of *Phytophthora*-induced symptoms in oak decline. *Remote Sensing of Environment*, 263, 112570.
  https://doi.org/10.1016/j.rse.2021.112570
  Índice de impacto (JCR): **10.164**. **Q1** *Remote sensing*, posición 1/32 (2020).
- Rafael M. Navarro-Cerrillo, Mª Ángeles Varo-Martínez, Cristina Acosta, Guillermo Palacios Rodríguez, **Rafael Sánchez-Cuesta**, Francisco J. Ruiz Gómez. **2019**. Integration of WorldView-2 and airborne laser scanning data to classify defoliation levels in *Quercus ilex* L. Dehesas affected by root rot mortality: Management implications. *Forest Ecology and Management*, 451, 117564. https://doi.org/10.1016/j.foreco.2019.117564
  Índice de Impacto (JCR): **3.558**. **Q1** *Forestry*, posición 7/67 (2020).
- Francisco J. Ruiz Gómez, Alejandro Pérez-de-Luque, **Rafael Sánchez-Cuesta**, José L. Quero and Rafael M. Navarro Cerrillo. **2018**. Differences in the response to acute drought and *Phytophthora cinnamomi* Rands infection in *Quercus ilex* L. seedlings. *Forests*, 9 (10), 634. https://doi.org/10.3390/f9100634 "Special Issue *Phytophthora* Infestations in Forest Ecosystems"
  Índice de Impacto (JCR): **2.633**. **Q1** *Forestry*, posición 13/67 (2020).
- Navarro-Cerrillo, R. M., Gómez, F. J. R., Cabrera-Puerto, R. J., **Sánchez-Cuesta, R.**, Rodríguez, G. P., & Pérez, J. L. Q. **2018**. Growth and physiological sapling responses of eleven *Quercus ilex* ecotypes under identical environmental conditions. *Forest Ecology and Management*, 415, 58-69. https://doi.org/10.1016/j.foreco.2018.01.004
  Índice de Impacto (JCR): **3.558**. **Q1** *Forestry*, posición 7/67 (2020).
- Ruiz-Gómez, F. J., Navarro-Cerrillo, R. M., Lara-Gómez, M. A., & **Sánchez-Cuesta, R**. **2016**. Aislamiento e identificación de oomicetos en focos de podredumbre radical de Andalucía y Extremadura. *Cuadernos de la Sociedad Española de Ciencias Forestales*, (42), 363-376. https://doi.org/10.31167/csef.v0i42.17489
  Google Scholar Metrics Índice H5: 4. *Ciencias Agrarias*.

- Ruiz Gómez, F. J., Navarro-Cerrillo, R. M., **Sánchez-Cuesta, R.**, & Pérez-de-Luque, A. **2015**. Histopathology of infection and colonization of *Quercus ilex* fine roots by *Phytophthora cinnamomi*. *Plant Pathology*, 64(3), 605-616. https://doi.org/10.1111/ppa.12310
  Índice de impacto (JCR): **2.590**. **Q2** *Agronomy*, posición 23/91 (2020).

Contribución a congresos, relacionado con la línea de investigación:

- **Rafael Sánchez-Cuesta**, Francisco J. Ruiz-Gómez, Joaquín Duque-Lazo, Pablo González-Moreno, Rafael M. Navarro-Cerrillo. **2021**. Factores ambientales que influyen en la dinámica espacio-temporal de la defoliación y la mortalidad de los *Quercus* en las dehesas del sur de España. XV Congreso Nacional de la Asociación Española de Ecología Terrestre: *El valor de la naturaleza para una sociedad global*. Plasencia (Cáceres. España). 18-22 de octubre de 2021. Ámbito: Nacional. Tipo de comunicación: oral.
- Roberto J. Cabrera-Puerto, Francisco J. Ruiz Gómez, **Rafael Sánchez-Cuesta**, Rafael Navarro, José Luis Quero. **2021**. Ecofisiología del estrés asociado a podredumbre radical en una dehesa de encina. XV Congreso Nacional de la Asociación Española de Ecología Terrestre: *El valor de la naturaleza para una sociedad global*. Plasencia (Cáceres. España). 18-22 de octubre de 2021. Ámbito: Nacional. Tipo de comunicación: póster.
- Francisco José Ruiz Gómez, José Luis Quero, **Rafael Sánchez-Cuesta**, Rafael María Navarro Cerrillo. **2019**. Study of fungal and oomycete plant pathogens in soils of holm oak dehesas of Andalusia: Influence of site conditions. 1st Meeting of the Iberian Ecological Society & XIV AEET Meeting: *Ecology: an integrative science in the Anthropocene*. Barcelona (España). February 4-7, 2019. Ámbito: Internacional. Tipo de comunicación: póster.
- Cabrera-Puerto, R.J., Ruiz-Gómez, F.J., **Sánchez-Cuesta, R.**, Navarro-Cerrillo, R.M., Hernández-Clemente, R., Quero Pérez, J.L. **2019**. Uso de sensores basados en tecnología IoT para monitorizar el decaimiento forestal: el caso de la encina y la podredumbre de raíz. IV Reunión Científica de Sanidad Forestal - SECF: *Ciencia y técnica frente a riesgos globales: coordinación y complementariedad*. ETS Ing. Huelva (España). 25-26 de septiembre de 2019. Ámbito: Nacional. Tipo de comunicación: oral.
- Francisco J. Ruiz, José L Quero, **Rafael Sánchez-Cuesta**, Roberto J. Cabrera Puerto, Rafael M. Navarro Cerrillo. **2018.** Assessing root rot susceptibility in progenies of seed collection stands of *Quercus ilex* L. in Andalusia. IV Reunión conjunta del Grupo de Trabajo de Repoblaciones Forestales de la SECF y el Grupo de Trabajo de Restauración Ecológica de la AEET; VIII Reunión del GT de Repoblaciones Forestales de la SECF; IV Reunión del GT de Restauración Ecológica de la AEET: *Restauración y Diversificación del Paisaje Rural: Estrategias y Técnicas*. Alcázar de San Juan (Ciudad Real. España). 17-19 de octubre de 2018. Ámbito: Nacional. Tipo de comunicación: póster.
- **Sánchez de la Cuesta, Rafael**. Patrón de distribución espacial de oomicetos bajo copa de encina en el Andévalo Occidental de Huelva. **2016.** V Congreso Científico de Investigadores en Formación de la Universidad de Córdoba: *Creando Redes*. Córdoba (España). 30 de noviembre, 1 y 2 de diciembre 2016. Ámbito: Nacional. Tipo de comunicación: póster.
- F.J. Ruiz, C. Morales, **R. Sánchez-Cuesta**, A. Pérez-de-Luque, A. Vannini and R.M. Navarro. **2016**. Molecular identification of Oomycota biodiversity in soils from "Los Alcornocales" Natural Park (Cádiz, Spain). 8th IOBC Working Group: *Integrated Protection in Oak Forests*. Córdoba (España). October 23-27, 2016. Ámbito: Internacional. Tipo de comunicación: póster.

- Ruiz-Gómez FJ, Navarro-Cerrillo R, Lara-Gómez MA, **Sánchez de la Cuesta R**. **2015**. Aislamiento e identificación de oomicetos en focos de podredumbre radical de Andalucía y Extremadura. III Reunión Científica de Sanidad Forestal. SECF. Madrid (España). 7-8 de octubre de 2015. Ámbito: Nacional. Tipo de comunicación: oral.

Artículos científicos no relacionados directamente con la línea de investigación:

- Navarro Cerrillo, R.M., **Sánchez de la Cuesta, R.**, De Rojas Martínez de Villarreal, P.I., Palacios-Rodríguez, G., **2021**. Caso práctico V. Restauración de dehesas de encina (*Quercus ilex* L. subsp. *ballota* Desf. Samp.) en Andalucía, en: Bases Técnicas y Ecológicas Del Proyecto de Repoblación Forestal. Ministerio para la Transición Ecológica y el Reto Demográfico (MITECO), Madrid, pp. 337–366. ISBN: 978-84-18508-57-8. https://doi.org/10.1016/j.foreco.2021.119824
- Navarro-Cerrillo, R.M., González-Moreno, P., Ruiz-Gómez, F.J., **Sánchez-Cuesta, R.**, Gazol, A., & Camarero, J.J. **2021**. Drought stress and pests increase defoliation and mortality rates in vulnerable *Abies pinsapo* forests. *Forest Ecology and Management*,
  Índice de Impacto (JCR): **3.558**. **Q1** *Forestry*, posición 7/67 (2020).
- A. M. García Moreno, **R. Sánchez-Cuesta**, C. Prades López, M. Verdum Virgos, P. Jové, M. Bejarano Medina, B. Abellanas Oar. El corcho como sustrato de cubiertas verdes (Proyecto GO SUBER). Revista Tecno Garden, pp. 39-43. 25 septiembre, **2020**.
- Carpio, A. J., Lora, Á., Martín-Consuegra, E., **Sánchez-Cuesta, R.**, Tortosa, F. S., & Castro, J. **2020**. The influence of the soil management systems on aboveground and seed bank weed communities in olive orchards. *Weed Biology and Management*, 20(1), 12-23. https://doi.org/10.1111/wbm.12195
  Índice de Impacto (JCR): **1.059**. **Q3** *Agronomy*, posición 64/91 (2020).
- Rea M. Hall, Nicole Penke, Monika Kriechbaum, Sophie Kratschmer, Vincent Jung, Simon Chollet, Muriel Guernion, Annegret Nicolai, Francoise Burel, Albin Fertil, Ángel Lora, **Rafael Sánchez-Cuesta**, Gema Guzmán, Jose Gómez, Daniela Popescu, Adela Hoble, Claudiu-Ioan Bunea, Johann G. Zaller, Silvia Winter. **2020**. Vegetation management intensity and landscape diversity alter plant species richness, functional traits and community composition across European vineyards. *Agricultural Systems*, 177, 102706. https://doi.org/10.1016/j.agsy.2019.102706
  Índice de Impacto (JCR): **5.370**. **Q1** *Agriculture, Multidisciplinary*, posición 4/58 (2020).
- G. Guzmán, J.M. Cabezas, **R. Sánchez-Cuesta**, Á. Lora, T. Bauer, P. Strauss, S. Winter, J.G. Zaller, J.A. Gómez. **2019.** A field evaluation of the impact of temporary cover crops on soil properties and vegetation communities in southern Spain vineyards. *Agriculture, Ecosystems and Environment*, 272, 135-145. https://doi.org/10.1016/j.agee.2018.11.010
  Índice de Impacto (JCR): **5.567**. **Q1** *Ecology*, posición 21/166 (2020).
- Loewe, V., Navarro-Cerrillo, R. M., García-Olmo, J., Riccioli, C., & **Sánchez-Cuesta, R**. **2017**. Discriminant analysis of Mediterranean pine nuts (*Pinus pinea* L.) from Chilean plantations by near infrared spectroscopy (NIRS). *Food Control*, 73, 634-643. https://doi.org/10.1016/j.foodcont.2016.09.012
  Índice de Impacto (JCR): **5.548**. **Q1** *Food Science & Technology*, posición 19/144 (2020).
- Navarro-Cerrillo, R. M., Camarero, J. J., Manzanedo, R. D., **Sánchez-Cuesta, R.**, López Quintanilla, J., & Sanchez Salguero, R. **2014**. Regeneration of *Abies pinsapo* within gaps created by *Heterobasidion annosum*-induced tree mortality in southern Spain. *Iforest-biogeosciences and Forestry*, 7(4), 209. https://doi.org/10.3832/ifor0961-007
  Índice de Impacto (JCR): **1.836**. **Q3** *Forestry*, posición 34/67 (2020).

<u>Contribución a congresos, no relacionado con la línea de investigación</u>:

- Roberto J. Cabrera-Puerto, Francisco J. Ruiz Gómez, **Rafael Sánchez-Cuesta**, Andrés Cortés Márquez, Rafael M. Navarro Cerrillo. **2018**. Bromatological and morphological characterization of acorns from Andalusian *Quercus ilex* L. seed collection stands. IV Reunión conjunta del Grupo de Trabajo de Repoblaciones Forestales de la SECF y el Grupo de Trabajo de Restauración Ecológica de la AEET; VIII Reunión del GT de Repoblaciones Forestales de la SECF; IV Reunión del GT de Restauración Ecológica de la AEET: *Restauración y Diversificación del Paisaje Rural: Estrategias y Técnicas*. Alcázar de San Juan (Ciudad Real. España). 17-19 de octubre de 2018. Ámbito: Nacional. Tipo de comunicación: póster.

Por todo lo anteriormente expuesto, consideran que el trabajo realizado reúne los requisitos establecidos para su presentación y, en consecuencia, se autoriza la exposición y defensa pública de la Tesis Doctoral "Patrón espacial de variables bióticas y abióticas implicadas en la mortalidad por podredumbre radical en *Quercus ilex* L. subsp. *ballota* (Desf.) Samp. en el suroeste de la Península Ibérica".

En Córdoba, 11 de febrero de 2022

Firma de los directores

NAVARRO CERRILLO RAFAEL MARIA - 50702674W

Firmado digitalmente por NAVARRO CERRILLO RAFAEL MARIA - 50702674W
Fecha: 2022.02.10 11:48:09 +01'00'

HERNANDEZ CLEMENTE ROCIO - 30957696H

Digitally signed by HERNANDEZ CLEMENTE ROCIO - 30957696H
DN: cn=HERNANDEZ CLEMENTE ROCIO - 30957696H, c=ES
Date: 2022.02.10 13:34:29 +01'00'

Fdo.: Dr. Rafael Mª Navarro Cerrillo.

Fdo.: Dra. Rocío Hernández Clemente

Firmado digitalmente por RUIZ GOMEZ FRANCISCO JOSE - 75097758K
Fecha: 2022.02.11 '13:45:45 +01'00

Fdo.: Dr. Francisco José Ruiz Gómez

Dedicado con especial cariño y admiración
a mi padre Rafael y a mi madre Nati quienes,
con su ejemplo de esfuerzo y dedicación constante,
me inculcan día a día los mejores valores para alcanzar
cualquier objetivo y superar los obstáculos de la vida al grito de…

"PALANTE"

¡¡Gracias por vuestro tiempo, por estar ahí siempre, os quiero!!

Agradecimientos

Como siempre dijo mi director Rafael Navarro, este tipo de trabajos se convierten en "Tesis de Grupo", por lo que son muchas las personas que de uno u otro modo han contribuido a alcanzar la tan ansiada meta de esta carrera de fondo y, por ello, merecen todo mi agradecimiento. En este sentido, es a ti, Rafa, en primer lugar y de forma destacada, como mi profesor, compañero y amigo, así como mi director de tesis y del Grupo de Investigación ERSAF al que pertenezco, a quien quiero agradecer todo tu apoyo y confianza en mí, desde el principio. Tú me diste la oportunidad de crecer profesional y personalmente, llevando mi nombre y mi trabajo a todos los ámbitos laborales. Gracias por transmitirme tu entusiasmo por la educación y la ciencia y por animarme a seguir adelante en los momentos más críticos. Ha sido un verdadero placer recorrer contigo cada kilómetro de este apasionante Trail y, estoy seguro, de que aún nos quedan muchas más cumbres por alcanzar.

A mis codirectores, compañeros y amigos, Rocío Hernández y Francisco J. Ruiz, por su apoyo en la organización de la estructura y desarrollo de las ideas del trabajo. Su joven, pero valiosa y destacada experiencia científica, me ha permitido avanzar con seguridad en cada reto que los objetivos de la tesis nos planteaban.

A los coautores de las publicaciones científicas que aparecen en esta Tesis Doctoral, Rafael Navarro-Cerrillo, José L. Quero, Francisco J. Ruiz-Gómez, Pablo González-Moreno, Joaquín Duque-Lazo, y a aquellos compañeros que me están ayudando a que el resto de los trabajos aquí reflejados se publiquen, Andrés Cortés-Márquez, Cristina Acosta-Muñoz, Mª Ángeles Varo-Martínez y Rocío Hernández-Clemente. Daros las gracias por vuestra disponibilidad, tiempo y experiencia científica, que me han enriquecido y motivado a seguir admirando la ciencia, y en especial a Fran Ruiz, Andrés Cortés, Alejandro Pérez, Roberto Cabrera y Vico, que con su inestimable ayuda en los tediosos trabajos de campo y de laboratorio, hicieron más amenos los difíciles momentos del arranque metodológico inicial.

A los profesores y compañeros de Ingeniería Forestal de la Universidad de Huelva y de Ingeniería de Montes de la Universidad de Córdoba por ayudarme a desarrollar mi carrera y amor por la naturaleza. Al Departamento de Ingeniería Forestal, mi segundo hogar, donde he encontrado grandes profesionales y amistades, entre las que admiro a Mª Carmen García Ortiz, mi compañera del PAS, siempre dispuesta a escucharme, ayudarme y levantarme el ánimo y, por supuesto, a mi Grupo de Investigación que, desde el 2008, me ha permitido crecer, disfrutar y compartir mil y una aventuras rodeado de grandes personas que sería difícil enumerarlas a todas sin dejarme a nadie atrás. Gracias a todos.

A mi gran amigo Paco Jiménez, él es mi mano derecha, mi apoyo constante y mi persona de confianza. Gracias por estar siempre ahí, hermano.

Y qué sería de la vida sin el apoyo incondicional de la familia. Tengo la gran fortuna de tener un papi y una mami (Rafael y Nati) que siempre me alentaron con amor y cariño a levantarme tras las caídas, a mantener la esperanza y a confiar en mí. Gracias por vuestro tiempo, sacrificio y valentía. Estoy muy orgulloso de vosotros y de la educación y ejemplo que me trasmitís cada día. Gracias a mi hermano Guillermo y a mi hermana Inma por todo vuestro apoyo y cariño, por tantos ratos que me dedicasteis en los estudios, sois para mí ejemplo de perseverancia frente a la vida. Gracias familia.

A mis abuelos con especial cariño que, desde el cielo me acompañáis una vez más como lo hicisteis presencialmente en otros tantos actos académicos; os regalo este trabajo y reto personal. Gracias por tanto.

A mi tía Anita, a la que quiero con pasión y es ejemplo de lucha y alegría constante, ella es la causante de haber conocido a mis amores, mi Reyes y mi Ismael, ellos me han abierto las puertas de su corazón, ellos son mi familia y mi hogar, las dos personas que me han devuelto la ilusión y la felicidad por la vida. Su cariño, valoración y respeto me han permitido superar las adversidades en este último tramo de la Tesis. Gracias, os quiero muchísimo.

"En los momentos más difíciles de tu vida,
Yo siempre estaré a tu lado"

Jesús de Nazaret

Mi Metamorfosis

***M**ágica es la vida*
como la misma estrella,
como el mismo hada
de la cenicienta.

***M**ágico el amor,*
mágico un te quiero,
mágica es la vida
en amor y sufrimiento.

***M**ágicas tus caricias,*
mágicos tus besos,
magia es tu sonrisa
que hace sentir al cuerpo.

María de los Reyes Valle Mellado (escritores Mellarienses)

Colaboración institucional

Los trabajos que forman parte de la presente Tesis Doctoral se han llevado a cabo con la ayuda de los proyectos INTERBOS (CGL2008-04503-C03-01), QUERCUSAT (CGL2013-40790-R) y ESPECTRAMED (CGL2017-86161-R), financiados por el Ministerio de Economía, Industria y Competitividad y el Ministerio de Ciencia e Innovación.

Los autores de los trabajos quieren agradecer a la Consejería de Medio Ambiente y Ordenación del Territorio (Junta de Andalucía) y en especial a su Equipo de la Red de Equilibrios Biológicos de la Agencia de Medio Ambiente y Agua (AMAYA) (Ángel Carrasco, José Manuel Ruiz, Sixto Rodríguez y a todos sus técnicos provinciales) por el apoyo logístico y técnico respecto al acceso a las parcelas de la Red SEDA (Red Andaluza de Seguimiento de Daños sobre Ecosistemas Forestales) y a la información de la base de datos asociada (REDIAM).

A la finca de Campo Baldío S.L. de Puebla de Guzmán (Huelva), y en especial a su director técnico (Celestino Jaldón Hidalgo), por el acceso a la información técnica de la forestación, así como a la zona de estudio.

Resumen

Desde la última mitad del siglo XX, los bosques de *Quercus* y dehesas del sur de la Península Ibérica vienen experimentando un progresivo deterioro forestal de sus masas arbóreas, denominado, de forma genérica, como decaimiento o *seca* de los *Quercus*. Este declive está motivado por multitud de factores bióticos y abióticos que actúan de forma independiente o como combinación de ellos, y entre los que destacan las perturbaciones motivadas por el cambio climático global, la falta de regeneración natural de los bosques, la escasez de silvicultura y de gestión agroganadera, así como la intensificación, cada vez mayor, del tránsito de material vegetal a nivel mundial, sin el suficiente control fitosanitario en los viveros que impida la invasión y la dispersión de plagas y enfermedades forestales. En este síndrome complejo, se ha identificado la acción primaria del oomiceto patógeno invasor no nativo de podredumbre radical, *Phytophthora cinnamomi* Rands., el cual provoca la muerte de raíces finas, generando síntomas de estrés hídrico que se presentan en forma de puntisecado regresivo de ramas y defoliación de la copa del árbol y, en ocasiones, la muerte del individuo.

Con esta Tesis Doctoral se pretende aumentar el conocimiento sobre la relación entre las características estructurales del arbolado y los factores abióticos (estructura física y química del suelo, topografía del paisaje y climatología) con la distribución espaciotemporal de oomicetos patógenos de podredumbre radical (*Phytophthora* spp. y *Pythium* spp.) en especies del género *Quercus* spp. A partir de estas relaciones, se ha estudiado cómo influyen sobre el estado de salud del arbolado (defoliación de las copas y mortalidad) la triple interacción patógeno-huésped-ambiente a diferentes escalas territoriales (árbol, rodal y región), y en diferentes tipos de formaciones vegetales, como son las repoblaciones forestales sobre tierras agrarias y las dehesas de *Quercus*, en Andalucía.

Para llevar a cabo esta investigación, el trabajo se estructuró en 7 capítulos que se describen a continuación.

El Capítulo 1, enmarca los antecedentes teóricos que sustentan la justificación de esta Tesis Doctoral y plantea los objetivos generales y específicos de la misma.

El Capítulo 2, aborda la importancia que tiene, en un momento puntual, la heterogeneidad de las propiedades fisicoquímicas del suelo, la humedad del suelo y la influencia de la cobertura del dosel de una repoblación forestal de *Quercus ilex*, a nivel de árbol individual, sobre la distribución espacial en suelo, a pequeña escala, de las unidades formadoras de colonias (ufc) de *Phytophthora cinnamomi*. Para ello se utilizaron Modelos Lineales Mixtos Generalizados e índices de agregación y agrupación de variables mediante la herramienta SADIE. Los resultados indicaron que las variables limo, materia orgánica, P, K y humedad del suelo, principalmente, influyeron sobre la distribución de ufc. La variabilidad de las condiciones de los micrositios, pueden predecir qué áreas alrededor de los árboles influyen en la mayor o menor disponibilidad de estos oomicetos en el suelo.

El Capítulo 3, muestra los patrones de distribución espacial, a escala de parcela, de las ufc del oomiceto *Phytophthora cinnamomi* en la rizosfera de plantaciones de *Q. ilex* y *Q. suber*, influenciados por la disposición de las propiedades fisicoquímicas, la humedad del suelo y las propiedades topográficas de la repoblación. Las implicaciones derivadas de las interacciones entre dichos factores bióticos y abióticos se observaron a través de los parámetros de defoliación y mortalidad del arbolado tras un periodo de 8 años, usando modelos de ecuaciones estructurales e índices de agregación y agrupación de variables mediante la herramienta SADIE. Los resultados muestran la mayor susceptibilidad de la encina frente al alcornoque en presencia del patógeno, con porcentajes de defoliación y mortalidad más elevados para la primera especie. A su vez los daños se correlacionaron con la textura y los nutrientes del suelo. En la defoliación de *Q. ilex*, influyó principalmente las propiedades químicas del suelo, mientras que para *Q. suber*, también influyó la topografía y la humedad del suelo. La mayor presencia de oomicetos se localizó en zonas de mayor humedad edáfica, menores pendientes, orientación norte y baja radiación solar.

El Capítulo 4, analiza el efecto de los factores bióticos, abióticos (edáficos, topográficos y ambientales) sobre el decaimiento forestal de los *Quercus* y sobre la propagación de oomicetos patógenos invasores no nativos de podredumbre radical (género *Phytophthor*a spp.) a escala regional de Andalucía. Se estudia la dinámica espaciotemporal de la defoliación y la mortalidad del arbolado registrada en la Red Regional de parcelas de Seguimiento de Daños de Andalucía (Red SEDA, ICP Nivel I, 2000-2016) en relación con la presencia de oomicetos y los valores medios y anuales ambientales. Se usaron varios enfoques estadísticos (curvas de supervivencia de Kaplan-Meier, gráficos de estimación de densidad Kernel y Modelos Lineales Mixtos Generalizados) para analizar 3635 árboles (152 parcelas). La defoliación y la mortalidad anuales se correlacionaron con la temperatura media anual, el Índice de Precipitación Evapotranspiración Estandarizada ($SPEI_{18}$verano y $SPEI_{1}$primavera), el contenido de materia orgánica del suelo y la precipitación anual, adquiriendo mayor relevancia la acción del patógeno en estas condiciones ambientales. Las redes regionales de sanidad forestal se muestran como herramienta crucial en las estrategias de gestión forestal adaptativa frente al cambio climático.

El Capítulo 5, evalúa y cartografía sobre una forestación de *Q. ilex* y *Q. suber*, los daños asociados al efecto de patógenos no nativos de podredumbre radical (*Phytophthora* spp.), a escala de árbol individual, utilizando técnicas LiDAR de alta densidad e imágenes multiespectrales de alta resolución. Para ello se utilizó el nivel de defoliación de 429 árboles que, mediante procesado de segmentación de copas, permitió obtener las métricas LiDAR e índices de vegetación basados en sus bandas espectrales. Ello dio lugar a la estimación de la defoliación mediante un modelo no paramétrico que permitió generar el mapa de daños de la plantación.

El Capítulo 6, aúna los conocimientos y resultados obtenidos en esta Tesis en forma de discusión general, aportando un enfoque global de los hitos más relevantes alcanzados a lo largo del estudio. Asimismo, se incluyen las limitaciones presentadas durante los trabajos y se expone el enfoque de las nuevas líneas de investigación que se derivan de esta Tesis.

El Capítulo 7, presenta las conclusiones generales de la Tesis, sintetizadas a continuación.

Los patrones de distribución espacial de las ufc del patógeno de podredumbre radical, *P. cinnamomi*, en dehesas de *Quercus* y repoblaciones de *Q. ilex* y *Q. suber*, implicados en la dinámica temporal de los procesos de defoliación y de mortalidad de estas especies arbóreas, están influenciados por la variabilidad de factores bióticos y abióticos del medio, como son las propiedades fisicoquímicas del suelo, la cobertura del dosel arbóreo, la presencia y estado fitosanitario de los huéspedes y su sistema radical, los cambios climatológicos, así como la heterogeneidad topográfica del paisaje. El análisis espacial a diferentes escalas de árbol, rodal y región puede servir como herramienta de predicción de áreas más susceptibles de albergar a estos oomicetos y, por tanto, como medio para aplicar estrategias de gestión forestal adaptativa frente al decaimiento de estos ecosistemas.

Palabras clave: decaimiento de *Quercus*, dehesas, forestación, *Phytophthora cinnamomi*, podredumbre radical, defoliación, mortalidad, SADIE, GLMMs, SEM, LiDAR, WorldView.

Summary

Since the last half of the 20th century, *Quercus* forests and dehesas in the south of the Iberian Peninsula have been experiencing a progressive forest deterioration of their tree stands, generically known as *Quercus* decline or *seca Quercus*. This decline is caused by a multitude of biotic and abiotic factors acting independently or in combination, including disturbances caused by global climate change, the lack of natural regeneration of forests, the scarcity of forestry and agro-livestock management, as well as the increasing intensification of the transit of plant material worldwide, without sufficient phytosanitary control in nurseries to prevent the invasion and spread of forest pests and diseases. In this complex syndrome, the primary action of the non-native invasive root rot pathogenic oomycete, *Phytophthora cinnamomi* Rands., has been identified, which causes the death of fine roots, generating symptoms of water stress in the form of regressive top-drying of branches and defoliation of the tree crown and, sometimes, death of the tree.

This PhD thesis aims to increase knowledge of the relationship between the structural characteristics of trees and abiotic factors (physical and chemical soil structure, landscape topography and climatology) with the spatiotemporal distribution of pathogenic root rot oomycetes (*Phytophthora* spp. and *Pythium* spp.) in species of the genus *Quercus* spp. Based on these relationships, we studied the influence of the triple interaction pathogen-host-environment on tree health (crown defoliation and mortality) at different territorial scales (tree, stand and region), and in different types of plant formations afforestation on agricultural land and *Quercus* dehesas in Andalusia.

To carry out this research, the work was structured in 7 chapters which are described below.

Chapter 1, frames the theoretical background that supports this doctoral Thesis's justification and sets out its general and specific objectives.

Chapter 2, addresses the importance of the heterogeneity of soil physicochemical properties, soil moisture and the influence of the canopy cover of a *Quercus ilex* afforestation, at individual tree level, on the small-scale spatial distribution of colony forming units (cfu) of *Phytophthora cinnamomi* in the soil. Generalised Linear Mixed Models and variable aggregation and clustering indices were used using the SADIE tool. The results indicated that silt, organic

matter, P, K and soil moisture variables mainly influenced the distribution of cfu. The variability of microsite conditions can predict which areas around the trees influence the greater or lesser availability of these oomycetes in the soil.

Chapter 3, shows the spatial distribution patterns, at plot scale, of cfu of the oomycete *Phytophthora cinnamomi* in the rhizosphere of *Q. ilex* and *Q. suber* plantations, influenced by the arrangement of physico-chemical properties, soil moisture and topographical properties of the stand. The implications derived from the interactions between these biotic and abiotic factors were observed through defoliation and tree mortality parameters after eight years, using structural equation models and aggregation and grouping indices of variables using the SADIE tool. The results show the greater susceptibility of holm oak versus cork oak in the presence of the pathogen, with higher percentages of defoliation and mortality for the former species. Damage was correlated with soil texture and nutrients. Defoliation of *Q. ilex* was mainly influenced by soil chemical properties, while for *Q. suber*, topography and soil moisture were also influential. The highest presence of oomycetes was located in areas with higher soil moisture, lower slopes, northern orientation and low solar radiation.

Chapter 4, analyses the effect of biotic, abiotic (edaphic, topographic and environmental) factors on *Quercus* forest decline and the spread of non-native invasive pathogenic root rot oomycetes (genus *Phytophthora* spp.) at a regional scale in Andalusia. The spatiotemporal dynamics of tree defoliation and mortality recorded in the Regional Network of Damage Monitoring Plots of Andalusia (SEDA Network, ICP Level I, 2000-2016) are studied in relation to the presence of oomycetes and mean and annual environmental values. Several statistical approaches (Kaplan-Meier survival curves, Kernel density estimation plots and Generalised Linear Mixed Models) were used to analyse 3635 trees (152 plots). Annual defoliation and mortality were correlated with mean annual temperature, Standardised Precipitation Evapotranspiration Index ($SPEI_{18}$summer and $SPEI_{1}$spring), soil organic matter content and annual precipitation, with pathogen action becoming more relevant under these environmental conditions. Regional forest health networks are shown to be a crucial tool in adaptive forest management strategies in the face of climate change.

Chapter 5, assesses and maps damage associated with the effect of non-native root rot pathogens (*Phytophthora* spp.) on a *Q. ilex* and *Q. suber* afforestation at the individual tree scale, using high-density LiDAR techniques

and high-resolution multispectral imagery. The defoliation level of 429 trees was used to obtain LiDAR metrics and vegetation indices based on their spectral bands by means of crown segmentation processing. This resulted in the estimation of defoliation using a non-parametric model that allowed the generation of the damage map of the plantation.

Chapter 6, brings together the knowledge and results obtained in this Thesis in a general discussion, providing a global approach to the most relevant milestones reached throughout the study. It also includes the limitations presented during the work and sets out the focus of the new lines of research arising from this Thesis.

Chapter 7, presents the general conclusions of the Thesis, which are synthesised below.

The spatial distribution patterns of the cfu of the root rot pathogen, *P. cinnamomi*, in *Quercus* dehesas and afforestations of *Q. ilex* and *Q. suber*, involved in the temporal dynamics of defoliation and mortality processes of these tree species, are influenced by the variability of biotic and abiotic environmental factors, such as soil physicochemical properties, tree canopy cover, the presence and phytosanitary status of the hosts and their root system, climatological changes, as well as the topographic heterogeneity of the landscape. Spatial analysis at different tree, stand and regional scales can serve as tool for predicting areas more susceptible to host these oomycetes and, therefore, to apply adaptive forest management strategies against the decline of these ecosystems.

Key words: *Quercus* decline, dehesas, afforestation, *Phytophthora cinnamomi*, root rot, defoliation, mortality, SADIE, GLMMs, SEM, LiDAR, WorldView.

Tabla de Contenidos

Índice de Tablas

Capítulo 1

Capítulo 2

Capítulo 3

Capítulo 4

Capítulo 5

Anexos

Supplementary material - Capítulo 2

Supplementary Material - Capítulo 3

Supplementary Material - Capítulo 4

Índice de Figuras

Capítulo 1

Capítulo 2

Capítulo 3

Capítulo 4

Capítulo 5

Capítulo 6

Anexos

Supplementary Material - Capítulo 2

Supplementary Material - Capítulo 3

Supplementary Material - Capítulo 4

Supplementary Material - Capítulo 5

Abreviaturas

AIC	Akaike's Information Criterion
ANN	Artificial Neural Network
ARVI	Atmospherically resistance vegetation index
BNDVI	Blue Normalized Difference Vegetation Index
CBH	Continental (dry-subhumid) Mediterranean climate of the Eastern circumbetic ranges and hills
CFI	Comparative Fit Index
ChlGREEN	Chlorophyll Green
CHM	Canopy Height Model
COV	Canopy cover
D800/550	Difference 800/550
D800/680	Difference 800/680
DC	Defoliation Class
DEM	Digital Elevation Model
DNS	Canopy density
ETRS	European Terrestrial Reference System
EVI	Enhanced vegetation index
FLAASH	Fast Line-of-sight Atmosphere Analysis of Spectral Hypercubes
FOV	Field of View
FTA	Forestación de Tierras Agrarias
GIS	Geographic Information System
GLI	Green Leaf Index
GLMM	Generalized Linear Mixed Models
GNDVI	Green Normalized Vegetation Index
GRNDVI	Green Red NDVI
GSD	Ground Sampling Distance
I_a	Índice de agregación
ICC	Intraclass Correlation Coefficient
ICP	International Co-operative Programme on Assessment and Monitoring of Air Pollution Effects on Forests
IDW	Inverse Distance Weighting

KDE (KD)	Kernel Density Estimation
kNN	K-Nearest-Neighbour
KUR	Kurtosis
LAI	Índices de Área Foliar
LIC2	Lichtenthaler indices 2
LiDAR	Light Detection and Ranging
LSCV	Leave-one-out least-squares cross-validation
MCARI1	Modified Chlorophyll Absorption in Reflectance Index 1
MCARI2	Modified Chlorophyll Absorption in Reflectance Index 2
MLG	Semi-oceanic Mediterranean climate of the lower Guadalquivir
MMG	Semi-continental (dry-subhumid) Mediterranean climate of the Middle Guadalquivir
MSI	Multispectral Instrument
MTR	Modelos de Transferencia Radiativa
MTVI1	Modified Triangular Vegetation Index 1
NARPH	Nistatina-Ampicilina Sódica-Rifampicina-Pentacloronitrobenceno-Hymexazol
NBR	Normalized Burn Ratio
NDMI	Normalized Difference Moisture Index
NDVI	Normalized Difference Vegetation Index
NIR	Near-Infrared Spectroscopy (from 780 nm to 2500 nm)
OSAVI	Optimized Soil Adjusted Vegetation Index
OWC	Oceanic Mediterranean climate of the windward coast
PBF	Semi-oceanic (subhumid-humid) Mediterranean climate of the Western peribetic foothills
PBM	Semi-oceanic (subhumid-humid) Mediterranean climate of the Western peribetic mountains
PCA	Principal Component Analysis
PNDVI	Pan NDVI
P_{nth}	nth percentile height
PSSRc1	Pigment Specific Simple Ratio C1
QAV	Mean quadratic height
RBNDVI	Red Blue NDVI
RMSEA	Root Mean Square Error of Approximation
SADIE	Spatial Analysis by Distance Indices

SAGA	System for Automated Geoscientific Analyses
SARVI	Soil and Atmospherically Resistant Vegetation Index
SAVI	Soil Adjusted Vegetation Index
SEDA	Red Andaluza de Seguimiento de Daños sobre Ecosistemas Forestales
SEM	Structural Equation Modelling
SIG	Sistemas de Información Geográfica
SKE	Skewness
SPEI	Standardised Precipitation-Evapotranspiration Index
SWIR	Short Wavelength Infrared
TDR	Time Domain Reflectometry
TLI	Tucker-Lewis Index
UAV	Unmanned Aerial Vehicle
ufc	Unidades formadoras de colonias
$v\ (v_i - v_j)$	Índice de agrupación (valores, altos o manchas – bajos o claros, de la variable, respectivamente)
VI	Vegetation Indices
VIF	Variance Inflation Factor
VWC	Volumetric Water Content
wi	Akaike weight of evidence

Capítulo 1

Introducción general

1 Los sistemas adehesados de *Quercus* en España

1.1 La dehesa: ecosistema único del bosque mediterráneo

Desde el siglo XVIII, momento en el que se tiene constancia del primer registro publicado en España del término *dehesa* (montado, en Portugal), han sido muchos los autores que han tratado de dar una definición lo más completa y ajustada posible a este agroecosistema único de origen antrópico, en el cual se ha venido manejando la vegetación (aclarado, podas, desbroces y siembras) para transformar el bosque mediterráneo original en un sistema agrosilvopastoral (San Miguel Ayanz, 1994). Las dehesas son sistemas de una gran complejidad y albergan una importante biodiversidad natural y multifuncional que se extienden principalmente por el área suroccidental de la Península Ibérica (3 mill. ha) (Figura 1) (Olea et al., 2005; Díaz y Pulido, 2009; Pinto-Correia et al., 2011).

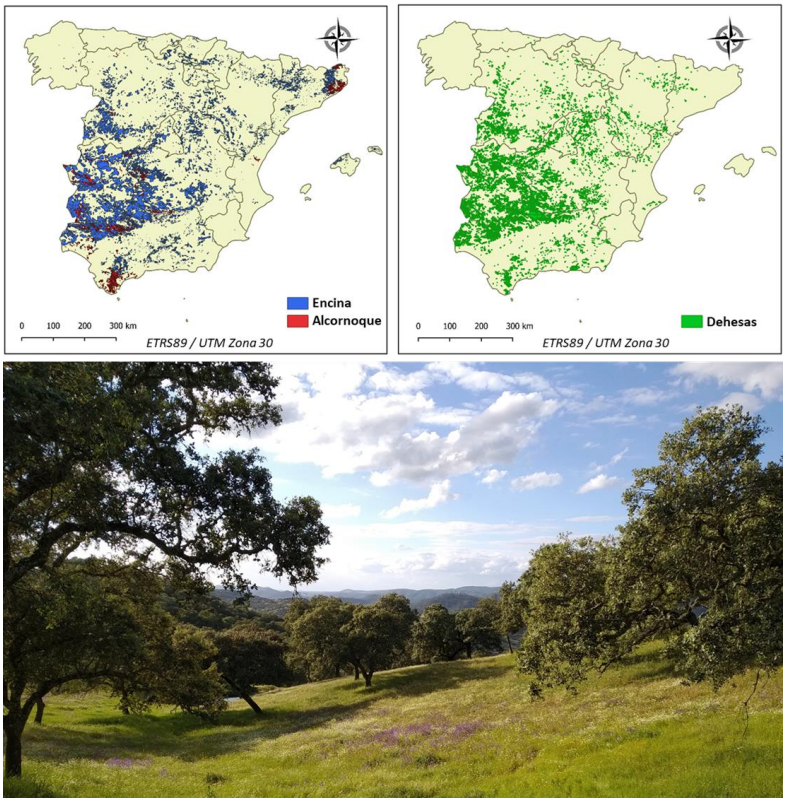

Figura 1. Mapas de distribución de *Quercus ilex* subsp. *ballota*, *Q. suber* (arriba izquierda) y ecosistemas de dehesa de *Quercus* (arriba derecha) en España (2,2 mill. ha). Aspecto de una dehesa de *Quercus* en el norte de la provincia de Huelva (España). Fuente: archivo del autor.

Como primera aproximación, la dehesa constituye un **sistema agrosilvopastoral** donde se aúnan el uso múltiple del territorio de forma espaciotemporal, con actividades agrícolas, ganaderas, cinegéticas y forestales, tratando de optimizar el enfoque productivo de los recursos y respetando el principio de conservación y sostenibilidad ambiental. En este sentido, la ganadería extensiva (principalmente, vacuno, ovino y/o porcino) constituye el aprovechamiento principal, no sólo desde un punto de vista económico sino también ecológico, pues mantiene mediante el pastoreo una buena estructura de los pastizales y regula el estrato arbustivo. De esta forma, y atendiendo al uso múltiple al que hace referencia este ecosistema, podrían incluirse como sistemas adehesados las forestaciones en tierras agrarias que sean objeto de pastoreo y donde se dirija al arbolado, mediante prácticas silvícolas, hacia una estructura de dehesa (Alejano Monge et al., 2011).

También se debe considerar a la dehesa como una **unidad de gestión** con vistas a su manejo técnico, compuesta por formaciones vegetales fragmentadas en teselas que se combinan de forma dinámica entre sí (monte arbolado, matorrales, pastizales, cultivos, forestaciones, etc.), dando lugar a hábitats con una composición y una estructura muy diferentes dependiendo del objetivo de las intervenciones humanas y de la intensidad del manejo que se realice sobre el territorio. Y como enfoque final, se debe tener en cuenta al sistema dehesa como **ecosistema**, situado principalmente en terrenos llanos o de pendiente moderada, y compuesto generalmente por dos estratos vegetales: uno arbóreo, más o menos disperso o hueco, con función estabilizadora-productiva y presencia fundamentalmente de especies de *Quercus* mediterráneos (*Q. ilex* ssp. *ballota* (Desf.) Samp; *Q. suber* L.; *Q. faginea* Lam; y *Q. canariensis* Willd.), en ocasiones mezclados con otras especies como el acebuche (*Olea europaea* L. ssp. *europaea* var. *sylvestris* Brot.), el pino piñonero (*Pinus pinea* L.) o el algarrobo (*Ceratonia siliqua* L.), entre otras; y el estrato herbáceo (pastizales y/o cultivos), con presencia o no de matorrales dispersos o en forma de manchas, cuyas características dependerán del estrato arbóreo y del aprovechamiento ganadero (San Miguel Ayanz, 1994; Costa et al., 2006; Alejano Monge et al., 2011).

1.2 ¿Cuál es el estado de las dehesas en Andalucía?

Según Costa et al. (2006), y los datos recogidos en el Mapa de Usos y Coberturas Vegetales del Suelo de Andalucía (Junta de Andalucía, 1999), la superficie de dehesas en esta región es de 1,26 millones de hectáreas, repartidas principalmente por Sierra Morena y las serranías gaditanas y, de manera dispersa, por las sierras Subbéticas y algunas campiñas. Dada su importancia, la Directiva 1992/43/CEE del Consejo, de 21 de mayo, de conservación de los hábitats naturales y de la flora y de la fauna silvestres, contempla como hábitats de interés comunitario los bosques esclerófilos para pastoreo. Además, la Unesco declaró a las Dehesas de Sierra Morena como Reserva de la Biosfera, dada la gran extensión que abarcan (424.000 ha) y su elevado valor ecológico, ambiental, agrario y cultural. De todo ello, se deriva el Pacto Andaluz por la Dehesa, mediante Acuerdo de 18 de octubre de 2005, del Consejo de Gobierno de la Junta de Andalucía, para promover su defensa, dada la diversidad y complejidad de las causas, tanto socioeconómicas, silvícolas, climáticas y fitosanitarias, entre otras, que están poniendo en grave peligro el equilibrio de los recursos y del sistema de explotación (Ley 7/2010, para la Dehesa).

La Ley 7/2010, de 14 de julio, para la Dehesa, en la Comunidad Autónoma de Andalucía, establece las siguientes definiciones que engloban a estos ecosistemas desde el punto de vista natural y de gestión:

- *Formación adehesada*: Superficie forestal ocupada por un estrato arbolado, con una fracción de cabida cubierta (superficie de suelo cubierta por la proyección de la copa de los árboles) comprendida entre el 5% y el 75%, compuesto principalmente por encinas, alcornoques, quejigos o acebuches, y ocasionalmente por otro arbolado, que permita el desarrollo de un estrato esencialmente herbáceo (pasto), para aprovechamiento del ganado o de las especies cinegéticas.
- *Dehesa*: Explotación constituida en su mayor parte por formación adehesada, sometida a un sistema de uso y gestión de la tierra basado principalmente en la ganadería extensiva que aprovecha los pastos, frutos y ramones, así como otros usos forestales, cinegéticos o agrícolas.

Son muchas las oportunidades y las fortalezas asociadas a la multifuncionalidad y a la diversidad de las dehesas, pero al mismo tiempo, dicho entramado agro-ecosistémico también implica constantes amenazas y debilidades que desestabilizan su equilibrio socioeconómico y ambiental.

Algunas de estas restricciones son (Junta de Andalucía, 2008; Alejano Monge et al., 2011):

- ✓ Pérdida de tradiciones y abandono progresivo de los aprovechamientos por falta de reemplazo generacional. Intensificación de los laboreos y actividades agrícolas.
- ✓ La baja fertilidad de los suelos, unido al fomento de las sobrecargas ganaderas, generan sistemas de escasa productividad poniendo en riesgo los pastizales naturales.
- ✓ Envejecimiento generalizado del arbolado, intensamente explotado durante periodos muy largos, con daños parciales o heridas, con escasa diversidad de clases de edad y una ausencia casi total de regeneración natural, por sobrepastoreo o intensificación de cultivos.
- ✓ Descoordinación entre políticas forestales y agrarias, con la consiguiente pérdida de oportunidades y rentabilidad de productos.
- ✓ Tendencia al abandono de las masas forestales por elevado coste de los tratamientos silvícolas de mantenimiento, con la consecuente acumulación de biomasa y con el elevado riesgo de incendios forestales.
- ✓ Expansión de los procesos de decaimiento asociados a agentes bióticos (plagas y enfermedades) y abióticos (cambio climático) cada vez más acusados.

Pese a las fronteras políticas y a la propia gestión agrosilvopastoral, los bosques de encinas y alcornoques de nuestra vecina Portugal son muy similares a los que se pueden encontrar en el suroeste de España. Estos sistemas han experimentado un continuo retroceso en la cobertura del dosel arbóreo entre 1965 y 2015 (Acácio et al., 2021), donde *Q. suber* ha decrecido un 57,9% y *Q. ilex* subsp. *ballota* un 71,1%, valores que, por su similitud ecológica y fitosanitaria, son muy afines a los que puedan estar experimentando estas especies en nuestros bosques. Principalmente estas pérdidas, se asociaron a áreas de escasa pendiente, con un uso más intensivo de la tierra y elevadas cargas ganaderas y con temperatura media más alta.

1.3 Forestación de tierras agrarias en Andalucía ¿el futuro de la dehesa?

Con objeto de diversificar la funcionalidad de las explotaciones agrícolas y ganaderas, entre 1993 y 1999, se promovió en Andalucía un primer programa de ayudas para fomentar la forestación de tierras agrarias (FTA) que permitiese obtener rendimientos económicos futuros sobre tierras marginales, incentivando el recurso cinegético, las actividades de recreo ambiental, el aprovechamiento de maderas, el corcho, las piñas, etc., así como una mejora de la calidad de los pastos influenciados por el estrato arbóreo generado, que beneficiase al ganado (Montiel Molina y Galiana Martín, 2004; Fernández Carrillo et al., 2016). Y, por otro lado, las FTA aportarían también beneficios ecosistémicos promoviendo hábitats más biodiversos y aprovechamientos, directos o indirectos, más variados, disminuyendo la erosión de los suelos y la desertización, regulando el régimen hídrico, creando sumideros de carbono frente al avance del cambio climático y, mejorando y poniendo en valor el paisaje en el entorno rural (Junta de Andalucía, 2008; Fernández Carrillo et al., 2016).

La superficie total forestada para dicho periodo en Andalucía fue de 120.080 ha (Vadell et al., 2019), de las cuales 82.755 ha fueron de encina y 1.393 ha de alcornoque (Tabla 1) (Navarro Cerrillo et al., 2009), donde Huelva fue la provincia de Andalucía con más superficie forestada, con un 40% de superficie sobre el total.

Tabla 1. Número de expedientes y superficie forestada (ha) con encina y alcornoque en Andalucía (Navarro Cerrillo et al., 2009).

	Encina		**Alcornoque**	
	Expedientes	Superficie (ha)	Expedientes	Superficie (ha)
Almería	314	11092	275	9
Cádiz	28	717	625	29
Córdoba	87	3020	375	15
Granada	97	2595	0	0
Huelva	984	44447	42504	1028
Jaén	78	2444	655	19
Málaga	94	3153	607	26
Sevilla	383	15287	10785	267
TOTAL	2065	82755	55826	1393

Entre otras especies utilizadas en las FTA como el algarrobo, el pino piñonero o el pino carrasco (*Pinus halepensis* Mill.), la encina y el alcornoque fueron las que más superficie aportaron al programa, ya que, además de las funcionalidades anteriormente citadas, contribuían, desde el punto de visto de los propietarios, a la regeneración, mejora y conservación de las dehesas.

La FTA, por las características de los suelos susceptibles de ser forestados, la densidad requerida en el programa (300 pies ha^{-1}) y el mantenimiento de las plantaciones, han creado estructuras en forma de rodales forestales, de densidad media (150-200 pies ha^{-1}), en terrenos de pendiente media o baja, agrícolas, degradados y/o marginales, principalmente, sobre superficies de cultivos herbáceos de secano y de eriales a pastos (Vadell et al., 2019). En muchas ocasiones, el impacto visual de estas intervenciones forestales fue destacado, a la vez que positivo, pues permitió recuperar espacios deteriorados en los entornos rurales (Montiel Molina y Galiana Martín, 2004)

Los trabajos de FTA con encina y alcornoque en Andalucía (Figura 2), constituyen un gran componente, por no decir el único, de las nuevas superficies de estas especies, y los sistemas forestales creados (plantaciones de densidad media o baja) son fundamentales como precursores de nuevas dehesas. Sin embargo, los resultados de la restauración de estos suelos agrícolas se ven comprometidos por numerosos factores, tales como el abandono de las plantaciones, la inadecuada selección del sitio y/o la especie, los incendios, la calidad de la planta de vivero, las marras por las condiciones climáticas o la presencia de plagas y enfermedades (Cuenca et al., 2016; Vadell et al., 2019), que comprometen la viabilidad de la vegetación a largo plazo. En ese sentido es necesario estudiar el impacto de dichos factores, así como las prácticas recomendadas de agroforestería para su gestión, que lleven a la plantación a formar parte de una diversificación y progreso de los paisajes agrícolas (Bertomeu García et al., 2019) formando ecosistemas más complejos a escala espaciotemporal, compuestos por mosaicos de vegetación y bosquetes, mejor adaptados al cambio climático (Sánchez-Oliver et al., 2014; Pereira y Navarro, 2015; Rey Benayas et al., 2015). La investigación actual sobre forestación aborda muchos de estos problemas como la idoneidad de especies y de sitio en condiciones de infección por podredumbre radical, ver, por ejemplo, (Duque-Lazo et al., 2018a).

Figura 2. Aspecto de una plantación de encinas (arriba) y de alcornoques (abajo) en la finca de Campo Baldío S.L. (Puebla de Guzmán – Huelva), dentro del programa de forestación de tierras agrarias en España. Fuente: archivo del autor.

De hecho, recientemente se ha puesto de manifiesto el riesgo que supone la forestación como transmisor de enfermedades a través de la planta de vivero, el uso de maquinaria o las prácticas de gestión (Jung et al., 2016; Fernández-Habas et al., 2019).

2 ¿Cuál es el estado fitosanitario actual de las dehesas en Andalucía?

Las dehesas de encinas, alcornoques y otros *Quercus*, conforman un paisaje muy intervenido por el hombre que, junto a las perturbaciones ocasionadas por los factores bióticos y abióticos (el cambio climático, la escasa fertilidad de los suelos, las plagas, las enfermedades, la falta de regeneración natural, etc.), ponen a la dehesa en un constante estado de desequilibrio, generando sobre el arbolado una pérdida de vigor y una sintomatología de deterioro progresivo, que viene expresada como defoliación y clorosis generalizada de la copa.

Desde los años 80-90 comenzaron a observarse de forma más patente estos procesos de debilitamiento y mortalidad sobre *Q. ilex* y *Q. suber*, a lo largo de toda la cuenca mediterránea y de forma más acusada en el suroeste de la Península Ibérica (Brasier, 1992). Es entonces cuando comienzan a surgir interrogantes sobre la causalidad de estos procesos de declive y se empieza a investigar sobre las causas subyacentes. ¿Se trataba de un episodio climático adverso de carácter puntual que provocaba lo que se denominó ***la Seca* de los *Quercus***, o existía detrás de este deterioro un complejo entramado de múltiples factores que generaban un proceso regresivo al que más tarde se le llamó **síndrome de decaimiento de los *Quercus***?

El término *Seca* comenzó a utilizarse de forma indiscriminada en todos los ámbitos y niveles de gestión de las dehesas (propietarios de fincas, técnicos, gestores forestales y la opinión pública en general), refiriéndose a cualquier alteración del estado fitosanitario normal observada en las encinas y los alcornoques (defoliación, muerte regresiva de tallos, abundante emisión de brotes adventicios o "chupones", necrosis del sistema radical, etc.) (Brasier, 1992, 1996), independientemente de su sintomatología, patrón y extensión de los daños y agentes presentes que los provocasen. Se tendía, por tanto, a generalizar con este nombre situaciones desfavorables y factores tan diversos como episodios climáticos adversos, prácticas de selvicultura inadecuadas y ataques de plagas y enfermedades sobre el arbolado, que afectaban a escalas e intensidades distintas, con objeto de dar una única solución a problemas independientes o con multitud de componentes implicados (Carrasco Gotarredona et al., 2009).

El *decaimiento forestal* es una enfermedad de etiología compleja, resultado de la acción de un número variable de factores bióticos y abióticos que causan un deterioro gradual y general de los árboles afectados hasta su muerte. Los factores implicados en el proceso de decaimiento son típicamente múltiples, y lo más importante, ninguno de ellos por separado es capaz de reproducir los síntomas observados en campo (Sánchez et al., 2000; Navarro Cerrillo et al., 2004). Los patrones de distribución espacial (focos de *seca*) y la evolución de la sintomatología del decaimiento (defoliación, puntisecado, muerte regresiva de ramas, chancros, brotes adventicios y necrosis radical), son diferentes a los efectos que pueda producir un evento de sequía o una enfermedad infecciosa concreta, pero en ocasiones, resulta muy difícil diferenciar si el deterioro se debe a una enfermedad de etiología compleja o decaimiento, a un factor biótico o abiótico concreto o inclusive a la propia senescencia natural de árboles individuales o de la masa, por lo que algunos procesos identificados como decaimiento, inicialmente, acaban asociándose a algún agente primario causal único, a posteriori, y en muchas ocasiones ligado a algún evento intenso del clima local o regional (Alejano Monge et al., 2011).

Los factores que intervienen en el proceso del decaimiento de los *Quercus* en las dehesas pueden agruparse en tres categorías (Navarro Cerrillo et al., 2004; Carrasco Gotarredona et al., 2009):

- Factores de Predisposición: prácticas de gestión inadecuadas que actúan a largo plazo debilitando al arbolado frente a los factores incitantes y contribuyentes.
    - Arbolado senescente y sobreexplotado.
    - Escasez de regenerado por sobrepastoreo.
    - Prácticas culturales inapropiadas que provocan heridas y daños irreversibles (podas, descorches, intensidad del laboreo).
- Factores Incitantes: agentes abióticos basados principalmente en alteraciones climáticas.
    - Incremento de las temperaturas.
    - Cambios en la intensidad y la distribución de las precipitaciones.
    - Mayor recurrencia de episodios climáticos extremos.
- Factores Contribuyentes: son aquellas enfermedades y plagas que, participando en los últimos estados del proceso de decaimiento, son los que provocan la muerte del arbolado.

El efecto combinado y repetido en el tiempo de estos tres factores ocasiona un debilitamiento progresivo del arbolado que se expresa a través de los síntomas del decaimiento y mortalidad del arbolado.

Así, la variedad de agentes o factores involucrados como desencadenantes de los procesos de decaimiento de los *Quercus* es muy amplia, como numerosos autores han identificado y constatado (Sánchez et al., 2000; Navarro Cerrillo et al., 2004; Carrasco Gotarredona et al., 2009; Alejano Monge et al., 2011). En este sentido, uno de los factores incitantes más destacados es el aumento del estrés abiótico impulsado por los episodios de sequía severos y recurrentes a consecuencia del cambio global (Gea-Izquierdo et al., 2020) entre otros, como los encharcamientos estacionales, la contaminación atmosférica y los cambios en el uso tradicional de las dehesas y montes, a los que les siguen como factores contribuyentes los ataques de insectos barrenadores (*Cerambyx velutinus* Brull. y *Prinobius germari* Dejean) y de hongos patógenos (*Phytophthora cinnamomi* Rands., *Pythium spiculum*, *Biscogniauxia mediterránea* (De Not.) Kuntze, *Botryosphaeria corticola* Phillips y *Brenneria quercina* Hauben) (Tabla 2).

Tabla 2. Biogeografía de *la Seca* de la encina y el alcornoque en Andalucía (Navarro Cerrillo et al., 2004).

Zona	Problema	Agente primario	Agente secundario	Principal problema silvícola
Sector Occidental	Enfermedad	*Phytophthora cinnamomi*	*Biscogniauxia mediterránea* *Botryosphaeria* sp. *Cerambyx welensii* *Prinobius germari* *Kermes ilicis*	Falta de regeneración
Sector Sierra Morena	Decaimiento		*Biscogniauxia mediterránea* *Cerambyx welensii* *Prinobius germari*	Falta de regeneración
Sector sierras Gaditano-malagañas	Enfermedad	*Botryosphaeria* sp.	*Biscogniauxia mediterránea* *Phytophthora cinnamomi*	Falta de regeneración Origen de las masas
Sector oriental	Sequía			Densidades excesivas

Sobre la base del conocimiento científico-técnico alcanzado hasta la fecha, el diagnóstico del deterioro del arbolado debe procurar diferenciar aquellas situaciones claras en las que actúa una enfermedad o plaga concreta, de aquellas en las que afectan múltiples factores intercambiables en el tiempo y el espacio produciendo un decaimiento forestal complejo (Alejano Monge et al., 2011).

Actualmente, la regresión y la mortalidad de los bosques y dehesas de *Q. ilex* y *Q. suber* en España se interpreta mediante diversos patrones que se combinan en el espacio, bien por procesos de decaimiento o por enfermedades de etiología simple (plagas o enfermedades). De entre estas últimas, la podredumbre de raíces en especies leñosas provocada por el patógeno *P. cinnamomi* es considerada como una de las principales causas desencadenantes de episodios graves de defoliación y mortalidad del arbolado (junto a otras especies de oomicetos de los géneros *Phytophthora* de Bary y *Pythium* Pringsh.), con más de 5000 especies de plantas susceptibles entre las que se encuentran la encina y el alcornoque (Jung et al., 2013).

3 Podredumbre de raíz en encina y alcornoque

3.1 Agentes de etiología simple del suelo: *Phytophthora cinnamomi* Rands.

Phytophthora cinnamomi es uno de los patógenos de podredumbre de raíces de plantas leñosas más destructivos del mundo (de Andrade Lourenço et al., 2020). Provoca la pudrición generalizada de las raíces absorbentes, llegando en ocasiones a limitar la capacidad del árbol para obtener agua y nutrientes del suelo, ocasionándole síntomas foliares similares a los que se dan por estrés hídrico durante los periodos de sequía. La sintomatología en las copas (clorosis, marchitez foliar, defoliación, puntisecado de brotes y ramas, etc.) puede expresarse de forma gradual a lo largo del tiempo (síndrome de muerte regresiva o lenta) o en forma de colapso repentino (síndrome de muerte súbita o apoplejía) siendo, en esta última modalidad, característica la marchitez general de las hojas adheridas a la copa (Sánchez et al., 2000, 2003) (Figura 3). La muerte regresiva suele presentarse más frecuentemente en climas frescos y húmedos (Sánchez et al., 2006).

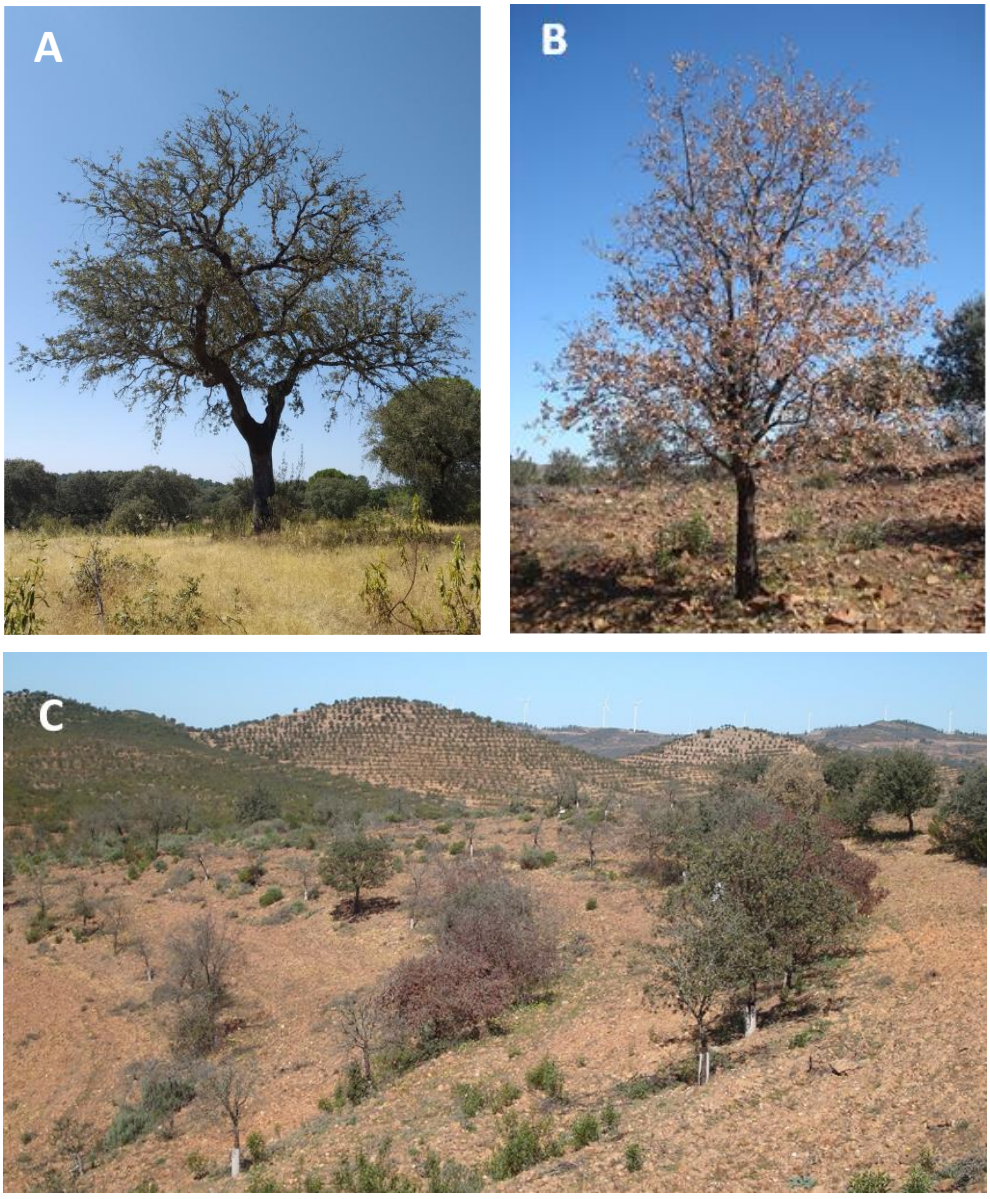

Figura 3. Sintomatología de muerte regresiva en arbolado adulto (A) y de repoblación (C) y muerte súbita en arbolado de repoblación (B y C), asociada al decaimiento. Fuente: archivo del autor.

La amplia distribución mundial y local, en cuanto a diversidad de ecosistemas en los que puede encontrarse este patógeno, se ve influenciada por la gran variedad de vectores que contribuyen a su dispersión, a pequeña y gran escala, como los desplazamientos de animales y el ser humano (Krull et

al., 2013), los movimientos de tierra asociados a las prácticas agrícolas o infraestructuras viarias (Weste y Taylor, 1971), los vectores de carácter ambiental como escorrentías por lluvia (Kinal et al., 1993; Ristaino y Gumpertz, 2000), las importaciones de material vegetal y sustratos infectados, así como las plantas de viveros empleadas en forestaciones con problemas de damping-off, ocasionados por patógenos de podredumbre radical (Jung et al., 2016). Así mismo, en función de la variabilidad de los condicionantes ambientales en tiempo y espacio, a *P. cinnamomi* se le considera un organismo capaz de pasar de fase necrótrofa a biótrofa o endófita, o a la inversa (Crone et al., 2013a, 2013b; Ruiz-Gómez et al., 2015), así como de reproducirse sexual o asexualmente, generando diversidad de estructuras infectivas y de supervivencia (hifas, oosporas, zoosporas, clamidosporas (Erwin y Ribeiro, 1996; Hardham, 2005; Jung et al., 2013) y con un amplio abanico de estrategias de colonización e infección frente a sus huéspedes (quimiotaxis, electrotaxis, autotaxis o autoagregación (Weste, 1983; Walker y van West, 2007), dotando a este organismo patógeno de gran plasticidad para adaptarse a cambios en las condiciones climáticas, edáficas y topográficas de cada zona.

En este sentido, Thomas Jung y colaboradores (2016) analizaron el grado de infestación que tienen los viveros europeos con especies del género *Phytophthora* spp., donde en el 91,5% de los estudiados se aislaron diferentes especies de este patógeno, y el 66% de las áreas objeto de plantaciones forestales y paisajísticas de árboles y arbustos, se encontraban infectadas con estos oomicetos de podredumbre de raíz. Este hecho supone un serio peligro para la estabilidad de los bosques naturales y seminaturales europeos y, en particular, de las dehesas y ecosistemas mediterráneos de *Quercus*.

3.2 Condiciones abióticas que pueden influir en la dispersión e infección de *P. cinnamomi*

Las condiciones ambientales de disponibilidad de agua y el rango de temperaturas son factores de gran importancia en el desarrollo y en el proceso de infección de *P. cinnamomi* (ver Capítulo IV). En este sentido, el oomiceto tiene la capacidad de completar su ciclo biológico y producir infección en un rango amplio de temperaturas comprendidas entre 5-35 ºC (Zentmyer, 1981; Caetano et al., 2009), sin observarse diferencias en la sintomatología de daños, cubriendo prácticamente todas las estaciones del año en el sur de Europa y sobreviviendo en el suelo en forma de estructuras de resistencia o en el interior de las raíces del hospedante. Así, las alteraciones

derivadas del cambio climático, como son los episodios de lluvias intensas con posibilidad de encharcamiento del terreno, combinado con sequías extremas prolongadas e incremento de las temperaturas, ayudarían a la dispersión espacio-temporal y al incremento de la patogenicidad de *P. cinnamomi*, fomentando así la colonización de nuevos huéspedes, agravando su estado fisiológico y potenciando los daños de la enfermedad (Sánchez et al., 2003; Bergot et al., 2004; Sánchez et al., 2005). El otoño y la primavera son las épocas más favorables para el proceso de infección del huésped, debido a factores como la mayor disponibilidad de agua libre en el suelo y las temperaturas del suelo, en el rango óptimo para que germinen las estructuras del patógeno (24-30 ºC) (Erwin y Ribeiro, 1996; Sánchez et al., 2002). En estos periodos se producen múltiples ciclos de infección, alternando entre las estructuras infectivas de las raíces (zoosporas) y las estructuras de resistencia características de los periodos desfavorables (clamidosporas) (Hardham, 2005).

Q. ilex y *Q. suber*, este último menos susceptible a la infección por *P. cinnamomi* que otros *Quercus* spp. (Maurel et al., 2001; Robin et al., 2001; Sánchez et al., 2005), experimentan de forma general, en condiciones de infección, una mejor respuesta ecofisiológica frente a situaciones de estrés hídrico no prolongadas que frente a estados de encharcamiento, debido a que su sistema radical presenta menor porcentaje de pudrición por el patógeno (Maurel et al., 2001; Robin et al., 2001; Ruiz-Gómez et al., 2019b). Sin embargo, en condiciones prolongadas de escasez de agua en el suelo, tras un periodo de encharcamiento previo, la respuesta ecofisiológica del árbol y sus reservas de carbono, se verían comprometidas (Gimeno et al., 2009; Galiano et al., 2012; Ruiz-Gómez et al., 2019b) poniendo en grave riesgo su supervivencia, más si cabe, si se produjese un evento puntual de lluvia en la época de sequía, donde el patógeno se vería favorecido de forma instantánea para infestar nuevas raíces (Sánchez et al., 2002, 2003, 2005; Ruiz-Gómez et al., 2018) y el huésped, por el contrario, vería agravada su situación por falta de una rápida respuesta fisiológica, provocándole incluso la muerte (Rodríguez-Molina et al., 2005).

Por otro lado, las condiciones topográficas del terreno, como la orientación y la pendiente de las laderas, condicionan el régimen hidrológico de la ladera (micro topografía) respecto al movimiento y la disponibilidad de agua en el terreno (ver Capítulos II y III). De esta manera, la confluencia de aguas hacia las vaguadas y las zonas bajas de menor pendiente, facilitan el

encharcamiento favoreciendo la dispersión de *P. cinnamomi* (Tuset et al., 2001; Moreira y Martins, 2005). En este sentido, diversos estudios han demostrado la interconexión y dependencia espacial entre las zonas afectadas por la enfermedad, a lo largo del tiempo y en un espacio limitado, dentro de las cuencas hidrográficas (Fernández-Habas et al., 2019), donde las manchas infectadas se expanden mediante patrones circulares en terreno llano y en forma parabólica en las laderas (Cardillo et al., 2018). En vaguadas, donde los periodos de encharcamiento son más prolongados, *P. cinnamomi* se multiplicaría y dispersaría más rápido que en las laderas, provocando un mayor daño sobre el arbolado.

P. cinnamomi parece ser más frecuente en suelos poco profundos, con baja fertilidad y bajos niveles de nutrientes minerales, especialmente de fósforo (Moreira y Martins, 2005). Respecto al contenido de nitrógeno en el suelo, en sus diferentes formas (amonio, nitrato), este elemento parece actuar como inhibidor del ciclo biológico de *P. cinnamomi* en las fases de germinación y esporulación (Tsao y Oster, 1981). La textura del suelo estrechamente relacionada con la disponibilidad de agua, y el índice pH, condicionan el comportamiento y la abundancia del oomiceto en el medio. Así, los perfiles de suelo con texturas gruesas presentan menor capacidad de retención de agua y posibilidad de encharcarse, afectando negativamente a la capacidad del patógeno de dispersarse e infestar (Gómez-Aparicio et al., 2012). En este sentido, todos aquellos factores que incrementen la compactación del suelo, como el pisoteo por ganado, la maquinaria pesada y los suelos arcillosos, favorecen la dispersión del patógeno y la infección del arbolado (Erwin y Ribeiro, 1996). En relación con el pH, este oomiceto se desarrolla mejor en suelos ácidos con índices superiores o iguales a 3,8 (Moreira y Martins, 2005), siendo su óptimo entre 5,5 y 6 (Zentmyer, 1980) y logrando soportar hasta índices de pH 7 (Serrano et al., 2011a, 2011b). Otros condicionantes de tipo antrópico como las prácticas agrícolas mediante laboreos intensivos y las prácticas ganaderas con sobrecarga de animales en áreas infectadas, favorecen la dispersión y el incremento de las unidades formadoras de colonias (ufc) o estructuras del oomiceto con capacidad de infestar más árboles y, por tanto, de incrementar la densidad de inóculo y la capacidad de dispersión del patógeno (Brasier et al., 1993).

Un óptimo estado nutricional y fisiológico del arbolado, relacionado directamente con la asimilación de carbono y un buen balance hídrico para crear nuevas raíces y hojas, capacita a las plantas para incrementar su

resistencia frente a posibles infecciones del patógeno (Jönsson, 2006). Algunos nutrientes (Ca, Al o N) intervienen en el ciclo biológico del patógeno y, a su vez, en los medios de defensa de los árboles frente a estos organismos. Concretamente, Serrano et al. (2013), demostraron en condiciones controladas que una óptima nutrición en calcio de plántulas de *Q. ilex*, aumentaría las defensas frente al ataque por *P. cinnamomi*, evitando así los daños característicos sobre el huésped tras repetidas infecciones, como son la alteración fisiológica y nutricional y la reducción del potencial hídrico, la conductancia estomática y la fotosíntesis del árbol, que se traducen en desequilibrio biológico mediante la pérdida de hojas y raíces.

Por último, hay que considerar los factores de origen antrópico y relacionados con el manejo agrosilvopastoral de la dehesa y los bosques de *Quercus* spp., como un grupo de factores abióticos con una gran influencia en el estado fitosanitario del arbolado y, en concreto, en la dispersión de los patógenos de podredumbre de raíz. En las dehesas, las labores agrícolas suponen uno de los vectores más relevantes en cuanto al movimiento de tierras para la transmisión del patógeno ligado a la contaminación de aperos y maquinaria (Worboys y Gadek, 2004; Dell et al., 2005; Duque-Lazo et al., 2018b).

3.3 Condiciones bióticas que influyen en la severidad, distribución y abundancia espacial de *P. cinnamomi* y otros patógenos oomicetos

Existen multitud de factores bióticos que pueden influir en los patrones espaciotemporales y de abundancia de *P. cinnamomi* en el suelo. Uno de los más importantes es el papel que la microbiota del suelo desempeña en la protección de las raíces de los árboles frente a factores estresantes como periodos de sequía y frente a los oomicetos patógenos de raíz, compitiendo con estos por el espacio y los recursos de la rizosfera (Corcobado et al., 2014; Balla et al., 2021). En este sentido, la abundancia de hongos ectomicorrícicos simbiontes que se asocian con las raíces del árbol, interactúan de forma compleja con estos oomicetos. Corcobado et al., (2014) demostraron en un trabajo realizado sobre localizaciones de encinar adehesado afectado por podredumbre de raíz, que las encinas en decaimiento mostraban menor tasa de micorrización que las encinas no afectadas, indicando que estos organismos simbiontes parecen actuar como barrera en la zona apical de las raíces del árbol, frente a la infección del patógeno. En este sentido, Ruiz-

Gómez et al., (2019a) observó que valores bajos de diversidad fúngica en el suelo estaban asociados a zonas de dehesa con mayores índices de defoliación del arbolado, donde destacan especies patógenas.

Por otro lado, la diversidad, composición e interrelación en el suelo entre comunidades patógenas de raíces de *Quercus*, géneros *Phytophthora* spp. y *Pythium* spp., afectan al grado de daños que ejercen sobre su huésped, compitiendo entre ellos por recursos y espacio, asociándose los daños más graves de defoliación del arbolado a una menor diversidad de oomicetos y principalmente referente a especies del género *Phytophthora* spp. (Ruiz-Gómez et al., 2016, 2019a). La presencia de hongos antagonistas también influye en la abundancia y la capacidad de causar daños de estos oomicetos, especialmente los hongos del género *Trichoderma* Persoon. Este género se ha asociado con la actividad antagonista frente a numerosas especies patógenas, convirtiéndose en un organismo comúnmente usado en estrategias de biocontrol de múltiples especies, como los oomicetos (Vinale et al., 2008; García-Núñez et al., 2017; Widmer et al., 2018; Ruiz-Gómez et al., 2019a). Estudios recientes han demostrado que algunas de estas especies de *Trichoderma* presentan un elevado potencial para el control de *P. cinnamomi* (Morales-Rodríguez et al., 2018; Ruiz-Gómez y Miguel-Rojas, 2021).

Otro factor para considerar en la distribución del patógeno es la misma presencia de sustrato para que los oommicetos completen su ciclo reproductivo. Gómez-Aparicio et al., (2012) observaron que, en un análisis de distribución espacial dentro de un foco de podredumbre de raíz en alcornoque, la abundancia de estos patógenos disminuía en las zonas donde el arbolado aparecía muerto, lo que concuerda con el carácter de *P. cinnamomi* y *Pythium* spp., que son especies que requieren de la presencia de raíces finas vivas para el crecimiento y dispersión de sus estructuras infectivas (Shearer y Tippett, 1989). En este sentido, la distribución espacial a pequeña escala de las raíces del huésped, considerando la encina y el alcornoque, pero también otras especies susceptibles como cistáceas (Moreira y Martins, 2005), ericáceas (Cardillo et al., 2018) o herbáceas perennes y cultivos (Serrano et al., 2010, 2011c) influyen de manera determinante en la evolución y dispersión de la infección. Una de las especies de leguminosas que crece de forma espontánea entre los pastizales del sur de la Península Ibérica, y también es usada frecuentemente como cultivo para alimentar al ganado en las dehesas es *Lupinus luteus* L. (altramuz amarillo), el cual se ha mostrado no solo como huésped susceptible de *P. cinnamomi,* sino que presenta un alto potencial

como planta reservorio de inóculo en su sistema radicular, aumentando los niveles en suelo de las estructuras infectivas del patógeno, y por tanto, relacionado con mayores tasas de podredumbre de las raíces de los *Quercus* spp. (Serrano et al., 2010, 2011c).

En relación con lo anterior, la estructura, densidad y diversidad del arbolado puro o mixto con mezcla de matorrales, generan unas condiciones de proyección de las copas y de disponibilidad de luz o de sombra sobre el suelo y de presencia de raíces y de hojarasca asociada con la mesofauna, que en interacción con el resto de factores bióticos del entorno, constituyen un sistema complejo de impulsores ecosistémicos relacionados entre sí que influyen en la abundancia y dispersión de los oomicetos de podredumbre de raíz (Cardillo et al., 2021; Gómez-Aparicio et al., 2012, 2017; Jiménez-Chacón et al., 2018; Sánchez-Cuesta et al., 2020).

4 El "problema espaciotemporal" de los agentes bióticos y abióticos asociados a *P. cinnamomi*

La heterogeneidad espacial de los componentes de cualquier proceso de carácter infectivo patógeno-huésped, como el que ocupa esta tesis doctoral, son fruto de un complejo conjunto de interacciones, donde se incluye la forma en que se distribuyen los factores ambientales bióticos y abióticos en el medio, y el tipo de respuesta de los organismos que cohabitan frente a esos factores (Milne, 1991). Esa distribución heterogénea de los organismos en el hábitat se puede producir a diferentes escalas espaciotemporales (Stewart, 2000; Dale y Fortin, 2014; Turner y Gardner, 2015). Por ello, es importante considerar el concepto de escala en la valoración de dicha heterogeneidad, desde la dimensión ecológica, de muestreo y analítica (Dungan et al., 2002) pues, dependiendo del nivel de detalle, se podrán mostrar las variables en el entorno como homogéneas o heterogéneas, por lo que la escala de muestreo en cada estudio deberá ser la adecuada para recoger la máxima variabilidad y representatividad del proceso estudiado (García, 2006).

La heterogeneidad de los factores bióticos y abióticos que intervienen en procesos patogénicos como el provocado por *Phytophthora cinnamomi*, ha sido estudiada a diferentes escalas, desde su distribución a nivel mundial (Burgess et al., 2017), como regional (Duque-Lazo et al., 2018b; Sánchez-Cuesta et al., 2021), de meso escala (Cardillo et al., 2018, 2021) y microescala (Gómez-Aparicio et al., 2012; Sánchez-Cuesta et al., 2020). De forma general,

los sistemas mediterráneos, objeto de nuestro estudio, son un claro ejemplo de esta heterogeneidad espaciotemporal de las condiciones ambientales, la distribución de las especies arbóreas de *Quercus* spp., y las propiedades del suelo (Andivia et al., 2015).

La variabilidad espaciotemporal de los factores que interaccionan en cualquier proceso de enfermedad forestal, conlleva no sólo la propia complejidad intrínseca a la heterogeneidad de los factores, sino a la necesidad del seguimiento y control de las causas, y su evolución mediante el estudio de los patrones de distribución de las variables, usando para ello unidades de muestreo y estudio a diferentes escalas (fincas, parcelas y redes de seguimiento de bosques) que sirvan como herramientas para abordar las relaciones inherentes al decaimiento forestal (Navarro-Cerrillo y Ruiz-Gómez, 2020). En el caso de la podredumbre radical de los *Quercus*, hay que añadir la dificultad, en muchas ocasiones, de atribuir visualmente la sintomatología de debilitamiento del arbolado al daño ocasionado por el oomiceto *P. cinnamomi*, debido a que los síntomas son inespecíficos y se pueden confundir con el daño ocasionado por otras enfermedades o el estrés hídrico (Robin et al., 1998; Jung et al., 2000; Sánchez et al., 2006). Normalmente se evalúan los síntomas de daño relacionados con la condición de la copa de los árboles, es decir, daño de ramas y brotes, el nivel de defoliación y el nivel de decoloración de la copa. Usando estos indicadores, las Redes de Seguimiento de Daños en los Bosques (Redes ICP, International Co-operative Programme on Assessment and Monitoring of Air Pollution Effects on Forests, (Lorenz, 1995; Parr et al., 2002), http://icp-forests.net/) permiten evaluar a largo plazo los efectos de los cambios ambientales en los principales ecosistemas forestales (Figura 4). Las redes ICP tienen protocolos de medición y diseño de muestreo, que permiten la integración del seguimiento de ecosistemas a nivel europeo, y la disponibilidad de datos armonizados para realizar estudios a escala regional. Por otro lado, la Comunidad Autónoma de Andalucía, al igual que otras CCAA, han reconocido la necesidad de un programa regional y nacional coherente de seguimiento integrado a largo plazo de los sistemas forestales, que dio lugar en Andalucía a la implantación de la Red Andaluza de Seguimiento de Daños sobre Ecosistemas Forestales "Red SEDA" (Figura 4) (Navarro-Cerrillo et al., 2000; Consejería de Medio Ambiente y Ordenación del Territorio, 2018) que evalúa el estado fitosanitario del arbolado, detectando tendencias y alteraciones tanto en el nivel de daño y abundancia de los agentes bióticos y abióticos, como en la defoliación, decoloración y mortalidad de los árboles. Sin

embargo, el análisis de los datos generados por estas Redes puede ser problemático, entre otras cosas debido a las limitaciones impuestas por la distribución sistemática de los puntos de muestreo, los protocolos de evaluación y medida, o las variables registradas, lo que obliga a integrar datos de otras redes e inventarios complementarios existentes para aprovechar al máximo estas evaluaciones (Galluzzi et al., 2018).

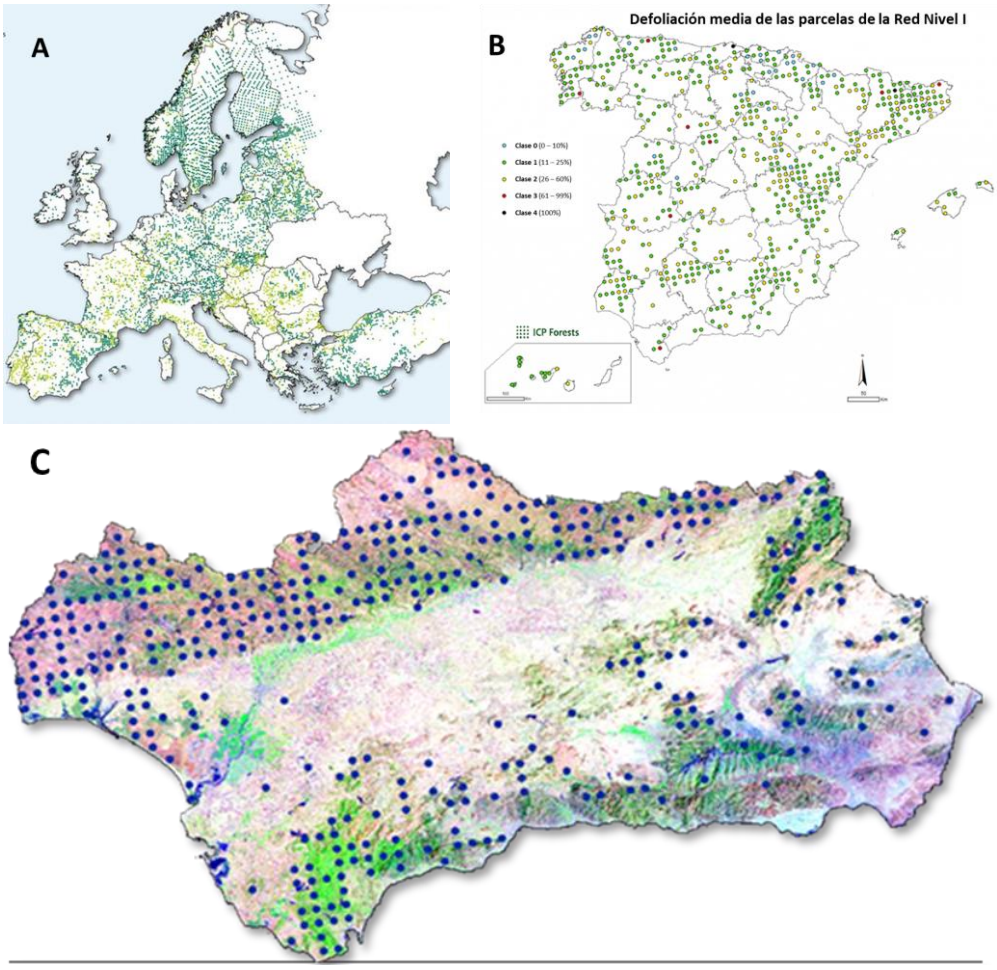

Figura 4. Red de parcelas (16 x 16 km) de Nivel I, del Programa de Cooperación Internacional para la Evaluación y el Seguimiento de los Efectos de la Contaminación Atmosférica en los Bosques "ICP Forest" a escala de Europa (A) y a escala nacional de España (B), y Red Andaluza de Seguimiento de Daños sobre Ecosistemas Forestales, que densifica las anteriores (8 x 8 km) "Red SEDA" al sur de España (C).

Por último, las Redes están aportando información sobre el comportamiento de varias enfermedades fúngicas forestales, que pueden volverse devastadoras debido a circunstancias tales como las interacciones con los factores abióticos, como la sequía y las inundaciones, que predisponen a los árboles al ataque de esos patógenos, modifican sus patrones de dispersión aumentando la incidencia de las enfermedades o el rango geográfico de las mismas (por ejemplo, al encontrar nuevos huéspedes y/o nuevos vectores potenciales), y pueden generar nuevas amenazas asociadas a los cambios genéticos en hospedantes y patógenos. En ese sentido, es importante que se estudien los patógenos con mayor potencial de producir daños graves para estimar la magnitud de la amenaza y prepararse para las condiciones cambiantes futuras (La Porta et al., 2008).

5 Las diferentes aproximaciones al "problema espaciotemporal"

La compleja heterogeneidad que albergan las interrelaciones y la distribución espacial de los factores bióticos y abióticos de cualquier ecosistema o proceso forestal, no sólo conlleva una gestión pormenorizada del estudio y del seguimiento en el propio medio natural, como se ha descrito anteriormente, sino que también precisa, a posteriori, del uso de herramientas geoestadísticas (Krige, 1951) que ayuden a analizar, en base a diversas áreas temáticas, los datos espacialmente explícitos que se generan (Maestre, 2006; Zavala et al., 2006; Klobučar, 2010). De esta forma, las diferentes técnicas de interpolación espacial como la regresión en procesos Gaussianos "kriging" (Burgess y Webster, 1980) o la distancia inversa ponderada "IDW" (Philip y Watson, 1982; Watson y Philip, 1985), son metodologías geoestadísticas cada vez más empleadas en procesos biológicos y en temáticas forestales tan diversas como la distribución espacial de nutrientes en suelo y árbol (Gallardo et al., 2000; Gallardo, 2003; Gallardo y Covelo, 2005; Covelo et al., 2008), la distribución de contaminantes en suelo (Qiao et al., 2019), la producción de pastos en dehesas (Gómez-Giráldez et al., 2019), la distribución de la microbiota en suelos forestales (Morris, 1999; Pennanen et al., 1999; Sánchez-Cuesta et al., 2020) o las estimaciones de pérdida de dosel arbóreo en bosques de *Quercus* spp. (Acácio et al., 2021).

Algunas de las herramientas de base geoestadística más empleadas en el análisis y la comprensión del complejo entramado de las interrelaciones

espaciotemporales de los ecosistemas forestales, y más concretamente, de los procesos de decaimiento forestal donde intervienen organismos patógenos de podredumbre radical como el oomiceto *Phytophthora cinnamomi*, se describen a continuación.

5.1 Análisis de los patrones de distribución espacial mediante índices de distancia "SADIE" (*Spatial Analysis by Distance Indices*)

Multitud de estudios de ámbito ecológico y forestal presentan los datos de sus resultados en forma de conteos, con numerosos ceros y distribuciones de Poisson y, por tanto, difíciles de analizar mediante técnicas geoestadísticas clásicas por no cumplir con la estacionariedad de la varianza o las distribuciones normales (Maestre et al., 2008). Para salvar estos inconvenientes, el Dr. Joe Perry y su grupo, implementaron un método de análisis espacial de conteos denominado SADIE (Perry y Hewitt, 1991; Perry, 1995, 1998; Perry et al., 1996, 1999), basado en el tipo de patrón de distribución espacial de las variables (agregado, regular o aleatorio) y en la estimación de la distancia mínima necesaria en el espacio para alcanzar la regularidad. La sencillez de su uso, la simplicidad matemático-estadística para la evaluación de los patrones espaciales de las variables y la amplia gama de recursos existentes para la visualización de los resultados, hacen de esta técnica una herramienta muy versátil (Maestre et al., 2008).

En el uso de SADIE se tiene en cuenta la localización espacial de los datos, sin que tengan que seguir distribuciones determinadas, y los resultados se ven únicamente condicionados por la heterogeneidad de los mismos en el espacio (Bell, 1998). Así, este método permite analizar los patrones espaciales de variables individuales en la zona de estudio a lo largo del tiempo y estimar la contribución de cada punto de muestreo al patrón espacial global (Maestre et al., 2008).

SADIE es una herramienta no paramétrica que caracteriza la forma en cómo se distribuye la variable en la zona de estudio mediante dos índices. El índice de agregación, I_a, que indica el patrón espacial general de cada variable en la zona de estudio y su tipo de distribución (agregado si $I_a > 1$, aleatorio si $I_a = 1$ y regular si $I_a < 1$), y el índice de agrupación, v, que permite delimitar entre todos los datos las zonas con presencia de manchas o áreas con valores altos de la variable ($v_i \geq 1{,}5$) y los claros o áreas con valores bajos de la variable ($v_j \leq -1{,}5$), mientras que los cercanos a 1 indican patrón aleatorio de esa unidad de

muestreo (Perry et al., 1999). De esta forma y mediante interpolación lineal, SADIE permite representar mediante mapeo, el valor de *v* de cada posición muestreada, facilitando la interpretación de los resultados.

Esta herramienta de análisis espacial, se presenta por tanto como un método muy adecuado para analizar los patrones de distribución espaciotemporales de multitud de variables bióticas y abióticas presentes en el medio, como propiedades edáficas, hongos patógenos, plantas, animales y procesos de decaimiento y mortalidad por plagas y enfermedades (Maestre et al., 2008), entre otros, pero también tiene sus limitaciones, en relación a que los datos de las variables deben ser valores enteros, las unidades de muestreo deben tener siempre la misma superficie y que los estadísticos de SADIE, especialmente el I_a, dependen del posicionamiento de las manchas y los claros en el espacio y, por tanto, no pueden describir todas las características del patrón espacial de la variable dentro del área de estudio, por lo que en este sentido, se hace necesario combinar esta técnica de análisis espacial con otras técnicas estadísticas complementarias (Quero, 2006; Maestre et al., 2008).

5.2 Técnicas de modelización predictiva del seguimiento, interacción y distribución espaciotemporal de agentes bióticos y abióticos

El seguimiento de las enfermedades forestales, como es el caso de las patologías asociadas a los oomicetos de suelo del género *Phytophthora* spp., es actualmente un reto para la conservación y el mantenimiento de la sostenibilidad de los ecosistemas forestales Mediterráneos, especialmente en el actual contexto de cambio global (Ruiz-Gómez et al., 2019b). Tanto el pronóstico como el diagnóstico son herramientas fundamentales y necesarias en la evaluación de dichos procesos, y en las posibles aplicaciones de control que se pudieran derivar. Estas herramientas, actualmente, incluyen modelos tanto de impacto o daños asociados como de evaluación de riesgos. Los primeros representan la condición de las especies forestales consideradas desde su evolución espaciotemporal, así como su relación con los factores bióticos y abióticos relacionados con el proceso, especialmente centrados en la relación de los patógenos principales con el resto de los factores. El desarrollo de estos modelos requiere de la presencia de bases de datos contrastadas, que son las que definen esta escala espaciotemporal. En dicho sentido, la presencia de redes de monitorización como la Red SEDA ofrecen una oportunidad única para desarrollar este tipo de modelos y descifrar la existencia de relaciones

causa-efecto entre la presencia de agentes patógenos y el estado fitosanitario del arbolado, teniendo en cuenta otros aspectos claves como son las condiciones climáticas en periodos de tiempo moderadamente largos o las diferencias en los usos del suelo en el ecosistema (Kelly y Meentemeyer, 2002; Meentemeyer et al., 2012).

La combinación de diferentes técnicas de modelado espaciotemporal resulta adecuada en este contexto para evaluar estos impactos. El concepto de escala temporal y espacial se puede combinar en técnicas estadísticas aplicando modelos mixtos (*Generalized Linear Mixel Models* – GLMM) utilizando la factorización espacial como variable aleatoria, o simplemente considerando factores de agrupamiento en otras técnicas estadísticas que evalúan el impacto de la enfermedad, como los análisis de supervivencia (*Kaplan-Meier*, o regresiones de Cox). Además, la fragmentación de las variables ambientales en clústeres homogéneos y su interacción a través de técnicas como la inferencia multimodelo nos ofrecen una potente herramienta para discriminar los principales fatores desencadenantes de estos procesos dentro de bases de datos muy complejas (Burnham y Anderson, 2002).

Sin embargo, estas aproximaciones presentan limitaciones desde el punto de vista espacial, que pueden ser recogidas por otras técnicas de modelización de probabilidades a nivel espacial, como las técnicas de estimación de densidad de probabilidades a partir de núcleos (*Kernel Density Estimation* – KDE) (Kenchington et al., 2014). Estas técnicas son más adecuadas para el análisis de la distribución espacial de daños a niveles de escala amplios (regiones de varias decenas de miles de Km^2), donde otras técnicas de interpolación o análisis espacial detallado, como por ejemplo SADIE, dejan de ser adecuadas por el nivel de detalle requerido.

Finalmente, para obtener una visión general de las relaciones entre los diversos parámetros, se pueden utilizar otras herramientas de análisis y clasificación no supervisada, incluyendo técnicas de *Machine Learning* (kNN, ANN, Random Forest…) u otras técnicas basadas en el análisis de la matriz de covarianzas entre factores exógenos y endógenos. Para este último tipo de análisis se utiliza una técnica estadística de común uso en ciencias sociales, pero que tiene un desarrollo limitado en ciencias ambientales, los SEM (*Structural Equation Modelling*). Esta herramienta es capaz de detectar patrones generales en un sistema, al mismo tiempo que testea relaciones de parámetros específicos del mismo con el modelo global y entre ellos, permitiendo así evaluar la estructura de los datos a varios niveles al mismo

tiempo, permitiéndonos comprobar la validez de hipótesis preestablecidas de comportamiento (por ejemplo, estructura ecosistémica) y relaciones específicas entre variables exógenas (explicativas) y endógenas (dependientes) del sistema, en todas las combinaciones posibles (Sutton-Grier et al., 2010). El establecimiento de modelos explicativos para estas relaciones podría arrojar luz sobre los mecanismos que regulan la intensidad de los procesos de podredumbre de raíz en encinares de Andalucía.

5.3 Los SIG y la Teledetección en la evaluación de los procesos de decaimiento forestal

Los sistemas de información geográfica (SIG) representan una herramienta fundamental en el desarrollo de análisis de características del territorio y procesos espacialmente distribuidos (Reque y Pérez, 2011). Entre estos procesos, los relacionados con el decaimiento forestal son susceptibles de ser representados espacialmente mediante la estimación de factores y características como la defoliación u otros síntomas asociados al estado fitosanitario. La firma espectral de la vegetación presenta regiones con una gran sensibilidad a los cambios en el estado fitosanitario del arbolado. La zona del infrarrojo cercano y medio se relaciona con cambios en la temperatura de copa producidos por el cierre o la apertura estomática, utilizándose como un indicador del estado hídrico del arbolado (Gerhards et al., 2019). Por su parte, la zona del *red edge*, localizada alrededor de los 720 nm, se ha relacionado con la eficiencia fotosintética. El desplazamiento de esta banda hacia rangos de longitud de onda más amplia puede guardar relación con una mayor actividad fotosintética en general, lo que daría lugar a mayor absorción alrededor de los 680 nm (Xie et al., 2018). Las imágenes hiper y multiespectrales nos permiten calcular índices de vegetación que utilizan la reflectancia en estas bandas, y que podemos utilizar en la extracción de rasgos de la vegetación a diferentes escalas.

Los métodos más precisos para obtener estas relaciones son aquellos que utilizan datos de sensores remotos con una alta resolución espacial (sub-métrica). Estos datos suelen ser tomados a través de plataformas aéreas no tripuladas (UAVs) o tripuladas (vuelos tripulados fotogramétricos). Estos sensores nos permiten crear modelos con gran detalle y precisión, a nivel de copa, pero que presentan limitaciones de cobertura espacial al aumentar la escala de trabajo, para lo cual se requieren sensores localizados a distancias superiores, como serían los sensores satelitales. Actualmente existen diversos

sensores activos, tanto en misiones de la ESA (Copernicus Hub) como de la NASA, que facilitan datos espectrales con una gran resolución espacial (Pléiades con precisión de 2 m en multiespectral y 0.5 m en pancromático), SPOT 6 y 7 (6 m en multiespectral y 1,5 m en pancromático) o WorldView 3 (1,24 m en multiespectral y 0,30 m en pancromático). Dichos sensores permiten la inversión de modelos calibrados a escala de paisaje y región con una gran precisión, aunque a menudo requieren de altas capacidades de computación. Para análisis de procesos espaciales a niveles de escala grandes (regionales, centenas a miles de km^2), existen otros sensores más adecuados, que presentan unas resoluciones espaciales medias, entre ellos uno de los más usados, por ser además de acceso público, los que portan las misiones Sentinel 2A y 2B, equipado con un sensor multiespectral que envía datos de infrarrojos de onda corta (SWIR) con una resolución espacial de 10 m con un campo de visión (FOV) de hasta 290 km.

Por otro lado, para una correcta interpretación de los índices espectrales en el seguimiento fitosanitario de masas arboladas, es necesario tener en cuenta los parámetros de estructura de dosel. Estos parámetros se refieren tanto a la estructura horizontal de la masa como a la estructura vertical de la copa, interfiriendo ambos factores en la modulación de la intensidad de la escala. Mientras que la estructura horizontal hace referencia a parámetros como la densidad y afecta de forma diferente a la obtención de rasgos de la vegetación en función de la escala espacial del sensor, la estructura vertical del arbolado se refiere a parámetros relacionados con la altura de la vegetación y la fracción de copa, además de la defoliación, que interactúan en la señal puntual que recibe el sensor en las diferentes longitudes de onda. En el caso de la vegetación, además resulta un parámetro clave, utilizado como herramienta de diagnóstico, en muchos de los procesos de decaimiento forestal estudiados en la actualidad. Para incluir estos parámetros en los modelos de análisis espacial que integran SIG y teledetección, existen actualmente dos aproximaciones diferentes. Una de ellas es la que usa la modelización de los parámetros de estructura de vegetación a través de modelos de transferencia radiativa (MTR). Dichos modelos simulan la firma espectral teórica de una hoja, una copa o un dosel, en función de características propias de la especie y otras del entorno, moduladas por parámetros obtenidos en los muestreos de campo, como índices de área foliar (LAI) y contenido en pigmentos. La segunda aproximación es la que se apoya en datos LiDAR para integrar en los modelos,

métricas relacionadas con estos parámetros de estructura. El uso combinado de métricas basadas en percentiles de la nube de puntos, junto con los modelos de altura de vegetación, pueden relacionarse con cambios en la densidad de copas de una especie determinada. Por ejemplo, el uso combinado de datos LiDAR junto con imágenes de alta resolución espacial de WorldView ha sido utilizado como herramienta en el análisis espacial de patrones de defoliación en dehesa de encina, con buenos resultados (Navarro-Cerrillo et al., 2019).

El acceso a estas herramientas de análisis y modelización es cada vez más común, y se plantea como una alternativa viable en el seguimiento de grandes repoblaciones y reforestaciones que, por su homogeneidad, facilitan en gran medida la obtención de rasgos de la vegetación relacionados con el estado fitosanitario, como la defoliación.

6 Hipótesis, objetivos de la Tesis y estructura

6.1 Hipótesis

La sostenibilidad de las dehesas y bosques de *Quercus* en el sur de la Península Ibérica se está viendo comprometida por la interacción de multitud de factores bióticos y abióticos, entre los que se encuentran las alteraciones climáticas y la dispersión y afección de plagas y enfermedades que generan un debilitamiento progresivo del arbolado, con un aumento en los niveles de defoliación del arbolado, y que, en muchas ocasiones, acaba provocando su muerte. En consecuencia, estos ecosistemas están experimentando un retroceso tanto en las densidades del arbolado como en su extensión. En este declive o decaimiento forestal de los *Quercus*, participa el oomiceto invasor *Phytophthora cinnamomi*, uno de los patógenos forestales más relevantes a escala mundial, por la cantidad de plantas huésped a la que afecta y los síntomas asociados a su presencia, que desencadenan frecuentemente la pérdida del arbolado.

La hipótesis general de esta Tesis es que el comportamiento biológico, la distribución espaciotemporal y el impacto de este patógeno en los ecosistemas de dehesas y bosques de *Quercus* mediterráneos, se puede ver influenciado tanto por la heterogeneidad de los factores abióticos presentes en el medio (características fisicoquímicas del suelo, topografía del terreno y climatología) como por los factores bióticos (microbiota del suelo, vegetación, estructura

del arbolado y su sistema radical) con los que interacciona en el complejo patógeno-huésped-ambiente. El estudio de estas interacciones aumentaría el conocimiento existente sobre el síndrome del decaimiento de los *Quercus*, a diferentes escalas espaciales (árbol, rodal y región) sobre diferentes estructuras de arbolado (de repoblación y de dehesa-bosque) y sobre especies distintas (encina y alcornoque). Los trabajos incluidos en esta tesis doctoral pretenden comprender mejor a este organismo patógeno y su interacción con el medio, con la intención de generar datos objetivos y modelos que permitan llevar a cabo estrategias de gestión integral precisas, que mitiguen la dispersión y el impacto del decaimiento en estos ecosistemas singulares y de alto valor ecológico.

6.2 Objetivos de la Tesis Doctoral

El ***objetivo general*** de esta Tesis Doctoral ha sido estudiar los patrones de distribución espacial y temporal en repoblaciones, dehesas y bosques de *Quercus* spp. en Andalucía, a diferentes escalas (árbol, rodal y región), de los oomicetos patógenos no nativos de podredumbre radical (*Phytophthora* spp. y *Pythium* spp.), condicionados por los patrones espaciotemporales de los factores bióticos y abióticos presentes en el medio con los que cohabitan, así como en la repercusión que dicha interacción ambiente-patógeno presenta sobre el nivel de defoliación de las copas y la mortalidad del arbolado.

Los cuatro ***objetivos específicos*** que desarrollan el objetivo global de la Tesis se presentan a continuación:

1. ¿Cómo influyen las propiedades fisicoquímicas del suelo en la abundancia y en el patrón de distribución espacial de *Phytophthora cinnamomi*, a nivel de microescala bajo el efecto individual de la proyección de copa de encinas de repoblación?

2. ¿Cuáles son los patrones de distribución espaciotemporal en el suelo de *Phytophthora cinnamomi* en una repoblación de encinas y alcornoques a escala de rodal y su relación con el nivel de defoliación y de mortalidad del arbolado, en respuesta a la interacción con las características fisicoquímicas de la rizosfera y la topografía del terreno?

3. ¿Qué factores bióticos y abióticos influyen en las dinámicas de variación espaciotemporal del porcentaje de defoliación y de la mortalidad del arbolado, en relación con la presencia de oomicetos de podredumbre radical en el suelo de las dehesas y bosques de *Quercus* spp, utilizando como

herramienta la Red Andaluza de Parcelas de Seguimiento de Daños (Red SEDA, ICP Forest Nivel I) a escala regional?

4. ¿Es posible cartografiar los patrones de daños, expresados en porcentaje de defoliación, mediante el uso de datos LiDAR y sensores multiespectrales de alta resolución espacial (World-View 2) en plantaciones de *Quercus* spp., a escala de árbol individual?

6.3 Estructura del documento de Tesis

Para cubrir los objetivos planteados en esta Tesis se plantearon diferentes aproximaciones metodológicas, que abordaron el análisis de las interacciones descritas en la hipótesis desde una escala experimental de planta individual hasta una escala de parcela-rodal y región, y planteando otras aproximaciones de parametrización espacial basadas en la modelización estadística, los SIG y la teledetección. El presente documento de memoria de Tesis Doctoral muestra el contexto de los trabajos realizados y los resultados obtenidos, estructurados en 7 capítulos que se describen a continuación:

El **Capítulo 1**, se presenta como una introducción general a la situación actual fitosanitaria que atraviesan las repoblaciones forestales, las dehesas y los bosques de *Quercus* spp. en Andalucía, así como los principales factores bióticos y abióticos que influyen en el decaimiento forestal, incidiendo en el agente patógeno no nativo *Phytophthora cinnamomi*, causante de la podredumbre radical de estas especies arbóreas y los factores que condicionan el comportamiento y distribución espacial de estos oomicetos en el suelo. Se aborda también la heterogeneidad espaciotemporal de dichos factores y las herramientas geoestadísticas empleadas para su análisis.

En el **Capítulo 2**, se analiza la influencia de la heterogeneidad de las propiedades físicas y químicas del suelo, la humedad edáfica y el efecto de la proyección de la copa a escala de árbol individual, sobre la distribución espacial de *P. cinnamomi* en la rizosfera. Para ello se recogieron 33 muestras de suelo por árbol en una cuadrícula de 4 x 4 m, bajo la copa de las encinas, se cuantificaron las unidades formadoras de colonias (ufc) del patógeno y se estudiaron 11 variables de suelo. Los datos se analizaron mediante modelos lineales mixtos y sus patrones espaciales mediante índices de distancia (SADIE). Los resultados de este trabajo se publicaron en la revista científica *Forests* (ISSN 1999-4907; Q1 "Forestry").

En el **Capítulo 3**, se estudian los procesos de interacción patógeno-huésped-ambiente, entre 2010 y 2018, en una repoblación de encinas y alcornoques con presencia de *P. cinnamomi* en el suelo, mediante el análisis de los patrones de distribución espacial de los factores bióticos y abióticos del medio, la abundancia de oomicetos en suelo y su influencia sobre el estado de salud del arbolado. Para ello se recolectaron al inicio del estudio, en dos parcelas de alcornoque y dos de encina, un total de 98 muestras de suelo analizando sus propiedades fisicoquímicas, la humedad edáfica y la carga de "ufc" de patógenos de podredumbre radical, se describió la topografía del terreno mediante el modelo de elevaciones, la hidrografía de las parcelas a nivel de microcuencas y la incidencia de la radiación solar. Así mismo, se caracterizó el estado silvícola de la repoblación (diámetros y alturas) y el estado fitosanitario (defoliación de copas y mortalidad, en 2018). Los datos se procesaron mediante análisis espacial por índices de distancia (SADIE) y a través de sistemas de ecuaciones estructurales (SEM).

En el **Capítulo 4**, se modelizó la influencia de los factores ambientales bióticos y abióticos (edáficos, topográficos y climáticos), en relación con la presencia de oomicetos de podredumbre radical (*Phytophthora* spp.), en dehesas de *Quercus* spp. de Andalucía, sobre la dinámica espaciotemporal del estado fitosanitario del arbolado, estimado a partir de datos de defoliación y mortalidad de 3635 árboles (principalmente, encinas y alcornoques) monitorizados en 152 parcelas de la Red Andaluza de Seguimiento de Daños sobre Ecosistemas Forestales (ICP Nivel I), durante el periodo 2001-2016. Para dicho estudio, se usaron técnicas de estimación de supervivencia de Kaplan-Meier, la evolución espaciotemporal de la defoliación y la mortalidad mediante Kernel Density Estimation y los modelos mixtos generalizados. Los resultados de este trabajo se publicaron en la revista científica *Forest Ecology and Management* (ISSN 0378-1127; Q1 "Forestry").

En el **Capítulo 5**, se evalúa la integración de datos LiDAR de alta densidad (12 puntos m^{-2}) e imágenes multiespectrales de alta resolución (sensor WorldView-2, 2 m, resolución espacial) para cartografiar los daños asociados a patógenos no nativos de podredumbre radical (*Phytophthora* spp.), en plantaciones de *Quercus ilex* y *Q. suber* a escala de árbol individual. El estudio utilizó información sobre la defoliación de 429 árboles, y un proceso de segmentación de árbol individual basado en información LiDAR, a partir de la cual se obtuvieron las métricas LiDAR y los valores de 18 índices de vegetación basados en bandas espectrales. El conjunto de variables se usó en

un modelo no paramétrico para la estimación de la defoliación. Finalmente, se invirtió el modelo para generar una cartografía de defoliación a escala de árbol individual.

El **Capítulo 6**, constituye una síntesis de los trabajos anteriores relacionándose entre ellos mediante la discusión general. Se abordan también las principales limitaciones encontradas en la investigación de los trabajos, y se plantean las vías de progreso y de trabajos futuros que complementen estos estudios para la mejora progresiva de estrategias de gestión adaptativa frente al decaimiento forestal y a los impactos del cambio climático en los ecosistemas mediterráneos de dehesas y bosques de *Quercus* en la Península Ibérica.

En el **Capítulo 7**, finalmente se expone la relación de las conclusiones generales derivadas de los resultados y de las investigaciones de esta Tesis Doctoral.

A continuación, se muestra a modo de síntesis en la Tabla 3, un esquema general descriptivo que contextualiza los cuatro capítulos centrales (Capítulos 2-5) de la investigación de esta Tesis Doctoral.

Tabla 3. Esquema general descriptivo de los Capítulos 2, 3, 4 y 5 de la Tesis Doctoral.

	Capítulo 2	**Capítulo 3**	**Capítulo 4**	**Capítulo 5**
Escala	Microescala "árbol" (48 m²)	Mesoescala "rodales" (1,24 ha)	Macroescala "región" (29.238 km²)	Mesoescala "forestación" (4,9 km²)
Árboles	4	359	3366	475
Especies	(1) *Q.i*	(2) *Q.i*	(4) *Q.i, Q.s, Q.f, Q.c*	(2) *Q.i, Q.s*
Parcelas	4 (4x4 m)	2 (≈80x80 m)	152 (Ø=100 m)	2 (≈80x80 m)
Estado forestal	Forestación	Forestación	Natural (dehesa/bosque)	Forestación
Evaluación (año)	Puntual (2008)	Temporal (2008-2018)	Temporal (2000-2016)	Fija (2018)
Variables de estudio	ufc Edáficas	ufc Edáficas Topográficas Dasométricas Defoliación	*P. cinnamomi* Edáficas Topográficas Climáticas Dasométricas Defoliación	ufc Dasométricas Defoliación LiDAR WV2
Muestras de suelo	132 (33 pie)	98 (49 parcela)	Indeterminado	---
Métodos de análisis	SADIE GLMM	SADIE SEM	K-M; KDE; GLMM	ML (RF; NN)

Q.i.: *Quercus ilex*; ***Q.s***.: Q. *suber*; ***Q.f***.: *Q. faginea*; ***Q.c***.: *Q. coccifera;* **ufc**: Unidades formadoras de colonias; ***P. cinnamomi***: *Phytophthora cinnamomi* (ausencia / presencia); **LIDAR**: Light Detection and Ranging; **WV2**: WorldView-2; **SADIE**: Spatial Analysis by Distance Indices; **GLMM**: Generalized Linear Mixed Model; **SEM**: Structural Equation Modeling; **K-M**: Kaplan-Meier (curvas de supervivencia); **KDE**: Kernel Density Estimation; **ML**: Machine learning; **RF**: Random Forest; **NN**: Neural Network.

7 Referencias

Acácio, V., Dias, F.S., Catry, F.X., Bugalho, M.N., Moreira, F., 2021. Canopy Cover Loss of Mediterranean Oak Woodlands: Long-term Effects of Management and Climate. Ecosystems. https://doi.org/10.1007/s10021-021-00617-9

Alejano Monge, R., Domingo Santos, J.M., Fernández Martínez, M., 2011. Manual para la gestión sostenible de las dehesas andaluzas, Foro para la defensa y conservación de la dehesa "ENCINAL" y la Universidad de Huelva. ed. Huelva, España.

Andivia, E., Fernández, M., Alejano, R., Vázquez-Piqué, J., 2015. Tree patch distribution drives spatial heterogeneity of soil traits in cork oak woodlands. Ann. For. Sci. 72, 549–559. https://doi.org/10.1007/s13595-015-0475-8

Balla, A., Silini, A., Cherif-Silini, H., Chenari Bouket, A., Moser, W.K., Nowakowska, J.A., Oszako, T., Benia, F., Belbahri, L., 2021. The Threat of Pests and Pathogens and the Potential for Biological Control in Forest Ecosystems. Forests 12, 1579. https://doi.org/10.3390/f12111579

Bell, E.D., 1998. Spatio-temporal dynamics of uk moths (Ph.D.). Ann Arbor, United States.

Bergot, M., Cloppet, E., Pérarnaud, V., Déqué, M., Marçais, B., Desprez-Loustau, M.-L., 2004. Simulation of potential range expansion of oak disease caused by *Phytophthora cinnamomi* under climate change. Glob. Change Biol. 10, 1539–1552. https://doi.org/10.1111/j.1365-2486.2004.00824.x

Bertomeu García, M., Torres, M., Pulido, F.J., Moreno Marcos, G., Giménez Fernández, J.C., 2019. Agroforestación: una alternativa a la forestación de tierras agrarias para la domesticación del paisaje rural. Cuad. Soc. Esp. Cienc. For. 133–148.

Brasier, C.M., 1996. *Phytophthora cinnamomi* and oak decline in southern Europe. Environmental constraints including climate change. Ann. Sci. For. 53, 347–358. https://doi.org/10.1051/forest:19960217

Brasier, C.M., 1992. Oak tree mortality in Iberia. Nature 360, 539.

Brasier, C.M., Robredo, F., Ferraz, J.F.P., 1993. Evidence for *Phytophthora cinnamomi* involvement in Iberian oak decline. Plant Pathol. 42, 140–145. https://doi.org/10.1111/j.1365-3059.1993.tb01482.x

Burgess, T.I., Scott, J.K., Mcdougall, K.L., Stukely, M.J.C., Crane, C., Dunstan, W.A., Brigg, F., Andjic, V., White, D., Rudman, T., Arentz, F., Ota, N., Hardy, G.E.S.J., 2017. Current and projected global distribution of *Phytophthora cinnamomi*, one of the world's worst plant pathogens. Glob. Change Biol. 23, 1661–1674. https://doi.org/10.1111/gcb.13492

Burgess, T.M., Webster, R., 1980. Optimal Interpolation and Isarithmic Mapping of Soil Properties: I The semi-variogram and punctual kriging. J. Soil Sci. 31, 315–331. https://doi.org/10.1111/j.1365-2389.1980.tb02084.x

Burnham, K.P., Anderson, D.R., 2002. Model Selection and Multimodel Inference: A Practical Information-Theoretic Approach., 2nd ed. ed. Springer-Verlag New York, Fort Collins, Colorado, USA.

Caetano, P., Ávila, A., Sánchez, M.E., Trapero, A., Coelho, A.C., 2009. *Phytophthora cinnamomi* populations on *Quercus* forests from Spain and Portugal, in: Phytophthoras in Forests and Natural Ecosystems. USDA Forest Service General Technical Report PSW-GTR-221, Albany, CA, pp. 261–269.

Cardillo, E., Abad, E., Meyer, S., 2021. Iberian oak decline caused by *Phytophthora cinnamomi*: A spatiotemporal analysis incorporating the effect of host heterogeneities at landscape scale. For. Pathol. 51, e12667. https://doi.org/10.1111/efp.12667

Cardillo, E., Acedo, A., Abad, E., 2018. Topographic effects on dispersal patterns of *Phytophthora cinnamomi* at a stand scale in a Spanish heathland. PLoS ONE 13. https://doi.org/10.1371/journal.pone.0195060

Carrasco Gotarredona, Á., Fernández Cancio, Á., Trapero Casas, A., López Pantoja, G., Sánchez Osorio, I., Ruiz Navarro, J.M., Jiménez Molina, J.J., Domínguez Nevado, L., Romero Martín, M. de los Á., Carbonero Muñoz, M.D., Sánchez Hernández, M.E., Lucas Caetano, P.C., Gil Hernández, P., Fernández Rebollo, P., Navarro Cerrillo, R.M., Sánchez de la Cuesta, R., Raposo Llobet, R., Rodríguez Reviriego, S., 2009. Procesos de Decaimiento Forestal (la Seca): Situación del Conocimiento, 1ª edición. ed. Consejería de Medio Ambiente, Córdoba, España.

Consejería de Medio Ambiente y Ordenación del Territorio, 2018. Manual para el establecimiento y la evaluación de las parcelas de la Red Andaluza de Seguimiento de Daños sobre Ecosistemas Forestales: Red SEDA y Red de PINSAPO. Junta de Andalucía.

Corcobado, T., Vivas, M., Moreno, G., Solla, A., 2014. Ectomycorrhizal symbiosis in declining and non-declining *Quercus ilex* trees infected with or free of *Phytophthora cinnamomi*. For. Ecol. Manag. 324, 72–80. https://doi.org/10.1016/j.foreco.2014.03.040

Costa, J.C., Martín, Á., Fernández, R., Estirado, M., 2006. Dehesas de Andalucía: caracterización ambiental. Consejería de Medio Ambiente, Junta de Andalucía, Sevilla, Spain.

Covelo, F., Rodríguez, A., Gallardo, A., 2008. Spatial pattern and scale of leaf N and P resorption efficiency and proficiency in a *Quercus robur* population. Plant Soil 311, 109–119. https://doi.org/10.1007/s11104-008-9662-9

Crone, M., McComb, J.A., O'Brien, P.A., Hardy, G.E.S.J., 2013a. Survival of *Phytophthora cinnamomi* as oospores, stromata, and thick-walled chlamydospores in roots of symptomatic and asymptomatic annual and herbaceous perennial plant species. Fungal Biol. 117, 112–123. https://doi.org/10.1016/j.funbio.2012.12.004

Crone, M., McComb, J.A., O'Brien, P.A., Hardy, G.E.S.J., 2013b. Annual and herbaceous perennial native Australian plant species are symptomless hosts of *Phytophthora cinnamomi* in the *Eucalyptus marginata* (jarrah) forest of Western Australia. Plant Pathol. 62, 1057–1062. https://doi.org/10.1111/ppa.12016

Cuenca, C., Melero, M., Cortina, J., 2016. Análisis de las políticas de restauración forestal en España (1983-2013). https://doi.org/10.31167/csef.v0i42.17423

Dale, M.R.T., Fortin, M.-J., 2014. Spatial Analysis: A Guide For Ecologists. Cambridge University Press.

de Andrade Lourenço, D., Branco, I., Choupina, A., 2020. Phytopathogenic oomycetes: a review focusing on *Phytophthora cinnamomi* and biotechnological approaches. Mol. Biol. Rep. 47, 9179–9188. https://doi.org/10.1007/s11033-020-05911-8

Dell, B., Hardy, G.E.S.J., Vear, K., 2005. History of *Phytophthora cinnamomi* management in Western Australia, in: Calver, M.C., Bigler-Cole, H., Bolton, G., Dargavel, J., Gaynor, A., Horwitz, P., Mills, J., Wardell-Johnston, G. (Eds.), A Forest Conscienceness: Proceedings 6th National Conference of the Australian Forest History Society. Millpress Science Publishers, Rotterdam, pp. 391–406.

Díaz, M., Pulido, F.J., 2009. 6310 Dehesas perennifolias de *Quercus* spp., in: VV.AA., Bases ecológicas preliminares para la conservación de los tipos de hábitat de interés comunitario en España. Ministerio de Medio Ambiente, y Medio Rural y Marino, Madrid, p. 69.

Dungan, J.L., Perry, J.N., Dale, M.R.T., Legendre, P., Citron-Pousty, S., Fortin, M.-J., Jakomulska, A., Miriti, M., Rosenberg, M.S., 2002. A balanced view of scale in spatial statistical analysis. Ecography 25, 626–640. https://doi.org/10.1034/j.1600-0587.2002.250510.x

Duque-Lazo, J., Navarro-Cerrillo, R.M., Ruíz-Gómez, F.J., 2018a. Assessment of the future stability of cork oak (*Quercus suber* L.) afforestation under climate change scenarios in Southwest Spain. For. Ecol. Manag. 409, 444–456. https://doi.org/10.1016/j.foreco.2017.11.042

Duque-Lazo, J., Navarro-Cerrillo, R.M., van Gils, H., Groen, T.A., 2018b. Forecasting oak decline caused by *Phytophthora cinnamomi* in Andalusia: Identification of priority areas for intervention. For. Ecol. Manag. 417, 122–136.

https://doi.org/10.1016/j.foreco.2018.02.045

Erwin, D.C., Ribeiro, O.K., 1996. *Phytophthora* diseases worldwide. American Phytopathological Society (APS Press).

Fernández Carrillo, M.A., Belmonte Serrato, F., Romero Díaz, M.A., Robledano Aymerich, F., 2016. La forestación de tierras agrarias en la Región de Murcia a través de los Programas de Desarrollo Rural en España: una medida con impacto medioambiental positivo en el medio rural, in: Crisis, globalización y desequilibrios sociales y territoriales en España [Recurso electrónico]: Aportación Española al 33º Congreso de Beijing: Comité Español de la Unión Geográfica Internacional. Centro Nacional de Información Geográfica, pp. 32–42.

Fernández-Habas, J., Fernández-Rebollo, P., Casado, M.R., García Moreno, A.M., Abellanas, B., 2019. Spatio-temporal analysis of oak decline process in open woodlands: A case study in SW Spain. J. Environ. Manage. 248, 109308. https://doi.org/10.1016/j.jenvman.2019.109308

Galiano, L., Martínez-Vilalta, J., Sabaté, S., Lloret, F., 2012. Determinants of drought effects on crown condition and their relationship with depletion of carbon reserves in a Mediterranean holm oak forest. Tree Physiol. 32, 478–489. https://doi.org/10.1093/treephys/tps025

Gallardo, A., 2003. Effect of tree canopy on the spatial distribution of soil nutrients in a Mediterranean Dehesa. Pedobiologia 47, 117–125. https://doi.org/10.1078/0031-4056-00175

Gallardo, A., Covelo, F., 2005. Spatial pattern and scale of leaf N and P concentration in a *Quercus robur* population. Plant Soil 273, 269–277. https://doi.org/10.1007/s11104-004-7943-5

Gallardo, A., Rodríguez-Saucedo, J.J., Covelo, F., Fernández-Alés, R., 2000. Soil nitrogen heterogeneity in a Dehesa ecosystem. Plant Soil 222, 71–82. https://doi.org/10.1023/A:1004725927358

Galluzzi, M., Rocchini, D., Canullo, R., McRoberts, R.E., Chirici, G., 2018. Mapping uncertainty of ICP-Forest biodiversity data: From standard treatment of diffusion to density-equalizing cartograms. Ecol. Inform. 48, 281–289. https://doi.org/10.1016/j.ecoinf.2018.06.005

García, D., 2006. La escala y su importancia en el análisis espacial. Ecosistemas 15.

García-Núñez, H.G., Martínez-Campos, Á.R., Hermosa-Prieto, M.R., Monte-Vázquez, E., Aguilar-Ortigoza, C.J., González-Esquivel, C.E., García-Núñez, H.G., Martínez-Campos, Á.R., Hermosa-Prieto, M.R., Monte-Vázquez, E., Aguilar-Ortigoza, C.J., González-Esquivel, C.E., 2017. Caracterización morfológica y molecular de cepas nativas de *Trichoderma* y su potencial de biocontrol sobre *Phytophthora infestans*. Rev. Mex. Fitopatol. 35, 58–79. https://doi.org/10.18781/r.mex.fit.1605-4

Gea-Izquierdo, G., Natalini, F., Cardillo, E., 2020. Holm oak death is accelerated but not sudden and expresses drought legacies. Sci. Total Environ. 141793. https://doi.org/10.1016/j.scitotenv.2020.141793

Gerhards, M., Schlerf, M., Mallick, K., Udelhoven, T., 2019. Challenges and Future Perspectives of Multi-/Hyperspectral Thermal Infrared Remote Sensing for Crop Water-Stress Detection: A Review. Remote Sens. 11, 1240. https://doi.org/10.3390/rs11101240

Gimeno, T.E., Pías, B., Lemos-Filho, J.P., Valladares, F., 2009. Plasticity and stress tolerance override local adaptation in the responses of Mediterranean holm oak seedlings to drought and cold. Tree Physiol. 29, 87–98. https://doi.org/10.1093/treephys/tpn007

Gómez-Aparicio, L., Domínguez-Begines, J., Kardol, P., Ávila, J.M., Ibáñez, B., García, L.V., 2017. Plant-soil feedbacks in declining forests: implications for species coexistence. Ecology 98, 1908–1921. https://doi.org/10.1002/ecy.1864

Gómez-Aparicio, L., Ibáñez, B., Serrano, M.S., De Vita, P., Ávila, J.M., Pérez-Ramos, I.M., García, L.V., Esperanza Sánchez, M., Marañón, T., 2012. Spatial patterns of soil pathogens in

declining Mediterranean forests: implications for tree species regeneration. New Phytol. 194, 1014–1024. https://doi.org/10.1111/j.1469-8137.2012.04108.x

Gómez-Giráldez, P.J., Aguilar, C., Caño, A.B., García-Moreno, A., González-Dugo, M.P., 2019. Remote sensing estimation of net primary production as monitoring indicator of holm oak savanna management. Ecol. Indic. 106, 105526. https://doi.org/10.1016/j.ecolind.2019.105526

Hardham, A.R., 2005. *Phytophthora cinnamomi*. Mol. Plant Pathol. 6, 589–604. https://doi.org/10.1111/j.1364-3703.2005.00308.x

Jiménez-Chacón, A., Homet, P., Matías, L., Gómez-Aparicio, L., Godoy, O., 2018. Fine Scale Determinants of Soil Litter Fauna on a Mediterranean Mixed Oak Forest Invaded by the Exotic Soil-Borne Pathogen *Phytophthora cinnamomi*. Forests 9, 218. https://doi.org/10.3390/f9040218

Jönsson, U., 2006. A conceptual model for the development of *Phytophthora* disease in *Quercus robur*. New Phytol. 171, 55–68. https://doi.org/10.1111/j.1469-8137.2006.01743.x

Jung, T., Blaschke, H., Oßwald, W., 2000. Involvement of soilborne *Phytophthora* species in Central European oak decline and the effect of site factors on the disease. Plant Pathol. 49, 706–718. https://doi.org/10.1046/j.1365-3059.2000.00521.x

Jung, T., Colquhoun, I.J., Hardy, G.E.S.J., 2013. New insights into the survival strategy of the invasive soilborne pathogen *Phytophthora cinnamomi* in different natural ecosystems in Western Australia. For. Pathol. 43, 266–288. https://doi.org/10.1111/efp.12025

Jung, T., Orlikowski, L., Henricot, B., Abad-Campos, P., Aday, A.G., Casal, O.A., Bakonyi, J., Cacciola, S.O., Cech, T., Chavarriaga, D., Corcobado, T., Cravador, A., Decourcelle, T., Denton, G., Diamandis, S., Doğmuş-Lehtijärvi, H.T., Franceschini, A., Ginetti, B., Green, S., Glavendekić, M., Hantula, J., Hartmann, G., Herrero, M., Ivic, D., Jung, M.H., Lilja, A., Keca, N., Kramarets, V., Lyubenova, A., Machado, H., Lio, G.M. di S., Vázquez, P.J.M., Marçais, B., Matsiakh, I., Milenkovic, I., Moricca, S., Nagy, Z.Á., Nechwatal, J., Olsson, C., Oszako, T., Pane, A., Paplomatas, E.J., Varela, C.P., Prospero, S., Martínez, C.R., Rigling, D., Robin, C., Rytkönen, A., Sánchez, M.E., Ros, A.V.S., Scanu, B., Schlenzig, A., Schumacher, J., Slavov, S., Solla, A., Sousa, E., Stenlid, J., Talgø, V., Tomic, Z., Tsopelas, P., Vannini, A., Vettraino, A.M., Wenneker, M., Woodward, S., Peréz-Sierra, A., 2016. Widespread *Phytophthora* infestations in European nurseries put forest, semi-natural and horticultural ecosystems at high risk of *Phytophthora* diseases. For. Pathol. 46, 134–163. https://doi.org/10.1111/efp.12239

Junta de Andalucía, 2008. Caracterización socioeconómica de la dehesa de Andalucía. Consejería de Agricultura y Pesca, Sevilla, España.

Junta de Andalucía, 1999. Mapa de usos y coberturas vegetales del suelo de Andalucía 1999.

Kelly, M., Meentemeyer, R.K., 2002. Landscape dynamics of the spread of sudden oak death. Photogramm. Eng. Remote Sens. 68, 1001–1010.

Kenchington, E., Murillo, F.J., Lirette, C., Sacau, M., Koen-Alonso, M., Kenny, A., Ollerhead, N., Wareham, V., Beazley, L., 2014. Kernel Density Surface Modelling as a Means to Identify Significant Concentrations of Vulnerable Marine Ecosystem Indicators. PLOS ONE 9, e109365. https://doi.org/10.1371/journal.pone.0109365

Kinal, J., Shearer, B.L., Fairman, R.G., 1993. Dispersal of *Phytophthora cinnamomi* through lateritic soil by laterally flowing subsurface water. Plant Dis. 77, 1085–1090.

Klobučar, D., 2010. Primjena geostatistike u uređivanju šuma. Šumar. List 134, 249–258.

Krige, D.G., 1951. A statistical approach to some basic mine valuation problems on the Witwatersrand. J. South. Afr. Inst. Min. Metall. 52, 119–139. https://doi.org/10.10520/AJA0038223X_4792

Krull, C.R., Waipara, N.W., Choquenot, D., Burns, B.R., Gormley, A.M., Stanley, M.C., 2013. Absence of evidence is not evidence of absence: Feral pigs as vectors of soil-borne pathogens. Austral Ecol. 38, 534–542. https://doi.org/10.1111/j.1442-9993.2012.02444.x

La Porta, N., Capretti, P., Thomsen, I.M., Kasanen, R., Hietala, A.M., Von Weissenberg, K., 2008. Forest pathogens with higher damage potential due to climate change in Europe. Can. J. Plant Pathol. 30, 177–195. https://doi.org/10.1080/07060661.2008.10540534

Lorenz, M., 1995. International Co-operative Programme on Assessment and Monitoring of Air Pollution Effects on Forests-ICP Forests-. Water. Air. Soil Pollut. 85, 1221–1226. https://doi.org/10.1007/BF00477148

Maestre, F.T., 2006. Análisis y modelización de datos espacialmente explícitos en Ecología. Ecosistemas 15.

Maestre, F.T., Escudero, A., Bonet, A., 2008. Introducción al análisis espacial de datos en ecología y ciencias ambientales: métodos y aplicaciones, Universidad Rey Juan Carlos. ed. Dykinson, S.L., Madrid.

Maurel, M., Robin, C., Capron, G., Desprez-Loustau, M.-L., 2001. Effects of root damage associated with *Phytophthora cinnamomi* on water relations, biomass accumulation, mineral nutrition and vulnerability to water deficit of five oak and chestnut species. For. Pathol. 31, 353–369. https://doi.org/10.1046/j.1439-0329.2001.00258.x

Meentemeyer, R.K., Haas, S.E., Václavík, T., 2012. Landscape Epidemiology of Emerging Infectious Diseases in Natural and Human-Altered Ecosystems. Annu. Rev. Phytopathol. 50, 379–402. https://doi.org/10.1146/annurev-phyto-081211-172938

Milne, B.T., 1991. Heterogeneity as a Multiscale Characteristic of Landscapes, in: Kolasa, J., Pickett, S.T.A. (Eds.), Ecological Heterogeneity, Ecological Studies. Springer, New York, NY, pp. 69–84. https://doi.org/10.1007/978-1-4612-3062-5_4

Montiel Molina, C., Galiana Martín, L., 2004. La restauración de paisajes forestales a través de la forestación de tierras agrarias. Cuad. Soc. Esp. Cienc. For. 193–198.

Morales-Rodríguez, C., Bastianelli, G., Aleandri, M., Chilosi, G., Vannini, A., 2018. Application of *Trichoderma* spp. Complex and Biofumigation to Control Damping-Off of *Pinus radiata* D. Don Caused by *Fusarium circinatum* Nirenberg and O'Donnell. Forests 9, 421. https://doi.org/10.3390/f9070421

Moreira, A.C., Martins, J.M.S., 2005. Influence of site factors on the impact of *Phytophthora cinnamomi* in cork oak stands in Portugal. For. Pathol. 35, 145–162. https://doi.org/10.1111/j.1439-0329.2005.00397.x

Morris, S.J., 1999. Spatial distribution of fungal and bacterial biomass in southern Ohio hardwood forest soils: fine scale variability and microscale patterns. Soil Biol. Biochem. 31, 1375–1386. https://doi.org/10.1016/S0038-0717(99)00047-4

Navarro Cerrillo, R.M., Fernández Rebollo, P., Trapero, A., Caetano, P., Romero, M.A., Sánchez, M.E., Fernández Cancio, A., Sánchez, I., López Pantoja, G., 2004. Los procesos de decaimiento de encinas y alcornoques. Dirección General de Gestión del Medio Natural. Consejería de Medio Ambiente. Junta de Andalucía., Sevilla.

Navarro Cerrillo, R.M., Pemán García, J., del Campo García, A.D., Moreno Sánchez, J., Lara Gómez, M.A., Díaz Hernández, J.L., Pousa Salvador, F., Piñón Castillo, F.M., 2009. Manual de especies para la forestación de tierras agrarias en Andalucía. Junta de Andalucía. Consejería de Agricultura y Pesca, Sevilla (Spain).

Navarro-Cerrillo, R.M., Fernandez Rebollo, P., Ruiz Navarro, J.M., 2000. Manual de campo para establecimiento de los puntos de la Red Andaluza de Daños sobre ecosistemas forestales en Andalucía.

Navarro-Cerrillo, R.M., Ruiz-Gómez, F.J., 2020. Seguimiento de plagas y enfermedades forestales en Andalucía: interpretación a diferentes escalas. Cuad. Soc. Esp. Cienc. For. 46, 33–56. https://doi.org/10.31167/csecfv0i46.19902

Navarro-Cerrillo, R.M., Varo-Martínez, M.Á., Acosta, C., Palacios Rodriguez, G., Sánchez-Cuesta, R., Ruiz Gómez, F.J., 2019. Integration of WorldView-2 and airborne laser scanning data to classify defoliation levels in *Quercus ilex* L. Dehesas affected by root rot mortality: Management implications. For. Ecol. Manag. 451, 117564. https://doi.org/10.1016/j.foreco.2019.117564

Olea, L., López-Bellido, R.J., Poblaciones, M.J., 2005. European types of silvopastoral systems in the Mediterranean area: dehesa. Silvopastoralism Sustain. Land Manag. Proc. Int. Congr. Silvopastoralism Sustain. Manag. Held Lugo Spain April 2004 30–35.

Parr, T.W., Ferretti, M., Simpson, I.C., Forsius, M., Kovács-Láng, E., 2002. Towards A Long-Term Integrated Monitoring Programme In Europe: Network Design in Theory and Practice. Environ. Monit. Assess. 78, 253–290. https://doi.org/10.1023/A:1019934919140

Pennanen, T., Liski, J., Bååth, E., Kitunen, V., Uotila, J., Westman, C.J., Fritze, H., 1999. Structure of the Microbial Communities in Coniferous Forest Soils in Relation to Site Fertility and Stand Development Stage. Microb. Ecol. 38, 168–179. https://doi.org/10.1007/s002489900161

Pereira, H.M., Navarro, L.M., 2015. Rewilding european landscapes. Springer Nature.

Perry, J. n., Winder, L., Holland, J. m., Alston, R. d., 1999. Red–blue plots for detecting clusters in count data. Ecol. Lett. 2, 106–113. https://doi.org/10.1046/j.1461-0248.1999.22057.x

Perry, J.N., 1998. Measures of Spatial Pattern for Counts. Ecology 79, 1008–1017. https://doi.org/10.1890/0012-9658(1998)079[1008:MOSPFC]2.0.CO;2

Perry, J.N., 1995. Spatial Analysis by Distance Indices. J. Anim. Ecol. 64, 303–314. https://doi.org/10.2307/5892

Perry, J.N., Bell, E.D., Smith, R.H., Woiwod, I.P., 1996. SADIE: software to measure and model spatial pattern. Asp. Appl. Biol. 46, 95–102.

Perry, J.N., Hewitt, M., 1991. A New Index of Aggregation for Animal Counts. Biometrics 47, 1505–1518. https://doi.org/10.2307/2532402

Philip, G.M., Watson, D.F., 1982. A precise method for determining contoured surfaces. APPEA J. 22, 205–212. https://doi.org/10.1071/aj81016

Pinto-Correia, T., Ribeiro, N., Sá-Sousa, P., 2011. Introducing the montado, the cork and holm oak agroforestry system of Southern Portugal. Agrofor. Syst. 82, 99. https://doi.org/10.1007/s10457-011-9388-1

Qiao, P., Li, P., Cheng, Y., Wei, W., Yang, S., Lei, M., Chen, T., 2019. Comparison of common spatial interpolation methods for analyzing pollutant spatial distributions at contaminated sites. Environ. Geochem. Health 41, 2709–2730. https://doi.org/10.1007/s10653-019-00328-0

Quero, J.L., 2006. SADIE como herramienta de cuantificación de la heterogeneidad espacial: casos prácticos en el Parque Nacional de Sierra Nevada (Granada, España). Ecosistemas 15.

Reque, J.A., Pérez, R.A., 2011. Del monte al rodal. Manual SIG de inventario forestal. Valladolid (Spain) Univ. de Valladolid.

Rey Benayas, J.M., Martínez-Baroja, L., Pérez-Camacho, L., Villar-Salvador, P., Holl, K.D., 2015. Predation and aridity slow down the spread of 21-year-old planted woodland islets in restored Mediterranean farmland. New For. 46, 841–853. https://doi.org/10.1007/s11056-015-9490-8

Ristaino, J.B., Gumpertz, M.L., 2000. New Frontiers in the Study of Dispersal and Spatial Analysis of Epidemics Caused by Species in the Genus *Phytophthora*. Annu. Rev. Phytopathol. 38, 541–576. https://doi.org/10.1146/annurev.phyto.38.1.541

Robin, C., Capron, G., Desprez-Loustau, M.L., 2001. Root infection by *Phytophthora cinnamomi* in seedlings of three oak species. Plant Pathol. 50, 708–716. https://doi.org/10.1046/j.1365-3059.2001.00643.x

Robin, C., Desprez-Loustau, M.-L., Capron, G., Delatour, C., 1998. First record of *Phytophthora cinnamomi* on cork and holm oaks in France and evidence of pathogenicity. Ann. Sci. For. 55, 869–883. https://doi.org/10.1051/forest:19980801

Rodríguez-Molina, M.C., Blanco-Santos, A., Palo-Núñez, E.J., Torres-Vila, L.M., Torres-Álvarez, E., Suárez-de-la-Cámara, M.A., 2005. Seasonal and spatial mortality patterns of holm oak seedlings in a reforested soil infected with *Phytophthora cinnamomi*. For. Pathol. 35, 411–422. https://doi.org/10.1111/j.1439-0329.2005.00423.x

Ruiz-Gómez, F.J., Miguel-Rojas, C., 2021. Antagonistic Potential of Native *Trichoderma* spp. against *Phytophthora cinnamomi* in the Control of Holm Oak Decline in Dehesas Ecosystems. Forests 12, 945. https://doi.org/10.3390/f12070945

Ruiz-Gómez, F.J., Navarro Cerrillo, R.M., Lara Gómez, M.A., Sánchez-Cuesta, R., 2016. Aislamiento e identificación de oomicetos en focos de podredumbre radical de Andalucía y Extremadura. Cuad. Soc. Esp. Cienc. For. 43, 363–376. https://doi.org/10.31167/csef.v0i42.17489

Ruiz-Gómez, F.J., Navarro-Cerrillo, R.M., Pérez-de-Luque, A., Oβwald, W., Vannini, A., Morales-Rodríguez, C., 2019a. Assessment of functional and structural changes of soil fungal and oomycete communities in holm oak declined dehesas through metabarcoding analysis. Sci. Rep. 9, 5315. https://doi.org/10.1038/s41598-019-41804-y

Ruiz-Gómez, F.J., Navarro-Cerrillo, R.M., Sánchez-Cuesta, R., Pérez-de-Luque, A., 2015. Histopathology of Infection and Colonization of *Quercus ilex* Fine Roots by *Phytophthora cinnamomi*. Plant Pathol. 64, 605–616. https://doi.org/10.1111/ppa.12310

Ruiz-Gómez, F.J., Pérez-de-Luque, A., Navarro-Cerrillo, R.M., 2019b. The Involvement of *Phytophthora* Root Rot and Drought Stress in Holm Oak Decline: from Ecophysiology to Microbiome Influence. Curr. For. Rep. 5, 251–266. https://doi.org/10.1007/s40725-019-00105-3

Ruiz-Gómez, F.J., Pérez-de-Luque, A., Sánchez-Cuesta, R., Quero, J.L., Navarro Cerrillo, R.M., 2018. Differences in the Response to Acute Drought and *Phytophthora cinnamomi* Rands Infection in *Quercus ilex* L. Seedlings. Forests 9, 634. https://doi.org/10.3390/f9100634

San Miguel Ayanz, A., 1994. La dehesa española. Origen, tipología, características y gestión. Fundación Conde del Valle de Salazar, Madrid.

Sánchez, M.E., Andicoberry, S., Trapero, A., 2005. Pathogenicity of three *Phytophthora* spp. causing late seedling rot of *Quercus ilex* ssp. *ballota*. For. Pathol. 35, 115–125. https://doi.org/10.1111/j.1439-0329.2004.00392.x

Sánchez, M.E., Caetano, P., Ferranz, J., Trapero Casas, A., 2000. El decaimiento y muerte de encinas en tres dehesas de la provincia de Huelva. Bol. Sanid. Veg. Plagas 26 4 447-464 2000.

Sánchez, M.E., Caetano, P., Ferraz, J., Trapero, A., 2002. *Phytophthora* disease of *Quercus ilex* in south-western Spain. For. Pathol. 32, 5–18. https://doi.org/10.1046/j.1439-0329.2002.00261.x

Sánchez, M.E., Caetano, P., Romero, M.A., Navarro, R.M., Trapero, A., 2006. *Phytophthora* root rot as the main factor of oak decline in southern Spain, in: Proceedings of the Third International IUFRO Working Party S07.02.09. Presented at the Progress in research on *Phytophthora* diseases of forest trees, Forest Research, Freising (Germany).

Sánchez, M.E., Sánchez Solana, J.E., Navarro Cerrillo, R.M., Fernández Rebollo, P., Trapero Casas, A., 2003. Incidencia de la podredumbre radical causada por *Phytophthora cinnamomi* en masas de *Quercus* en Andalucía. Bol. Sanid. Veg. Plagas 29, 87–108.

Sánchez-Cuesta, R., Navarro-Cerrillo, R.M., Quero, J.L., Ruiz-Gómez, F.J., 2020. Small-Scale Abiotic Factors Influencing the Spatial Distribution of *Phytophthora cinnamomi* under Declining *Quercus ilex* Trees. Forests 11, 375. https://doi.org/10.3390/f11040375

Sánchez-Cuesta, R., Ruiz-Gómez, F.J., Duque-Lazo, J., González-Moreno, P., Navarro-Cerrillo, R.M., 2021. The environmental drivers influencing spatio-temporal dynamics of oak defoliation and mortality in dehesas of Southern Spain. For. Ecol. Manag. 485, 118946. https://doi.org/10.1016/j.foreco.2021.118946

Sánchez-Oliver, J.S., Rey Benayas, J.M., Carrascal, L.M., 2014. Differential effects of local habitat and landscape characteristics on bird communities in Mediterranean afforestations motivated by the EU Common Agrarian Policy. Eur. J. Wildl. Res. 60, 135–143. https://doi.org/10.1007/s10344-013-0759-y

Serrano, M.S., De Vita, P., Fernández-Rebollo, P., Sánchez, M.E., 2011a. Control de la podredumbre radical de encinas mediante fertilizantes inorgánicos II: efecto "in vitro" del Ca y el K en la capacidad infectiva de "*Phytophthora cinnamomi*." Bol. Sanid. Veg. Plagas 37, 109–118.

Serrano, M.S., De Vita, P., Fernández-Rebollo, P., Sánchez, M.E., 2011b. Control de la podredumbre radical de encinas mediantes fertilizantes inorgánicos III: efecto de la aplicación al suelo de fertilizantes cálcicos y potásicos. Bol. Sanid. Veg. Plagas 37, 119–127.

Serrano, M.S., Fernández-Rebollo, P., De Vita, P., Carbonero, M.D., Sánchez, M.E., 2011c. The role of yellow lupin (*Lupinus luteus*) in the decline affecting oak agroforestry ecosystems. For. Pathol. 41, 382–386. https://doi.org/10.1111/j.1439-0329.2010.00694.x

Serrano, M.S., Fernández-Rebollo, P., De Vita, P., Carbonero, M.D., Trapero, A., Sánchez, M.E., 2010. *Lupinus luteus*, a new host of *Phytophthora cinnamomi* in Spanish oak-rangeland ecosystems. Eur. J. Plant Pathol. 128, 149–152. https://doi.org/10.1007/s10658-010-9652-7

Serrano, M.S., Fernández-Rebollo, P., De Vita, P., Sánchez, M.E., 2013. Calcium mineral nutrition increases the tolerance of *Quercus ilex* to *Phytophthora* root disease affecting oak rangeland ecosystems in Spain. Agrofor. Syst. 87, 173–179. https://doi.org/10.1007/s10457-012-9533-5

Shearer, B.L., Tippett, J.T., 1989. Jarrah dieback: the dynamics and management of *Phytophthora cinnamomi* in the jarrah (Eucalyptus marginata) forest of south-western Australia, Department of Conservation and Land Management. ed, Research Bulletin. CALM, Como, Western, Australia.

Stewart, A.J.A., 2000. The world is heterogeneous: Ecological consequences of living in a patchy environment. Ecol. Consequences Environ. Heterog. 1–8.

Sutton-Grier, A.E., Kenney, M.A., Richardson, C.J., 2010. Examining the relationship between ecosystem structure and function using structural equation modelling: A case study examining denitrification potential in restored wetland soils. Ecol. Model. 221, 761–768. https://doi.org/10.1016/j.ecolmodel.2009.11.015

Tsao, P.H., Oster, J.J., 1981. Tsao, P. H., & Oster, J. J. (1981). Relation of ammonia and nitrous acid to suppression of *Phytophthora* in soils amended with nitrogenous organic substances. Phytopathology 71, 53–59.

Turner, M.G., Gardner, R.H., 2015. Landscape ecology in theory and practice: pattern and process, 2nd ed. Springer, New York, NY.

Tuset, J.J., Cots, F., Hinarejos, C., Mira, J.L., 2001. Suspensiones de zoosporas de *Phytophthora cinnamomi* que causan la "seca" en cinco especies de *Quercus* mediterráneos. Bol. Sanid. Veg. Plagas 27, 103–115.

Vadell, E., de-Miguel, S., Centeno, G.F., Robla, E., Cuzzi, M.L., García, J.P., 2019. La forestación de tierras agrícolas: balance de un instrumento de política forestal para el cambio del uso de la tierra. Cuad. Soc. Esp. Cienc. For. 1–20.

Vinale, F., Sivasithamparam, K., Ghisalberti, E.L., Marra, R., Woo, S.L., Lorito, M., 2008. *Trichoderma*–plant–pathogen interactions. Soil Biol. Biochem. 40, 1–10. https://doi.org/10.1016/j.soilbio.2007.07.002

Walker, C.A., van West, P., 2007. Zoospore development in the oomycetes. Fungal Biol. Rev. 21, 10–18. https://doi.org/10.1016/j.fbr.2007.02.001

Watson, D.F., Philip, G.M., 1985. A refinement of inverse distance weighted interpolation. Refinement Inverse Distance Weight. Interpolat. 2, 315–327.

Weste, G., 1983. Population dynamics and survival of *Phytophthora* [Plant pathogenic fungi].

Weste, G.M., Taylor, P., 1971. The invasion of native forest by *Phytophthora cinnamomi*. I. Brisbane Ranges, Victoria. Aust. J. Bot. 19, 281–294. https://doi.org/10.1071/bt9710281

Widmer, T.L., Johnson-Brousseau, S., Kosta, K., Ghosh, S., Schweigkofler, W., Sharma, S., Suslow, K., 2018. Remediation of *Phytophthora ramorum*-infested soil with *Trichoderma asperellum* isolate 04-22 under ornamental nursery conditions. Biol. Control 118, 67–73. https://doi.org/10.1016/j.biocontrol.2017.12.007

Worboys, S., Gadek, P.A., 2004. Rainforest dieback: risks associated with roads and walking track access in the Wet Tropics World Heritage Area. School of Tropical Biology, James Cook University Cairns Campus, and Cooperative Research Centre for Tropical Rainforest Ecology and Management. Rainforest CRC, Cairns (Australia).

Xie, Q., Dash, J., Huang, W., Peng, D., Qin, Q., Mortimer, H., Casa, R., Pignatti, S., Laneve, G., Pascucci, S., Dong, Y., Ye, H., 2018. Vegetation Indices Combining the Red and Red-Edge Spectral Information for Leaf Area Index Retrieval. IEEE J. Sel. Top. Appl. Earth Obs. Remote Sens. 11, 1482–1493. https://doi.org/10.1109/JSTARS.2018.2813281

Zavala, M.A., Díaz-Sierra, R., Purves, D., Zea, G.E., Urbieta, I.R., 2006. Modelos espacialmente explícitos. Rev. Ecosistemas 15. https://doi.org/10.7818/re.2014.15-3.00

Zentmyer, G.A., 1981. The effect of Temperature on Growth and Pathogenesis of *Phytophthora cinnamomi*. Phytopathology 66, 925–928.

Zentmyer, G.A., 1980. *Phytophthora cinnamomi* and the diseases it causes. Monograph, American Phytopathological Society, Univ. California, Riverside, USA.

Capítulo 2

Factores abióticos a pequeña escala que influyen en la distribución espacial de *Phytophthora cinnamomi* bajo árboles de *Quercus ilex* en decaimiento

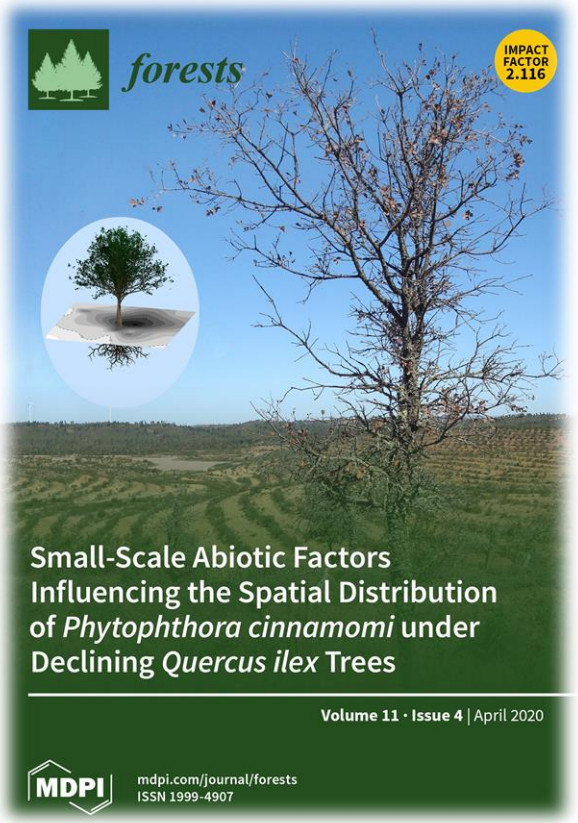

Sánchez-Cuesta, R., Navarro-Cerrillo, R.M., Quero, J.L., Ruiz-Gómez, F.J., **2020**. Small-scale abiotic factors influencing the spatial distribution of *Phytophthora cinnamomi* under declining *Quercus ilex* trees. *Forests* 11, 375.
https://doi.org/10.3390/f11040375 (Open Access)

This article belongs to the Special Issue "*Phytophthora* Infestations in Forest Ecosystems" (June 2021) https://doi.org/10.3390/books978-3-0365-0801-6

Resumen

La podredumbre radical causada por *Phytophthora* se considera uno de los factores principales asociados a la mortalidad de la encina (*Quercus ilex* L.). La efectividad y precisión del patógeno transmitido por el suelo y su gestión podrían verse influenciados por la heterogeneidad espacial del suelo. Este factor es de especial relevancia en muchas repoblaciones forestales del suroeste de España, las cuales se llevaron a cabo sin control fitosanitario de las plántulas de vivero. Seleccionamos un área de estudio situada en una repoblación forestal de *Q. ilex* de 15 años, infectada por *Phytophthora cinnamomi* Rands. Las muestras de suelo (n_{total} = 132) fueron tomadas en una cuadrícula bajo 4 árboles, de forma sistemática, y se analizaron para cuantificar 12 variables, las unidades formadoras de colonias (ufc) de *P. cinnamomi* más 11 propiedades físicas y químicas del suelo. El análisis combinado de todas las variables se realizó con modelos lineales generalizados mixtos (MLGM), y los patrones espaciales de las ufc se caracterizaron mediante un índice de agregación (I_a) y un índice de agrupación (ν) mediante SADIE. Los valores de ufc oscilaron entre 0 y 211 ufc g^{-1}, y el MLGM construido con las variables limo, P, K y humedad del suelo explicó en mayor medida la distribución de las ufc. El análisis espacial mostró que 9 de las 12 variables presentaban agregación espacial (I_a > 1) y agrupación de manchas locales ($\nu_i \geq 1{,}5$) para la materia orgánica, el limo y el Ca. Los patrones espaciales de las ufc de *P. cinnamomi* bajo plantación de encinas están relacionados con las variables edáficas y la cobertura del dosel. El análisis espacial a pequeña escala de la variabilidad del micrositio puede predecir qué áreas circundantes a los árboles pueden influir en la menor disponibilidad de ufc de oomicetos.

Abstract

Phytophthora root rot is considered one of the main factors associated with holm oak (*Quercus ilex* L.) mortality. The effectiveness and accuracy of soilborne pathogen and management could be influenced by soil spatial heterogeneity. This factor is of special relevance in many afforestations of southwestern Spain, which were carried out without phytosanitary control of the nursery seedlings. We selected a study area located in a 15-year-old afforestation of *Q. ilex*, known to be infested by *Phytophthora cinnamomi* Rands. Soil samples (n_{total} = 132) were taken systematically from a grid under 4 trees, and analysed to quantify 12 variables, the colony forming units (cfu) of *P. cinnamomi* plus 11 physical and chemical soil properties. The combined analysis of all variables was performed with linear mixed models (GLMM), and the spatial patterns of cfu were characterised using an aggregation index (I_a) and a clustering index (ν) by SADIE. Cfu values ranged from 0 to 211 cfu g^{-1}, and the GLMM built with the variables silt, P, K and soil moisture explained the cfu distribution to the greatest extent. The spatial analysis showed that 9 of the 12 variables presented spatial aggregation (I_a > 1), and the clustering of local patches ($\nu_i \geq 1.5$) for organic matter, silt, and Ca. The spatial patterns of the *P. cinnamomi* cfu under planted holm oak trees are related to edaphic variables and canopy cover. Small-scale spatial analysis of microsite variability can predict which areas surrounding trees can influence lower oomycetes cfu availability.

Keywords: GLMM; holm oak decline; tree mortality; root rot.; plantation; dehesas; montados; open forests

1 Introduction

Mediterranean-like savannas of the southern Iberian Peninsula (hereafter dehesas) are important ecosystems threatened by socioeconomic, climatic and phytosanitary factors. Currently, dehesas are affected by tree mortality caused by root rot (Jiménez et al., 2008; Camilo-Alves et al., 2013). After three decades of research and development, holm oak (*Quercus ilex* subsp. *ballota* (Desf.) Samp.) decline remains the most-important cause of tree loss in southern Spain and Portugal (Ruiz-Gómez et al., 2016). Oak decline has been related to management factors, as well as to the influence of climatic factors, such as severe droughts (González-Alonso, 2008). However, there is a broad consensus that biotic agents (pests and diseases) act as triggers for mortality episodes, in the context of a continuously-deteriorating ecosystem with limited regeneration capacity (Vettraino et al., 2002; Pérez-Sierra et al., 2013).

The root rot caused by soilborne pathogens from the genera *Phytophthora* spp. and *Pythium* spp. is considered one of the most-important causes triggering mortality of holm oak (Trapero et al., 2000; Navarro Cerrillo et al., 2004; Camilo-Alves et al., 2013), causing rot of fine-roots, leading to water and nutritive stress (Oßwald et al., 2014), and therefore changes in tree physiology (Ruiz Gómez et al., 2018) which are visible in terms of defoliation and chlorosis, and in many cases tree death. These oomycetes remain as resistance structures either in soil, infected roots or debris under unfavourable conditions (Jung et al., 2016), waiting for suitable biotic and abiotic conditions for germination, leading to sporangia production and the subsequent release of zoospores which then infect new host roots (Marais et al., 2002).

Due to the heterogeneity of the holm oak fine root distribution, and thus the heterogeneity of the soil rhizosphere in dehesas, it is often necessary to carry out large sampling efforts to avoid false negative outcomes in diagnosis of root rot caused by *Phytophthora* spp. (Hüberli et al., 2000; Zamora Rojas et al., 2014). This soil heterogeneity has been proved to be related with the horizontal canopy distribution in several *Quercus* spp. (Ashton and Larson, 1996; Mauer et al., 2017). Biotic and abiotic factors such as soil microbiota community (Aponte et al., 2014; Carranca et al., 2015; Ruiz Gómez et al., 2019), and soil moisture and mineral nutrients (Gallardo, 2003; Cubera and Moreno, 2007; Quero et al., 2013; Andivia et al., 2015) are also related to the

spatial distribution of the tree canopy, mainly due to the differences in the soil exposure to solar radiation and its contribution to processes involved in organic matter formation and mineral deposition (Cappai et al., 2017).

The spatial distribution of the pathogen inoculum in the soil appears to be influenced by rhizosphere heterogeneity, but there is a lack of studies of soil microbiota spatial distribution in forest soils at a small-scale (Gómez-Aparicio et al., 2012; Ibáñez et al., 2015). Colony forming units (hereafter, cfu) is the number of propagules which produce countable colonies after sowing in selective medium plates (Romero et al., 2007). It is often used as an indicator of the abundance of the inoculum of *Phytophthora* spp. and other oomycetes in the soil. The density of cfu of *Phytophthora cinnamomi* Rands has been related to calcium content or plant diversity in Mediterranean oak forests (Gómez-Aparicio et al., 2012; Serrano et al., 2012). Thus, it has been hypothesized that the spatial distribution of soil physicochemical properties associated with the tree crown may influence the density of the oomycete cfu concentration, and therefore the small-scale spatial distribution of the soil pathogen (Gallardo, 2003; Cubera and Moreno, 2007; Quero et al., 2013; Andivia et al., 2015).

Furthermore, the afforestation programmes implemented in Spain at the end of the 20th century and the beginning of the 21st, in the context of the European Economic Community's aid scheme for forestry measures in agriculture (directives EEC-2080/92, and 1698/2005) have led to 232 000 ha of tree plantations in Andalusia, of which 82 775 ha are *Q. ilex* (Vadell et al., 2016). The afforestation programme funded plantation costs, conservation and maintenance, without paying attention to the phytosanitary control of the nursery seedlings at the time of planting. This lack of phytosanitary control is considered a threat to seedling survival and a reason for the spread of potential soil pathogens (Jung et al., 2016; Lehtijärvi et al., 2017), especially when dealing with invasive alien pathogens such as *Phytophthora* spp., since biological invasion is one of the main drivers of global change in Mediterranean climates (Burgess et al., 2017).

The main objective of this study was to evaluate the effect of several soil and plant parameters on the spatial distribution and aggregation of *P. cinnamomi* cfu in holm oak. For this purpose, we selected as a case-study an afforestation on former agricultural land, to take advantage of the homogeneity of plant genotype and age, climatic variables and soil conditions among the selected individuals. The specific objectives were: (i) to evaluate the effect of the tree crown cover and the soil physicochemical characteristics

on the spatial distribution of the cfu; and (ii) to model the relationships between spatial patterns of cfu, tree crown cover and soil variables to evaluate the predictive capacity of these variables. Once these objectives were met, we intended to ascertain which microsite variables are potentially more important regarding the presence and spatial distribution of *P. cinnamomi*. This could help to guide the sampling effort for the diagnosis of root rot, and to determine the predisposition of soils to host the pathogen according to their physical and chemical characteristics.

2 Material and Methods

2.1 Study zone

The study was carried out in a *Q. ilex* afforestation site located in Puebla de Guzmán (Andalusia - southern Spain, coordinates ETRS89, UTM30N: 120 500 mW, 4 167 500 mN, 185–188 m a.s.l.). The area is characterised by a mean annual temperature of 16.8 °C and a mean annual rainfall of 570 mm (Meteorological Station of IFAPA, Puebla de Guzman, coordinates ETRS89, UTM30N: 124 659 mW, 4 164 620 mN; 195 m a.s.l. Institute of Agronomic and Fishery Research and Training-IFAPA, Junta de Andalusia), with a dry thermo-Mediterranean climate (120–150 biologically-dry days) with hot and dry summers and mild winters. The area has an undulating relief (slope between 5 and 10%, Supplementary Material, Table S2.1). Soils are shallow and acidic in nature, with rocky outcrops of slate and schists, an almost total absence of free calcium carbonate and sometimes a slight surface layer of organic matter. The site was cropped periodically before 1990 and has been left fallow since this date, supporting a mixture of native herbaceous species associated with former agricultural land and shrubs (*Cistus ladanifer* L.). A holm oak plantation was established in 1995. The planting area was sub-soiled, using a ripper with a single tine, to a depth of 60 cm and soil clods were broken up using a spring harrow and culta-mulcher, to provide a more-level surface for the plantation. The planting was done by hand following a systematic spatial pattern of distribution, with a density of 312 plants ha^{-1} (4 × 8 m spacing), using tree shelter. No additional soil treatments were carried out after the afforestation.

2.2 Soil sampling design

In spring (April) 2010, the plot (100 m^2) was established to include four *Q. ilex* trees with symptoms of oak decline (mean defoliation 30%) and previously shown to be infested by *P. cinnamomi* (Newbiotechnic S.A., NBT-No. 41/04/PR/PSX). The effects of practices carried out during cultivation and plantation management were homogeneous for the selected trees. The four trees were regular in size (DBH = 9.5 ± 0.5 cm; H = 2.5 ± 0.1 m). Visual phytosanitary assessment was carried out following the European Network of Damage in Forest Masses manual (Eichhorn et al., 2017). The trees ranged in crown damage (defoliation) from Class 1 (10 < slight defoliation ≤ 25%) to Class 3 (60 < severe defoliation ≤ 95%) (Supplementary Material, Table S2.1). Apart from *P. cinnamomi*, no other biotic agents contributing to the aboveground symptoms were identified during the visual inspection. The presence of root rot was confirmed in all cases through roots diagnosis (loss of secondary fine roots, discoloration and softness).

Under each tree crown, a sampling grid was established north facing, following the methodology proposed by Gallardo (2003), and included two grid sizes (Figure 1): a general grid (G) 1 × 1 m (n = 16) in a 4 × 4 m quadrat centred in the trunk, and 0.5 × 0.33 m (n = 24) grid, which were concentrated within the general sampling quadrat according to the crown cover (crown position: O = Outside, T = Transition and I = Inside). Some of the points of the general and concentrated grids were the same, with a total of 33 points sampled per tree (n) (Figure 1). Finally, two categories were established: outside of the crown cover (OC, n = 22) and inside of the crown cover (IC, n = 11). The tree crown projection was obtained with the help of a plumb line, marking the vertical projection of the crown margins over the grid. Regarding orientation, all the points belonging to the A and B quadrats were considered as North points (N) and the ones located in the C and D quadrats, as South points (S).

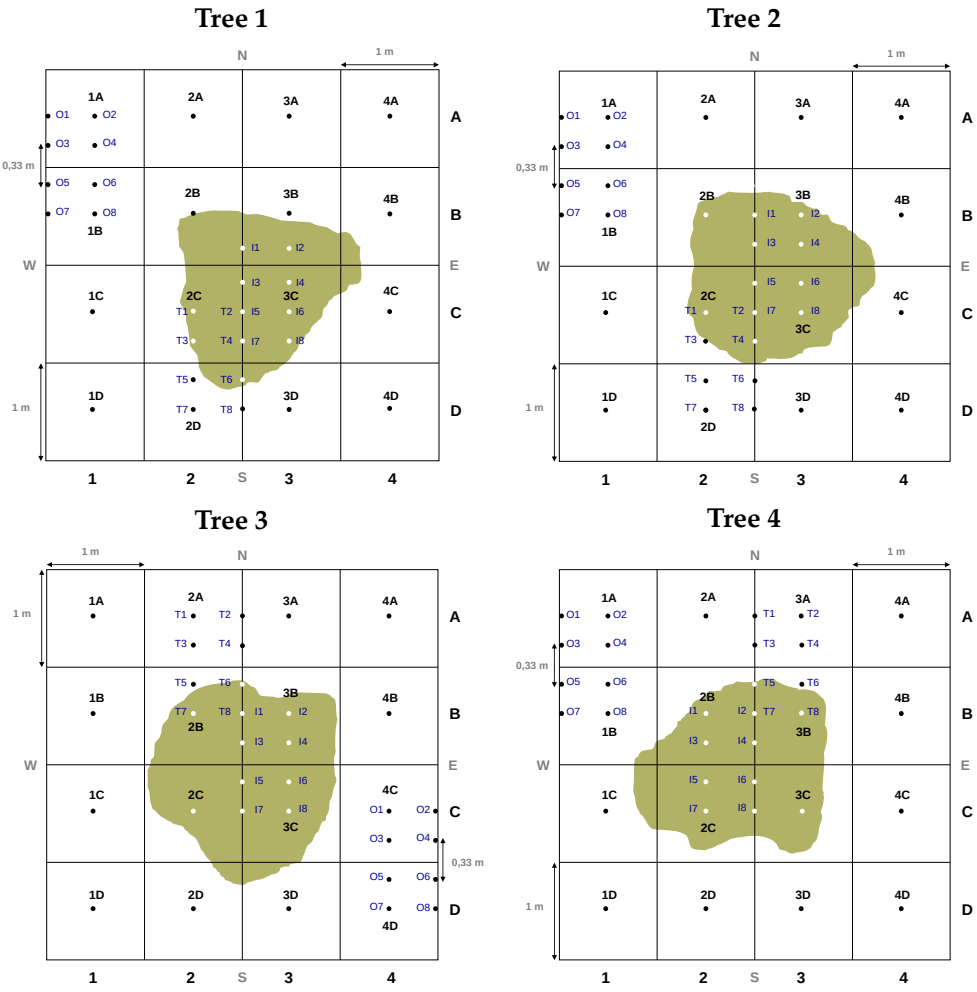

Figure 1. Soil sample design (according to Gallardo et al. (Gallardo, 2003) at two different scales: general grid (1 × 1 m) (G, n = 16) and specific position grid (0.5 × 0.33 m) corresponding to inside of the crown cover (I, n = 8), transition (T, n = 8), and outside of the crown cover (O, n = 8) for each of the four sampled trees. The black points belong to the group outside of the crown cover (OC, n = 22) and the white points belong to the group inside of the crown cover (IC, n = 11). The letters N, E, S and W, indicate the cardinal points.

2.3 Processing and analysis of soil samples

In spring (April) 2010, soil samples were taken at each point of the grid (n_{total} = 132). The soil surface layer and the decomposing organic matter layer were removed from a square of 30 × 30 cm centred on the grid point, and a homogeneous soil sample of approximately 1 kg was extracted from the mineral horizon, over the point, to a depth of 20 cm, with the help of a spade

(Zamora Rojas et al., 2014). Each sample was placed in a sealed plastic bag to prevent loss of moisture, properly labelled and preserved in an ice-cooler (in the absence of light, at approximately 4 °C) during its transfer to the laboratory. The soil samples were air-dried at room temperature for 48 h and then processed by hand, eliminating the rough fraction after mechanical milling and crushing. Prior to aliquot separation, the fine fraction was homogenised and passed through a 2-mm-Ø sieve. In total, 12 variables (11 edaphic variables plus cfu abundance) were evaluated for each soil sample. First, one aliquot of approximately 100 g was separated for quantification of *P. cinnamomi* cfu, and other aliquot of approximately 500 g, was sent to Innoagral laboratories, Grupo Hespérides Biotech S.L., (Sevilla, Spain) for the analysis of 10 soil physicochemical variables (% of clay, silt, and sand, pH, organic matter in soil, total nitrogen, carbon-nitrogen ratio and amount of phosphorus, calcium and potassium) (Supplementary Material, Table S2.2).

Finally, soil moisture (% volumetric content of water) was measured at a depth of 12 cm at all of the sampling points, with a Time Domain Reflectometry (TDR) sensor (Field Scout TDR 100, Spectrum Technologies, Inc. Aurora, IL USA), at the same time as the collection of soil samples.

2.4 Quantification of cfu

Ten grams of each homogenised aliquot of soil for cfu analysis, previously dried at room temperature, was suspended in 100 mL 0.2% agar solution, as described in Romero et al. (2007). The solution was gently shaken and 1 mL of the soil suspension was plated with a 1000 µl pipette on 10 Petri plates for each soil sample, containing NARPH selective medium (Hüberli et al., 2000). The soil suspension was carefully distributed over the surface of the selective medium with the help of an inoculation loop. The plates were incubated at room temperature in darkness for 24 h, after which the soil suspension was removed with sterile water. Colonies growing on each plate were counted after an additional 72 h of incubation after washing.

The hyphal bodies that had grown in the culture medium were quantified visually by light contrast with a 10 × 1 magnifying glass (Nikon SMZ800, Nikon Corp., Tokyo, Japan) and a millimetre mesh. Some growing structures were identified through the observation of aleatory chosen NARPH dishes under microscope (Motic BA310E, Motic Instruments Co., Ltd., Chengdu, China) to ensure that no other organisms different from *P. cinnamomi* were counted. This species was easy identified through the

characteristic aseptate coralloid hyphae with clustered hyphal swellings. The sum of the cfu for the 10 replicates per sample was expressed as cfu/g of dry soil. Due to the positive identification of *P. cinnamomi* on the soil, through molecular methods, and the results of the checking of aleatorily chosen NARPH plates, all the cfu counted were considered directly related with *P. cinnamomi* cfu abundance.

2.5 Statistical analysis

All the variables were examined for normality (Shapiro-Wilk test, $P < 0.05$) and homoscedasticity (Levene test, $P < 0.05$). When the data did not fit to a normal distribution, the variable was subjected to a square root or logarithmic transformation. Once the normality and homoscedasticity requirements were met, the variables N, OM, C/N, percentage of silt and sand, pH and Ca were analysed using one-way analysis of variance (ANOVA), considering crown position and orientation as independent factors. In those cases where the variables were significant, Tukey's test for multiple comparisons of means was used to check for differences (Rohlf and Sokal, 1981). In the case of the non-normal variables (cfu, clay percentage, P, K and moisture), a Kruskal-Wallis (H) mean comparison test and the Mann-Whitney U test were applied for pairs of independent groups ($P < 0.05$). When Mann-Whitney U test was used for mean comparisons on the I-O-T grids, the α threshold to reject the null hypothesis was corrected according to Bonferroni ($P < 0.0167$) (Hazra and Gogtay, 2016). Specific correlations between the soil variables and cfu were determined using a non-parametric Spearman rho coefficient (ρ) at a significance level of 5% ($P < 0.05$), including soil variables that did not follow a normal distribution. Statistical analysis was performed using "R" version 3.3.1. (R Development Core Team, 2017).

The spatial patterns of cfu were characterised using Spatial Analysis by Distance Indices (SADIE), implemented in the program "SADIEShell v2.0" and the aggregation index (I_a) and clustering index (ν) were calculated per plot (Quero, 2006; Winder et al., 2019). The I_a provides information on the overall spatial pattern of each environmental variable. According to Quero et al., (Perry and Dixon, 2002) the spatial pattern is aggregated if $I_a > 1$, random if I_a is close to one and regular if $I_a < 1$. The index ν measures the degree of clustering of the data into patches (mean ν_i: areas of high values of the target variable) and gaps (mean ν_j: areas of low values). Then, ν was contoured by kriging in a two-dimensional map showing their spatial distribution of patches

($\nu \geq 1.5$) and gaps ($\nu \leq -1.5$) using Surfer 10.1 (Golden Software, Colorado, USA). An independent SADIE analysis was performed for each variable and tree. Afterwards the mean values of I_a for all the variables in the four trees were calculated and were also represented using the bilinear interpolation method in Surfer 10.1.

Finally, the relationship of the soil variables with the inoculum concentration and crown cover was assessed through a generalized linear mixed model (GLMM). This methodology allows the analysis of non-normal data that involve fixed or random effects (Bates et al., 2014). The GLMM was implemented through the "lme4" package. The cfu variable was modelled through Poisson distribution with log transformation. The independent variables were previously filtered using a Variance Inflation Factor (VIF) threshold of 10, and the tree and crown position were selected as random effects (Bolker et al., 2009). Despite the relevance of crown position as the main factor of this study explaining spatial distribution of several variables, this factor did not present significant influence over the cfu variable when used in the model as fixed effect. Different model configurations were tested, providing the use of crown position and tree as random effects the best result. Autocorrelation of the output model was evaluated through the analysis of model residuals and correlation matrix of fixed effects. The model was selected based on the lowest value of Akaike's Information Criterion (AIC), which indicates the optimal fit, and the influence of effects was tested through a likelihood ratio test (Schielzeth, 2010). Comparison between Random Effects influence was performed through ANOVA linear model deleting each effect with glmerControl optimization type "bobyqa" (package "lmer4") and the influence of single fixed factors through automatic model reduction and Chi-squared test.

3 Results

3.1 Spatial distribution of the cfu

The cfu values of soil samples ranged from 0 to 211 cfu g^{-1}, for all four trees, showing significant correlation with the tree defoliation level ($\rho = 0.986$, $P < 0.05$). Moreover, cfu showed significant differences according to the crown cover factor (I, T and O; $H_{I\text{-}O} = 20.886$, $P_{I\text{-}O} < 0.001$; $H_{O\text{-}T} = 20.491$, $P_{O\text{-}T} < 0.001$; $H_{I\text{-}T} = 7.549$, $P_{I\text{-}T} < 0.01$). The I-grid showed a significant greater concentration of cfu than O grid in all cases ($U_{I\text{-}O} = 174.5$, $P_{I\text{-}O} < 0.001$), and the T-grid

presented more variability in its results depending on the tree (Table 1). Moreover, a significantly higher cfu value in the IC grid was observed with respect to OC ($H_{IC\text{-}OC}$ = 27.4; $U_{IC\text{-}OC}$ = 882.5, $P_{IC\text{-}OC}$ < 0.001).

Table 1. Colony forming units of each tree (cfu sample^{-1}, mean ± standard error) according to sample grid and sample position with respect to tree crown cover. Mean cfu: mean value of cfu considering all the samples; *n*: number of soil samples per grid under each tree; I: inside crown intensive grid; T: transition intensive grid; O: outside crown intensive grid; IC: all samples inside crown cover; OC: all samples outside crown cover. Different lowercase letters in superscript indicate significant differences between position with respect to crown cover (Mann-Whitney U Test, P < 0.05 for IC-OC comparisons and P < 0.0167 for I-O-T comparisons). No comparisons were made between means corresponding to different factors (I, O and T with IC and OC).

		Position respect to crown cover				
Tree	**Mean cfu** *n* = 33	**I** *n* = 8	**T** *n* = 8	**O** *n* = 8	**IC** *n* = 11	**OC** *n* = 22
1	12 ± 3	22 ± 5^{a}	6 ± 4^{b}	5 ± 2^{b}	23 ± 7^{a}	6 ± 2^{b}
2	13 ± 5	34 ± 13^{a}	4 ± 3^{b}	3 ± 2^{b}	26 ± 10^{a}	7 ± 6^{b}
3	19 ± 8	38 ± 20^{a}	39 ± 26^{a}	0 ± 0^{b}	44 ± 21^{a}	5 ± 4^{b}
4	44 ± 10	119 ± 26^{a}	49 ± 11^{b}	16 ± 6^{c}	100 ± 22^{a}	16 ± 4^{b}
Mean	22 ± 4	53 ± 11^{a}	24 ± 8^{b}	6 ± 2^{b}	48 ± 9^{a}	9 ± 2^{b}

The highest value of cfu in the T-grid occurred in trees with higher level of defoliation (trees 3 and 4, 35 and 70%, respectively). As in the I-grid, the cfu value of IC samples was directly proportional to the defoliation level, being significantly higher for tree 4. Moreover, cfu was significantly higher in points located on the north side of the grid (H_{cfu} = 8.422, P < 0.01).

3.2 Spatial distribution of edaphic variables

Significant differences were found between the overall positions for all variables, except for N, C/N, silt and moisture (Table 2). Clay, P and K were also significantly different between IC and OC (H_{clay} = 6.3, P_{clay} < 0.05; H_P = 4.6, P_P < 0.05; and H_K = 4.2, P_K < 0.0167), but regarding the concentrated grids (I, T and O positions) only OM, Clay and P presented differences. OM, clay and phosphorus were higher at points of the I grid in a significant extent to O grid ($F_{I\text{-}O\ (OM)}$ = 5.5, $P_{I\text{-}O\ (OM)}$ < 0.0167; $U_{I\text{-}O\ (clay)}$ = 318.0, $P_{I\text{-}O\ (clay)}$ < 0.0167; $U_{I\text{-}O\ (P)}$ = 327.0, $P_{I\text{-}O\ (P)}$ < 0.0167).

Table 2. Edaphic variables. Mean values (mean ± standard error) according to sample grid and position respect to tree crown cover. *n*: total number of samples. I: inside crown grid; T: transition grid; O: outside crown grid. IC: samples inside crown cover; OC: samples outside crown cover; (ρ): Spearman correlation coefficient between cfu (n = 132) and physicochemical soil parameters. Different letters in superscript indicate significant differences with respect to crown cover (Tukey test for normal distributed variables, $P < 0.05$ and Mann-Whitney U Test for non-normal distributed variables, $P < 0.05$ for IC-OC comparisons and $P < 0.0167$ for I-O-T comparisons †). No comparisons were made between means corresponding to different factors (I, O and T with IC and OC).

	Position with respect to crown cover					
Variable	**I** n = 32	**T** n = 32	**O** n = 32	**IC** n = 44	**OC** n = 88	**Corr. coef. (ρ)**
N (%)	0.19±0.01^{a}	0.18±0.01^{a}	0.18±0.01^{a}	0.19±0.01^{a}	0.17±0.01^{a}	−0.045
OM (%)	1.91±0.11^{b}	1.47±0.12^{b}	1.77±0.11^{a}	1.78±0.08^{a}	1.61±0.07^{a}	−0.008
C/N	6.67±0.52^{a}	5.13±0.49^{a}	6.25±0.54^{a}	6.09±0.39^{a}	5.98±0.36^{a}	0.020
Clay † (%)	27.17±1.01^{b}	28.21±0.90^{ab}	26.85±1.33^{a}	25.43±0.84^{a*}	28.66±0.67^{b*}	−0.398***
Silt (%)	37.28±1.36^{a}	38.86±1.16^{a}	37.68±1.28^{a}	38.49±1.23^{a}	37.25±0.69^{a}	−0.026
Sand (%)	35.54±2.03^{a}	32.93±1.34^{a}	35.48±2.17^{a}	36.08±1.72^{a}	34.09±1.07^{a}	0.242**
P † (mg/kg)	32.45±9.05^{b}	7.41±3.38^{b}	19.58±6.94^{a}	27.07±6.55^{a*}	12.19±3.31^{b*}	0.109
pH	5.13±0.06^{a}	5.17±0.04^{a}	5.20±0.05^{a}	5.13±0.04^{a}	5.19±0.03^{a}	0.319***
Ca (meq/100 g)	0.70±0.04^{a}	0.59±0.03^{a}	0.73±0.05^{a}	0.64±0.03^{a}	0.67±0.03^{a}	0.374***
K † (meq/100 g)	0.50±0.13^{a}	0.20±0.02^{a}	0.22±0.05^{a}	0.41±0.09^{a*}	0.19±0.02^{b*}	0.352***
Moisture † (%)	15.04±1.24^{a}	15.75±0.65^{a}	15.24±0.77^{a}	15.25±0.84^{a}	15.30±0.46^{a}	0.066

The Kruskal-Wallis test showed significant differences for clay, P and K relative to the IC and OC grids (H_{clay} = 6.304, $P_{clay} < 0.05$; H_P = 4.564, $P_P < 0.05$; H_K = 4.232, $P_K < 0.05$). Similarly, to the cfu results (Table 1), P and K had significantly higher concentrations under the crown cover, while clay had significantly lower percentages (Table 2). Regarding orientation, OM (F_{OM} = 6.049, $P < 0.05$), pH (F_{pH} = 5.543, $P < 0.05$), Ca (F_{Ca} = 14.792, $P < 0.05$) and K (H_K = 2746, $P < 0.01$) presented significant differences between North and South sides, with higher values in North side, except in the case of OM.

Moreover, the analysis of the Spearman's bivariate correlations showed a significant and positive relationship between cfu and sand (ρ = 0.242, $P < 0.01$), pH (ρ = 0.319, $P < 0.001$), Ca (ρ = 0.374, $P < 0.001$) and K (ρ = 0.352, $P < 0.001$), and a significant and negative one with clay (ρ = −0.398, $P < 0.001$).

3.3 Spatial analysis and location of edaphic variables and relationship with cfu

All variables showed spatial aggregation (I_a > 1) in at least one tree (Figure 2). The aggregation was significant (P < 0.05) for clay in trees 2, 3 and 4; OM, P and silt in trees 2 and 4; Ca in trees 3 and 4; the soil moisture for trees 2 and 3; and K and sand only in trees 1 and 4, respectively. In all other options, the variables tend to be random (I_a ≈ 1, P > 0.05, Figure 2). Overall, nine of the twelve variables analysed with SADIE presented significant spatial aggregation patterns and up to six did so for trees 2 and 4, with the latter the most defoliated.

The clustering indices (ν) showed the presence of patches ($\nu_i \geq 1.5$) and/or gaps ($\nu_j \leq -1.5$) for all variables with I_a > 1 (Figure 2; Supplementary Material, Figure S2.1). Clay showed significant patches (P < 0.05) for trees 2 and 3 and gaps also for tree 3 under the crown cover, tending to cluster in tree 4. Organic matter showed clustering patches for trees 1, 2 and 4, as well as gaps for tree 2. Phosphorus and silt showed significant patches and gaps for trees 2 and 4, and Ca for trees 3 and 4, tending also to gaps in these trees. Soil moisture showed significant patches for trees 2 and 3 as well as gaps for tree 2, and K showed significant patches and gaps only for tree 1.

The remaining edaphic variables (N, C/N, sand, pH, Ca, K and moisture) did not show any significant aggregation patterns (I_a ≈ 1) or significant clustering of patches and gaps, for all trees.

On the other hand, cfu showed a local aggregated distribution pattern (I_a > 1) that was not strong enough to contribute significantly (P > 0.05) to the overall aggregation of the influence of the crown area (Figure 2), but these clustering patches (ν > 1.5) were found under the crown cover of all trees as well as in the immediate transition zone (Figure 3).

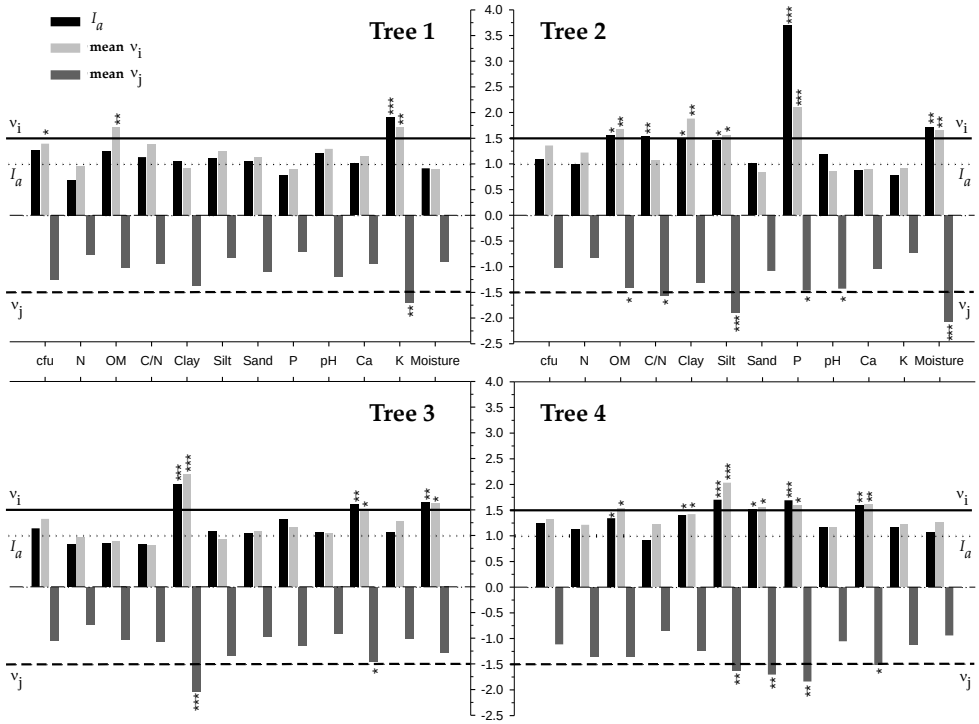

Figure 2. Aggregation indices (I_a) and clustering indices (ν) for the study of 12 variables in the four sampled oaks. The horizontal dotted line $I_a = 1$ indicates the limit of the type of distribution pattern of the variable ($I_a > 1$ aggregated, $I_a < 1$ regular and $I_a = 1$ random). The horizontal continuous line (mean $v_i \geq 1.5$) indicates the limit for which the index ν is grouped into patches, i.e., higher values of a given variable. The horizontal discontinuous line (mean $v_j \leq -1.5$) indicates the limit for which the index ν is grouped into gaps, i.e., lower values of a given variable. * - $P < 0.05$; ** - $P < 0.01$; *** - $P < 0.001$.

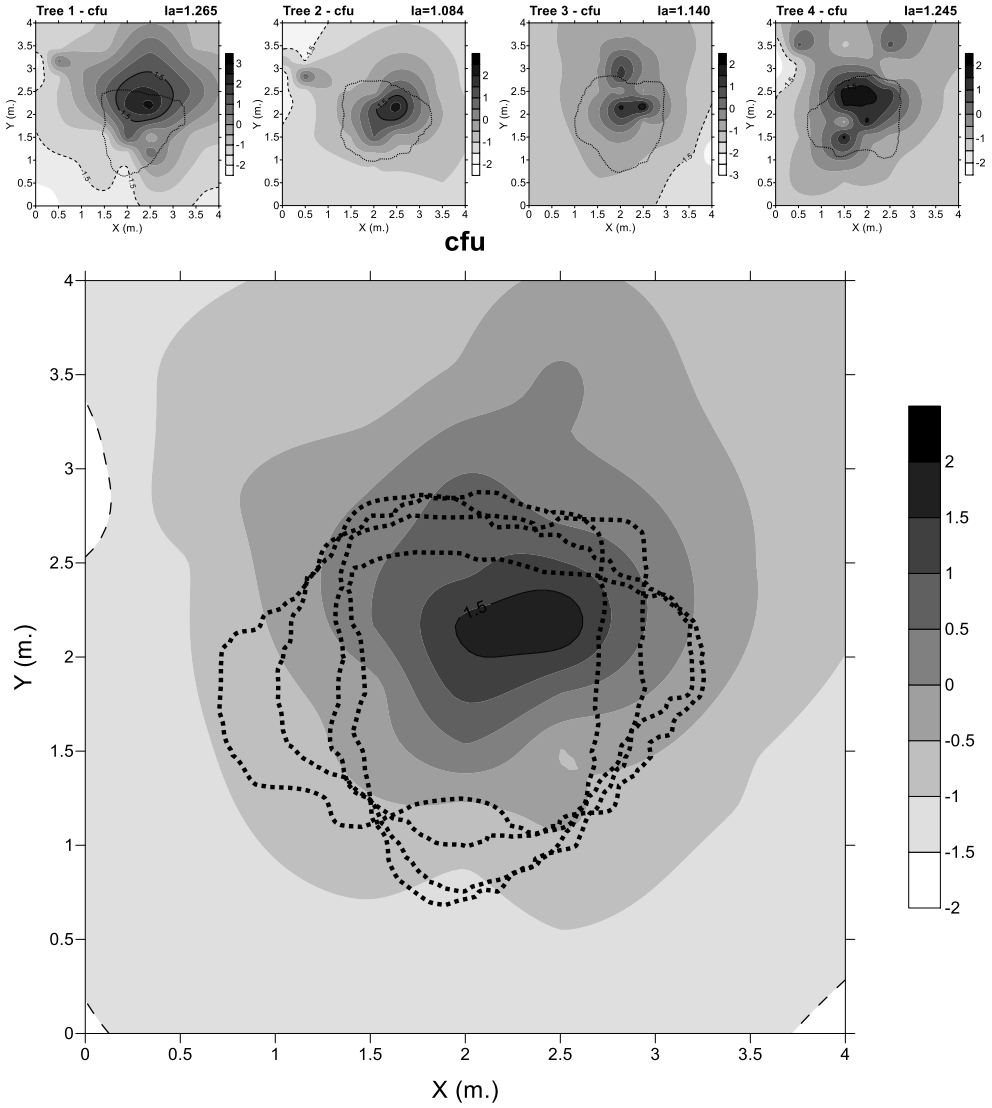

Figure 3. Maps of clustering indices (ν) of the cfu for the four sampled trees (top) and the mean for all the trees (bottom). The dark areas show cfu clustering patches (ν > 1.5) delimited by a continuous line, and the light areas show clustering gaps (ν < −1.5) delimited by a discontinuous line. The dotted lines represent the crown cover of each tree. (I_a): General aggregation index. Legend (ν) is unitless.

The variables that presented the most aggregated mean pattern were P, OM, K and clay (Figure 4). Phosphorous and OM tended to accumulate under crown cover as well as in the transition zone, with this tendency being obvious in trees 2-4, and to a lesser extent in tree 1. Potassium showed a tendency to

be clustered under crown cover, being more evident in trees 3 and 4, which had higher levels of defoliation (35 and 70%, respectively).

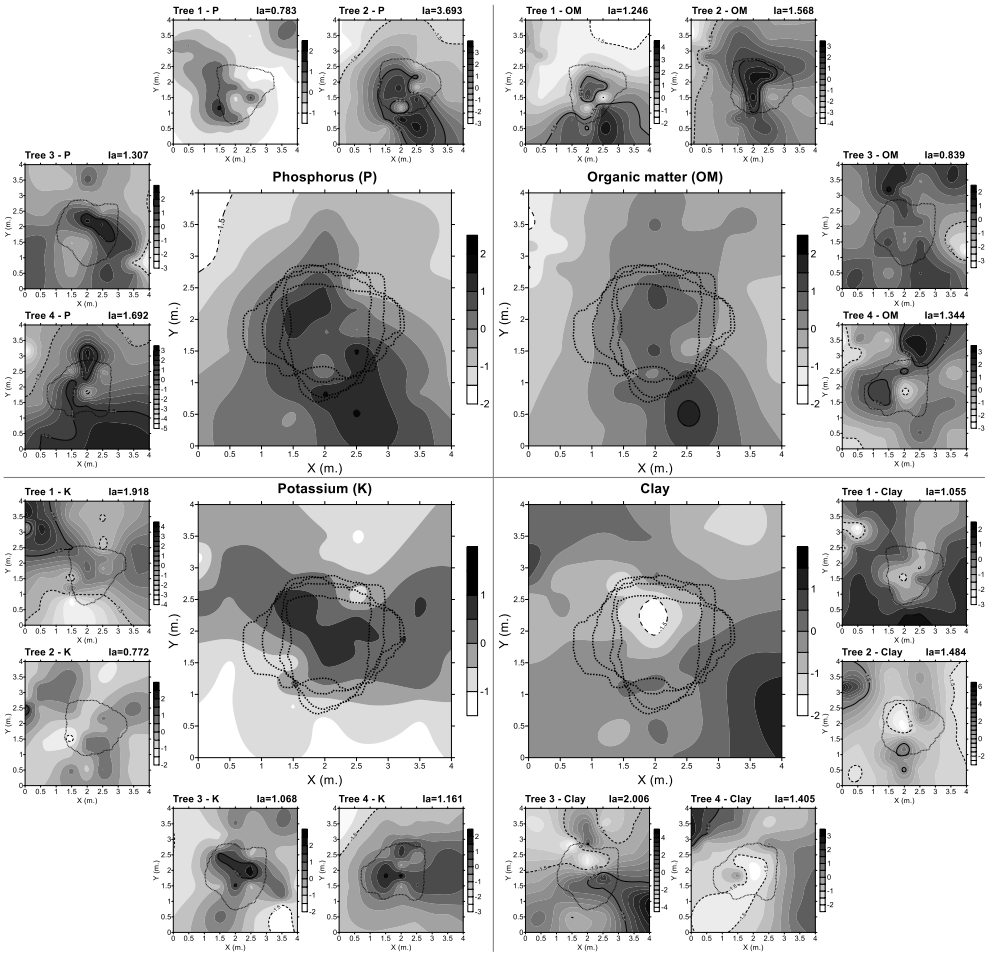

Figure 4. Maps of clustering indices (ν) of edaphic variables (P: phosphorus, OM: organic matter, silt and clay) whose aggregation index (I_a) presents statistical significance in at least two trees (Figure 2) and/or significant differences in the mean value between grids respect to crown cover (Table 2), for the four sampled trees (small maps) and the mean of all trees (large maps), projected to 4 × 4 m surface. The darker areas show clustering patches of edaphic variables (ν > 1.5) are delimited by a continuous line, and the light areas show edaphic variables clustering gaps (ν < −1.5) are delimited by a discontinuous line. The dotted lines represent the crown cover of each tree. In the upper right corner of each sampling unit, the overall general aggregation pattern (I_a) is indicated. Legend (ν) is unitless.

Clay showed a dominance of gaps under the crown cover, which is clearer in trees 2 and 4, with patches and gaps in tree 2 (ν_i = 1.884) and 3 (ν_i = 2.187; ν_j = −2.045) and smaller gaps with a tendency to randomness in tree 1.

Potassium showed, under the crown, a dominance of spots in trees 3 and 4 and a tendency to be in gaps in tree 1 (ν_j = −1.698) and 2. For P there was, under the crown, a dominance of spots in trees 2 (ν_i = 2.098), 3 and 4 (ν_i = 1.592), and a tendency to randomness in tree 1. Organic matter showed a dominance of patches under the crown in tree 1 (ν_i = 1.721) and 2 (ν_i = 1.669), small patches and gaps in tree 4 (ν_i = 1.532) and a tendency to randomness in tree 3.

The remaining edaphic variables (N, C/N, silt, sand, pH, Ca, and moisture) showed randomness in spatial distribution of patches and gaps for the most trees (Supplementary Material, Figure S2.1).

3.4 Generalized linear mixed model for cfu

Eight out the 11 edaphic variables (OM, C/N, clay, silt, P, Ca, K and moisture) were selected to test different mixed models using the tree and the position under the crown (IC/OC) as random effects. Finally, the generalised mixed model that fitted best to the cfu distribution was the one constructed by the variables silt, P, K and moisture as fixed effects, considering both tree and position as random effects, which presented model variances of 1.205 and 1.229, respectively (dimensionless). The likelihood ratio test showed also the significant influence of both random effects in the overall model (Table 3).

Table 3. Generalized Linear Mixed Model effects Chi-squared test. First row shows the optimal model Akaike Information Criteria (AIC). Df: Degrees of freedom. *P*: Significance level.

Single effects influence		Df	AIC	*P*
None			2703.8	
Random effects	*Tree*	6	4876.2	< 0.001
	Position	6	4103.0	< 0.001
Fixed effects	*Silt*	1	2704.8	0.082
	K	1	2754.4	< 0.001
	P	1	2933.8	< 0.001
	Moisture	1	3864.5	< 0.001

Although the deletion of silt only produced marginal differences in the resulting model (Table 3), this parameter was finally included in the output model because of the lower AIC compared with the model constructed without this variable. Moreover, when the four selected variables, including silt were considered as fixed effects, they contributed significantly ($P < 0.05$) to the model (Table 4).

No significant correlation was found between the fixed effects, and the residuals showed a normal distribution (D = 0.122, *P* = 0.099), showing therefore the absence of autocorrelation between fixed factors. The final model showed also a strong Intraclass Correlation Coefficient (Adjusted ICC = 0.975) indicating that clustering by position under the crown accounted for a high proportion of the total variability, and data within each cluster were well correlated.

4 Discussion

This work shows the existence of small-scale spatial patterns in the distribution of cfu of *P. cinnamomi* under holm oak trees, related to texture, P, pH, Ca, K and moisture distribution in soil. Our results are consistent with those obtained in other studies, where the canopy cover of woody plants has been shown to have an important effect on soil properties (Gallardo, 2003; Gea-Izquierdo et al., 2010; Simón et al., 2013; Andivia et al., 2015) and these, in turn, on soil microorganisms (Gómez-Aparicio et al., 2012; Quero et al., 2013); in this case, on the frequency of *P. cinnamomi* (Ruiz-Gómez et al., 2016). Additionally, our results show a significant linear relationship between the values of the cfu and the edaphic variables (texture, P, pH, Ca, K and moisture), which correlate with the presence in soil of these oomycetes (Sánchez et al., 2002).

Although crown defoliation is usually the main factor assessed when studying holm oak health status in relation to root rot (González et al., 2017; Navarro-Cerrillo et al., 2019), this factor was not considered in our work. This analysis would have required different experimental design, considering a plot with a wider range of crown defoliation and health status, a healthy plot with similar soil conditions as a control, and more biological repetitions for each defoliation level. Such increase in the number of repetitions would have been a big challenge regarding the sampling intensity established under each tree in our study. In this work the plot was chosen by its homogeneous conditions in order to determine if soil microsite changes driven by crown cover influence were related with cfu distribution. Thus, we assumed that our chosen plots had similar disease conditions. Moreover, SADIE or spatial analysis use in few plots can be assessed because of an implicitly high sample size (Maestre and Quero, 2008). Notwithstanding, and despite the relevance of our findings, it is important to indicate that the low number of trees used in our study would limit the transferability of the results.

4.1 The abundance of cfu and soil parameters are influenced by the canopy cover

The soil samples were collected in spring (April) 2010, in an area severely affected by root rot in Andalusia (Sánchez et al., 2000), and showed cfu values similar or slightly superior to those obtained in comparable work in the Iberian Peninsula, with inoculum concentrations ranging between 3 and 130 cfu g^{-1} (Rodríguez et al., 2004; Jiménez et al., 2008; Serrano et al., 2014). In this sense, the observed defoliation level in the absence of other biotic agents (pests and diseases) is considered to be caused mainly by the root pathogen *P. cinnamomi* (Sánchez et al., 2002; Romero et al., 2007).

The sampled trees were located in a 15-year-old plantation at low density (≈ 312 trees ha^{-1}) with scattered shrub cover (*Cistus ladanifer* L.). The low presence of herbaceous and shrub species allows the existence of a homogeneous root system with abundant fine roots, which in the case of the holm oak rhizosphere, is allocated mainly in the area under the canopy cover (Ruiz-Gómez et al., 2019). In previous studies, it has been found a significant relationship between soil biological components and the rhizosphere under the crown (Gómez-Aparicio et al., 2012; Ibáñez et al., 2015).

Moreover, there was a tendency for the highest concentration of cfu to group under the crown on the northern side, independently of the different slopes present in the studied trees. This aggregation of cfu might be related with the microclimate that the tree crown's shade generates on the ground, driven by differences in nutrients and organic matter. Other authors have reported similar aggregation patterns in soils under holm and cork oaks (Gallardo, 2003; Gea-Izquierdo et al., 2010; Andivia et al., 2015). Furthermore, the greater presence of fine roots under the crown cover (Canadell and Rodà, 1991; Silva and Rego, 2004) agrees with the fine root distribution observed in several Mediterranean oak species (Lopez et al., 1998), and should be considered another relevant driver influencing this cfu distribution pattern. Woody plant cover influences the edaphic properties, as well as the related plant and faunal communities (Gallardo, 2003; Eldridge et al., 2011; Andivia et al., 2015), establishing an important and direct relationship between the fertility and presence of soilborne pathogens and thus influencing the health status of the tree (Gómez-Aparicio et al., 2012; Corcobado, 2013). Moreover, other soil characteristics such as texture, porosity, fertility, organic matter, cultivation methods and the presence of host plants are other factors involved

in the presence of resistant structures in the soil (García Moreno et al., 2016). In our work, some outliers detected in the cfu values outside the crown were closely related to the presence of clusters of *Cistus ladanifer* (data not shown). Those data were not eliminated from the analysis because it might be considered that the effects of the presence of the shrub clusters on the studied variables should be similar to the effect of the presence of the trees (Moreira and Martins, 2005).

The spatial analysis showed that 9 out of the 12 variables analysed with SADIE presented spatial aggregation ($I_a > 1$, $P < 0.05$) in some of the studied trees, and 11 out of the 12 variables did so for the most defoliated tree (#4), but only 6 with significant probability. Results on the spatial distribution of nutrients in the current study agreed with those observed by Gallardo (2003) and Andivia et al. (2015), where all variables showed spatial heterogeneity. Nitrogen and OM tended to be clumped under the crown cover for all trees, except tree 4 in the case of N. The N cycle is closely related to the processes of organic matter in soils, although it seems to be little influenced by the presence of roots and mycorrhizae (Ruiz-Gómez et al., 2019). The soil content of P is also linked to soil biological and chemical processes, and forms clusters under the crown cover in three (trees 1, 2 and 4) of the four trees studied. Roots and mycorrhizae play an important role in the mineralisation of the P in organic matter through the activity of phosphatases (Satyaprakash et al., 2017); thus, the probable extension of roots beyond the crown cover could explain P distribution within and around the crown (Rodà et al., 1999; Shen et al., 2011). In this sense, soil N and P concentrations depend on the rate of mineralisation and their uptake by roots and microorganisms (Gallardo, 2003; Sardans and Peñuelas, 2013), and on the interactions with soil mineral components in the case of P (Delgado-Baquerizo et al., 2013; Sardans and Peñuelas, 2013). Potassium should show less spatial dependence on the tree crown than the rest of the essential elements as it is not linked to the organic soil components; however, it showed aggregation of clusters in trees 3 and 4. These contrasting results among trees may be related with other processes such as the cortical runoff of K leaching from leaves and other aboveground plant organs (Aber and Melillo, 2001; Gallardo, 2003; Sardans and Peñuelas, 2013).

4.2 Concentration of cfu was influenced by the spatial distribution of edaphic variables

The significant correlations between the concentration of cfu and the edaphic variables, clay, P and K, were related to differences in general values and/or significant aggregation patterns with respect to crown cover. These results provide evidence of the influence of crown cover on soil conditions and cfu. The lifecycle of *P. cinnamomi* and other oomycetes is driven by soil conditions, persists in the soil as resistance structures when the conditions are unfavourable, and proliferates through zoospores when soil temperature and moisture are adequate (Corcobado, 2013). Therefore, the influence of crown cover on soil conditions might have an indirect influence on the number of cfu.

For all trees, the concentration of clay was lower under the crown cover. Locations under the tree cover showed higher cfu levels accompanied with lower clay and higher sand percentages. Other studies have reported loam medium texture under crown cover and clay-loam medium texture outside (Brown, 2003). Although the differences in soil texture were significant for the crown cover, the effect of those differences on cfu concentration would be lower than the effect of the presence of fine roots, which are supposed to be concentrated under the crown. The root rot of *Q. ilex* affects mostly the fine roots, the most serious effects being on roots growing in relatively dry soils, eventually undergo short flooding due to extreme precipitation events (Brown, 2003; Oßwald et al., 2014; Burgess et al., 2017). Therefore, it might be considered that the presence of fine roots and soil moisture are more influential environmental drivers for the presence of microorganisms compared with changes in soil texture.

In our study pH and Ca showed a positive correlation with cfu. High concentrations of Ca and high pH values in the soil are related on the literature with the inhibition of the pathogen growth and the accumulation of survival structures of oomycetes (Serrano et al., 2012, 2013; Burgess et al., 2017). However, the overall values we found for pH and Ca did not differ regarding crown position and presented small variations among all the samples. All the soil samples analysed were acidic ($5.1 < pH < 5.5$) and the Ca^{2+} values ranged from 0.56 to 0.78 meq $100g^{-1}$ (from 0.28 to 0.4 mMol Ca each 100 g of soil) (Table 2). The pH was very close to the interval established as the optimum for the development and infection of several soilborne pathogen oomycetes in

laboratory tests, including *P. cinnamomi* (optimum pH between 5.5 and 6.0) (Zentmyer, 1980), and the concentration of Ca was 100 fold lower than the necessary to inhibit the mycelium growth of *P. cinnamomi* on in vitro tests (Serrano et al., 2012). Therefore, Ca and pH should not be considered in our case as factors influencing the distribution of cfu, since the range of Ca and pH values could not produce differences in the behaviour of the pathogen.

The cfu values were predicted to a significant extent by the GLMM using silt and moisture as variables, together with P and K, demonstrating that there is an influence of soil conditions on cfu abundance apart from tree crown influence. The output model might be considered site-specific because it is dependent on a set of microsite characteristics. However, the results suggest that there exists a significant influence of the soil variables contributing to the suitability of the microsite environment for *P. cinnamomi*.

The levels of P and K were significantly different due to crown position, presenting higher values under the tree crown. However, when the influence of crown position was taken out of the analysis, considering it as a random effect in the mixed model, both P and K concentration explained to a significant extent the cfu values. Both P and K were present in higher concentrations under the crown, following the same trend as cfu. Other studies showed that N, P, K, OM and the biomass of microorganisms tend to concentrate under the crown (Gallardo et al., 2000; Cubera and Moreno, 2007). It could be considered that the influence of these soil parameters on the number of cfu is related to the suitability of the microenvironment for oomycetes to complete their lifecycle. Some oomycetes species, including several pathogenic *Phytophthora* spp., have the ability to either survive or complete their lifecycle as saprobes (Hardham, 2005; Cerri et al., 2017; Ruiz Gómez et al., 2019), despite their poor ability to compete with other saprophytic organisms (Dunstan et al., 2010). Therefore, higher levels of organic matter and nutrients might lead to an increase of oomycete resistance structures under a saprophytic environment.

The cfu distribution seems to be favoured mainly by the grouping of silt patches. Silt is considered to equilibrate the clay-sand trend of the soil. Texture and porosity are directly influenced by the silt percentage in intermediate textured soils. In our study, the crown cover did not significantly influence soil moisture or aggregation patterns. However, the mixed model showed that crown cover clearly influenced the cfu abundance. The same occurred with silt, when it was considered as fixed effect in the model. Soils

with higher silt percentage retain more water (Garrido Valero, 1994; Brown, 2003), and with higher water content oomycetes are more readily able to produce sporangia and release zoospores (Jeon et al., 2016; Tecon and Or, 2017). In contrast, as these soils become drier, oomycetes produce resistant survival structures.

5 Conclusions

The distribution of *P. cinnamomi* cfu in soils associated with *Q. ilex* was not random in the soil but showed distribution patterns predictable to some degree, influenced by the crown cover, orientation and the levels of soil moisture and fertility. Our results could be useful to increase the sampling efficiency of the field surveys. Soil sampling searching for *P. cinnamomi* in holm oak dehesas would be oriented to those areas most likely to contain the pathogen identified in our work, allowing a greater number of trees to be sampled. This work also highlights the dynamics of soil properties in the presence of tree cover. Clear differences and aggregated spatial patterns in key soil elements were where shown to be influenced by canopy cover. The cfu tend to concentrate in the North side, probably influenced by the shadow of the crown cover, and in zones with more organic matter, nutrients and well-textured soils. In our case, the influence of the texture was driven mainly by silt concentration due to the low variation of clay and sand in the studied area.

Due to the homogeneity of environmental conditions in the selected plot, the output GLMM must be considered site-specific, but we demonstrate that it is a useful tool to study the influence of soil parameters in the distribution of microbial community due to the elimination of random effects, mainly the influence of canopy cover. The spatial analysis of the biotic and abiotic factors involved in oak root rot processes can be an effective management tool predicting favourable areas regarding spatial heterogeneity, quantification and distribution for those parameters that limit the development of *P. cinnamomi*, thus favouring oak establishment and survival in afforestation practices. However, further research is needed to assess the abundance of *Phytophthora* spp. and other oomycetes in soils with more heterogeneous conditions, in order to clarify whether generalized models can be used to predict cfu amounts, particularly in Mediterranean dehesa and montados ecosystems and in oak afforestation.

6 References

Aber, J.A., Melillo, J.M., 2001. Terrestrial Ecosystems, 2nd ed. Brooks/Cole Publishing, Pacific Grove, California.

Andivia, E., Fernández, M., Alejano, R., Vázquez-Piqué, J., 2015. Tree patch distribution drives spatial heterogeneity of soil traits in cork oak woodlands. Ann. For. Sci. 72, 549–559. https://doi.org/10.1007/s13595-015-0475-8

Aponte, C., Matías, L., González-Rodríguez, V., Castro, J., García, L.V., Villar, R., Marañón, T., 2014. Soil nutrients and microbial biomass in three contrasting Mediterranean forests. Plant Soil 380, 57–72. https://doi.org/10.1007/s11104-014-2061-5

Ashton, M.S., Larson, B.C., 1996. Germination and seedling growth of *Quercus* (section Erythrobalanus) across openings in a mixed-deciduous forest of southern New England, USA. For. Ecol. Manag. 80, 81–94. https://doi.org/10.1016/0378-1127(95)03636-9

Bates, D., Mächler, M., Bolker, B., Walker, S., 2014. Fitting Linear Mixed-Effects Models using lme4. ArXiv14065823 Stat.

Bolker, B.M., Brooks, M.E., Clark, C.J., Geange, S.W., Poulsen, J.R., Stevens, M.H.H., White, J.S.S., 2009. Generalized linear mixed models: a practical guide for ecology and evolution. Trends Ecol. Evol. 24, 127–135. https://doi.org/10.1016/j.tree.2008.10.008

Brown, R.B., 2003. Soil Texture, Fact Sheet SL-29. Soil and Water Science Department, Florida Cooperative Extensión Service, Institute of Food and Agriculture Sciences, University of Florida.

Burgess, T.I., Scott, J.K., Mcdougall, K.L., Stukely, M.J.C., Crane, C., Dunstan, W.A., Brigg, F., Andjic, V., White, D., Rudman, T., Arentz, F., Ota, N., Hardy, G.E.St.J., 2017. Current and projected global distribution of *Phytophthora cinnamomi*, one of the world's worst plant pathogens. Glob. Change Biol. 23, 1661–1674. https://doi.org/10.1111/gcb.13492

Camilo-Alves, C. de S. e P., Clara, M.I.E. da, Ribeiro, N.M.C. de A., 2013. Decline of Mediterranean oak trees and its association with *Phytophthora cinnamomi*: a review. Eur. J. For. Res. 132, 411–432. https://doi.org/10.1007/s10342-013-0688-z

Canadell, J., Rodà, F., 1991. Root biomass of *Quercus ilex* in a montane Mediterranean forest. Can. J. For. Res. 21, 1771–1778. https://doi.org/10.1139/x91-245

Cappai, C., Kemanian, A.R., Lagomarsino, A., Roggero, P.P., Lai, R., Agnelli, A.E., Seddaiu, G., 2017. Small-scale spatial variation of soil organic matter pools generated by cork oak trees in Mediterranean agro-silvo-pastoral systems. Geoderma, 5th International Symposium on Soil Organic Matter 2015 304, 59–67. https://doi.org/10.1016/j.geoderma.2016.07.021

Carranca, C., Castro, I.V., Figueiredo, N., Redondo, R., Rodrigues, A.R.F., Saraiva, I., Maricato, R., Madeira, M.A.V., 2015. Influence of tree canopy on N2 fixation by pasture legumes and soil rhizobial abundance in Mediterranean oak woodlands. Sci. Total Environ. 506–507, 86–94. https://doi.org/10.1016/j.scitotenv.2014.10.111

Cerri, M., Sapkota, R., Coppi, A., Ferri, V., Foggi, B., Gigante, D., Lastrucci, L., Selvaggi, R., Venanzoni, R., Nicolaisen, M., Ferranti, F., Reale, L., 2017. Oomycete Communities Associated with Reed Die-Back Syndrome. Front. Plant Sci. 8. https://doi.org/10.3389/fpls.2017.01550

Corcobado, T., 2013. Influencia de "*Phytophthora cinnamomi*" Rands en el decaimiento de "*Quercus ilex* L." y su relación con las propiedades del suelo y las ectomicorrizas. Universidad de Extremadura, España.

Cubera, E., Moreno, G., 2007. Effect of land-use on soil water dynamic in dehesas of Central–Western Spain. Catena, Soil Water Erosion in Rural Areas 71, 298–308. https://doi.org/10.1016/j.catena.2007.01.005

Delgado-Baquerizo, M., Maestre, F.T., Gallardo, A., Bowker, M.A., Wallenstein, M.D., Quero, J.L., Ochoa, V., Gozalo, B., García-Gómez, M., Soliveres, S., García-Palacios, P., Berdugo, M.,

Valencia, E., Escolar, C., Arredondo, T., Barraza-Zepeda, C., Bran, D., Carreira, J.A., Chaieb, M., Conceição, A.A., Derak, M., Eldridge, D.J., Escudero, A., Espinosa, C.I., Gaitán, J., Gatica, M.G., Gómez-González, S., Guzman, E., Gutiérrez, J.R., Florentino, A., Hepper, E., Hernández, R.M., Huber-Sannwald, E., Jankju, M., Liu, J., Mau, R.L., Miriti, M., Monerris, J., Naseri, K., Noumi, Z., Polo, V., Prina, A., Pucheta, E., Ramírez, E., Ramírez-Collantes, D.A., Romão, R., Tighe, M., Torres, D., Torres-Díaz, C., Ungar, E.D., Val, J., Wamiti, W., Wang, D., Zaady, E., 2013. Decoupling of soil nutrient cycles as a function of aridity in global drylands. Nature 502, 672–676. https://doi.org/10.1038/nature12670

Dunstan, W.A., Rudman, T., Shearer, B.L., Moore, N.A., Paap, T., Calver, M.C., Dell, B., Hardy, G.E.St.J., 2010. Containment and spot eradication of a highly destructive, invasive plant pathogen (*Phytophthora cinnamomi*) in natural ecosystems. Biol. Invasions 12, 913–925. https://doi.org/10.1007/s10530-009-9512-6

Eichhorn, J., Roskams, P., Potočić, N., Timmermann, V., Ferretti, M., Mues, V., Szepesi, A., Durrant, D., Seletković, I., Schroeck, H.-W., Nevalnien, S., Filippo Bussotti, García, P., Wulff, S., 2017. Part IV: Visual assessment of crown condition and damaging agents., in: UNECE ICP Forests Programme Co-ordinating Centre. Manual on methods and criteria for harmonized sampling, assessment, monitoring and analysis of the effects of air pollution on forests. Thünen Institute of Forest Ecosystems, Eberswalde, Germany, p. 54.

Eldridge, D.J., Bowker, M.A., Maestre, F.T., Roger, E., Reynolds, J.F., Whitford, W.G., 2011. Impacts of shrub encroachment on ecosystem structure and functioning: towards a global synthesis. Ecol. Lett. 14, 709–722. https://doi.org/10.1111/j.1461-0248.2011.01630.x

Gallardo, A., 2003. Effect of tree canopy on the spatial distribution of soil nutrients in a Mediterranean Dehesa. Pedobiologia 47, 117–125. https://doi.org/10.1078/0031-4056-00175

Gallardo, A., Rodríguez-Saucedo, J.J., Covelo, F., Fernández-Alés, R., 2000. Soil nitrogen heterogeneity in a Dehesa ecosystem. Plant Soil 222, 71–82. https://doi.org/10.1023/A:1004725927358

García Moreno, A.M., Fernández Rebollo, P., Ortiz Berrocal, F., Carbonero Muñoz, M.D., 2016. Podredumbre radical, descripción y control aplicado a los ecosistemas de dehesa.

Garrido Valero, M.S., 1994. Interpretación de análisis de suelos. Ministerio de Agricultura, Pesca y Alimentación, Madrid.

Gea-Izquierdo, G., Allen-Díaz, B., San Miguel, A., Canellas, I., 2010. How do trees affect spatio-temporal heterogeneity of nutrient cycling in mediterranean annual grasslands? Ann. For. Sci. 67, 112.

Gómez-Aparicio, L., Ibáñez, B., Serrano, M.S., De Vita, P., Ávila, J.M., Pérez-Ramos, I.M., García, L.V., Esperanza Sánchez, M., Marañón, T., 2012. Spatial patterns of soil pathogens in declining Mediterranean forests: implications for tree species regeneration. New Phytol. 194, 1014–1024. https://doi.org/10.1111/j.1469-8137.2012.04108.x

González, M., Romero, M., Ramo, C., Serrano, M.S., Sánchez, M.E., 2017. Control of *Phytophthor*a root rot on Mediteranean *Quercus* spp. Using fosetyl-Al trunk injections. M. http://dx.doi.org/10.13039/501100000780

González-Alonso, C., 2008. Analysis of the oak decline in Spain; la seca (Bachelor Thesis in Forest Management). Swedish University of Agricultural Sciences, SLU - Uppsala.

Hardham, A.R., 2005. *Phytophthora cinnamomi*. Mol. Plant Pathol. 6, 589–604. https://doi.org/10.1111/j.1364-3703.2005.00308.x

Hazra, A., Gogtay, N., 2016. Biostatistics Series Module 3: Comparing Groups: Numerical Variables. Indian J. Dermatol. 61, 251–260. https://doi.org/10.4103/0019-5154.182416

Hüberli, D., Tommerup, I.C., Hardy, G.E.St.J., 2000. False-negative isolations or absence of lesions may cause mis-diagnosis of diseased plants infected with *Phytophthora cinnamomi*. Australas. Plant Pathol. 29, 164–169. https://doi.org/10.1071/AP00029

Ibáñez, B., Gómez-Aparicio, L., Ávila, J.M., Pérez-Ramos, I.M., García, L.V., Marañón, T., 2015. Impact of tree decline on spatial patterns of seedling-mycorrhiza interactions: Implications for regeneration dynamics in Mediterranean forests. For. Ecol. Manag. 353, 1–9. https://doi.org/10.1016/j.foreco.2015.05.014

Jeon, S., Krasnow, C.S., Kirby, C.K., Granke, L.L., Hausbeck, M.K., Zhang, W., 2016. Transport and Retention of *Phytophthora capsici* Zoospores in Saturated Porous Media. Environ. Sci. Technol. 50, 9270–9278. https://doi.org/10.1021/acs.est.6b01784

Jiménez, J.J., Serrano, M.S., Vicente, M., Fernández, P., Trapero Casas, A., Sánchez Hernández, E., 2008. Nuevas especies de *Pythium* que causan podredumbre radical de *Quercus* en España y Portugal. Bol. Sanid. Veg. Plagas 34 549-562 2008.

Jung, T., Orlikowski, L., Henricot, B., Abad-Campos, P., Aday, A.G., Aguín Casal, O., Bakonyi, J., Cacciola, S.O., Cech, T., Chavarriaga, D., Corcobado, T., Cravador, A., Decourcelle, T., Denton, G., Diamandis, S., Doğmuş-Lehtijärvi, H.T., Franceschini, A., Ginetti, B., Green, S., Glavendekić, M., Hantula, J., Hartmann, G., Herrero, M., Ivic, D., Horta Jung, M., Lilja, A., Keca, N., Kramarets, V., Lyubenova, A., Machado, H., Magnano di San Lio, G., Mansilla Vázquez, P.J., Marçais, B., Matsiakh, I., Milenkovic, I., Moricca, S., Nagy, Z.Á., Nechwatal, J., Olsson, C., Oszako, T., Pane, A., Paplomatas, E.J., Pintos Varela, C., Prospero, S., Rial Martínez, C., Rigling, D., Robin, C., Rytkönen, A., Sánchez, M.E., Sanz Ros, A.V., Scanu, B., Schlenzig, A., Schumacher, J., Slavov, S., Solla, A., Sousa, E., Stenlid, J., Talgø, V., Tomic, Z., Tsopelas, P., Vannini, A., Vettraino, A.M., Wenneker, M., Woodward, S., Peréz-Sierra, A., 2016. Widespread *Phytophthora* infestations in European nurseries put forest, semi-natural and horticultural ecosystems at high risk of *Phytophthora* diseases. For. Pathol. 46, 134–163. https://doi.org/10.1111/efp.12239

Lehtijärvi, A., Aday Kaya, A.G., Woodward, S., Jung, T., Doğmuş Lehtijärvi, H.T., 2017. Oomycota species associated with deciduous and coniferous seedlings in forest tree nurseries of Western Turkey. For. Pathol. 47, e12363. https://doi.org/10.1111/efp.12363

Lopez, B., Sabate, S., Gracia, C., 1998. Fine roots dynamics in a Mediterranean forest: effects of drought and stem density. Tree Physiol. 18, 601–606. https://doi.org/10.1093/treephys/18.8-9.601

Maestre, F.T., Quero, J.L., 2008. Análisis espacial mediante índices de distancia (SADIE), in: Introducción al Análisis Espacial de Datos En Ecología y Ciencias Ambientales: Métodos y Aplicaciones. Universidad Rey Juan Carlos, Madrid, pp. 637–648.

Marais, L.J., Menge, J.A., Bender, G.S., Feber, B., 2002. *Phytophthora* root rot. Avoresearch Calif. Avocado Comm. Publ. 2.

Mauer, O., Houškova, K., Mikita, T., 2017. The root system of pedunculate oak (*Quercus robur* L.) at the margins of regenerated stands. J. For. Sci. 63, 22–33. https://doi.org/10.17221/85/2016-JFS

Moreira, A.C., Martins, J.M.S., 2005. Influence of site factors on the impact of *Phytophthora cinnamomi* in cork oak stands in Portugal. For. Pathol. 35, 145–162. https://doi.org/10.1111/j.1439-0329.2005.00397.x

Navarro Cerrillo, R.M., Fernández Rebollo, P., Trapero, A., Caetano, P., Romero, M.A., Sánchez, M.E., Fernández Cancio, A., Sánchez, I., López Pantoja, G., 2004. Los procesos de decaimiento de encinas y alcornoques. Dirección General de Gestión del Medio Natural. Consejería de Medio Ambiente. Junta de Andalucía., Sevilla.

Navarro-Cerrillo, R.M., Varo-Martínez, M.Á., Acosta, C., Palacios Rodriguez, G., Sánchez-Cuesta, R., Ruiz Gómez, F.J., 2019. Integration of WorldView-2 and airborne laser scanning data to classify defoliation levels in *Quercus ilex* L. Dehesas affected by root rot mortality: Management implications. For. Ecol. Manag. 451, 117564. https://doi.org/10.1016/j.foreco.2019.117564

Oßwald, W., Fleischmann, F., Rigling, D., Coelho, A.C., Cravador, A., Diez, J., Dalio, R.J., Horta Jung, M., Pfanz, H., Robin, C., Sipos, G., Solla, A., Cech, T., Chambery, A., Diamandis, S., Hansen, E.,

Jung, T., Orlikowski, L.B., Parke, J., Prospero, S., Werres, S., 2014. Strategies of attack and defence in woody plant–*Phytophthora* interactions. For. Pathol. 44, 169–190. https://doi.org/10.1111/efp.12096

Pérez-Sierra, A., López-García, C., León, M., García-Jiménez, J., Abad-Campos, P., Jung, T., 2013. Previously unrecorded low-temperature *Phytophthora* species associated with *Quercus* decline in a Mediterranean forest in eastern Spain. For. Pathol. 43, 331–339. https://doi.org/10.1111/efp.12037

Perry, J.N., Dixon, P.M., 2002. A new method to measure spatial association for ecological count data. Écoscience 9, 133–141. https://doi.org/10.1080/11956860.2002.11682699

Quero, J.L., 2006. La heterogeneidad en ecología: herramientas de cuantificación y aplicaciones para la restauración. Acta Granatense 4/5, 107–114.

Quero, J.L., Maestre, F.T., Ochoa, V., García-Gómez, M., Delgado-Baquerizo, M., 2013. On the Importance of Shrub Encroachment by Sprouters, Climate, Species Richness and Anthropic Factors for Ecosystem Multifunctionality in Semi-arid Mediterranean Ecosystems. Ecosystems 16, 1248–1261. https://doi.org/10.1007/s10021-013-9683-y

R Development Core Team, 2017. R: A language and environment for statistical computing. R Foundation for Statistical Computing, Vienna, Austria. 2016.

Rodà, F., Retana, J., Gracia, C.A., Bellot, J., 1999. Ecology of Mediterranean Evergreen Oak Forests. Springer Science & Business Media, Verlag Berlin (Germany).

Rodríguez, M., Sánchez, M.E., Trapero, A., 2004. Desarrollo de un método eficaz para la cuantificación de *Phytophthora cinnamomi* en muestras de suelo, in: XII Congreso de La Sociedad Española de Fitopatología. Presented at the PB-32, Lloret de Mar, Girona (Spain).

Rohlf, F.J., Sokal, R.R., 1981. Statistical tables. W. H. Freeman, San Francisco, California, USA.

Romero, M.A., Sánchez, J.E., Jiménez, J.J., Belbahri, L., Trapero, A., Lefort, F., Sánchez, M.E., 2007. New *Pythium* Taxa Causing Root Rot on Mediterranean *Quercus* Species in South-west Spain and Portugal. J. Phytopathol. 155, 289–295. https://doi.org/10.1111/j.1439-0434.2007.01230.x

Ruiz Gómez, F., Pérez-de-Luque, A., Sánchez-Cuesta, R., Quero, J., Navarro Cerrillo, R., 2018. Differences in the response to acute drought and *Phytophthora cinnamomi* Rands Infection in *Quercus ilex* L. seedlings. Forests 9, 634. https://doi.org/10.3390/f9100634

Ruiz Gómez, F.J.R., Navarro-Cerrillo, R.M., Pérez-de-Luque, A., Oβwald, W., Vannini, A., Morales-Rodríguez, C., 2019. Assessment of functional and structural changes of soil fungal and oomycete communities in holm oak declined dehesas through metabarcoding analysis. Sci. Rep. 9, 5315. https://doi.org/10.1038/s41598-019-41804-y

Ruiz-Gómez, F.J., Navarro Cerrillo, R.M., Lara Gómez, M.A., Sánchez-Cuesta, R., 2016. Aislamiento e identificación de oomicetos en focos de podredumbre radical de Andalucía y Extremadura, in: III Reunión del Grupo de Trabajo de Sanidad Forestal. Presented at the Decaimiento, Cuad. Soc. Esp. Cienc. For., Madrid, pp. 363–376.

Ruiz-Gómez, F.J., Navarro-Cerrillo, R.M., Pérez-de-Luque, A., Oβwald, W., Vannini, A., Morales-Rodríguez, C., 2019. Assessment of functional and structural changes of soil fungal and oomycete communities in holm oak declined dehesas through metabarcoding analysis. Sci. Rep. 9, 5315. https://doi.org/10.1038/s41598-019-41804-y

Sánchez, M., Caetano, P., Ferraz, J., Trapero, A., 2002. *Phytophthora* disease of *Quercus ilex* in south-western Spain. For. Pathol. 32, 5–18.

Sánchez, M.E., Caetano, P., Ferranz, J., Trapero Casas, A., 2000. El decaimiento y muerte de encinas en tres dehesas de la provincia de Huelva. Bol. Sanid. Veg. Plagas 26 4 447-464 2000.

Sardans, J., Peñuelas, J., 2013. Plant-soil interactions in Mediterranean forest and shrublands: impacts of climatic change. Plant Soil 365, 1–33. https://doi.org/10.1007/s11104-013-1591-6

Satyaprakash, M., Nikitha, T., Reddi, E.U.B., Sadhana, B., Vani, S.S., 2017. Phosphorous and phosphate solubilising bacteria and their role in plant nutrition. Int J Curr Microbiol App Sci 6, 2133–2144.

Schielzeth, H., 2010. Simple means to improve the interpretability of regression coefficients: Interpretation of regression coefficients. Methods Ecol. Evol. 1, 103–113. https://doi.org/10.1111/j.2041-210X.2010.00012.x

Serrano, M.S., De Vita, P., Fernández-Rebollo, P., Sánchez-Hernández, M.E., 2012. Calcium fertilizers induce soil suppressiveness to *Phytophthora cinnamomi* root rot of *Quercus ilex*. Eur. J. Plant Pathol. 132, 271–279. https://doi.org/10.1007/s10658-011-9871-6

Serrano, M.S., Fernández-Rebollo, P., De Vita, P., Sánchez, M.E., 2013. Calcium mineral nutrition increases the tolerance of *Quercus ilex* to *Phytophthora* root disease affecting oak rangeland ecosystems in Spain. Agrofor. Syst. 87, 173–179. https://doi.org/10.1007/s10457-012-9533-5

Serrano, M.S., Leal, R., Vita, P.D., Fernández-Rebollo, P., Sánchez, M.E., 2014. Control of *Phytophthora cinnamomi* by soil application of calcium fertilizers in a Dehesa ecosystem in Spain. Integr. Prot. Oak For. IOBC-WPRS Bull. 101, 139–143.

Shen, J., Yuan, L., Zhang, J., Li, H., Bai, Z., Chen, X., Zhang, W., Zhang, F., 2011. Phosphorus Dynamics: From Soil to Plant. Plant Physiol. 156, 997–1005. https://doi.org/10.1104/pp.111.175232

Silva, J.S., Rego, F.C., 2004. Root to shoot relationships in Mediterranean woody plants from Central Portugal. Biologia (Bratisl.) 59, 109–115.

Simón, N., Montes, F., Díaz-Pinés, E., Benavides, R., Roig, S., Rubio, A., 2013. Spatial distribution of the soil organic carbon pool in a Holm oak dehesa in Spain. Plant Soil 366, 537–549. https://doi.org/10.1007/s11104-012-1443-9

Tecon, R., Or, D., 2017. Biophysical processes supporting the diversity of microbial life in soil. FEMS Microbiol. Rev. 41, 599–623. https://doi.org/10.1093/femsre/fux039

Trapero, A., Sánchez, M.E., Pérez de Algaba, A., Romero, M.A., Navarro, N., Varo, R., Gutiérrez, J., 2000. Enfermedades de especies forestales en Andalucía. Agricultura 821.

Vadell, E., de-Miguel, S., Pemán, J., 2016. Large-scale reforestation and afforestation policy in Spain: A historical review of its underlying ecological, socioeconomic and political dynamics. Land Use Policy 55, 37–48. https://doi.org/10.1016/j.landusepol.2016.03.017

Vettraino, A.M., Barzanti, G.P., Bianco, M.C., Ragazzi, A., Capretti, P., Paoletti, E., Luisi, N., Anselmi, N., Vannini, A., 2002. Occurrence of *Phytophthora* species in oak stands in Italy and their association with declining oak trees. For. Pathol. 32, 19–28. https://doi.org/10.1046/j.1439-0329.2002.00264.x

Winder, L., Alexander, C., Griffiths, G., Holland, J., Woolley, C., Perry, J., 2019. Twenty years and counting with SADIE: Spatial Analysis by Distance Indices software and review of its adoption and use. Rethink. Ecol. 4, 1–16. https://doi.org/10.3897/rethinkingecology.4.30890

Zamora Rojas, E., Andicoberry de los reyes, S., Sánchez Clemente, M.E., 2014. ANEXO A.1. IV EL DECAIMIENTO Y LA PODREDUMBRE RADICAL EN LAS DEHESAS ANDALUZAS, in: Ecosistemas de Dehesa: Desarrollo de Políticas y Herramientas Para La Gestión y Conservación de La Biodiversidad (Life Biodehesa Project). Consejería de Medio Ambiente y Ordenación del territorio, Sevilla (Spain).

Zentmyer, G.A., 1980. *Phytophthora cinnamomi* and the diseases it causes. Monograph, American Phytopathological Society, Univ. California, Riverside, USA.

Capítulo 3

La incidencia de *Phytophthora cinnamomi* en las forestaciones de *Quercus* depende más de las características de sitio que de la disponibilidad de huéspedes

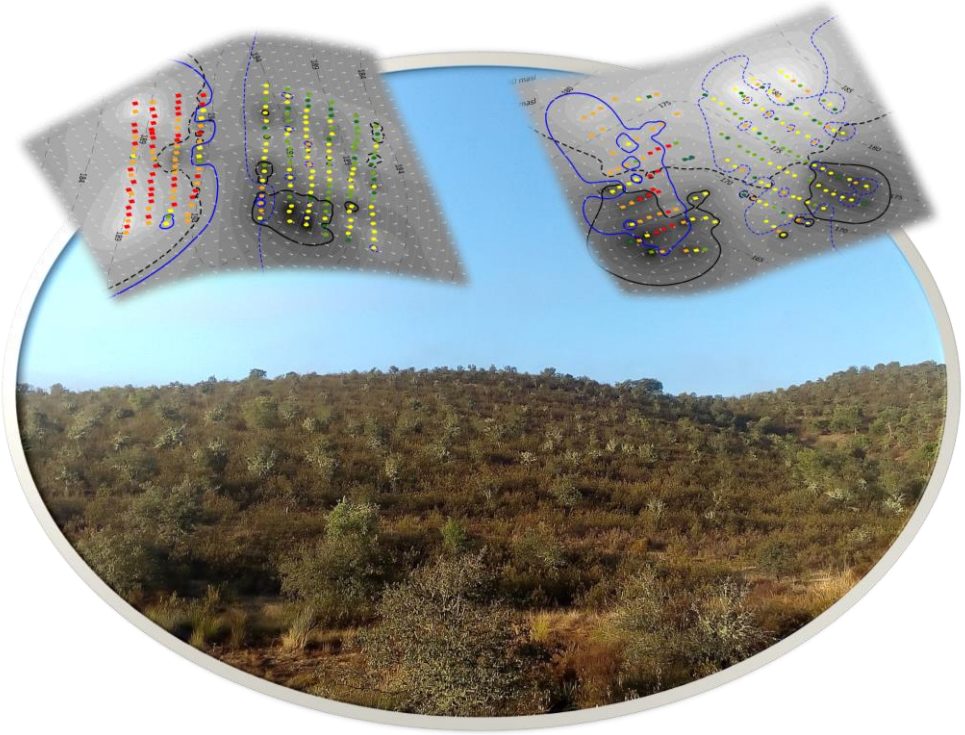

Sánchez-Cuesta, R., González-Moreno, P., Cortés-Márquez, A., Navarro-Cerrillo, R.M., Ruiz-Gómez, F.J., **2022**. *Phytophthora cinnamomi* occurrence in oak afforestation depends on site characteristics rather than on host availability. *New Forests* (Submitted).

Resumen

El decaimiento y la mortalidad de las especies de *Quercus* en todo el mundo se interpreta a través de las interacciones de varios factores en el espacio y el tiempo. Entre estos factores, *Phytophthora cinnamomi* ha sido identificado como uno de los principales agentes bióticos que desencadenan la mortalidad de *Quercus ilex* y *Q. suber* en la Cuenca Mediterránea. Sin embargo, hay pocos ejemplos en la literatura que estudien la interacción entre *P. cinnamomi* y los factores ambientales del lugar o que evalúen los efectos de los factores ambientales sobre el sistema huésped-patógeno. En este estudio examinamos cómo las características y la distribución espacial del suelo y la topografía influyen en los efectos de *P. cinnamomi* sobre el estado fitosanitario de las plantaciones de encinas y alcornoques utilizando el Análisis Espacial mediante Índices de Distancia (SADIE) y el Modelo de Ecuaciones Estructurales (SEM). Los resultados mostraron la alta influencia del suelo (textura, nutrientes, composición química y humedad) y la topografía (orientación, incidencia solar e hidrología) sobre la abundancia del patógeno, así como la menor susceptibilidad del alcornoque, pero más relacionada con la presencia de inóculo que la de la encina. Estos resultados pusieron de manifiesto los beneficios de las forestaciones mixtas en comparación con las monoespecíficas, aumentando la resiliencia de la forestación, y la importancia de una escala precisa para la caracterización del suelo y la topografía que evite el fracaso de la forestación.

Abstract

Decline and mortality of *Quercus* species worldwide is interpreted through the interactions of several factors in space and time. Among these factors, *Phytophthora cinnamomi* has been identified as a major biotic agent triggering mortality of *Quercus ilex* and *Q. suber* in the Mediterranean basin. However, there are few examples in the literature studying the interaction between *P. cinnamomi* and site environmental factors or assessing effects of environmental drivers over the host-pathogen system. In this study we examined how both characteristics and spatial distribution of soil and topography influence the effects of *P. cinnamomi* over the phytosanitary status of holm and cork oak plantations using Spatial Analysis by Distance Indices (SADIE) and Structural Equation Modelling (SEM). Results showed the high influence of soil (texture, nutrients, chemical composition, and moisture) and topography (orientation, solar incidence, and hydrology) over the pathogen abundance, as well as lower susceptibility of cork oak, but more related to the inoculum presence than holm oak. These results highlighted the benefits of mixed afforestation compared with monospecific ones, increasing afforestation resilience, and the importance of a precise scale for the characterization of soil and topography preventing afforestation failure.

Keywords: Oak afforestation, *dehesa*, oak decline, *Phytophthora cinnamomi*, SADIE, Structural Equation Models

1 Introduction

Oaks are amongst the most diverse and widespread genus in the Northern hemisphere, with some sclerophyllous species well adapted to Mediterranean ecosystems. Holm oak (*Quercus ilex* L.) and cork oak (*Quercus suber* L.) are the dominant oak species in the Mediterranean Basin, representing an outstanding example of ecological and socio-economic sustainability of forest ecosystems (Moreno and Pulido, 2009; Ruiz-Gómez et al., 2019). Both species are currently threatened by oak decline, a global issue particularly relevant in Mediterranean ecosystems, which represents one of the main threats for these ecosystems in a context of global change (Burgess et al., 2017). This worldwide phenomenon is explained through the interactions of environmental factors and biotic agents at different temporal and spatial scales (Rodríguez-Calcerrada et al., 2017; Sánchez-Cuesta et al., 2021). Although those events are complex processes, some biotic agents involved in the syndrome presents simple – and identifiable – aetiology (de Sampaio e Paiva Camilo-Alves et al., 2013). Among the latter, the root rot caused by soilborne oomycetes is considered the most damaging disease in northern hemisphere oak forests. Specially, *Phytophthora cinnamomi* is a cosmopolitan soilborne pathogen, occurring in a wide variety of ecosystems, mostly in warm-temperate and dry forests worldwide, causing its most severe impacts in Mediterranean-type climates (Burgess et al., 2017). It is the case of oak forests of the western Iberian Peninsula, *P. cinnamomi* is a major threat for the sustainability of holm and cork oak Mediterranean Savannah-like rangelands (*dehesas*) (Ruiz-Gómez et al., 2019). Like other soilborne oomycetes, *P cinnamomi* produces asexual motile spores with flagellum (zoospores) which allows them to move in the soil through water (Hardham and Blackman, 2018). It develops several survival structures able to persist in decaying plants and in bulk soil for long periods (Crone et al., 2013), giving to this species a relevant high dispersal capacity.

On the other hand, environmental abiotic factors are key drivers in decline processes (Manion and Lachance, 1992). Abiotic stressors such as drought might be the main cause of oak decline outbreaks (Gentilesca et al., 2017), as well pathogen effects on plant community dynamics are generally dependent on abiotic factors (Colangelo et al., 2018; Eck et al., 2019). Despite its relevance, their influence in oak decline have been scarcely studied in water-limited Mediterranean ecosystems (Gómez-Aparicio et al., 2017; Homet

et al., 2019; Domínguez-Begines et al., 2020; Sánchez-Cuesta et al., 2021). Previous studies suggest that the environmental factors influenced plant-pathogen relationship leading to direct and indirect effects, prompting the need to consider them in a context of local environmental conditions. For instance, plant emergence after suppressing pathogen activity through fungicide applications was modulated by water availability (Domínguez-Begines et al., 2020), showing this factor different influence in 6 months-old seedlings mortality (Ruiz-Gómez et al., 2018). Site conditions, such as slope, aspect and soil characteristics are other abiotic factors with major influence on the water retention capacity and soil dynamics modulating habitat suitability for *P. cinnamomi* This is strongly affected by environmental conditions at scales of few meters, including also aboveground vegetation, light availability, and soil chemical composition (Sánchez-Cuesta et al., 2020). Therefore, abiotic factors influence oak physiology both in a direct manner (e.g., water and nutrient availability), and indirectly (e.g., slope and hidrology) by their influence over the suitability of soil environment for *P. cinnamomi* (Cardillo et al., 2018; Sena et al., 2018; Fernández-Habas et al., 2019).

To increase the knowledge of direct and indirect effects of biotic and abiotic factors in oak decline, it is necessary to assess changes on the plant-pathogen interaction along contrasting site conditions while keeping the vegetation structure. In this regard, an oak afforestation infested by *P. cinnamomi* with contrasting local environmental conditions would be a good model for unravelling the landscape dynamics of soilborne pathogen oomycetes related with site characteristics. In this study we examined how both characteristics and spatial distribution of soil and topography influence the effects of *P. cinnamomi* over the phytosanitary status of holm and cork oak plantations using Spatial Analysis by Distance Indices (SADIE) and Structural Equation Modelling (SEM). To achieve our goals, we established two specific objectives: (1) testing spatial variation and aggregation in the inoculum abundance of *P. cinnamomi,* tree health status (defoliation and mortality) and environmental conditions including soil, topography, and tree cover features; (2) finding the key interacting drivers (i.e., soil, topography, and *P. cinnamomi* occurrence) related to defoliation and mortality over cork oak and holm oak afforestation. Our results will provide a useful approach for distinguishing microsite mechanisms related to damage associated to *Phytophthora cinnamomi* and their impact on the suitability of afforestation practices in areas affected by oak decline.

2 Material and methods

2.1 Study site

This study was conducted in a homogeneous afforestation of *Quercus ilex* and *Q. suber* (490 ha) established in 1995 and located in Puebla de Guzmán (Andalusia- southern Spain, coordinates ETRS89, UTM29N: 650 000 m E, 4 160 000 m N, Figure 1).

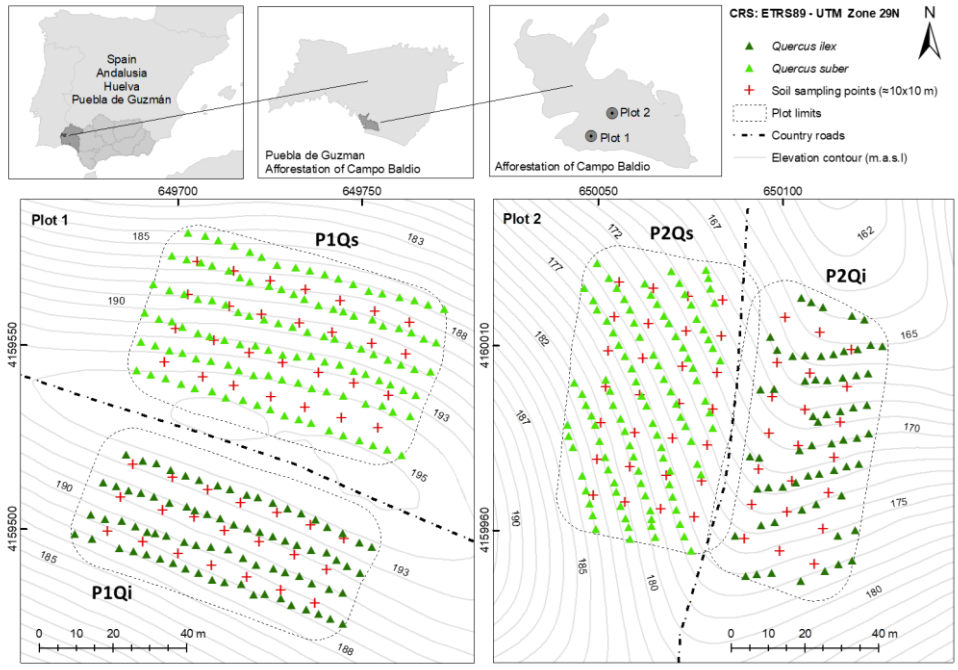

Figure 1. Location, appearance, and layout of study plots P1 (left) and P2 (right). Distribution of soil sampling points (red crosses) and *Q. ilex* (dark green triangles) and *Q. suber* (light green triangles). (Campo Baldío afforestation – Puebla de Guzmán – Huelva – Spain).

Elevation ranges between 120 and 221 m a.s.l., on low to moderate slope (0-18%). Climate is characterized as dry thermo-Mediterranean with hot and dry summers and mild winters. Mean monthly air temperature varies between 16.8 °C to 27 °C, with an average annual rainfall of 570 mm, presenting a drier season (monthly rainfall below 50 mm) from June to September. Soils are in general acid and shallow, with superficial presence of slate and schists, scarcity of free calcium carbonate and low superficial content of organic matter. Aboveground vegetation is mainly conformed by a

mixture of native herbaceous species and shrubs of *Cistus* spp. A holm and cork oaks afforestation were carried out in 1995, with a 5x6 m planting frame (density 330 trees ha^{-1}). Cork oaks were planted mainly in northern side of hills attending to their lesser ecological suitability coping with hydric stress, being the rest of the surface occupied by holm oak. The planting was performed after intensive soil preparation, using disc harrows (20 cm depth) followed by linear subsoiling with a shank (40 cm depth) along the planting line. No fertilization or irrigation was carried out over the afforestation (Lara-Gómez et al., 2020).

2.2 Experimental design

In March 2010, two plots (P_1 and P_2) were established in the study area, searching for soil and vegetation homogeneity (slope, aspect, and soil conditions in each plot), but also for representativity of the differences in the environmental conditions (Figure 1). Plots were established in areas of contact between *Q. ilex* and *Q. suber*, separated by a central boundary in P1 dividing north and south aspect, and by a central runoff in P2. Each plot was then divided in two subplots, those including only holm oak trees (P_1Qi, P_2Qi) and those including only cork oak trees (P_1Qs, P_2Qs). Plots were located searching for the wider differences in aspect for each species between the two subplots, south for *Q. ilex*-P_1Qi and northwest for P_2Qi; and north for *Q. suber*, P1Qs and northeast for P_2Qs subplots.

A permanent grid of 49 quadrats (10x10 m, approximately) was established in each plot with a Manual Total Station (Leica FlexLine TS03), comprising 28 sectors within the cork oak subplots and 21 sectors for holm oak. Trees that entered the 10-meter influence zone around each grid with a tolerance of 5 cm were included on the study plots (P_1Qi = 78 trees; P_1Qs = 119 trees; P_2Qi = 61 trees; P_2Qs = 101 trees). A total of 359 trees were evaluated (Figure 1).

The topographic characteristics of plots were analysed using digital elevation model (DEM), slope, aspect, and solar radiation in raster format (5x5 m pixel resolution for DEM, and 10x10 m for the rest, represented in the coordinate system ETRS89, projected in UTM for time zone 30N – EPSG: 25830) downloaded from the Andalusian Environmental Information Network – REDIAM (https://descargasrediam.cica.es) (Supplementary Material, Table S3.1). Raster information were resampled to a resolution of 0.5×0.5 m trough Inverse Distance Weight (IDW) method (Output cell size:

0.5; Power: 2; Search radius: variable; Number of points – 12; Maximum distance: length of the extent's diagonal) (Bartier and Keller, 1996), and topographic values were extracted from resulting rasters for each sampling point and tree using geoprocessing tools in QGis 3.16 (QGIS.org, 2022).

2.3 Tree status characterization

In April 2010 and April 2018, field campaigns for data collection were carried out. The diameter at breast height (1.3 m; DBH, cm) and height (H, m) of all trees in the plots were measured using a caliper (Haglöf Mantax caliper, Långsele, Sweden) and a Vertex (Haglöf Vertex III and Transponder T3, Långsele, Sweden) (Supplementary Material, Table S3.1-S3.2). Crown defoliation (Def, %) was determined following the classification of ICP Forest-European Network methodology (Ferretti et al., 1994; Eichhorn et al., 2016), and trees classified (Defoliation Class – DC) in five categories: DC-0 (no defoliation ≤ 10%), DC-1 (10 < light defoliation ≤ 25%), DC-2 (25 < moderate defoliation ≤ 60%), DC-3 (60 < severe defoliation ≤ 99%) and DC-4 (dead = 100%) (Table 1). Trees presented symptoms of oak decline, mainly in holm oaks with mean defoliation values in *Q. ilex* increasing from 30% in 2010 to 81% in 2018, and from 13% in 2010 to 35% in 2018 in *Q. suber*. *Phytophthora cinnamomi* was identified in the soil through molecular analyses (Newbiotechnic S.A., NBT - No. 41/04/PR/PSX). In 2010, no tree mortality was recorded in the study plots. During the process of phytosanitary tree assessment, no damage by other biotic or abiotic agents differing of *P. cinanmomi* was observed in both 2010 and 2018 field campaigns.

2.4 Soil sampling and processing

In April 2010, soil samples were taken in the centre of each of the 49 quadrats to carry out the soil physicochemical analysis and the quantification of the amount of oomycetes inoculum (colony forming units, cfu) (Figure 1). At each sampling point, the soil top layer, including litter and decomposing organic matter, was first removed on a 30x30 cm square and then a soil cores of 30 cm length and 9 cm diameter were taken. Cores were stored in plastic containers and preserved at 4-6 ºC during its transfer to the laboratory.

The soil samples were processed in laboratory following the same protocol of Sánchez-Cuesta et al. (2020); samples were air-dried at room temperature for 48 h and then homogenized by hand, eliminating the rough fraction after mechanical milling, and crushing, and passed through a 2-mm-Ø

sieve. One aliquot of approximately 100 g was separated for quantification of cfu, and other aliquot of approximately 500 g, was used for the determination of 23 different edaphic variables. Analyses were carried out by the Agri-food laboratory of Cordoba (Junta de Andalucía, Spain) and in the laboratory of the ERSAF group (Forest Engineering Department, University of Córdoba, Spain). (Supplementary Material, Table S3.1).

Additionally, volumetric water content (VWC) was measured in all sampling points, at a depth of 12 cm, at three times during 2010 (May, July, and December) (Supplementary Material, Table S3.1) using a Time Domain Reflectometry (TDR) sensor (TDR mod 100, Spectrum Technologies, Inc., Plainfield, IL, USA).

2.5 Quantification of cfu

Colony forming units were estimated following the same methodology described in Sánchez-Cuesta et al. (2020). Briefly, ten grams of fine fraction of the homogenized soil were suspended in 100 ml 0.2% agar solution. and placed on NARPH selective medium (10 technical repetitions for each soil sample). Subsequently, plates were incubated at room temperature in darkness for 24 h before removing soil suspension. Colonies growing on each plate were counted after an additional 72 h of incubation with a light contrast with a 10x1 magnifying glass (Nikon SMZ800, Nikon Corp., Tokyo, Japan). The inoculum abundance was calculated as the sum of the colonies for the 10 plates per sample and expressed as cfu g^{-1} of dry soil.

2.6 Statistical analysis

Normality of site variables (Kolmogorov-Smirnov test with Lilliefors correction, $n > 50$, $P < 0.05$; Shapiro-Wilk test, $n \leq 50$, $P < 0.05$) and homoscedasticity (Levene test, $P < 0.05$) were tested. Variables that did not fit the normal distribution were transformed by square root, inverse and logarithmic functions and normality and homoscedasticity were tested again. The differences of means between subplots (P_1Qi-P_1Qs-P_2Qi-P_2Qs) for variables with normal distribution and homoscedastic were analysed using one-way analysis of variance (ANOVA, $P < 0.05$), corrected by Bonferroni's procedure ($P < 0.0083$). When the variables fit to a normal distribution but were heteroscedastic the difference among treatments was analysed using Tamhane test ($P < 0.05$). The comparison of means between species (Qi-Qs) for variables with normal distribution and homoscedasticity was analysed

using Student's *t*-test ($P < 0.05$). When the variables fit to a normal distribution but were heteroscedastic the comparison of means was analysed using Welch's *t*-test. In the case of non-normal variables (percentage of defoliation, cfu, C/N ratio, Ca, percentage of soil moisture, DEM, orientation and solar), the Kruskal-Wallis test (H, $P < 0.05$) and the Mann-Whitney U test for independent group pairs with Bonferroni correction ($P < 0.0083$) were applied.

The relationships among tree characteristics, defoliation and cfu interpolated at tree level (IDW method, Output cell size: 0.5; Power: 2; Search radius: variable; Number of points: 12; Maximum distance: length of the extent's diagonal), and environmental variables (e.g., soil characteristics and topography) were evaluated with the non-parametric Spearman rho coefficient (ρ) at 5% significance level ($P < 0.05$).

The spatial patterns of the studied variables were analysed using Spatial Analysis by Distance Indices (SADIE), implemented in the program "SADIEShell v2.0" (Perry, 1995; Perry et al., 1996) and the aggregation index (I_a) and clustering index (ν) were calculated per plot following the methodology indicated in Sánchez-Cuesta et al (2020). The index ν, which measures the degree of clustering of the data, showing patches ($\nu_i \geq 1.5$) and gaps ($\nu_j \leq -1.5$) was contoured by kriging in a two-dimensional map showing their spatial distribution using Surfer 10.1 (Golden Software, Colorado, USA). An independent SADIE analysis was performed for each variable. Afterwards the mean values of aggregation index (I_a) for all the variables in the study area were calculated.

To test both the structure of the overall relationship between drivers and response variables, and between each pair of variables, Structural Equation Modelling (SEM) analysis was performed. SEM provides information about the fit of a putative multivariate model as well as parameterization of specific relationships between model drivers and dependent variables (Sutton-Grier et al., 2010). The analysis was carried out at tree level for the whole dataset and for the two subsets considering the different species (Overall dataset, dataset for only *Q. ilex* plots and dataset for only *Q. suber* plots). To reduce the high number of environmental variables, five different latent variables were determined for each of the main environmental characteristic groups (topographic characteristics – Topographic –, soil chemical composition – Chemical –, soil macro and micro-nutrients – Nutrients –, soil humidity – Moisture –, and physical properties of soil –

Physical –, Supplementary material, Table S3.1). The characteristics composing each latent variable were the most representative variables for each natural group of each dataset, chosen using Principal Component Analysis (PCA) (Table 1).

Table 1. Latent variables for the three SEM analyses carried out. Analysis means the dataset used for the analysis (Overall: All the data together; *Q. ilex*: Only data for *Q. ilex* subplots; *Q. suber*: Only data for *Q. suber* subplots). N. of comp.: Number of components retained for the PCA optimum solution without rotation (eigenvalue above 1). Cum. Var.: Percentage of the variance of the dataset explained by the retained components (eigenvalue above 1). The symbol =~ refers to the latent variable construction in the R-code of Lavaan R package.

Analysis	Latent variables	N. of comp.	Cum. Var.
Overall	Topographic =~ DEM + Orien + Solar	1	58.08%
	Chemical =~ CEC + pH + C/N + SOC	1	66.27%
	Nutrients =~ Ca + P + Cu + Mn + N	1	75.40%
	Physical =~ Fden + Fine + Sand + Silt	1	72.04%
	Moisture =~ M_5 + M_7	2	81.44%
Q. ilex	Topographic =~ Orien + Solar	2	85.49%
	Chemical =~ CEC + OM + SOC + pH	1	83.00%
	Nutrients =~ Ca + K + Cu + Zn + Mn	1	73.02%
	Physical =~ Root + Fine + Sand + Silt	1	72.46%
	Moisture =~ M_7	1	65.38%
Q. suber	Topographic =~ DEM + Slope	1	76.32%
	Chemical =~ CEC + SOC + pH	1	74.13%
	Nutrients =~ Ca + Cu + Fe + Mn	1	77.96%
	Physical =~ Fine + Tden + Clay + Sand	1	78.51%
	Moisture =~ M_5 + M_7	1	65.37%

For each group, only variables with communality over 0.6 for the principal components with eigenvalues over 1, and without collinearity problems were retained. To ensure representativity of latent variables they were only considered for the SEM analysis when the first component resulting of the linear combination of all the chosen variables explained over the 50% of the total variance of the dataset.

SEM offers a chi-square test for model fit with data structure. When the *p*-value of this test is non-significant, SEM can be considered as confirmatory analysis because the model structure and the data structure (variance and

covariance matrices) do not differ significantly. In our case we test the assumption that topography, soil moisture and physicochemical properties of the soil would influence directly nutrient content, cfu abundance and defoliation, as well as nutrients availability might influence defoliation and cfu in a direct way, and that cfu and defoliation would be related between them (Figure 2).

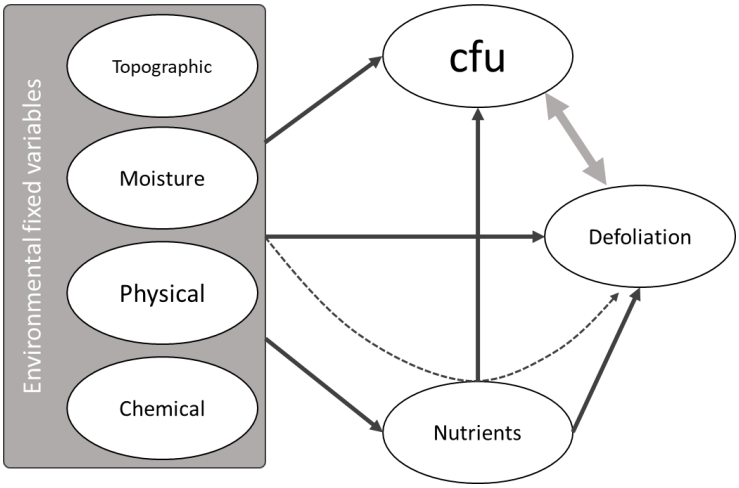

Figure 2. Conceptual model for relationships between environmental variables, soil nutrient content, pathogen abundance and defoliation. Regular arrows show direct effects, double headed arrow means interdependency and dashed line indicates indirect effects.

Comparative Fit Index (CFI), Tucker-Lewis Index (TLI) and Root Mean Square Error of Approximation (RMSEA) were used to test the goodness of the model fit (Sutton-Grier et al., 2010). To evaluate the variability explained by the model for each endogenous (dependent) variable, R^2 values were calculated. The relationship between variables were showed by standardized coefficients and z-test was carried out for test the direct effects of latent variables over endogenous ones, establishing significance level at p-value of 0.05. Indirect and mediator effects were also tested by testing the interaction of fixed parameters following (Finch and French, 2015). Covariances were evaluated to elucidate trend correlations between variables into the model structure. The standardized coefficients of each variable relevance and their significance tests in each latent variable were showed in the Supplementary Material, Table S3.3. To determine the best model, different combinations of interaction between the five latent variables and the endogenous variables (cfu and defoliation) were tested, including the saturated model, and the best

one was chosen testing differences in the Aikake Information Criteria trough ANOVA analysis (Finch and French, 2015).

All the reported analyses were performed in R 3.3.2 (R Core Team, 2022), with support of packages "*adespatial*" (Dray et al., 2017), "*ade4*" (Dray and Dufour, 2007) and "*glmmADMB*" (Fournier et al., 2012). SEM analyses were carried out with the help of the package "*lavaan*" (Rosseel, 2012) and were represented using "*semPlot*" (Epskamp and Epskamp, 2019).

3 Results

3.1 Phytosanitary status

Average defoliation was high (53 ± 2 %), with significant differences among holm and cork oaks (H = 156.2, $P < 0.05$) (Table 2). Holm oaks were mostly classified in the highest defoliation classes (77.7% in DC3 and DC4) meanwhile 90% of cork oak trees were classified in the medium and low defoliation classes (DC0 to DC2). Overall cfu values ranged between 0 and 159 cfu g^{-1} without differences comparing between species. However, when data were assessed also considering defoliation classes, the highest cfu abundance corresponded to holm oaks with moderate defoliation levels (DC2; 29 ± 5 cfu g^{-1}). The lowest cfu abundance (7 ± 2 cfu g^{-1}) was found in dead trees (i.e., DC4), a class that appear only in holm oak.

In the holm oak subplots, cfu values showed a significant and inverse correlation with crown defoliation (ρ = -0.431, $P < 0.01$) (Supplementary Material, Table S3.4). The subplot P_1Qi, (*Q. ilex* in southern exposure), presented the highest defoliation average (89% ± 2%) as well as the highest percentage of dead trees (51.3%) and the lowest mean abundance of cfu (2 ± 0.1 cfu g^{-1}). P_2Qi (*Q. ilex* in northwest orientation) showed the second highest defoliation average (70% ± 4%), together with a tree mortality rate of 21.3% and the highest mean abundance of cfu (30 ± 3 cfu g^{-1}).

In the cork oak subplots, the cfu values did not show significant correlation with crown defoliation (ρ = 0.118, $P > 0.05$). The two cork oak subplots (P_1Qs - P_2Qs) did not present tree mortality. P_1Qs, located in north orientation, showed the lowest defoliation (33% ± 2%), with the second lowest concentration of cfu (6 ± 1 cfu g^{-1}). Finally, P_2Qs, oriented to the northeast, presented similar defoliation rate (38% ± 2%) but with higher concentration of cfu (26 ± 3 cfu g^{-1}) (Table 2).

Defoliation class (DC=%)	All (*n*=359)			Subplots											Species					
				P_1Qi (*n*=78)			P_1Qs (*n*=119)			P_2Qi (*n*=61)			P_2Qs (*n*=101)			*Q. ilex* (*n*=139)			*Q. suber* (*n*=220)	
	cfu	Def_{18}	%	cfu	Def_{18}	%	cfu	Def_{18}	%	cfu	Def_{18}	%	cfu	Def_{18}	%	cfu	Def_{18}	%	cfu	Def_{18}	%
0 (0-10)	14±4	9±0	10.0	NA	NA	0.0	5±1	9±1	14.3	20±11	8±1	6.6	24±9	10±0	14.9	20±11	8±1	2.9	14±5	9±0	14.5
1 (11-25)	10±2	20±1	17.8	10±9	20±0	2.6	5±1	19±1	29.4	28±10	20±2	6.6	15±4	20±1	22.8	22±8	20±1	4.3	9±2	20±1	26.4
2 (26-60)	20±3	43±1	35.9	9±4	45±3	9.0	7±1	42±1	51.3	39±5	46±3	23.0	34±6	42±1	46.5	29±5	46±2	15.1	19±3	42±1	49.1
3 (61-99)	16±3	85±1	21.4	2±0	90±1	37.2	18±7	81±4	5.0	30±6	86±2	42.6	17±6	77±2	15.8	15±3	88±1	39.6	17±5	78±2	10.0
4 (100) *	7±2	100±0	14.8	1±0	100±0	51.3	NA	NA	0.0	24±5	100±0	21.3	NA	NA	0.0	7±2	100±0	38.1	NA	NA	0.0
cfu average •	15±1		100	$2±0^a$		100	$6±1^b$		100	$30±3^c$		100	$26±3^c$		100	$15±2^a$		100	$15±2^a$		100
Def_{18} average •	53±2			89±2[a]			33±2[b]			70±4[c]			38±2[b]			81±2[a]			35±1[b]	

Table 2. Colony forming units (cfu sample^{-1}, mean ± standard error) interpolated to the tree position, percentage of average defoliation for the tree's crowns and the percentage presence of trees in each plot, distributed by defoliation classes (DC=%), and grouped by treatments (subplots and species). Different lowercase letters in superscripts indicate significant differences between treatments for the cfu and Def_{18} variables (Kruskal-Wallis Test, $P < 0.05$ and Mann-Whitney U Test with correction of the Bonferroni Test, $P < 0.0083$). • - non-normal distributed variables. * Dead tree; *n* = number of trees; NA – Not Available.

3.2 Relationship between tree status and environmental characteristics

Soil chemical analysis showed low to very low concentrations of components and nutrients regarding standard values, except for N (0.12% ± 0.01%), Mg (2.55 ± 0.06 meq / 100 g), OM (2.53% ± 0.07%), K (0.25 ± 0.01 meq / 100 g), Ca (3.22 ± 0.12 meq / 100 g) and Na (0.33 ± 0.00 meq / 100 g) (Supplementary Material, Table S3.1). The lowest values of soil moisture correspond to the summer season (M_7) and the highest to the winter season (M_{12}), with the soil remaining below the permanent wilting point, except in winter season. Comparing species, significant differences were found for all variables except for the variables Root, Fden, SOC, OM, Zn, Fe, pH, M5, M7 and DEM. Winter soil moisture (M_{12}) was significantly different between species, being slightly higher in the subplots with lower solar incidence (Supplementary Material, Table S3.1 and S3.4).

Regarding Spearman's bivariate correlations (Table 3), the Def_{2018} for holm oak was significant ($P < 0.01$) and positively correlated ($\rho = 0.432$) with gravel's percentage, and negatively ($\rho < -0.4$) with cfu, fine's percentage, Ca, C/N, Cu, Mn, and pH. In addition, Spearman's correlation for cfu on holm oak was significant ($P < 0.01$) and positive ($\rho > 0.4$) for the variables root, fine's percentage, N, Ca, CEC, C/N, SOC, OM, Cu, Zn, and pH, and negative ($\rho < -0.4$) with gravel's percentage, Na, M_5 and the number of hours of annual solar incidence (solar) (Table 3).

The defoliation (Def_{2018}) of cork oaks was not significantly correlated with any soil physical variables, and only slightly related with some chemical variables and nutrient content. In the case of topography, holm oak defoliation only showed significant relationship with sun exposure (Solar). However, cfu showed a significant ($P < 0.01$) and positive ($\rho > 0$) relationship with many more variables in the Qs subplots, greater with Ca, Cu, and pH and also relevant with DEM and Solar.

Table 3. Spearman's bivariate correlation between the defoliation in 2018 (Def_{2018}) and colony forming units (cfu) with the rest of studied variables for the whole dataset (All), and for *Q. ilex* (Qi) and *Q. suber* (Qs) subplots datasets. * $P < 0.05$. ** $P < 0.01$.

	Def_{2018}			cfu		
	All	**Qi**	**Qs**	**All**	**Qi**	**Qs**
Def_{18}	1.000	1.000	1.000	-0.206**	-0.431**	0.118
Cfu	-0.206**	-0.471**	0.119	1.000	1.000	1.000
Root	-0.042	-0.373**	0.076	0.244*	0.472**	0.05
Fden	-0.132*	-0.089	-0.05	0.093	0.210	0.007
Tden	0.047	0.189*	-0.041	0.045	-0.045	0.121
Grav	0.383**	0.432**	0.068	-0.203*	-0.513**	0.067
Fine	-0.383**	-0.432**	-0.064	0.203*	0.513**	-0.067
Clay	-0.510**	-0.278**	-0.052	0.072	0.276	-0.168
Sand	0.438**	0.302**	-0.003	-0.204*	-0.385*	0.003
Silt	-0.146**	-0.259**	0.137	0.393**	0.317*	0.393**
N	-0.448**	-0.381**	0.127	0.441**	0.506**	0.345**
P	0.516**	0.344**	-0.072	-0.184	-0.182	-0.135
K	0.08	-0.247**	0.02	0.059	0.350*	-0.165
Na	0.032	0.317**	0.146*	-0.276**	-0.530**	-0.091
Mg	-0.155**	0.265**	-0.002	-0.237*	-0.258	-0.242
Ca	-0.434**	-0.418**	0.180**	0.454**	0.482**	0.473**
Cu	-0.233**	-0.435**	0.143*	0.453**	0.424**	0.446**
Zn	0.02	-0.256**	0.107	0.366**	0.476**	0.289*
Fe	0.135*	-0.051	-0.093	-0.116	0.010	-0.211
Mn	-0.304**	-0.444**	0.164*	0.371**	0.335*	0.377**
CEC	-0.457**	-0.376**	0.031	0.451**	0.631**	0.292*
C/N	-0.428**	-0.439**	-0.076	0.200*	0.508**	-0.108
SOC	-0.214**	-0.342**	0.013	0.372**	0.557**	0.176
OM	-0.058	-0.260**	-0.016	0.288**	0.416**	0.198
pH	-0.137**	-0.412**	0.191**	0.521**	0.497**	0.509**
H_5	-0.129*	0.071	-0.104	-0.181	-0.134	-0.220
H_7	-0.08	0.335**	-0.218**	-0.434**	-0.554**	-0.317*
H_{12}	-0.407**	-0.268**	-0.091	0.171	0.213	0.051
DEM	0.034	0.232**	-0.011	-0.492**	-0.606**	-0.383**
Slope	-0.380**	0.172*	-0.114	0.007	-0.231	0.056
Orien	0.349**	0.184*	0.129	-0.244*	-0.541**	0.144
Solar	0.461**	0.371**	0.213**	-0.127	-0.590**	0.322*

3.3 Spatial analysis of environmental characteristics and tree condition

All the soil variables analysed with SADIE showed spatial aggregation (I_a > 1) in at least one of the plots (Figure 3). Twelve variables showed significant aggregation in P_1 and P_2 (clay, sand, N, P, Ca, CEC, Mn, pH, M_{12}, DEM, slope and solar; P < 0.05). The variables Tden, C/N, M_5 and orientation showed only aggregation patterns in P_1, and cfu, gravel's percentage, fine's percentage, silt, K, Na, Mg, OM, Cu, Fe and M_7 only showed aggregation in P_2. The variables sand, P, Ca, CEC, and Solar presented the highest aggregation indices in both plots (P < 0.001), following by order for clay, N, Mn, pH, M_{12}, DEM and slope (P < 0.05) (Figure 3).

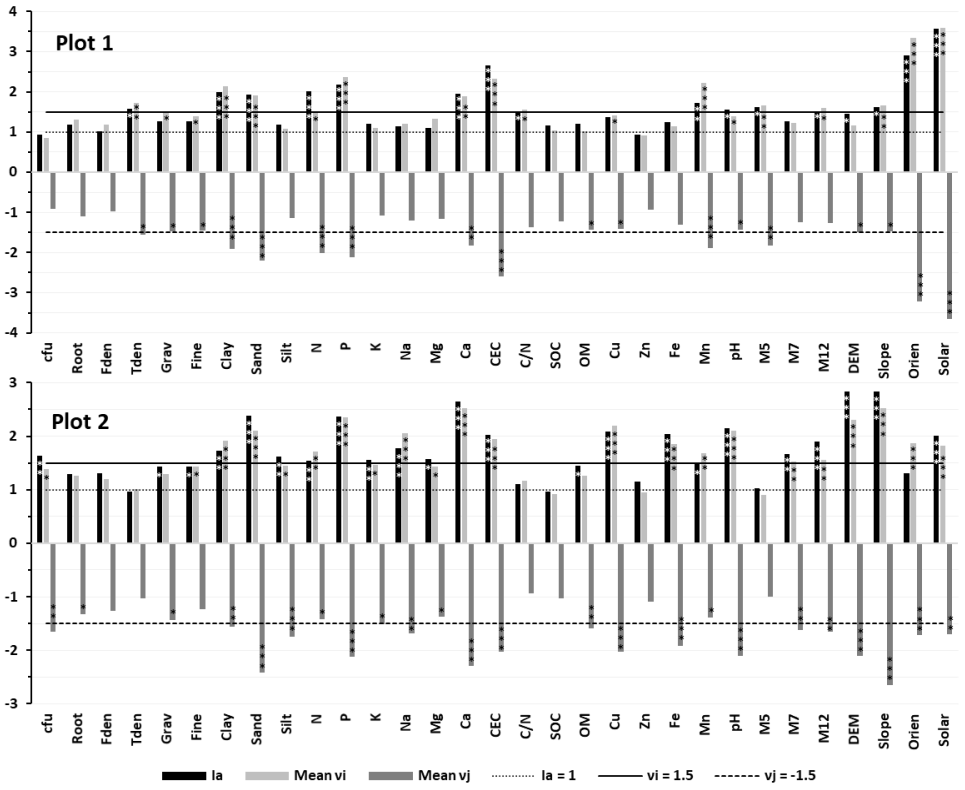

Figure 3. Aggregation indices (I_a) and clustering indices (ν) for the study of 31 soil variables in the Plot 1 and 2. The horizontal dotted line I_a = 1 indicates the limit of the type of distribution pattern of the variable (I_a > 1 aggregated, I_a < 1 regular and I_a = 1 random). The horizontal continuous line (mean $\nu_i \geq 1.5$) indicates the limit for which the index ν is grouped into patches, i.e., higher values of a given variable. The horizontal discontinuous line (mean $\nu_j \leq -1.5$) indicates the limit for which the index ν is grouped into gaps, i.e., lower values of a given variable. * - P < 0.05; ** - P < 0.01; *** - P < 0.001.

Regarding the spatial clustering, the variables clay, sand, P, Ca, CEC, and solar presented significant patches ($\nu_i \geq 1.5$) and gaps ($\nu_j \leq -1.5$) in both P_1 and P_2 plots, and the variables N, Mn, M_{12} and slope only significant patches ($P < 0.05$) (Figure 3, Supplementary Material, Figures S3.1 and S3.2). Other variables showed different patterns between the two plots. In P_2, the variables Na, Cu, Fe and M_7 showed significant patches and gaps ($P < 0.01$) and silt, K and OM, only gaps ($P < 0.05$), all of them showing significant aggregation ($P < 0.05$). On the other hand, significant patches and gaps for Tden and M5, and only patches for C/N, were identified for P_1 ($P < 0.05$) (Figure 3, Supplementary Material, Figures S3.1 and S3.2).

Regarding species, several soil variables showed differences in the clustering patterns between *Q. ilex* and *Q. suber* subplots. The variables fine's percentage, clay, N, Mg, Ca, CEC, C/N, Cu and Mn showed cluster patterns, in the form of patches ($\nu_i \geq 1.5$) in cork oak subplots, and in form of gaps ($\nu_j \leq -1.5$) in holm oak subplots. On the contrary, gravel, sand and P showed patches in holm oak subplots and gaps in cork oak subplots (Figure 3, Supplementary Material, Figures S3.1 and S3.2).

The spatial clustering analysis of cfu per subplots showed a patchy structure ($\nu_i \geq 1.5$; $P < 0.05$) in cork oak subplots (P_1Qs and P_2Qs) and, specifically, in areas of lower elevation and lower slope for P_1Qs (Figure 4). However, in the holm oak subplot, which were South-exposed (P_1Qi), the analysis showed gaps for cfu ($\nu_j \leq -1.5$; $P < 0.05$). In turn, trees with the highest crown defoliation classes (2-4) were concentrated in the holm oak zone, while the lowest defoliation classes (0-2) were mostly located in cork oak subplots, being the class 0 only assigned to cork oak trees. In P_1Qs, the most defoliated cork oak trees (classes 2-3) were concentrated near the patches of cfu (Figure 4).

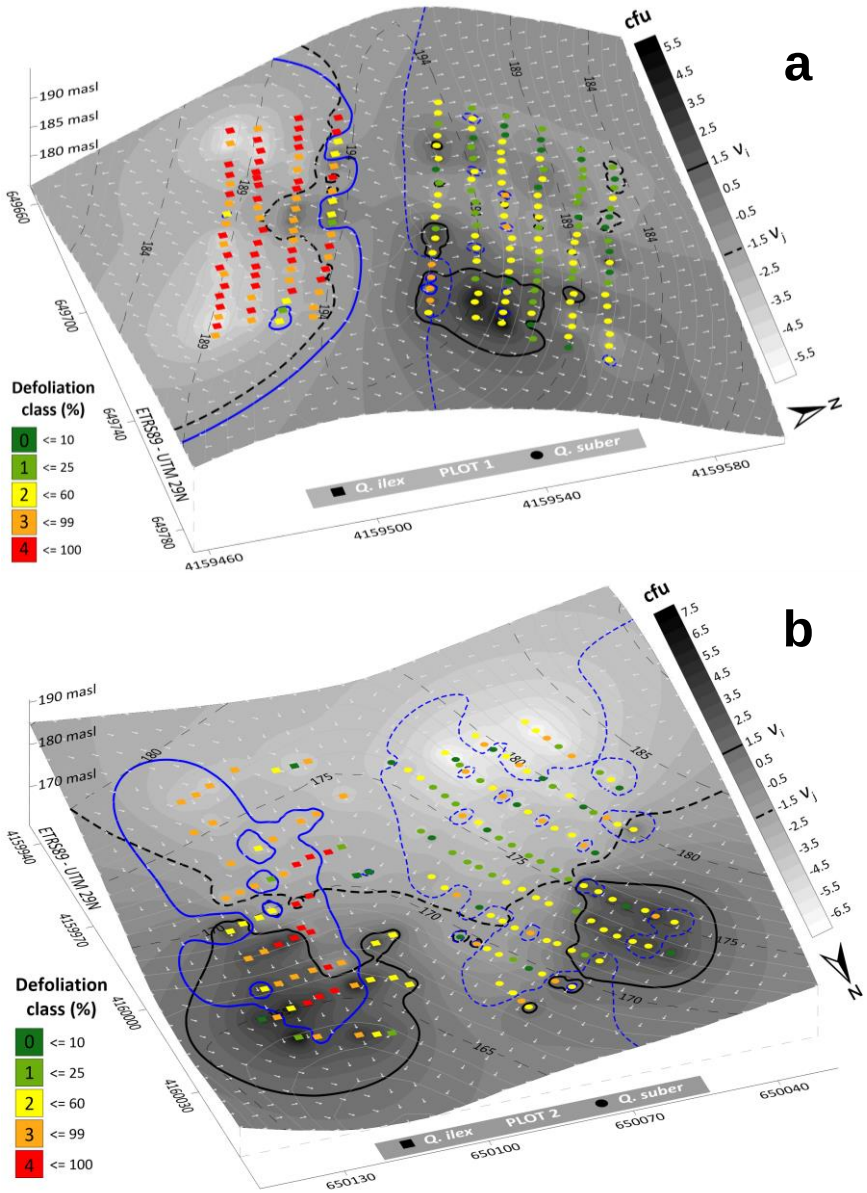

Figure 4. 3D topographical representation of the study plots with the spatial clustering of tree defoliation. a: Plot 1; b: Plot 2. Blue continuous line: (ν > 1.5): clustering of high defoliation classes; Blue discontinuous line (ν < -1.5): clustering of low defoliation classes. The black and white gradient in the background indicates the cfu clustering indices (ν). The dark areas show high cfu concentration with clustering patches (ν > 1.5) delimited by a black continuous line and the light areas show low cfu concentration with clustering gaps (ν < -1.5) delimited by a thick black discontinuous line. Legend (ν) is unitless. The coloured squares (holm oaks) and circles (cork oaks), represent the classes of defoliation in 2018 of the tree crowns. Dashed grey lines are contour lines of the land (equal m.a.s.l) while the small white arrows indicate the hydrological flow.

The patches of cfu in P_2 were in the areas of runoff confluence and lower slope, appearing significant gaps in the Southern areas of the plot, with the highest elevation and slope, mainly in the cork oak subplot (P_2Qs) (Figure 4). The holm oaks of P_2 presenting the highest crown defoliation classes (DC2-4) were concentrated near to the patches of cfu. These areas of spatial accumulation of cfu presented also higher mortality rate (Table 1; Figure 4; Supplementary Material, Table S3.4, Figure S3.2).

In summary, areas with the higher presence of *P. cinnamomi* (cfu) in both plots were characterized for a loamy texture with silt concentration patches (compared to sandy and clay soils), with high level of N, low levels of K and Ca, higher cation exchange capacity, pH and micronutrient concentration (Cu, Zn and Mn), higher edaphic humidity, lower slope, north exposure and lower levels of solar radiation (Figure 4; Supplementary Material, Table S3.4 and Figure S3.2). Those areas coincided with higher defoliation rates and higher mortality only in P2Qi, without clear trends in the rest of subplots.

3.4 SEM analysis

The best SEM model for the whole dataset included the five latent variables (Figure 6a) but did not fit the data structure ($P < 0.001$), presenting a high RMSEA value (RMSEA > 0.06). However, when datasets for holm oak and cork oak were differentiated, SEM fitted the data structure, and the goodness of model fit was very good (RMSEA < 0.05; TLI > 0.9; CFI > 0.9), appearing differences in the model structure between species (Figures 6b and 6c). In both cases (for holm oak subplots and cork oak subplots), topography and soil humidity presented significant effect over cfu, but for the case of *Q. suber*, also with significant indirect effect, due to the influence of topography over soil moisture ($Z_{topo\text{-}hum}^{Q.ilex} = -2.22$, $P < 0.05$; $Z_{topo\text{-}hum}^{Q.suber} = -2.28$, $P < 0.05$). In the case of *Q. ilex*, the only latent variable influencing defoliation was soil chemistry, meanwhile for *Q. suber*, defoliation was also influenced by topography (DEM) and soil moisture (M_5). Highest positions in the plot and higher soil moisture in May decreased defoliation rates in the case of cork oak.

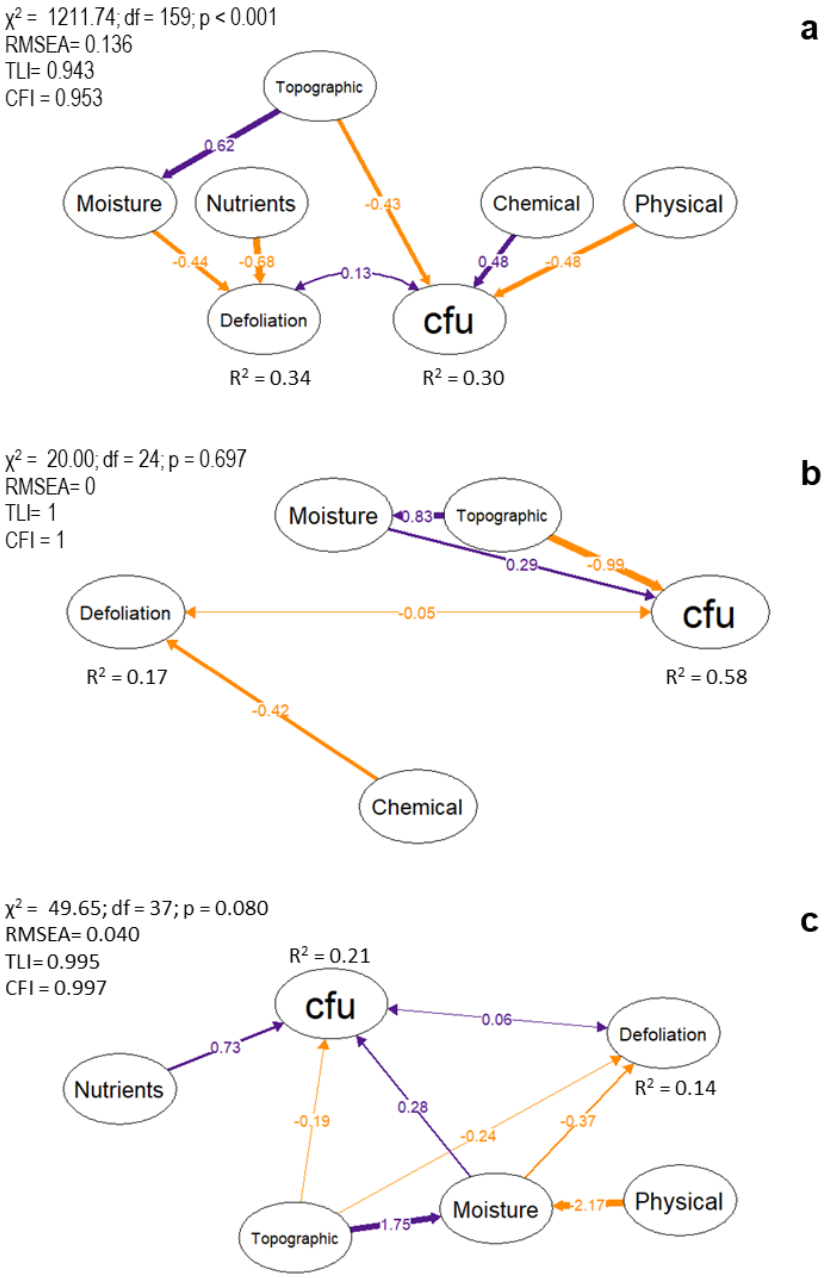

Figure 5. Graphical representation of structural paths of SEM. a: model for all the data. b: model for *Q. ilex* subplots. c: model for *Q. suber* subplots. Single-headed arrows represent direct effects. Double-headed arrows represent covariance relationship. Colours meant direct (purple) or inverse (orange) relationship between nodes. Arrow labels represent standardized values for the regression matrix. Arrow thickness is proportional to the weight of the regression in the model. Only significant direct regressions were showed ($P < 0.05$). R-square values represented the variance of the dependent variable explained by the overall model.

The model presented more significant effects for *Quercus suber* subplots, as for example the direct influence of soil nutrient composition over cfu (Z = 7.51, $P < 0.001$) and the inverse influence of physical properties over soil humidity (Z = -2.59, $P < 0.01$), which did not appear in holm oak subplots. Moreover, in the case of *Q. ilex* subplots the combination of topography and soil moisture explained in a great extent the soil cfu variance (58%). Noteworthy defoliation and cfu covaried in all the cases, but in the case of holm oak the variation was slight and inverse.

4 Discussion

This work shows an example of holm and cork oak afforestation established on former agricultural lands under the EU afforestation program in Southwest of the Iberian Peninsula, affected by decline and mortality processes, in which *Phytophthora cinnamomi* plays a key role (Jung et al., 2016; Sánchez-Cuesta et al., 2020). Our results represent a new contribution to the analysis of the spatial distribution patterns of *P. cinnamomi* in the soil rhizosphere of holm and cork oaks, showing new insights and confirming previous hypothesis of their relationship with defoliation and mortality. Agreeing with previous works, the response of an 8-years afforestation affected by *P. cinnamomi* root rot was related to physicochemical and topographic features (Fernández-Habas et al., 2019; Sánchez-Cuesta et al., 2020), the tree cover (Gallardo, 2003; Simón et al., 2013; Andivia et al., 2015) and the pathogen presence (Gómez-Aparicio et al., 2012; Quero et al., 2013). In fact, the health status of trees, and specifically crown defoliation, was mediated by direct and indirect relationships between these components and varied at small scale due to changes in microsite conditions and host species.

4.1 Tree response to pathogen abundance

Defoliation is considered as the main variable to assess root rot damage (Pollastrini et al., 2016). In this work, holm oak showed the higher defoliation values (89% ± 2%) and percentage of dead trees (51.3%) than cork oak without significant changes in cfu. These results support previous hypothesis indicating that holm oak is extremely vulnerable to *P. cinnamomi* (Serrano et al., 2012, 2015), being cork oak more tolerant to infection (Robin et al., 2001; Rodríguez-Molina et al., 2002). The difference between species symptoms might be explained by the higher rate of fine roots turnover of holm oak compared with cork oak, which might be related to the higher rates of fine

root rot caused by *P. cinnamomi* in controlled experiments (Robin et al., 2001; Moralejo et al., 2009; León et al., 2017). Higher rates of fine root growth and pathogen abundance are associated to higher consumption of nutrients and reserves and to changes in metabolism (Ruiz Gómez, 2018; San-Eufrasio et al., 2021).

Both species showed similar values of cfu; however, this variable showed a significant and inverse correlation with crown defoliation on holm oak, but not in cork oak. Previous works reported that despite cfu is a reliable indicator of the widespread occurrence of *P. cinnamomi*, this variable might not be directly related to defoliation levels (Navarro-Cerrillo et al., 2019; Ruiz-Gómez et al., 2019; Sánchez-Cuesta et al., 2020, 2021). A plausible explanation in this study is the high mortality rate found in the holm oak plots, limiting the availability of susceptible plant tissue to be infected. A similar result was found by Gómez-Aparicio et al. (2012) showing that in areas with dead oak trees, the soil inoculum density of *P. cinnamomi* and *Pythium* spp. decreased significantly. An alternative explanation is the direct influence of environmental characteristics on the pathogen occurrence irrespective of plant host species. In fact, our results showed that solar incidence, orientation, soil humidity and other soil characteristics directly influenced pathogen abundance, with lower values of cfu in the most exposed locations.

4.2 Spatial analysis of soil characteristics, pathogen abundance and tree status

The spatial aggregation analysis showed relevant clustering patterns associating defoliation and cfu with soil physical and chemical characteristics, as previously reported in other works (Gyeltshen et al., 2021). For holm oak, we found opposite trends for defoliation and cfu regarding soil characteristics, with higher defoliation rates in soils with high percentage of gravel, low percentage of fine fraction and low pH, and higher cfu abundance in finer-grained soils with high nutrients content and pH. However, many other variables influenced cfu in a significant extent, including soil moisture, organic matter content and the number of hours of annual solar incidence. However, cork oak defoliation did not show significant correlation with soil variables but with cfu, which did show positive relationship with nutrients, chemical composition, and pH in *Q. suber* subplots. Some of these relationships should be considered with caution, since the ranges of the variables could be narrow and thus biologically non-significant, leading the microsite effects and the

autocorrelation of plots to false statistically significant results. For instance, Ca concentration was in general very low compared with standard values but showed significant correlation with cfu. However., did not present significant effects in the variability of the latent variable "Chemical" in any case, nor indirect influence over cfu or defoliation when SEM analysis was carried out. Similar result was obtained for Ca in a previous work at tree level (Sánchez-Cuesta et al., 2020).

On the other hand, the lower inoculum levels in the highly affected holm oak subplot might seem contradictory but agrees with the knowledge on the interaction between host and pathogen and the behavior of *P. cinnamomi*. The abundance of cfu at tree scale has been related to microclimate under the tree crown, differences in nutrients and organic matter, or the greater presence of fine roots under the crown cover (Sánchez-Cuesta et al., 2020). Such conditions are altered in the process of plant-pathogen interaction. Root rot reduces drastically the secondary root system of holm oak increasing tree defoliation and death, and consequently also increasing solar radiation incidence over the soil and hindering the living conditions of microbiota and soil pathogens (Gómez-Aparicio et al., 2012), as might be the case in the south-facing subplot. Moreover, the presence of low inoculum levels is not a guarantee of low disease incidence. *Phytophthora cinnamomi* might rapidly increase their inoculum levels in soil under favourable conditions due to their asexual cycle (Hardham, 2005; Oßwald et al., 2014), changing from biotroph to necrotrophic and being able to complete a single cycle into the host roots in only 3 days (Ruiz Gómez et al., 2015). Therefore, the low levels of cfu do not allow us to rule out the causality of the pathogen on the symptoms of holm oak decline.

Generally, defoliation in the holm oak subplots appeared associated with less water retention capacity and nutrients availability in concordance with the limiting character of water and nutrients in Mediterranean semiarid environments (de Sampaio e Paiva Camilo-Alves et al., 2013). On the other hand, in the most favourable North-facing orientations, defoliation seems to be more related with the pathogen, as showed by the aggregation of high levels of defoliation and mortality in P_2Qi and defoliation in P_1Qs, over the cfu patches, even considering the most tolerant character of cork oak.

Despite the necessary precautions mentioned in the previous paragraphs, and even considering the presence of *P. cinnamomi* as factor triggering oak decline in this afforestation, results showed that tree symptoms

were modulated mainly by the specie and the topographic conditions. On this regard, cfu abundance was favoured mainly by fine soil textures on rich organic soils, in concordance with previous studies (Homet et al., 2019; Sánchez-Cuesta et al., 2020).

4.3 Relationship of soil variables, pathogen abundance and tree status

The ecological processes established in plant-soil interactions influence many different environmental characteristics, adapting ecosystems after afforestation in a quicker way that it can be thought (Bárcena et al., 2014; Cappai et al., 2017). When SEM models were tested for the whole dataset, the results did not show significant fit for the hypothesis structure, but when datasets were separated considering species, indices showed excellent fitting results. Moreover, the common paths were non-stationary, agreeing with the differences between cork oak and holm oak regarding the tolerance to root rot (Robin et al., 2001; Rodríguez-Molina et al., 2002). This result shows the different adaptability of cork and holm oak to site environment conditions, and how species selection modulates soil changes in the mixed afforestation.

Only the influence of topography over soil moisture and cfu abundance was constant for all subplots, explaining up to 58% of cfu variability in the case of holm oak. This can be considered as indicator of the high relevance of both characteristics over the pathogen abundance, agreeing with the spatial analysis results. Water availability, including soil capacity, together with topography have been previously identified as the main abiotic limitations for afforestation establishment (Pemán García et al., 2021; Ramón Vallejo et al., 2012). The significant covariance between cfu and defoliation in the SEM models indicates that their relationship is modulated by intermediate effects, which vary for each of the studied species. This observation is consistent with the results of the spatial aggregation analysis. SEM results showed a direct but negative influence of topography and soil moisture on cork oak defoliation, showing more defoliated trees concentrated around the patches of cfu in northern exposure (P_1Qs). In the case of holm oak, higher variability of defoliation rates corresponded to more constant (and higher) values of cfu, which might be related with higher impacts of the pathogen over trees standing in more favourable conditions (North-facing, close to a runoff). On the other hand, the higher variability of defoliation in cork oak corresponded with higher variability of cfu values, which appeared in P_2Qs, the *Q. suber*

subplot with higher solar incidence. Both covariance and direct effects of topography and humidity over cork oak defoliation might be related with a significant influence of environmental factors over their health status. This hypothesis is also confirmed by the direct influence of soil nutrients and organic matter over cfu in cork oak subplots, detaching inoculum levels to tree crown status in this case, persisting in soils under favourable conditions without lead to a significant decline symptom.

In summary, when datasets for holm oak and cork oak were differentiated, SEM showed that topography and soil moisture presented significant effects over cfu. Model results reinforce previous conclusions such as the influence of dry soils, eventually undergo short flooding over root rot infection on *Q. ilex* and *Q. suber* forests (Corcobado et al., 2013a, 2013b). Similar results have been also observed in other woody species, showing that it is a common behaviour of this oomycete species in different ecosystems (Davison, 2018).

5 Conclusions

Our study confirms that the distribution and abundance of *P. cinnamomi* at landscape level is not just determined by host availability but also by the spatial distribution of site conditions, highlighting the influence of soil water availability, soil structure, nutrients, and topography. Some of these variables also directly influence tree defoliation, but others such as exposition and soil physical characteristics modulate tree health status indirectly through their influence over the pathogen abundance. Inoculum abundance was more influenced by the soil and topographic characteristics than by the mere presence of the host and the availability of fine roots to colonize. Therefore, topography and soil should be characterized on a precise scale developing preventive strategies to reduce the risk of afforestation failure.

Differences between cork and holm oak in response to the pathogen infection, and how each species influences the soil characteristics, were noteworthy. Our results highlighted the benefits of mixed afforestation compared with monospecific ones, taking advantage of the heterogeneity of site conditions, and increasing afforestation resilience. Additionally, results reported here provide a baseline to predict the regional distribution of recent outbreaks of *P. cinnamomi* on *Quercus* plantations on agricultural lands, considering the appropriate site variables when forecasting priority areas for

intervention. However, further research is needed to assess the abundance of *Phytophthora* spp. and other oomycetes in soils with more heterogeneous conditions, and to clarify whether Modelling techniques can be used to predict cfu amounts, particularly in Mediterranean *dehesa* and *montados* ecosystems and in oak afforestation.

6 References

Andivia, E., Fernández, M., Alejano, R., Vázquez-Piqué, J., 2015. Tree patch distribution drives spatial heterogeneity of soil traits in cork oak woodlands. Annals of Forest Science 72, 549–559. https://doi.org/10.1007/s13595-015-0475-8

Bárcena, T.G., Gundersen, P., Vesterdal, L., 2014. Afforestation effects on SOC in former cropland: oak and spruce chronosequences resampled after 13 years. Global Change Biology 20, 2938–2952. https://doi.org/10.1111/gcb.12608

Bartier, P.M., Keller, C.P., 1996. Multivariate interpolation to incorporate thematic surface data using inverse distance weighting (IDW). Computers & Geosciences 22, 795–799. https://doi.org/10.1016/0098-3004(96)00021-0

Burgess, T.I., Scott, J.K., Mcdougall, K.L., Stukely, M.J.C., Crane, C., Dunstan, W.A., Brigg, F., Andjic, V., White, D., Rudman, T., Arentz, F., Ota, N., Hardy, G.E.St.J., 2017. Current and projected global distribution of *Phytophthora cinnamomi*, one of the world's worst plant pathogens. Glob Change Biol 23, 1661–1674. https://doi.org/10.1111/gcb.13492

Cappai, C., Kemanian, A.R., Lagomarsino, A., Roggero, P.P., Lai, R., Agnelli, A.E., Seddaiu, G., 2017. Small-scale spatial variation of soil organic matter pools generated by cork oak trees in Mediterranean agro-silvo-pastoral systems. Geoderma, 5th International Symposium on Soil Organic Matter 2015 304, 59–67. https://doi.org/10.1016/j.geoderma.2016.07.021

Cardillo, E., Acedo, A., Abad, E., 2018. Topographic effects on dispersal patterns of *Phytophthora cinnamomi* at a stand scale in a Spanish heathland. PLoS One 13. https://doi.org/10.1371/journal.pone.0195060

Colangelo, M., Camarero, J.J., Borghetti, M., Gentilesca, T., Oliva, J., Redondo, M.-A., Ripullone, F., 2018. Drought and *Phytophthora* Are Associated With the Decline of Oak Species in Southern Italy. Front. Plant Sci. 9, 1595. https://doi.org/10.3389/fpls.2018.01595

Corcobado, T., Cubera, E., Moreno, G., Solla, A., 2013a. *Quercus ilex* forests are influenced by annual variations in water table, soil water deficit and fine root loss caused by *Phytophthora cinnamomi*. Agricultural and Forest Meteorology 169, 92–99. https://doi.org/10.1016/j.agrformet.2012.09.017

Corcobado, T., Solla, A., Madeira, M.A., Moreno, G., 2013b. Combined effects of soil properties and *Phytophthora cinnamomi* infections on *Quercus ilex* decline. Plant Soil 373, 403–413. https://doi.org/10.1007/s11104-013-1804-z

Crone, M., McComb, J.A., O'Brien, P.A., Hardy, G.E.S.J., 2013. Survival of *Phytophthora cinnamomi* as oospores, stromata, and thick-walled chlamydospores in roots of symptomatic and asymptomatic annual and herbaceous perennial plant species. Fungal Biology 117, 112–123. https://doi.org/10.1016/j.funbio.2012.12.004

Davison, E.M., 2018. Relative importance of site, weather and *Phytophthora cinnamomi* in the decline and death of *Eucalyptus marginata* – jarrah dieback investigations in the 1970s to 1990s. Australasian Plant Pathol. 47, 245–257. https://doi.org/10.1007/s13313-018-0558-8

de Sampaio e Paiva Camilo-Alves, C., da Clara, M.I.E., de Almeida Ribeiro, N.M.C., 2013. Decline of Mediterranean oak trees and its association with *Phytophthora cinnamomi*: a review. Eur J Forest Res 132, 411–432. https://doi.org/10.1007/s10342-013-0688-z

Domínguez-Begines, J., Ávila, J.M., García, L.V., Gómez-Aparicio, L., 2020. Soil-borne pathogens as determinants of regeneration patterns at community level in Mediterranean forests. New Phytologist 227, 588–600. https://doi.org/10.1111/nph.16467

Dray, S., Blanchet, G., Borcard, D., Guenard, G., Jombart, T., Larocque, G., Wagner, H.H., 2017. adespatial: Multivariate multiscale spatial analysis. R package version 0.0-9.

Dray, S., Dufour, A.B., 2007. The ade4 package: implementing the duality diagram for ecologists. Journal of Statistical Software 22, 1–20.

Eck, J.L., Stump, S.M., Delavaux, C.S., Mangan, S.A., Comita, L.S., 2019. Evidence of within-species specialization by soil microbes and the implications for plant community diversity. PNAS 116, 7371–7376. https://doi.org/10.1073/pnas.1810767116

Eichhorn, J., Roskams, P., Ferretti, M., Mues, V., Szepesi, A., 2016. Visual assessment of crown condition and damaging agents. Manual Part IV, in: Manual on Methods and Criteria for Harmonized Sampling, Assessment, Monitoring and Analysis of the Effects of Air Pollution on Forests. UNECE ICP Forests Programme Co-ordinating Centre, Eberswalde, Germany, p. 49.

Epskamp, S., Epskamp, M.S., 2019. Package 'semPlot.' R Package Version 1.

Fernández-Habas, J., Fernández-Rebollo, P., Casado, M.R., García Moreno, A.M., Abellanas, B., 2019. Spatio-temporal analysis of oak decline process in open woodlands: A case study in SW Spain. Journal of Environmental Management 248, 109308. https://doi.org/10.1016/j.jenvman.2019.109308

Ferretti, M., Sánchez Peña, G., Economou, A., Beccu, E., Canu, G., Cocco, S., Bussotti, F., Cenni, E., Cozzi, A., Conceição Andrada, M., 1994. Especies forestales mediterráneas: guía para la evalución de las copas, CEC-UN/ECE. ed. LINNAEA ambiente Srl, Bruselas, Ginebra.

Finch, W.H., French, B.F., 2015. Latent Variable Modeling with R. Routledge, New York. https://doi.org/10.4324/9781315869797

Fournier, D.A., Skaug, H.J., Ancheta, J., Ianelli, J., Magnusson, A., Maunder, M.N., Nielsen, A., Sibert, J., 2012. AD Model Builder: using automatic differentiation for statistical inference of highly parameterized complex nonlinear models. Optimization Methods and Software 27, 233–249. https://doi.org/10.1080/10556788.2011.597854

Gallardo, A., 2003. Effect of tree canopy on the spatial distribution of soil nutrients in a Mediterranean Dehesa. Pedobiologia 47, 117–125. https://doi.org/10.1078/0031-4056-00175

Gentilesca, T., Camarero, J.J., Colangelo, M., Nolè, A., Ripullone, F., 2017. Drought-induced oak decline in the western Mediterranean region: an overview on current evidences, mechanisms and management options to improve forest resilience. iForest - Biogeosciences and Forestry 10, 796. https://doi.org/10.3832/ifor2317-010

Gómez-Aparicio, L., Domínguez-Begines, J., Kardol, P., Ávila, J.M., Ibáñez, B., García, L.V., 2017. Plant-soil feedbacks in declining forests: implications for species coexistence. Ecology 98, 1908–1921. https://doi.org/10.1002/ecy.1864

Gómez-Aparicio, L., Ibáñez, B., Serrano, M.S., De Vita, P., Ávila, J.M., Pérez-Ramos, I.M., García, L.V., Esperanza Sánchez, M., Marañón, T., 2012. Spatial patterns of soil pathogens in declining Mediterranean forests: implications for tree species regeneration. New Phytologist 194, 1014–1024. https://doi.org/10.1111/j.1469-8137.2012.04108.x

Gyeltshen, J., Dunstan, W.A., Grigg, A.H., Burgess, T.I., St. J. Hardy, G.E., 2021. The influence of time, soil moisture and exogenous factors on the survival potential of oospores and chlamydospores of *Phytophthora cinnamomi*. Forest Pathology 51, e12637. https://doi.org/10.1111/efp.12637

Hardham, A.R., 2005. *Phytophthora cinnamomi*. Molecular Plant Pathology 6, 589–604. https://doi.org/10.1111/j.1364-3703.2005.00308.x

Hardham, A.R., Blackman, L.M., 2018. *Phytophthora cinnamomi*. Molecular Plant Pathology 19, 260–285. https://doi.org/10.1111/mpp.12568

Homet, P., González, M., Matías, L., Godoy, O., Pérez-Ramos, I.M., García, L.V., Gómez-Aparicio, L., 2019. Exploring interactive effects of climate change and exotic pathogens on *Quercus suber* performance: Damage caused by *Phytophthora cinnamomi* varies across contrasting scenarios of soil moisture. Agricultural and Forest Meteorology 276–277, 107605. https://doi.org/10.1016/j.agrformet.2019.06.004

Jung, T., Orlikowski, L., Henricot, B., Abad-Campos, P., Aday, A.G., Casal, O.A., Bakonyi, J., Cacciola, S.O., Cech, T., Chavarriaga, D., Corcobado, T., Cravador, A., Decourcelle, T., Denton, G., Diamandis, S., Doğmuş-Lehtijärvi, H.T., Franceschini, A., Ginetti, B., Green, S., Glavendekić, M., Hantula, J., Hartmann, G., Herrero, M., Ivic, D., Jung, M.H., Lilja, A., Keca, N., Kramarets, V., Lyubenova, A., Machado, H., Lio, G.M. di S., Vázquez, P.J.M., Marçais, B., Matsiakh, I., Milenkovic, I., Moricca, S., Nagy, Z.Á., Nechwatal, J., Olsson, C., Oszako, T., Pane, A., Paplomatas, E.J., Varela, C.P., Prospero, S., Martínez, C.R., Rigling, D., Robin, C., Rytkönen, A., Sánchez, M.E., Ros, A.V.S., Scanu, B., Schlenzig, A., Schumacher, J., Slavov, S., Solla, A., Sousa, E., Stenlid, J., Talgø, V., Tomic, Z., Tsopelas, P., Vannini, A., Vettraino, A.M., Wenneker, M., Woodward, S., Peréz-Sierra, A., 2016. Widespread *Phytophthora* infestations in European nurseries put forest, semi-natural and horticultural ecosystems at high risk of *Phytophthora* diseases. Forest Pathology 46, 134–163. https://doi.org/10.1111/efp.12239

Lara-Gómez, M.A., Navarro-Cerrillo, R.M., Ceacero, C.J., Ruiz-Goméz, F.J., Díaz-Hernández, J.L., Palacios Rodriguez, G., 2020. Use of Aerial Laser Scanning to Assess the Effect on C Sequestration of Oak (*Quercus ilex* L. subsp. *ballota* [Desf.] Samp-*Q. suber* L.) Afforestation on Agricultural Land. Geosciences 10, 41. https://doi.org/10.3390/geosciences10020041

León, I., García, J., Fernández, M., Vázquez-Piqué, J., Tapias, R., 2017. Differences in root growth of *Quercus ilex* and *Quercus suber* seedlings infected with *Phytophthora cinnamomi*. Silva Fennica 51. https://doi.org/10.14214/sf.6991

Manion, P.D., Lachance, D., 1992. Forest Decline Concepts. APS Press.

Moralejo, E., García-Muñoz, J.A., Descals, E., 2009. Susceptibility of Iberian trees to *Phytophthora ramorum* and *P. cinnamomi*. Plant Pathology 58, 271–283. https://doi.org/10.1111/j.1365-3059.2008.01956.x

Moreno, G., Pulido, F.J., 2009. The Functioning, Management and Persistence of Dehesas, in: Rigueiro-Rodróguez, A., McAdam, J., Mosquera-Losada, M.R. (Eds.), Agroforestry in Europe: Current Status and Future Prospects, Advances in Agroforestry. Springer Netherlands, Dordrecht, pp. 127–160. https://doi.org/10.1007/978-1-4020-8272-6_7

Navarro-Cerrillo, R.M., Varo-Martínez, M.Á., Acosta, C., Palacios Rodriguez, G., Sánchez-Cuesta, R., Ruiz Gómez, F.J., 2019. Integration of WorldView-2 and airborne laser scanning data to classify defoliation levels in *Quercus ilex* L. Dehesas affected by root rot mortality: Management implications. Forest Ecology and Management 451, 117564. https://doi.org/10.1016/j.foreco.2019.117564

Oßwald, W., Fleischmann, F., Rigling, D., Coelho, A.C., Cravador, A., Diez, J., Dalio, R.J., Horta Jung, M., Pfanz, H., Robin, C., Sipos, G., Solla, A., Cech, T., Chambery, A., Diamandis, S., Hansen, E., Jung, T., Orlikowski, L.B., Parke, J., Prospero, S., Werres, S., 2014. Strategies of attack and defence in woody plant–*Phytophthora* interactions. For. Path. 44, 169–190. https://doi.org/10.1111/efp.12096

Pemán García, J., Navarro Cerrillo, R., Prada Saez, M.A., Serrada Hierro, R. (Eds.), 2021. Bases técnicas y ecológicas del proyecto de repoblación forestal. Ministerio para la Transición Ecológica y el Reto Demográfico.

Perry, J.N., 1995. Spatial Analysis by Distance Indices. Journal of Animal Ecology 64, 303–314. https://doi.org/10.2307/5892

Perry, J.N., Bell, E.D., Smith, R.H., Woiwod, I.P., 1996. SADIE: software to measure and model spatial pattern. Aspects of Applied Biology 46, 95–102.

Pollastrini, M., Feducci, M., Bonal, D., Fotelli, M., Gessler, A., Grossiord, C., Guyot, V., Jactel, H., Nguyen, D., Radoglou, K., Bussotti, F., 2016. Physiological significance of forest tree defoliation: Results from a survey in a mixed forest in Tuscany (central Italy). Forest Ecology and Management 361, 170–178. https://doi.org/10.1016/j.foreco.2015.11.018

QGIS.org, 2022. QGIS Geographic Information System. QGIS Association.

Quero, J.L., Maestre, F.T., Ochoa, V., García-Gómez, M., Delgado-Baquerizo, M., 2013. On the Importance of Shrub Encroachment by Sprouters, Climate, Species Richness and Anthropic Factors for Ecosystem Multifunctionality in Semi-arid Mediterranean Ecosystems. Ecosystems 16, 1248–1261. https://doi.org/10.1007/s10021-013-9683-y

R Core Team, 2022. R: A language and environment for statistical computing. R Foundation for Statistical Computing, Vienna, Austria.

Ramón Vallejo, V., Smanis, A., Chirino, E., Fuentes, D., Valdecantos, A., Vilagrosa, A., 2012. Perspectives in dryland restoration: approaches for climate change adaptation. New Forests 43, 561–579. https://doi.org/10.1007/s11056-012-9325-9

Robin, C., Capron, G., Desprez-Loustau, M.L., 2001. Root infection by *Phytophthora cinnamomi* in seedlings of three oak species. Plant Pathology 50, 708–716. https://doi.org/10.1046/j.1365-3059.2001.00643.x

Rodríguez-Calcerrada, J., Sancho-Knapik, D., Martin-StPaul, N.K., Limousin, J.-M., McDowell, N.G., Gil-Pelegrín, E., 2017. Drought-Induced Oak Decline—Factors Involved, Physiological Dysfunctions, and Potential Attenuation by Forestry Practices, in: Gil-Pelegrín, E., Peguero-Pina, J.J., Sancho-Knapik, D. (Eds.), Oaks Physiological Ecology. Exploring the Functional Diversity of Genus *Quercus* L., Tree Physiology. Springer International Publishing, Cham, pp. 419–451. https://doi.org/10.1007/978-3-319-69099-5_13

Rodríguez-Molina, M.C., Torres-Vila, L.M., Blanco-Santos, A., Núñez, E.J.P., Torres-Álvarez, E., 2002. Viability of holm and cork oak seedlings from acorns sown in soils naturally infected with *Phytophthora cinnamomi*. Forest Pathology 32, 365–372. https://doi.org/10.1046/j.1439-0329.2002.00297.x

Rosseel, Y., 2012. Lavaan: An R package for structural equation modeling and more. Version 0.5–12 (BETA). Journal of statistical software 48, 1–36.

Ruiz Gómez, F.J., 2018. Study of the interaction between root rot oomycetes and *Quercus ilex* L. Universidad de Córdoba, Idep - Universidad de Córdoba.

Ruiz Gómez, F.J., Navarro-Cerrillo, R.M., Sánchez-Cuesta, R., Pérez-de-Luque, A., 2015. Histopathology of infection and colonization of *Quercus ilex* fine roots by *Phytophthora cinnamomi*. Plant Pathology 64, 605–616. https://doi.org/10.1111/ppa.12310

Ruiz-Gómez, F.J., Pérez-de-Luque, A., Navarro-Cerrillo, R.M., 2019. The Involvement of *Phytophthora* Root Rot and Drought Stress in Holm Oak Decline: from Ecophysiology to Microbiome Influence. Curr Forestry Rep 5, 251–266. https://doi.org/10.1007/s40725-019-00105-3

Ruiz-Gómez, F.J., Pérez-de-Luque, A., Sánchez-Cuesta, R., Quero, J.L., Navarro Cerrillo, R.M., 2018. Differences in the Response to Acute Drought and *Phytophthora cinnamomi* Rands Infection in *Quercus ilex* L. Seedlings. Forests 9, 634. https://doi.org/10.3390/f9100634

Sánchez-Cuesta, R., Navarro-Cerrillo, R.M., Quero, J.L., Ruiz-Gómez, F.J., 2020. Small-Scale Abiotic Factors Influencing the Spatial Distribution of *Phytophthora cinnamomi* under Declining *Quercus ilex* Trees. Forests 11, 375. https://doi.org/10.3390/f11040375

Sánchez-Cuesta, R., Ruiz-Gómez, F.J., Duque-Lazo, J., González-Moreno, P., Navarro-Cerrillo, R.M., 2021. The environmental drivers influencing spatio-temporal dynamics of oak defoliation

and mortality in dehesas of Southern Spain. Forest Ecology and Management 485, 118946. https://doi.org/10.1016/j.foreco.2021.118946

San-Eufrasio, B., Castillejo, M.Á., Labella-Ortega, M., Ruiz-Gómez, F.J., Navarro-Cerrillo, R.M., Tienda-Parrilla, M., Jorrín-Novo, J.V., Rey, M.-D., 2021. Effect and Response of *Quercus ilex* subsp. *ballota* [Desf.] Samp. Seedlings From Three Contrasting Andalusian Populations to Individual and Combined *Phytophthora cinnamomi* and Drought Stresses. Frontiers in Plant Science 12, 17.

Sena, K., Crocker, E., Vincelli, P., Barton, C., 2018. *Phytophthora cinnamomi* as a driver of forest change: Implications for conservation and management. Forest Ecology and Management 409, 799–807. https://doi.org/10.1016/j.foreco.2017.12.022

Serrano, M.S., De Vita, P., Fernández-Rebollo, P., Sánchez-Hernández, M.E., 2012. Calcium fertilizers induce soil suppressiveness to *Phytophthora cinnamomi* root rot of *Quercus ilex*. Eur J Plant Pathol 132, 271–279. https://doi.org/10.1007/s10658-011-9871-6

Serrano, M.S., Ríos, P., González, M., Sánchez, M.E., 2015. Experimental minimum threshold for *Phytophthora cinnamomi* root disease expression on *Quercus suber*. Phytopathologia Mediterranea 54, 461–464.

Simón, N., Montes, F., Díaz-Pinés, E., Benavides, R., Roig, S., Rubio, A., 2013. Spatial distribution of the soil organic carbon pool in a Holm oak dehesa in Spain. Plant Soil 366, 537–549. https://doi.org/10.1007/s11104-012-1443-9

Sutton-Grier, A.E., Kenney, M.A., Richardson, C.J., 2010. Examining the relationship between ecosystem structure and function using structural equation modelling: A case study examining denitrification potential in restored wetland soils. Ecological Modelling 221, 761–768. https://doi.org/10.1016/j.ecolmodel.2009.11.015

Capítulo 4

Factores ambientales que influyen en la dinámica espaciotemporal de la defoliación y la mortalidad de los *Quercus* en las dehesas del sur de España

Sánchez-Cuesta, R., Ruiz-Gómez, F.J., Duque-Lazo, J., González-Moreno, P., & Navarro-Cerrillo, R.M., **2021**. The environmental drivers influencing spatio-temporal dynamics of oak defoliation and mortality in dehesas of Southern Spain. *Forest Ecology and Management*, 485, 118946.
https://doi.org/10.1016/j.foreco.2021.118946 (open access)

Resumen

Los ecosistemas de *Quercus* se han visto afectados globalmente por episodios de declive, que implican eventos extremos de defoliación y mortalidad, durante las últimas décadas. Tanto los factores abióticos como los bióticos parecen desencadenar estos procesos, incluyendo la propagación de patógenos invasores no nativos (por ejemplo, *Phytophthora* spp.). Sin embargo, tenemos un conocimiento limitado de cómo interactúan estos factores en un contexto espaciotemporal. Las redes regionales de seguimiento de la salud de los bosques son una herramienta relevante pero poco utilizada que nos permite desentrañar los patrones de defoliación y mortalidad de los árboles a lo largo del tiempo en relación con los factores ambientales y silvícolas. En este estudio, utilizamos una combinación de enfoques estadísticos (es decir, Kaplan-Meier, Kernel Density Estimation y Modelos Mixtos Generalizados) para analizar 3635 registros de robles (152 parcelas) de la Red Regional de Sanidad Forestal de Andalucía (España) (2001-2016, ICP Nivel I). De este modo, se estudió la variación espaciotemporal de la defoliación y la mortalidad en dehesas de *Quercus* spp. en relación con la presencia de oomicetos y los valores medios y anuales de los factores ambientales relacionados con el decaimiento del roble. La defoliación y la mortalidad anuales se correlacionaron con la temperatura media anual, el Índice de Precipitación-Evapotranspiración Estandarizado (SPEI 18 de verano y 1 de primavera) y el contenido de materia orgánica del suelo. El efecto de los oomicetos en el declive del bosque estuvo mediado por factores ambientales, teniendo mayor importancia en suelos ricos y años húmedos. Estos resultados implican que la variación en la defoliación y la mortalidad está claramente vinculada a cambios espaciotemporales relevantes en los factores ambientales. Las redes regionales de sanidad forestal son una parte crucial de las estrategias de gestión forestal adaptativa para reducir significativamente la incertidumbre respecto a los impactos del cambio climático en los ecosistemas de robles mediterráneos. La información oportuna proporcionada aquí podría conducir a mejores prácticas silvícolas, medidas preventivas contra la propagación del oomiceto y la implementación de herramientas de alerta temprana, para ofrecer evaluaciones precisas del riesgo de defoliación y de mortalidad en una escala espaciotemporal significativa.

Abstract

Quercus ecosystems have been affected globally by decline episodes, involving extreme defoliation and mortality events, during recent decades. Both abiotic and biotic factors seem to trigger these processes, including the spread of non-native invasive pathogens (e.g., *Phytophthora* spp.). However, we have limited understanding of how these factors interact in a spatio-temporal context. Regional forest health monitoring networks are a relevant but rarely used tool that enables us to disentangle the patterns of tree defoliation and mortality over time in relation to environmental and silvicultural drivers. In this study, we used a combination of statistical approaches (i.e., Kaplan-Meier, Kernel Density Estimation and generalized mixed models) to analyse 3635 records of oak trees (152 plots) from the Regional Forest Health Network of Andalusia (Spain) (2001-2016, ICP Level I). In this way, we studied the spatio-temporal variation of defoliation and mortality in dehesas of *Quercus* spp. in relation to oomycetes occurrence and the average and annual values of environmental factors related to oak decline. The annual defoliation and mortality were correlated with the mean annual temperature, Standardised Precipitation-Evapotranspiration Index (SPEI 18 summer and 1 spring) and soil organic matter content. The effect of oomycetes on forest decline was mediated by environmental factors, having greater importance in rich soils and wet years. These results imply that variation in defoliation and mortality is clearly linked to relevant spatio-temporal changes in environmental factors. Regional forest health networks are a crucial part of adaptive forest management strategies to significantly narrow the uncertainty regarding climate change impacts on Mediterranean oak woodland ecosystems. The timely information provided here could lead to better silvicultural practices, preventive measures against the spread of the oomycete and the implementation of early warning tools, to deliver accurate assessments of the defoliation and mortality risk on a meaningful spatio-temporal scale.

Keywords: Defoliation, Mortality, regional networks, Kernel Density Estimations, forest decline, climate change, dehesas ecosystems.

1 Introduction

Forest pests and diseases contribute to natural shifts in community composition, ecosystem processes, landscape-scale biotic disturbances and disturbance regimes structure via their impacts on both individual trees and whole ecosystems (Mordecai, 2011; Cobb and Metz, 2017; Simler-Williamson et al., 2019). However, the combined threats to forest ecosystems posed by climate change, the introduction of invasive species and other anthropogenic impacts have rapidly increased their vulnerability at large spatio-temporal scales, originating widespread forest decline processes (Millar and Stephenson, 2015; Trumbore et al., 2015; Ghelardini et al., 2016). Therefore, it is important to integrate a systematic approach, including the environmental drivers related to tree mortality, to understand these processes and predict future shifts in pest and pathogen dynamics in relation to tree health (Oliva et al., 2014; Anderegg et al., 2015; Hartmann et al., 2018).

Global pattern of forest decline is particularly relevant in the most representative ecosystem of the Southern Iberian Peninsula: the Mediterranean-like savannas dominated by *Quercus* species (hereafter, *dehesas*). *Dehesas* are agro-sylvo-pastoral ecosystems managed intentionally to maintain a grass or crop understory, as part of a multifunctional agroforestry unit (Moreno and Pulido, 2009). In the Southern Iberian Peninsula, a combination of abiotic and biotic factors is weakening the health of *dehesas* in multiple ways, causing extensive defoliation and mortality events (Sánchez et al., 2006; de Sampaio e Paiva Camilo-Alves et al., 2013; Sallé et al., 2014; Lieutier and Paine, 2016). Despite the resilience of these systems to drought and high temperatures (Gentilesca et al., 2017), seasonal variation and extreme events can cause large mortality events, particularly in a close interaction with pests and diseases (Natalini et al., 2016). Among these factors, oak decline in *dehesas* has been mainly related to root rot caused by the non-native pathogen *Phytophthora cinnamomi* and other soilborne oomycetes like *P. quercina*, *P. plurivora*, *P. gonapodyides* and *Pythium spiculum* (Brasier et al., 1993; Sánchez et al., 2002; Jiménez et al., 2008; Corcobado et al., 2010; Redondo et al., 2015; Ruiz-Gómez et al., 2019a). Since the late 90s, *Phytophthora cinnamomi* has been considered one of the main agents behind of holm and cork oak death in South-West of the Iberian Peninsula (Brasier et al., 1993). Nevertheless, recently it has been demonstrated that other pathogenic oomycetes could lead to decline symptoms and death in several

oak species including *Q. ilex* and *Q. suber* (Romero et al., 2007; Corcobado et al., 2010; Ruiz-Gómez et al., 2019a). Moreover, several studies have showed that other important factors regulating oak decline are soil microbial diversity, including Ectomycorrhizae abundance (Corcobado et al., 2014b; Ruiz-Gómez et al., 2019a).

Root rot constrains tree water uptake by destroying fine roots (Redondo et al., 2015; Ruiz-Gómez et al., 2015; Ruiz-Gómez et al., 2019a), which interacts with other physiological disturbances triggered by the presence of the pathogen inside root tissues (Ruiz-Gómez et al., 2018). This process causes an unprecedented mortality risk which is not restricted to small, supressed trees, as is habitual in Mediterranean ecosystems, but mainly affects medium to large trees (Ibáñez et al., 2015). Several authors have found that the potential distribution of *P. cinnamomi* in the Iberian Peninsula will increase under different climate change scenarios (Duque-Lazo et al., 2018; Hernández-Lambraño et al., 2018). In this new ecological context, understanding the environmental factors that trigger annual mortality and defoliation events in oak *dehesa* ecosystems is of paramount importance to ensure their sustainability and multifunctional character.

Little effort has been made to forecast forest health in near real time, besides creating static potential occurrence scenarios for global warming for the coming decades (Dietze et al., 2018; Duque-Lazo et al., 2018). This type of medium-term forecasting scenario allows policy makers, governments and stakeholders' associations to plan their strategies in the long-term (e.g., more than 20 years). Nevertheless, most management decisions related to forest health, provision of ecosystem services and management relate to the short or near-term (daily to annual) (Pinto-Correia and Azeda, 2017). After more than a decade of functioning, Forest Health Networks (e.g., ICP Forest, International Co-operative Program on Assessment and Monitoring of Air Pollution Effects on Forests) could start contributing to the filling of this major gap in forest research. Particularly, environmental monitoring networks could help the study of the specific mechanisms behind the complex spatio-temporal relationships among crown condition, mortality and various environmental stress factors (Hartmann et al., 2018; Senf et al., 2018; Seidling, 2019). At the regional scale, several Forest Health Networks have been established to study spatial patterns of exposure of forests to biotic and abiotic risk factors (Bussotti and Pollastrini, 2017; Popa et al., 2017), facilitating the study of these patterns at a relevant, manageable scale.

Together with mortality, defoliation has been frequently used to assess forest health (Peñuelas et al., 2001; Carnicer et al., 2011; Ferretti et al., 2014). Defoliation *a priori* is not an indicator of mortality but rather a physiological response to the interruption of growth (Dobbertin, 2005; MacLean, 2016; DeSoto et al., 2020). Thus, the temporal patterns of defoliation could show the existence of a "point of no return" at which permanent damage is done, leading ultimately to tree mortality (Carnicer et al., 2011; Ferretti et al., 2014).

Using the *dehesa* ecosystem in Andalusia (Spain) as a case study, we addressed the spatio-temporal trends of defoliation and mortality, as well as the identification of the core environmental drivers (i.e., climatic, soil and topographic variables) related to those processes. To achieve this objective, we used a forest health monitoring scheme that has systematically collected information from all forest ecosystems in Andalusia since 2000, the "Red Andaluza de Seguimiento de Daños sobre Ecosistemas Forestales" (hereinafter, SEDA). This monitoring scheme was initiated as part of the European network of monitoring plots, ICP-Forests-Level I (Navarro-Cerrillo et al., 2000). The SEDA plots are located at the vertex of an 8 x 8 km grid and are used to gather information annually on the condition of the same 24 trees, recording symptoms of forest health (defoliation and crown discolouration, 5-year tree growth, level of damage and abundance of biotic and abiotic agents, among others). This study had three specific objectives: i) to describe the current spatio-temporal distribution of defoliation and mortality of *Quercus* spp. *dehesas* in the Andalusia SEDA network, using Kernel Density Estimation (KDE) and regional survival analysis, ii) to identify the most significant environmental drivers triggering annual defoliation and mortality, using generalized mixed models, and iii) to understand the effect of oomycetes occurrence (including *P. cinnamomi*), both alone and when interacting with other factors, on *dehesa* health. The SEDA database provides a long-term monitoring system to help unravel these questions, providing the clues to predict future trends of forest decline processes and, consequently, serving as a tool for managing and planning ecosystem services, and preventing and adapting to changes in forest dynamics, on a large geographical scale (Meentemeyer et al., 2012; Axelson et al., 2019).

2 Material and methods

2.1 Study area

The study area comprises the northern distribution of *dehesas* of *Quercus* spp. (*Q. ilex, Q. suber, Q. faginea* and *Q. coccifera*) in the region of Andalusia (Spain), located in the South of the Iberian Peninsula, between 37° and 39° N latitude (28,467 km^2, Figure 1). *Dehesas* are distributed mainly in the northern part (e.g., Sierra Morena) of the region, along a climatic gradient covering an average annual precipitation range of 660 mm (440–1,100 mm) and an average annual temperature range of 10 °C (8–18 °C) (Costa et al., 2006) (Sierra Morena) (Figure 1). According to the climatic classification system proposed by Gómez-Zotano et al. (2015), six main defined climate types were selected (Figure 1, average annual temperature and precipitation): Oceanic Mediterranean climate of the windward coast – OWC – (16.1-18.8 °C, 500-900 mm), Semi-oceanic Mediterranean climate of the lower Guadalquivir – MLG – (16.5-18.5 °C, 510-780 mm), Semi-continental (dry-subhumid) Mediterranean climate of the Middle Guadalquivir – MMG – (15.0-18.0 °C, 435-800 mm), Semi-oceanic (subhumid-humid) Mediterranean climate of the Western peribetic foothills – PBF – (15.1-18.4 °C, 630-1170 mm), Semi-oceanic (subhumid-humid) Mediterranean climate of the Western peribetic mountains – PBM – (12.5-17.0 °C, 680-1175 mm), and Continental (dry-subhumid) Mediterranean climate of the Eastern circumbetic ranges and hills – CBH – (13.0-17.3 °C, 450-800 mm).

2.2 Defoliation and mortality data

The 152 plots used were selected from the SEDA network for the period 2000 to 2016 (https://descargasrediam.cica.es/repo/s/RUR?path=%2F05_CALIDAD_AMBIENTAL%2F04_ECOSISTEMAS_FORESTALES%2F01_EQUILIBRIOS_BIOLOGICOS%2FRedSedaPinsapo). These plots are located on the intersection or node of an 8 x 8 km grid established by a systematic sampling design (Figure 1) in which 24 trees were selected per plot (6 trees per quadrant, NE, SE, SW and NW). For this study, we used the criteria established by the Law of the Dehesa (7/2010, of 14 July, for the Dehesa, Andalusia, Figure 1) for plot selections: i) total tree cover between 5% and 75%; and ii) *Quercus* species represent more than 90% of the total tree cover. Of the 152 plots (N=3366 trees), 80 plots were pure *Q. ilex*, and the rest a mixture of *Quercus* spp. Defoliation data were collected annually during the summer (2001-2016)

for all the trees present in each plot, using the methodology of the ICP-Forests manual (Eichhorn et al., 2016). For each tree, defoliation was classified into one of 20 percentage classes (between 0 and 100) by comparison with a local "reference tree", according to the inter-calibration at the national level (Sánchez Peña et al., 2010; Ferretti et al., 2016); this was performed by the same independent teams. If any of the trees died, due to either anthropogenic or natural causes, the death was recorded and the tree was replaced by another, similar tree within the plot to continue with the defoliation estimation. Replacement trees were excluded from this study and the raw data were refined and organised into a reliable database.

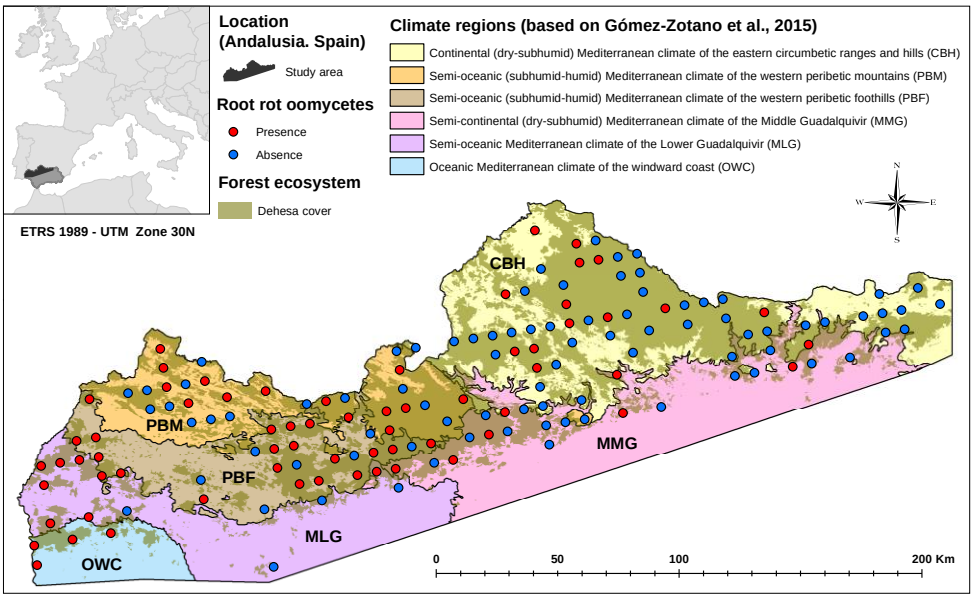

Figure 1. Location of tracking plots of Dehesas of *Quercus* spp. with presence/absence of root rot oomycetes, selected of the SEDA Network within Andalusia-Spain (Sierra Morena and the Andévalos of Huelva).

2.3 Presence of root rot

We used the presence of root rot oomycetes, instead of only *P. cinnamomi*, as a proxy for the root rot incidence probability, differentiating between infested (root rot oomycete positive diagnosis) and non-infested (root rot oomycete negative diagnosis) plots.

The presence of root rot oomycetes in the plots was evaluated in three different ways. First, historical data of *Phytophthora* spp. identification in the SEDA plots were compiled from the SEDA database and previous, related works found in the literature (Duque-Lazo et al., 2018; Hernández-Lambraño et al., 2018; Ruiz-Gómez et al., 2019a). To avoid the common uncertainties about metabarcoding or other DNA-based techniques as a diagnostic tool, the identification of root rot oomycetes through these techniques was taken into account in order to classify plot as infested only when the analysis was done over a SEDA plot showing decline symptoms in several years up to the end of the study period. Second, the presence of *Phytophthora* spp. and *Pythium spiculum* in several plots was evaluated in the laboratories of the University of Córdoba and the Consejería de Agricultura, Ganadería, Pesca y Desarrollo Sostenible, through classical isolation methods (Jeffers and Martin, 1986; Erwin and Ribeiro, 1996; Sánchez et al., 2002). These diagnostics were carried out during the season in which the presence of *P. cinnamomi* or *P. spiculum* was registered in the SEDA Network database, but there is not record of the precise date in which samples were collected or analysis was carried out. The results of these diagnostic analyses are included in the public database of the SEDA network. Third, the probability of oomycete root rot incidence in plots without reliable information concerning soil diagnosis was assessed following a methodology based on the distribution and severity of tree decline symptoms (Sancho et al., 2018), emphasising the temporal dynamics of tree crown defoliation, the level of damage caused by biotic and abiotic agents and their abundance. When plots presented high and progressive defoliation with clear positive trend until the end of the study period and occasionally tree sudden death, and no other biotic or abiotic agent showed abundance or damage level over 2 (in a 0-3 scale) apart from the agent identified as T8-3 in the SEDA database (Other/unknow agents), (Consejería de Medio Ambiente y Ordenación del Territorio, 2018) plots were considered as infested. Plots where other biotic agents (e.g., *Cerambyx* spp.) were present and caused damage that was moderate/important and/or sustained over time and plots

with punctual and destructive abiotic agents (e.g., fire, cutting down of trees, etc.) were not considered as infested plots through this methodology.

Finally, 66 plots showed a positive diagnosis for root rot oomycetes (infested plots) and 86 a negative diagnosis (non-infested) in the period 2000-16 (Table S4.1 and Table S4.2, Supplementary Material).

2.4 Environmental variables

The dataset contains several categories of variables: mean climatic (e.g., temperature, precipitation), annual climatic (temperature, precipitation and drought index), topographic (e.g., slope, aspect) and soil (e.g., texture, soil pH) (Table S4.3, Supplementary Material). All data layers were downloaded from the Andalusian Environmental Information Network – REDIAM (https://descargasrediam.cica.es/repo/s/RUR?path=%2F05_CALIDAD_AMBIENTAL%2F04_ECOSISTEMAS_FORESTALES%2F01_EQUILIBRIOS_BIOLOGICOS%2FRedSedaPinsapo). The mean climatic data (1971-2000) and the topographic and soil data were extracted from the Forest Biomass project of Andalusia at 100 m resolution (see methods in Guzmán-Álvarez et al., (2012)). Annual climatic variables (estimates for each year in the time series) were calculated from interpolations of the monthly precipitation and temperature data of all the official weather stations in Andalusia, at 500 and 100 m resolution, respectively (available at REDIAM). We then calculated several climatic variables for each year and plot from the SEDA time series, based on the *dehesa* dynamics and the biology of root rot oomycetes and its potential relationship with environmental variables (de Sampaio e Paiva Camilo-Alves et al., 2013; Sánchez-Cuesta et al., 2020). The temperature-related variables were mean temperature for each year and up to three years previously, mean temperature in spring for each year and the previous one, and mean temperature in summer and winter for each year. For precipitation, we calculated the rainfall (mm) for annual (January to December) and hydrological (September to August) period. We also estimated the precipitation from up to three years previously and the accumulated rainfall of the two, three and five previous years. We calculated the SPEI drought index (Vicente-Serrano et al., 2010) as the monthly difference between the precipitation and potential evapotranspiration, for different timescales (1, 3, 6, 18 and 24 months). The scale is achieved by aggregating the monthly SPEI index from the current time to up to 24 months ago, using a rectangular kernel (i.e., all previous months have equal weight; (Vicente-Serrano et al., 2010)).

Each timescale will have an effect in a different sub-hydrological system (Vicente-Serrano et al., 2010). For instance, short timescales are mainly related to soil water content and river discharge in headwater areas, medium timescales are related to reservoir storages and discharge in the middle course of rivers and long timescales are related to variations in groundwater storage. Evapotranspiration was estimated per plot with the Thornthwaite equation, using the monthly temperature and latitude. SPEI was calculated per month and timescale for all the study period, using the SPEI R package (Beguería and Vicente-Serrano, 2017), and was then averaged per year for the summer and spring seasons.

2.5 Mortality analysis

We used the Kaplan-Meier estimation method to create tree survival curves and to determine the probabilities of survival (with the associated 95% confidence intervals) for the studied period (2001-2016), separately for all the study area and each climatic region (see study area section). Time series for each tree were constructed between the year of plot establishment (2001) and the date of tree death. Chi-squared tests were used to statistically compare the *Quercus* spp. mortality in the infested and non-infested plots. The log-rank test, which can be used to compare curves from different groups (Riffenburgh, 2012), was performed to analyse differences in survival between the climatic regions. The statistical analyses were performed using the R *survival*, *ggplot2*, *ggfortify* and *ranger* Survival Analysis packages (Fox and Carvalho, 2012).

2.6 Spatio-temporal patterns of defoliation and mortality

Kernel Density Estimation (KDE) was used to assess the spatio-temporal correlation patterns of the defoliation and mortality. This is a non-parametric method which estimates the probability density function of random variables (Kenchington et al., 2014) and has been widely used for the estimation of forest variables (Wandresen et al., 2019). The distribution patterns of defoliation and mortality were explored based on finite data samples (O'Brien et al., 2012) and KDE was calculated for each year of the time series (2001-2016), weighting observations by the number of dead individuals recorded and the defoliation levels. We selected a Gaussian kernel density (KD) function, and the optimal bandwidth was estimated using leave-one-out least-squares cross-validation (LSCV) for bivariate KD bandwidths estimation in the *sparr* R package (Davies et al., 2011).

2.7 Temporal modelling of defoliation and mortality

We used Generalized Linear Mixed Models (GLMMs) in a multimodel inference approach (Burnham and Anderson, 2002) to analyse the relationship between mortality and defoliation levels and climatic (mean and annual), topographic and soil variables. We modelled the error terms of the defoliation model as a log-normal distribution while mortality (i.e., the presence of at least one dead tree) was modelled with a binomial distribution and logit link (i.e., logistic regression). The inventory plot ID was included as a random effect in the model to account for temporal pseudo replication.

Prior to modelling we checked the explanatory variables for collinearity using pair-wise Pearson's correlation tests (Figure S4.1, Supplementary Material). For fixed variables (mean climatic, topographic and soil) we excluded those with correlation values higher than 0.6 and then selected the ones with the best biological rationality. The annual climatic variables (temperature, precipitation and SPEI) were highly correlated within groups and thus we selected the non-correlated variable with the highest explanatory power for each environmental variable group and for each dependent variable using univariate GLMMs.

We performed multimodel inference based on an all-subsets selection of GLMMs, using Akaike's information criterion corrected for a large number of predictors (AICc) (Burnham and Anderson, 2002). For all combinations tested, all models within four AICc units of the best model (delta < 4) were considered as the set of best models given the selected predictors. This threshold is within the limits adopted in other studies (Grueber et al., 2011; González-Moreno et al., 2013). Within the best model subset, we calculated the Akaike weight of evidence (wi) for each candidate model to rank the predictors in order of importance in relation to the response variables. The wi of each predictor was estimated as the sum of the model AICc weights across all models in which the selected predictor appeared. This means that the predictor with the highest wi (i.e., closest to one) has the highest relative importance (compared to the other predictors) in the explanation of the response variables within the given data (Burnham and Anderson, 2002). In addition, multimodel inference was used to estimate regression coefficients and their confidence intervals (with the adjusted standard error) within the best model subset (i.e., the conditional average for models having delta < 4). The coefficient of a given selected predictor was calculated as the sum of the

predictor´s coefficient multiplied by the wi, across all possible models where the predictor was present (Burnham and Anderson, 2002). This multimodel inference approach was performed in a hierarchical way. First, we implemented separate models for each group of predictors (climatic, topographic and soil) and identified those variables with higher significance in the conditional averaging method. The best variables per group were then used to establish the final set of best-candidate models for each dependent variable. Finally, the best model identified using multimodel inference per dependent variable (lowest AICc) was used to study the interaction of the environmental variables with the presence of root rot oomycetes. All statistical analyses were performed with R-CRAN software (R Development Core Team, 2017), using the package *MuMIn* (Bartoń, 2020).

2.8 Statistical analysis

The distributions of all variables were assessed for normality and homoscedasticity using Anderson-Darling and Levene tests, respectively (Korkmaz et al., 2014). When a variable did not fit a normal distribution, it was log-transformed, and the normality was tested again.

In the case of the normally distributed variables, differences between infested and non-infested plots, or between climatic regions, were evaluated using ANOVA followed by the Bonferroni Intervals test for mean comparisons. For variables which did not fit a normal distribution, the non-parametric Kruskal-Wallis test was performed, followed by the Pairwise Comparison test with Bonferroni's correction.

Time series were analysed using partial least square regression, to assess the presence of significant trends over time, and the Wilcoxon pairwise test, to evaluate differences between groups (Kosiorowski et al., 2019). All the statistical analyses were carried out in the R environment v 3.6.3 (R Development Core Team, 2017), running on RStudio 1.1 (Team RStudio, 2016).

3 Results

3.1 Mortality analysis

The percentage tree mortality for the studied period (2001-2016) was 4.2% and 9.5% for non-infested and oomycete-infested plots, respectively, being significantly different according to the Kaplan-Meier analysis (Figure 2). The percentage mortality varied among the climatic zones in Andalusia. The OWC zone did not host any tree death events during the period in any of the four plots included in this region. The Circumbetica hills zone (CBH) showed significantly lower mortality rates and the PBF zone the highest ones, without differences among the rest of the climatic zones (MLG, MMG and PBM) (Table S4.4, Supplementary Material). When survival was analysed in relation to the presence of root rot in the plot and the climatic zone to which the plot belongs, the mortality rates were highest in infested PBM plots (Table S4.5, Supplementary Material). The Middle Guadalquivir zone (MMG) was the only one which presented significantly higher mortality rates for non-infested plots (Figure 2); it had rates for non-infested plots similar to those of other Western zones (MLG and PBF), but lower values of mortality for infested plots (Table S4.5, Supplementary Material). The differences between infested and non-infested plots were greatest in the PBM zone, where the survival rate was the lowest for trees located in the infested plots (Figure 2, Table S4.5, Supplementary Material).

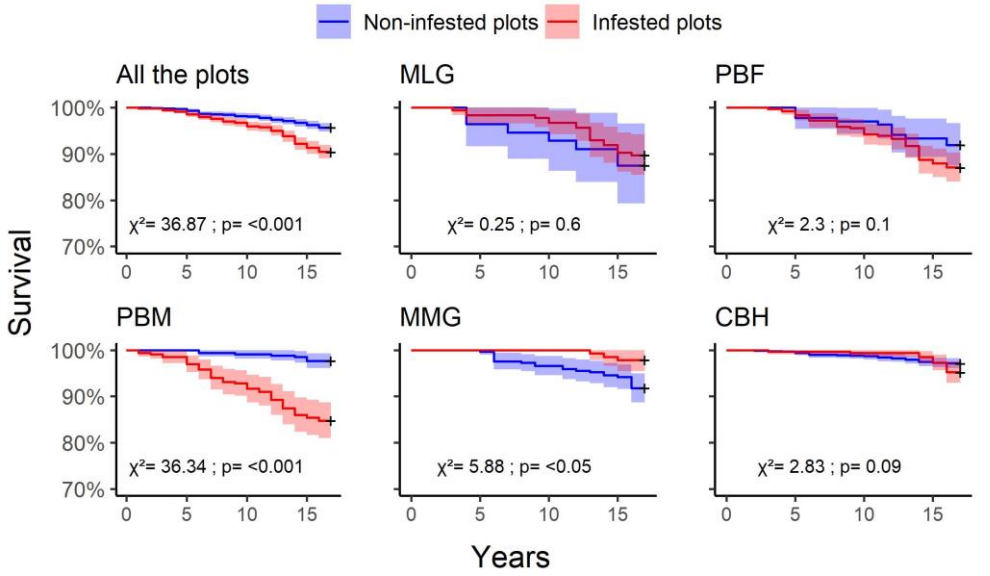

Figure 2. Survival probability graph of *Quercus* spp. using Kaplan-Meier for the study area. X-axis, years since the beginning of the monitoring of the phytosanitary status of the trees on the plots (year 2000) Y-axis, proportion of surviving trees. MLG: Semi-oceanic Mediterranean climate of the lower Guadalquivir; PBF: semi-oceanic (subhumid-humid) Mediterranean climate of the western peribetic foothills; PBM: semi-oceanic (sub-humid-humid) Mediterranean climate of the western peribetic mountains; MMG: Semi-continental (dry-subhumid) Mediterranean climate of the Middle Guadalquivir; CBH: continental (dry-sub-humid) Mediterranean climate of eastern circumbetic ranges and hills.

3.2 Spatial and temporal trends in defoliation and mortality

The annual plot-averaged defoliation and mortality within Andalusia during the period 2001–2016 showed different spatial patterns (Figure 3, Figure 4). Defoliation showed a significant trend, decreasing with the geographical longitude of the location of the plot (Figure S4.2, Supplementary Material), and exhibited more relevant values in the Western zones (i.e., OWC, MLG and PBM), particularly from 2011 in OWC (Figure S4.3, Supplementary Material). Overall, defoliation differed significantly among the climatic zones ($F=15.54$; $P < 0.001$), the values being significantly lower in CBH and MMG plots than in MLG and PBF plots (Table S4.6, Supplementary Material). The KDE approach highlighted some areas (in the Western part) that were particularly affected in more recent years (2016), but the presence of symptoms was generalised in all the northern part of the region. Plot-averaged mortality values were also higher in western zones, with a

generalised low incidence in the initial part of the study (before 2006) and higher incidence in eastern plots at the end (Figure 4).

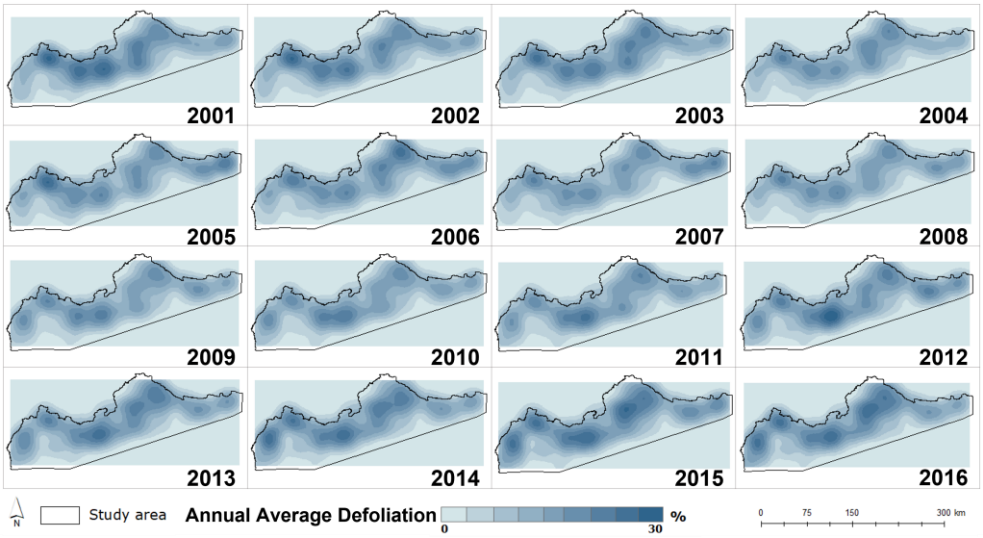

Figure 3. Estimate evolution of defoliation of *Quercus* spp. related to root rot from 2001 – 2016 using Kernel density. SEDA Network of Andalusia.

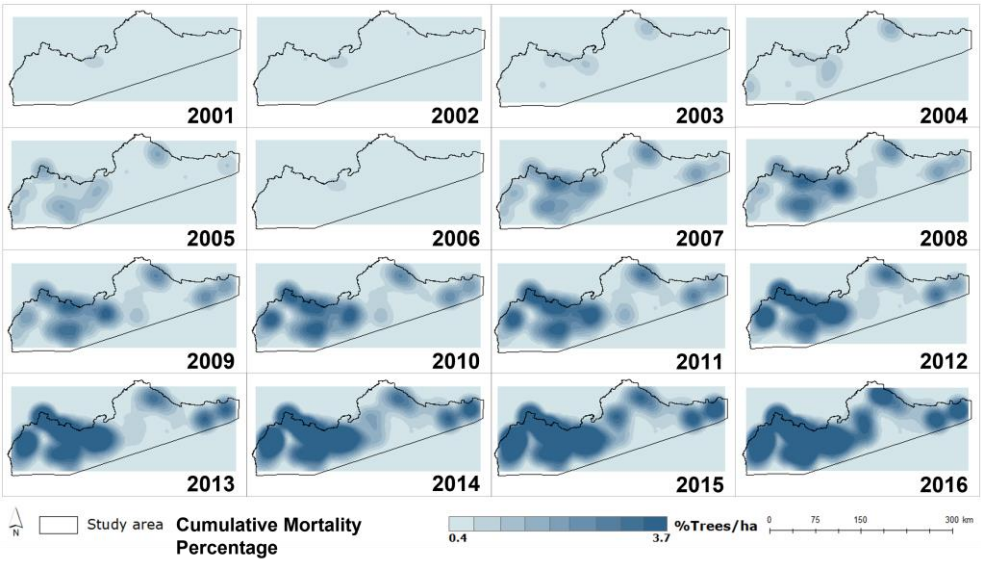

Figure 4. Estimate evolution of mortality of *Quercus* spp. related to root rot from 2001 – 2016 using Kernel density. SEDA Network of Andalusia.

Across time, the defoliation levels for infested and non-infested plots were rather similar within zones, without significant differences between infested and non-infested plots, except in the CBH zone, which showed higher rates of defoliation in infested plots (Wilcoxon statistic W=6.5; $P < 0.05$), and the PBM zone, which showed significantly higher values in non-infested plots (W=10.55, $P < 0.01$). In the MLG climatic zone, infested plots had defoliation levels that were clearly higher during the period 2006-2011 (Figure S4.3, Supplementary Material).

3.3 Defoliation model

As the climatic variables were highly correlated, for the final model we selected the best predictor of defoliation per group (temperature, precipitation and SPEI), using univariate models. For the temperature variables, annual mean temperature was the best predictor (Table S4.7, Supplementary Material). The mean temperature of the current year was more relevant than the mean temperatures of previous years, and the mean temperatures per season (spring or summer) (Table S4.7, Supplementary Material). Regarding the precipitation variables, the most important was the precipitation accumulated in the last two hydrological years. The longer temporal values of SPEI (18-24 months) for the summer period were the most important (Table S4.7, Supplementary Material).

Regarding the full model, the only variables explaining a significant percentage of the defoliation were annual temperature and summer SPEI (18 months scale), with a positive and a negative relationship, respectively (Table 1). The accumulated precipitation of the previous two hydrological years was marginally significant (Table 1, Figure 5b), while the presence of pathogenic oomycete root rot and the rest of the topographical and soil variables were not significant (Table 1). We found a significant interaction between the presence of oomycete root rot and both SPEI 18 (beta: 0.012, t: 2.9, $P < 0.001$) and the precipitation of the last two years (beta: -0.014, t: -2.6, $P < 0.001$). Specifically, non-infested plots showed less defoliation in wet years, in comparison to infested plots (Figures 5a, 5b). The summer SPEI 18 showed a significant tendency to decrease during the study period, which was significantly related to increases in defoliation (Figure 6a, Table S4.9, Supplementary Material).

Table 1. Defoliation model. Multimodel inference results of the averaged best models explaining % defoliation (conditional average on models < 4 AICc). For each predictor we provide the estimated coefficient, standard and adjusted error, significance, and accumulated weights (importance). In bold significant variables ($P < 0.05$). See variable explanation in Table S3.

	Estimate	SE	Adj. SE	z value	Pr(>|z|)	Sum Weights	N. models
(Intercept)	1.110	0.007	0.007	163.457	<0.001		
ta	0.025	0.006	0.006	4.129	<0.001	1.00	14
$spei_{18}$_summ	-0.009	0.002	0.002	3.705	<0.001	1.00	14
prech_2lag	-0.005	0.003	0.003	1.666	0.096	0.62	8
Sd	-0.010	0.006	0.006	1.635	0.102	0.58	7
Ca	-0.005	0.007	0.007	0.814	0.416	0.31	6
Oom	0.002	0.013	0.013	0.122	0.903	0.25	6

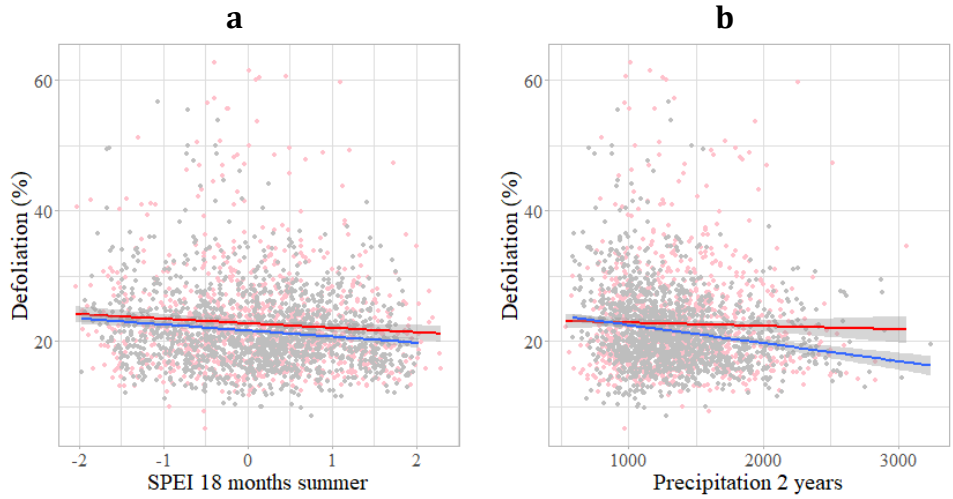

Figure 5. Interaction between drought proxies a) standardized precipitation evapotranspiration index 18-months accumulated-$SEPI_{18}$ and b) precipitation of the last two years to explain defoliation levels in *Quercus* stands. Red line and dots represent plots with oomycete presence, while blue line and grey dots correspond to plots without oomycete.

3.4 Mortality model

The best predictors of mortality per group (temperature, precipitation and SPEI), when using univariate models, were similar to those for defoliation. Of the temperature variables, annual mean temperature was the best predictor. The mean temperature of the current year was more relevant than the mean temperatures of previous years (Table S4.8, Supplementary Material). Regarding the precipitation variables, the most important were the precipitation of the last calendar year and the accumulated precipitation of the last two calendar years (Table S4.8, Supplementary Material). Among the SPEI group, drought during spring at the one-month scale was the most important variable, followed by SPEI during summer at the 18-month scale (Table S4.8, Supplementary Material).

Considering the full model, the probability of mortality was related negatively to spring SPEI at the one-month scale and positively to mean annual temperature (Table 2). Spring SPEI 1 had a trend similar to that of summer SPEI 18, with a significant decrease during the study period (Figure 6b; Table S4.9, Supplementary Material), and was also correlated significantly and negatively with the mortality incidence (Table S4.9, Supplementary Material).

Table 2. Mortality model. Multimodel inference results of the averaged best models explaining probability of tree mortality (conditional average on models < 4 AICc). For each predictor we provide the estimated coefficient, standard and adjusted error, significance, and accumulated weights (importance). In bold significant variables ($P < 0.05$). See variable explanation in Table S3.

	Estimate	SE	Adj. SE	z value	Pr(>|z|)	Sum Weights	N. models
(Intercept)	-3.305	0.19	0.193	17.156	<0.001		
spei$_{1}$_spr	-0.219	0.09	0.090	2.444	0.015	1.00	42
ta	0.548	0.18	0.176	3.110	0.002	1.00	42
OM	0.302	0.14	0.137	2.202	0.028	0.90	36
prec_1lag	-0.216	0.12	0.123	1.753	0.080	0.75	28
tmh	-0.285	0.2	0.205	1.392	0.164	0.50	22
Oom	0.289	0.29	0.291	0.992	0.321	0.30	14
CEC	-0.108	0.14	0.136	0.789	0.430	0.27	14
spei$_{18}$_summ	0.024	0.16	0.158	0.152	0.879	0.24	13
Ca	-0.005	0.22	0.219	0.023	0.982	0.21	12

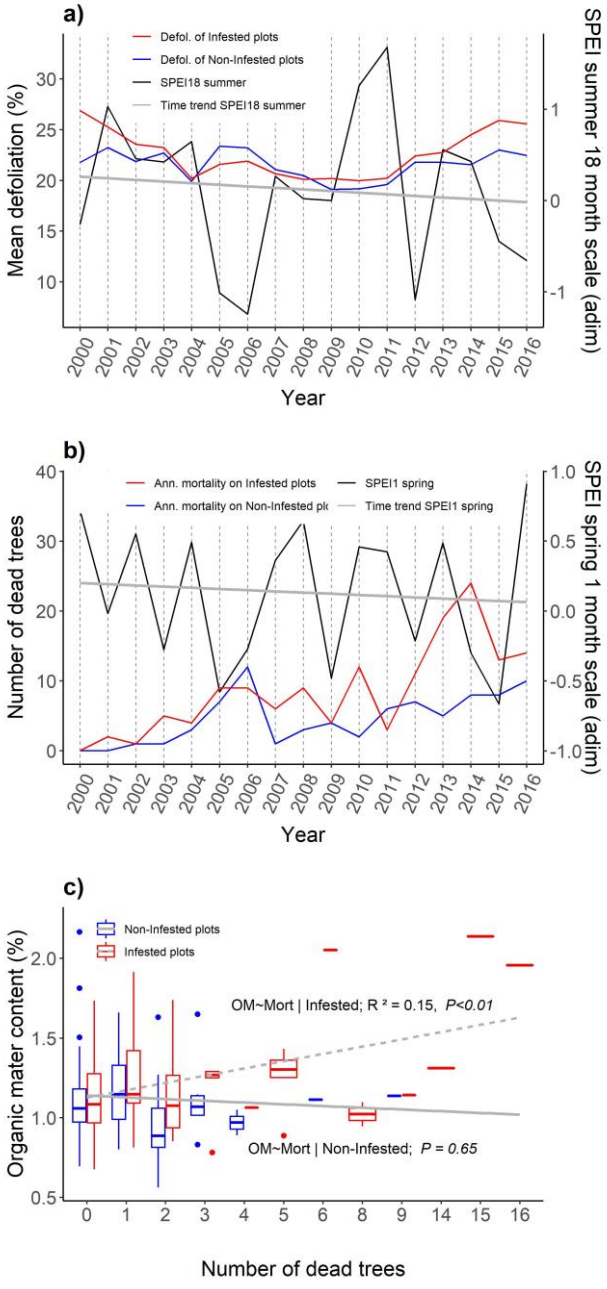

Figure 6. Evaluation of studied core drivers with significant effect on the defoliation and mortality spatial-temporal models. a) trend for SPEI 18 months summer compared with defoliation (see regression results in Supplementary Material, Table S4.9) b) trend for SPEI 1 month spring compared with annual mortality events (see regression results in Supplementary Material, Table S4.9) c) Boxplot distribution of Organic Matter content in plots with and without infestation and accumulated mortality events on each plot during the period.

Interestingly, the probability of mortality was higher for plots in which the soil had a higher content of organic material. We found a significant interaction between *P. cinnamomi* presence and the proportion of organic material in soil (beta: 0.67, z-value 2.65, $P < 0.001$). Specifically, for rich soils, infested plots showed higher mortality than non-infested plots (Figure 6c). The total number of annual tree deaths per plot was significantly correlated with the soil organic matter (OM) content in infested plots, but there was no correlation for non-infested ones (Figure 6c). The infested plots with higher soil OM contents had higher mortality rates, whereas in the non-infested plots with the maximum values of OM there were no deaths during the study period, and all the non-infested plots with OM values above 1.5% showed low mortality rates (3 deaths or fewer during the study). The rest of the variables, including the presence of *P. cinnamomi*, were not significantly related to mortality.

4 Discussion

Our study confirms the importance of both abiotic and biotic factors in the triggering of forest dieback. Our study shows increasing defoliation and mortality with a continuous temporal and spatial trend, in agreement with other findings at regional and continental levels (Peñuelas et al., 2001; Carnicer et al., 2011; Duque-Lazo and Navarro-Cerrillo, 2017).

4.1 Spatial and temporal patterns of mortality and defoliation

Our empirical results from Andalusia show low values of accumulated tree mortality of *Q. ilex* (2.3%, 2001-2016). However, the annual mortality rate (0.153%) was 5-10 times higher than that obtained from other forest health networks, ranging between 0.010 and 0.015% (Mantgem and Stephenson, 2007) and 0.001 and 0.03% for *Quercus* spp. (Lines et al., 2010). The *Q. ilex* mortality related to *P. cinnamomi* has been found to be high at the local scale in very-affected areas, with mortality rates of up to 59% for *Q. ilex* in a 10-year period (Natalini et al., 2016). However, the discrepancy between our findings and these studies could be mainly caused by the different data sources (e.g., low-density monitoring networks with 1 plot/64 km^2 *vs*. intensive inventory in high-damage areas) (Romero de los Reyes et al., 2007). The biologically-most-plausible interpretation of these results is that pathogenic oomycetes (e.g., *P. cinnamomi* and related species) are contributing to the increasing mortality rates. However, other possible causes of the increase in mortality

should be considered - such as primary pests (Duque-Lazo and Navarro-Cerrillo, 2017), droughts (Natalini et al., 2016; Gea-Izquierdo et al., 2020), soil microbial diversity and oomycete community evenness, ectomycorrhizae presence and abundance (Corcobado et al., 2014b; Ruiz-Gómez et al., 2019a) or complex interactions (senescence with age, mismanagement, etc.) (Moreno-Fernández et al., 2019).

The annual defoliation rate of *Q. ilex* showed moderate average values (30%, 2001-2016), similar to those obtained for *Q. ilex* in the European and Spanish health networks (Klap et al., 2000; Carnicer et al., 2011; de la Cruz et al., 2014; Michel and Seidling, 2017). The defoliation in relation to the presence of root rot oomycetes, as well as when considering both infection and climate-zone factors together, was rather aleatory. Some zones had higher defoliation rates for infested plots and others showed higher rates for non-infested ones, depending on their longitudinal location, which was the only clear trend for defoliation. Other authors concluded that defoliation is actually a weak indicator as a symptom of root rot, due to the great influence of several environmental factors - mainly seasonal drought and high temperatures - on the regulation of crown foliage density (Camarero et al., 2015; Navarro-Cerrillo et al., 2019; Gea-Izquierdo et al., 2020). This agrees with our results, since climatic drivers (Summer SPEI 18 and Ta) are the core drivers explaining defoliation variability across time in the model.

Our modelling approach, using KDE, revealed temporal trends in defoliation and mortality: both increased with time, especially mortality. The higher oak mortality in the west, spreading to the north-east during the study period, and the increase in defoliation in the western part agree with previous studies (Duque-Lazo et al., 2016, 2018; Hernández-Lambraño et al., 2018) which reported high *P. cinnamom*i densities in western areas of Andalusia. This might be linked to two factors: first, the spatial pattern of *P. cinnamomi*, related to its initial dispersion area in southern Portugal and Spain (Serrano et al., 2012); and second, the aridity gradient from west to east (Iglesias et al., 2016). These factors may interact with the age and management practices (e.g., lack of regeneration, inappropriate management and overgrazing) of the Mediterranean oak woodlands (López-Sánchez et al., 2016). Therefore, a continuous increase in oak woodlands decline can be expected in the coming years (Gil-Pelegrín et al., 2017; Duque-Lazo et al., 2018; Hernández-Lambraño et al., 2018).

4.2 Response of defoliation and mortality to environmental variables

Tree defoliation and mortality were mainly related to climatic factors, both annual and average. Particularly, we found that the incidence of defoliation in warm areas increased in dry years, which may be related to heat stress (Camarero et al., 2015; Burgess et al., 2017; Duque-Lazo et al., 2018). Specifically, the best predictors of annual defoliation were the annual mean temperature (climate average for 30 years, 1971-2000) and the summer SPEI with an 18-month scale for each year in the time series, while the accumulated precipitation of the previous two hydrological years was marginally significant. Dry periods in already-hot areas could lead to defoliation without the involvement of oomycetes (Camarero et al., 2015; Ruiz-Gómez et al., 2018). The relevance of longer timescales in the drought and precipitation indices suggests that average defoliation might be an accumulative process responding to long-term drought rather than an immediate response to an anomalous dry year. This pattern was confirmed in the review by Barbeta and Peñuelas (2016), who indicated that defoliation of holm oak is correlated with drought indices at scales of more than seven months. The ability of Holm oak to tap groundwater might reduce the exposure of trees to short-term drought (affecting evapotranspiration and soil moisture) (David et al., 2004; Barbeta et al., 2015). However, a long exposure to drought might deplete groundwater resources, producing an increase in defoliation and eventually mortality.

In contrast to defoliation, the probability of mortality was more associated with short-scale SPEI. In fact, the highest correlation was found for SPEI in spring with a one-month scale, indicating a high probability of mortality after a dry spring. This result agrees with Natalini et al. (2016), who found a clear relationship of increasing temperature and aridity with the growth suppression and widespread mortality of *Q. ilex* that has occurred since 2005. Also, Moreno-Fernández et al. (2019) found increasing levels of tree decline with warmer conditions and more intense human management.

In contrast, Barbeta et al. (2013) found the opposite pattern in a long-term drought experiment, suggesting higher resilience of holm oak to short rather than long-term droughts. Probably, this contrasting pattern is explained by the differences in the measurement of mortality between the studies (occurrence of mortality versus mortality rate) (Barbeta and Peñuelas,

2016). It is likely that a strong drought during spring, when trees should build up their water reserves, could easily kill at least one weak or young tree.

Other variables, like topographic (e.g., slope and aspect) and soil (e.g., calcium content, soil depth or pH) features, contributed less to the final models (Moreira and Martins, 2005; Corcobado et al., 2013). This finding contrasts with previous studies showing the importance of site variables as better spatial predictors of the crown condition than regional climatic variables. The only relevant soil factor was the proportion of organic material; interestingly, the mortality was higher in richer soils, which seems to be related to the impact of oomycetes.

4.3 Response of defoliation and mortality to oomycetes occurrence

This work compiled the most comprehensive up to date database of root rot oomycete identification for Andalusian region, using all the reliable sources beyond the SEDA Network database. Despite the large potential of this unprecedent database, some criticisms should be considered. On the classic diagnostic procedures, the date of sample collection would be relevant for the reliability of the data, considering the possibility that under certain environmental conditions, the pathogen could be present but undetectable. However, in the SEDA network, when a plot still having decline symptoms in subsequent years without positive isolation of root rot oomycetes, the diagnostic was repeated (Consejería de Medio Ambiente y Ordenación del Territorio, 2018), and if there was not positive isolation during the overall period, the plot was assessed through the third methodology of infestation classification (see material and methods section).

Regarding the data coming from eDNA studies, it would be considered that the identification of pathogen DNA material into the soil is only an evidence of the presence of this species at an unknow moment but not of the presence of this pathogen at the moment of the sample collection. Notwithstanding the errors and uncertainties associated with eDNA metabarcoding studies are mitigated by thoughtful study design (Deiner et al., 2017). Overall, we consider the lack of reliable register of the diagnostic date as the main criticism of our root rot oomycete database, but this issue did not influence the model outcome due to the time span of our dataset, and the endpoint nature of the classification of plots as infested or not infested.

In contrast to previous studies (e.g., (Chadfield and Pautasso, 2012; Duque-Lazo et al., 2016)), we did not find evidence associating defoliation with the simple occurrence of oomycetes. However, we found a significant interaction between environmental factors and oomycetes root rot occurrence in the explanation of both defoliation and mortality. Specifically, in wet years, infested plots showed higher defoliation than non-infested plots. Higher precipitation will produce long-lasting water saturation of soil during the year, increasing the likelihood of dispersal and sporulation of *P. cinnamomi* and other oomycetes species. Water saturation allows zoospores to spread and infect further fine roots of the tree or neighbouring trees (Hardham, 2005). Similarly, other studies have found a higher probability of P. cinnamomi occurrence close to water sources (Hernández-Lambraño et al., 2019) or in topographic depressions (de Sampaio e Paiva Camilo-Alves et al., 2013).

We also found a significant interaction between the presence of oomycetes and the proportion of OM in soil. Specifically, for soils with higher OM content, infested plots showed higher mortality than non-infested plots (Figure 6c). Interestingly, several studies have found the opposite pattern, suggesting that *P. cinnamomi* and related species are often supressed in rich soils where OM exceeds 5% (Thompson et al., 2014), probably related to an interaction with the richer biological component of soil (Hardham, 2005). Although this may seem contrary to our results, it should be considered that *dehesa* soils are generally deficient in OM (Marañón, 1988). Overall, the OM content of the studied plots was low, ranging between 0.56 and 2.24% (below 1.5% in 90% of the plots). The higher mortality incidence on infested plots was related with higher OM contents, but the higher absolute OM contents corresponded to non-infested plots with low accumulated mortality. In previous studies we demonstrated that, in *dehesa* conditions (poor soils) the OM variation at the microscale was correlated with the abundance of *P. cinnamomi* inoculum on holm oak rhizosphere (Sánchez-Cuesta et al., 2020). Soils richer in OM also tend to be more acidic and with higher water retention, conditions found to enhance the *P. cinnamomi* impact in the southern Iberian Peninsula (Serrano et al., 2012; Corcobado et al., 2013; de Sampaio e Paiva Camilo-Alves et al., 2013; Sánchez-Cuesta et al., 2020).

In addition, although this work did not address specifically the role of soil microbial diversity in oak decline, we must also consider this aspect in the regulation of soil-borne pathogens and their effects on their hosts (Vinale et

al., 2008; Corcobado et al., 2014a; Ruiz-Gómez et al., 2018; Ruiz-Gómez et al., 2019a). Higher biodiversity indices were related with low abundances of pathogenic oomycetes and low diversity and evenness of the oomycete community was related with high defoliation rates on infested plots (Ruiz-Gómez et al., 2019b).

4.4 Management implications

Forest Health Networks represent a key data source to develop strategies to prevent the spread of holm oak decline (Duque-Lazo et al., 2016; Duque-Lazo and Navarro-Cerrillo, 2017). Forest management oriented to increase tree vitality should use this information (Tiberi et al., 2016). Based on a systematic regional Forest Health Network this study has identified the key factors triggering mortality and defoliation events at large scale. Particularly, the models implemented here could be used as an early-warning tool to forecast the climatic risk of these forests under changing drought conditions based on SPEI values of the previous months. The reliability of these results could be improved with higher ancillary data availability. For instance, in this study we have improved the coverage of infection classification by root rot using three complementary methods. Further studies should increase the robustness of the classification by more specific and targeted molecular methods. Regarding silvicultural practices, our results support the application of an adaptive management based on ecohydrological silviculture (del Campo et al., 2019) as a tool to fight oak decline in the eastern part of the *dehesa* distribution in Andalusia. Meanwhile these early, the management of stands in western Andalusia that are undergoing decline should be focused more on the containment and eradication of the pathogen.

5 Conclusions

The results support the importance of systematic large-scale and long-term monitoring of forest health, combined with information about relevant environmental variables and biotic and abiotic agents. Large-scale monitoring of tree health would increase our understanding of the factors influencing the dynamics of biotic agents. In fact, our results identify the key factors influencing the crown damage and mortality of evergreen oaks in the Southern Iberian Peninsula which have been related to intense droughts in warm areas and the interaction with OM and the occurrence of oomycetes in the soil. This information could be used to develop appropriate silvicultural

practices together with control measures for biotic agents, to protect the Mediterranean oak woodlands from decline processes.

6 References

Anderegg, W.R.L., Hicke, J.A., Fisher, R.A., Allen, C.D., Aukema, J., Bentz, B., Hood, S., Lichstein, J.W., Macalady, A.K., McDowell, N., Pan, Y., Raffa, K., Sala, A., Shaw, J.D., Stephenson, N.L., Tague, C., Zeppel, M., 2015. Tree mortality from drought, insects, and their interactions in a changing climate. New Phytol. 674–683. https://doi.org/10.1111/nph.13477

Axelson, J., Battles, J., Bulaon, B., Cluck, D., Cousins, S., Cox, L., Estes, B., Fettig, C., Hefty, A., Hishinuma, S., Hood, S., Kocher, S., McMahon, D., Mortenson, L., Koltunov, A., Kuskulis, E., Poloni, A., Ramirez, C., Restaino, C., Safford, H., Slaton, M., Smith, S., Tubbesing, C., Wayman, R., Young, D., 2019. The California Tree Mortality Data Collection Network — Enhanced communication and collaboration among scientists and stakeholders. Calif. Agric. 73, 55–62.

Barbeta, A., Mejía-Chang, M., Ogaya, R., Voltas, J., Dawson, T.E., Peñuelas, J., 2015. The combined effects of a long-term experimental drought and an extreme drought on the use of plant-water sources in a Mediterranean forest. Glob. Change Biol. 21, 1213–1225. https://doi.org/10.1111/gcb.12785

Barbeta, A., Ogaya, R., Peñuelas, J., 2013. Dampening effects of long-term experimental drought on growth and mortality rates of a Holm oak forest. Glob. Change Biol. 19, 3133–3144. https://doi.org/10.1111/gcb.12269

Barbeta, A., Peñuelas, J., 2016. Sequence of plant responses to droughts of different timescales: lessons from holm oak (*Quercus ilex*) forests. Plant Ecol. Divers. 9, 321–338. https://doi.org/10.1080/17550874.2016.1212288

Bartoń, K., 2020. MuMIn: Multi-Model Inference.

Beguería, S., Vicente-Serrano, S.M., 2017. SPEI: Calculation of the Standardised Precipitation-Evapotranspiration Index. R package version 1.7.

Brasier, C.M., Robredo, F., Ferraz, J.F.P., 1993. Evidence for *Phytophthora cinnamomi* involvement in Iberian oak decline. Plant Pathol. 42, 140–145. https://doi.org/10.1111/j.1365-3059.1993.tb01482.x

Burgess, T.I., Scott, J.K., Mcdougall, K.L., Stukely, M.J.C., Crane, C., Dunstan, W.A., Brigg, F., Andjic, V., White, D., Rudman, T., Arentz, F., Ota, N., Hardy, G.E.S.J., 2017. Current and projected global distribution of *Phytophthora cinnamomi*, one of the world's worst plant pathogens. Glob. Change Biol. 23, 1661–1674. https://doi.org/10.1111/gcb.13492

Burnham, K.P., Anderson, D.R., 2002. Model Selection and Multimodel Inference: A Practical Information-Theoretic Approach., 2nd ed. ed. Springer-Verlag New York, Fort Collins, Colorado, USA.

Bussotti, F., Pollastrini, M., 2017. Observing Climate Change Impacts on European Forests: What Works and What Does Not in Ongoing Long-Term Monitoring Networks. Front. Plant Sci. 8. https://doi.org/10.3389/fpls.2017.00629

Camarero, J.J., Franquesa, M., Sangüesa-Barreda, G., 2015. Timing of Drought Triggers Distinct Growth Responses in Holm Oak: Implications to Predict Warming-Induced Forest Defoliation and Growth Decline. Forests 6, 1576–1597. https://doi.org/10.3390/f6051576

Carnicer, J., Coll, M., Ninyerola, M., Pons, X., Sánchez, G., Peñuelas, J., 2011. Widespread crown condition decline, food web disruption, and amplified tree mortality with increased climate change-type drought. Proc. Natl. Acad. Sci. 201010070. https://doi.org/10.1073/pnas.1010070108

Chadfield, V., Pautasso, M., 2012. *Phytophthora ramorum* in England and Wales: which environmental variables predict county disease incidence? For. Pathol. 42, 150–159. https://doi.org/10.1111/j.1439-0329.2011.00735.x

Cobb, R.C., Metz, M.R., 2017. Tree Diseases as a Cause and Consequence of Interacting Forest Disturbances. Forests 8, 147. https://doi.org/10.3390/f8050147

Consejería de Medio Ambiente y Ordenación del Territorio, 2018. Manual para el establecimiento y la evaluación de las parcelas de la Red Andaluza de Seguimiento de Daños sobre Ecosistemas Forestales: Red SEDA y Red de PINSAPO. Junta de Andalucía.

Corcobado, T., Cubera, E., Juárez, E., Moreno, G., Solla, A., 2014a. Drought events determine performance of *Quercus ilex* seedlings and increase their susceptibility to *Phytophthora cinnamomi*. Agric. For. Meteorol. 192–193, 1–8. https://doi.org/10.1016/j.agrformet.2014.02.007

Corcobado, T., Cubera, E., Pérez-Sierra, A., Jung, T., Solla, A., 2010. First report of *Phytophthora gonapodyides* involved in the decline of *Quercus ilex* in xeric conditions in Spain. New Dis. Rep. 22, 33. https://doi.org/10.5197/j.2044-0588.2010.022.033

Corcobado, T., Solla, A., Madeira, M.A., Moreno, G., 2013. Combined effects of soil properties and *Phytophthora cinnamomi* infections on *Quercus ilex* decline. Plant Soil 373, 403–413. https://doi.org/10.1007/s11104-013-1804-z

Corcobado, T., Vivas, M., Moreno, G., Solla, A., 2014b. Ectomycorrhizal symbiosis in declining and non-declining *Quercus ilex* trees infected with or free of *Phytophthora cinnamomi*. For. Ecol. Manag. 324, 72–80. https://doi.org/10.1016/j.foreco.2014.03.040

Costa, J.C., Martín, Á., Fernández, R., Estirado, M., 2006. Dehesas de Andalucía: caracterización ambiental. Consejería de Medio Ambiente, Junta de Andalucía, Sevilla, Spain.

David, T.S., Ferreira, M.I., Cohen, S., Pereira, J.S., David, J.S., 2004. Constraints on transpiration from an evergreen oak tree in southern Portugal. Agric. For. Meteorol. 122, 193–205. https://doi.org/10.1016/j.agrformet.2003.09.014

Davies, T.M., Hazelton, M.L., Marshall, J.C., 2011. sparr: Analyzing Spatial Relative Risk Using Fixed and Adaptive Kernel Density Estimation in R. J. Stat. Softw. 039.

de la Cruz, A.C., Gil, P.M., Fernández-Cancio, Á., Minaya, M., Navarro-Cerrillo, R.M., Sánchez-Salguero, R., Grau, J.M., 2014. Defoliation triggered by climate induced effects in Spanish ICP Forests monitoring plots. For. Ecol. Manag. 331, 245–255. https://doi.org/10.1016/j.foreco.2014.08.010

de Sampaio e Paiva Camilo-Alves, C., da Clara, M.I.E., de Almeida Ribeiro, N.M.C., 2013. Decline of Mediterranean oak trees and its association with *Phytophthora cinnamomi*: a review. Eur. J. For. Res. 132, 411–432. https://doi.org/10.1007/s10342-013-0688-z

Deiner, K., Bik, H.M., Mächler, E., Seymour, M., Lacoursière-Roussel, A., Altermatt, F., Creer, S., Bista, I., Lodge, D.M., Vere, N. de, Pfrender, M.E., Bernatchez, L., 2017. Environmental DNA metabarcoding: Transforming how we survey animal and plant communities. Mol. Ecol. 26, 5872–5895. https://doi.org/10.1111/mec.14350

del Campo, A.D., González-Sanchis, M., Molina, A.J., García-Prats, A., Ceacero, C.J., Bautista, I., 2019. Effectiveness of water-oriented thinning in two semiarid forests: The redistribution of increased net rainfall into soil water, drainage and runoff. For. Ecol. Manag. 438, 163–175. https://doi.org/10.1016/j.foreco.2019.02.020

DeSoto, L., Cailleret, M., Sterck, F., Jansen, S., Kramer, K., Robert, E.M.R., Aakala, T., Amoroso, M.M., Bigler, C., Camarero, J.J., Čufar, K., Gea-Izquierdo, G., Gillner, S., Haavik, L.J., Hereş, A.-M., Kane, J.M., Kharuk, V.I., Kitzberger, T., Klein, T., Levanič, T., Linares, J.C., Mäkinen, H., Oberhuber, W., Papadopoulos, A., Rohner, B., Sangüesa-Barreda, G., Stojanovic, D.B., Suárez, M.L., Villalba, R., Martínez-Vilalta, J., 2020. Low growth resilience to drought is related to future mortality risk in trees. Nat. Commun. 11, 545. https://doi.org/10.1038/s41467-020-14300-5

Dietze, M.C., Fox, A., Beck-Johnson, L.M., Betancourt, J.L., Hooten, M.B., Jarnevich, C.S., Keitt, T.H., Kenney, M.A., Laney, C.M., Larsen, L.G., Loescher, H.W., Lunch, C.K., Pijanowski, B.C., Randerson, J.T., Read, E.K., Tredennick, A.T., Vargas, R., Weathers, K.C., White, E.P., 2018. Iterative near-term ecological forecasting: Needs, opportunities, and challenges. Proc. Natl. Acad. Sci. 115, 1424–1432. https://doi.org/10.1073/pnas.1710231115

Dobbertin, M., 2005. Tree growth as indicator of tree vitality and of tree reaction to environmental stress: a review. Eur. J. For. Res. 124, 319–333. https://doi.org/10.1007/s10342-005-0085-3

Duque-Lazo, J., Navarro-Cerrillo, R.M., 2017. What to save, the host or the pest? The spatial distribution of xylophage insects within the Mediterranean oak woodlands of Southwestern Spain. For. Ecol. Manag. 392, 90–104. https://doi.org/10.1016/j.foreco.2017.02.047

Duque-Lazo, J., Navarro-Cerrillo, R.M., van Gils, H., Groen, T.A., 2018. Forecasting oak decline caused by *Phytophthora cinnamomi* in Andalusia: Identification of priority areas for intervention. For. Ecol. Manag. 417, 122–136. https://doi.org/10.1016/j.foreco.2018.02.045

Duque-Lazo, J., van Gils, H., Groen, T.A., Navarro-Cerrillo, R.M., 2016. Transferability of species distribution models: The case of *Phytophthora cinnamomi* in Southwest Spain and Southwest Australia. Ecol. Model. 320, 62–70. https://doi.org/10.1016/j.ecolmodel.2015.09.019

Eichhorn, J., Roskams, P., Ferretti, M., Mues, V., Szepesi, A., 2016. Visual assessment of crown condition and damaging agents. Manual Part IV, in: Manual on methods and criteria for harmonized sampling, assessment, monitoring and analysis of the effects of air pollution on forests. UNECE ICP Forests Programme Co-ordinating Centre, Eberswalde, Germany, p. 49.

Erwin, D.C., Ribeiro, O.K., 1996. *Phytophthora* diseases worldwide. American Phytopathological Society (APS Press).

Ferretti, M., König, N., Granke, O., 2016. Quality assurance within the ICP forests monitoring programme. Manual Part III, in: Manual on Methods and Criteria for Harmonized Sampling, Assessment, Monitoring and Analysis of the Effects of Air Pollution on Forests. UNECE ICP Forests Programme Co-ordinating Centre, Eberswalde, Germany, p. 10.

Ferretti, M., Nicolas, M., Bacaro, G., Brunialti, G., Calderisi, M., Croisé, L., Frati, L., Lanier, M., Maccherini, S., Santi, E., Ulrich, E., 2014. Plot-scale modelling to detect size, extent, and correlates of changes in tree defoliation in French high forests. For. Ecol. Manag., Monitoring European forests: detecting and understanding changes 311, 56–69. https://doi.org/10.1016/j.foreco.2013.05.009

Fox, J., Carvalho, M.S., 2012. The RcmdrPlugin.survival Package: Extending the R Commander Interface to Survival Analysis. J. Stat. Softw. 49, 1–32. https://doi.org/10.18637/jss.v049.i07

Gea-Izquierdo, G., Natalini, F., Cardillo, E., 2020. Holm oak death is accelerated but not sudden and expresses drought legacies. *Sci. Total Environ*. 141793. https://doi.org/10.1016/j.scitotenv.2020.141793

Gentilesca, T., Camarero, J.J., Colangelo, M., Nolè, A., Ripullone, F., 2017. Drought-induced oak decline in the western Mediterranean region: an overview on current evidences, mechanisms and management options to improve forest resilience. IForest - Biogeosciences For. 10, 796. https://doi.org/10.3832/ifor2317-010

Ghelardini, L., Pepori, A.L., Luchi, N., Capretti, P., Santini, A., 2016. Drivers of emerging fungal diseases of forest trees. For. Ecol. Manag. 381, 235–246. https://doi.org/10.1016/j.foreco.2016.09.032

Gil-Pelegrín, E., Peguero-Pina, J.J., Sancho-Knapik, D., 2017. Oaks and People: A Long Journey Together, in: Gil-Pelegrín, E., Peguero-Pina, J.J., Sancho-Knapik, D. (Eds.), Oaks Physiological Ecology. Exploring the Functional Diversity of Genus *Quercus* L., Tree Physiology. Springer International Publishing, Cham, pp. 1–11. https://doi.org/10.1007/978-3-319-69099-5_1

Gómez-Zotano, J., Alcántara-Manzanares, J., Olmedo-Cobo, J.A., Martínez-Ibarra, E., 2015. La sistematización del clima mediterráneo: identificación, clasificación y caracterización climática de Andalucía (España). Rev. Geogr. Norte Gd. 161–180. https://doi.org/10.4067/S0718-34022015000200009

González-Moreno, P., Pino, J., Carreras, D., Basnou, C., Fernández-Rebollar, I., Vilà, M., 2013. Quantifying the landscape influence on plant invasions in Mediterranean coastal habitats. Landsc. Ecol. 28, 891–903. https://doi.org/10.1007/s10980-013-9857-1

Grueber, C.E., Nakagawa, S., Laws, R.J., Jamieson, I.G., 2011. Multimodel inference in ecology and evolution: challenges and solutions. J. Evol. Biol. 24, 699–711. https://doi.org/10.1111/j.1420-9101.2010.02210.x

Guzmán Álvarez, J.R., Venegas Troncoso, J., Seseña Rengel, A., Sillero Almazán, M.L., Rodríguez Álvarez, J.A., 2012. Biomasa forestal en Andalucía. 1. Modelo de existencias, crecimiento y producción. Coníferas. Consejería de Agricultura, Pesca y Medio Ambiente. Junta de Andalucía, Sevilla, Spain.

Hardham, A.R., 2005. *Phytophthora cinnamomi*. Mol. Plant Pathol. 6, 589–604. https://doi.org/10.1111/j.1364-3703.2005.00308.x

Hartmann, H., Moura, C.F., Anderegg, W.R.L., Ruehr, N.K., Salmon, Y., Allen, C.D., Arndt, S.K., Breshears, D.D., Davi, H., Galbraith, D., Ruthrof, K.X., Wunder, J., Adams, H.D., Bloemen, J., Cailleret, M., Cobb, R., Gessler, A., Grams, T.E.E., Jansen, S., Kautz, M., Lloret, F., O'Brien, M., 2018. Research frontiers for improving our understanding of drought-induced tree and forest mortality. New Phytol. 218, 15–28. https://doi.org/10.1111/nph.15048

Hernández-Lambraño, R.E., de la Cruz, D.R., Sánchez-Agudo, J.Á., 2019. Spatial oak decline models to inform conservation planning in the Central-Western Iberian Peninsula. For. Ecol. Manag. 441, 115–126. https://doi.org/10.1016/j.foreco.2019.03.028

Hernández-Lambraño, R.E., González-Moreno, P., Sánchez-Agudo, J.Á., 2018. Environmental factors associated with the spatial distribution of invasive plant pathogens in the Iberian Peninsula: The case of *Phytophthora cinnamomi* Rands. For. Ecol. Manag. 419–420, 101–109. https://doi.org/10.1016/j.foreco.2018.03.026

Ibáñez, B., Gómez-Aparicio, L., Ávila, J.M., Pérez-Ramos, I.M., García, L.V., Marañón, T., 2015. Impact of tree decline on spatial patterns of seedling-mycorrhiza interactions: Implications for regeneration dynamics in Mediterranean forests. For. Ecol. Manag. 353, 1–9. https://doi.org/10.1016/j.foreco.2015.05.014

Iglesias, E., Báez, K., Diaz-Ambrona, C.H., 2016. Assessing drought risk in Mediterranean Dehesa grazing lands. Agric. Syst. 149, 65–74. https://doi.org/10.1016/j.agsy.2016.07.017

Jeffers, S.N., Martin, S.B., 1986. Comparison of two media selective for *Phytophthora* and *Pythium* species. Plant Dis. 70, 1038–1043.

Jiménez, J.J., Sánchez, J.E., Romero, M.A., Belbahri, L., Trapero, A., Lefort, F., Sánchez, M.E., 2008. Pathogenicity of *Pythium spiculum* and *P. sterilum* on feeder roots of *Quercus rotundifolia*. Plant Pathol. 57, 369–369. https://doi.org/10.1111/j.1365-3059.2007.01627.x

Kenchington, E., Murillo, F.J., Lirette, C., Sacau, M., Koen-Alonso, M., Kenny, A., Ollerhead, N., Wareham, V., Beazley, L., 2014. Kernel Density Surface Modelling as a Means to Identify Significant Concentrations of Vulnerable Marine Ecosystem Indicators. PLOS ONE 9, e109365. https://doi.org/10.1371/journal.pone.0109365

Klap, J.M., Oude Voshaar, J.H., De Vries, W., Erisman, J.W., 2000. Effects of Environmental Stress on Forest Crown Condition in Europe. Part IV: Statistical Analysis of Relationships. Water. Air. Soil Pollut. 119, 387–420. https://doi.org/10.1023/A:1005157208701

Korkmaz, S., Goksuluk, D., Zararsiz, G., 2014. MVN: An R Package for Assessing Multivariate Normality. R J. 6, 151–162.

Kosiorowski, D., Rydlewski, J.P., Snarska, M., 2019. Detecting a structural change in functional time series using local Wilcoxon statistic. Stat. Pap. 60, 1677–1698. https://doi.org/10.1007/s00362-017-0891-y

Lieutier, François, Paine, T.D., 2016. Responses of Mediterranean Forest Phytophagous Insects to Climate Change, in: Paine, T.D., Lieutier, Francois (Eds.), Insects and Diseases of Mediterranean Forest Systems. Springer International Publishing, Cham, pp. 801–858. https://doi.org/10.1007/978-3-319-24744-1_28

López-Sánchez, A., Perea, R., Dirzo, R., Roig, S., 2016. Livestock vs. wild ungulate management in the conservation of Mediterranean dehesas: Implications for oak regeneration. For. Ecol. Manag. 362, 99–106. https://doi.org/10.1016/j.foreco.2015.12.002

MacLean, D.A., 2016. Impacts of insect outbreaks on tree mortality, productivity, and stand development. Can. Entomol. 148, S138–S159. https://doi.org/10.4039/tce.2015.24

Mantgem, P.J.V., Stephenson, N.L., 2007. Apparent climatically induced increase of tree mortality rates in a temperate forest. Ecol. Lett. 10, 909–916. https://doi.org/10.1111/j.1461-0248.2007.01080.x

Marañón, T., 1988. Agro-sylvo-pastoral systems in the Iberian Peninsula: Dehesas and Montados. Rangel. Arch. 10, 255–258.

Meentemeyer, R.K., Haas, S.E., Václavík, T., 2012. Landscape Epidemiology of Emerging Infectious Diseases in Natural and Human-Altered Ecosystems. Annu. Rev. Phytopathol. 50, 379–402. https://doi.org/10.1146/annurev-phyto-081211-172938

Michel, A., Seidling, W., 2017. Forest Condition in Europe: 2017 Technical Report of ICP Forests. Report under the UNECE Convention on Long-range Transboundary Air Pollution (CLRTAP). BFWDokumentation 24/2017, Vienna: BFW Austrian Research Centre for Forests.

Millar, C.I., Stephenson, N.L., 2015. Temperate forest health in an era of emerging megadisturbance. Science 349, 823–826. https://doi.org/10.1126/science.aaa9933

Mordecai, E.A., 2011. Pathogen impacts on plant communities: unifying theory, concepts, and empirical work. Ecol. Monogr. 81, 429–441. https://doi.org/10.1890/10-2241.1

Moreira, A.C., Martins, J.M.S., 2005. Influence of site factors on the impact of *Phytophthora cinnamomi* in cork oak stands in Portugal. For. Pathol. 35, 145–162. https://doi.org/10.1111/j.1439-0329.2005.00397.x

Moreno, G., Pulido, F.J., 2009. The Functioning, Management and Persistence of Dehesas, in: Rigueiro-Rodróguez, A., McAdam, J., Mosquera-Losada, M.R. (Eds.), Agroforestry in Europe: Current Status and Future Prospects, Advances in Agroforestry. Springer Netherlands, Dordrecht, pp. 127–160. https://doi.org/10.1007/978-1-4020-8272-6_7

Moreno-Fernández, D., Ledo, A., Martín-Benito, D., Cañellas, I., Gea-Izquierdo, G., 2019. Negative synergistic effects of land-use legacies and climate drive widespread oak decline in evergreen Mediterranean open woodlands. For. Ecol. Manag. 432, 884–894. https://doi.org/10.1016/j.foreco.2018.10.023

Natalini, F., Alejano, R., Vázquez-Piqué, J., Cañellas, I., Gea-Izquierdo, G., 2016. The role of climate change in the widespread mortality of holm oak in open woodlands of Southwestern Spain. Dendrochronologia 38, 51–60. https://doi.org/10.1016/j.dendro.2016.03.003

Navarro-Cerrillo, R.M., Fernandez Rebollo, P., Ruiz Navarro, J.M., 2000. Manual de campo para establecimiento de los puntos de la Red Andaluza de Daños sobre ecosistemas forestales en Andalucía.

Navarro-Cerrillo, R.M., Varo-Martínez, M.Á., Acosta, C., Palacios Rodriguez, G., Sánchez-Cuesta, R., Ruiz Gómez, F.J., 2019. Integration of WorldView-2 and airborne laser scanning data to

classify defoliation levels in *Quercus ilex* L. Dehesas affected by root rot mortality: Management implications. For. Ecol. Manag. 451, 117564. https://doi.org/10.1016/j.foreco.2019.117564

O'Brien, S.H., Webb, A., Brewer, M.J., Reid, J.B., 2012. Use of kernel density estimation and maximum curvature to set Marine Protected Area boundaries: Identifying a Special Protection Area for wintering red-throated divers in the UK. Biol. Conserv., Seabirds and Marine Protected Areas planning 156, 15–21. https://doi.org/10.1016/j.biocon.2011.12.033

Oliva, J., Stenlid, J., Martínez-Vilalta, J., 2014. The effect of fungal pathogens on the water and carbon economy of trees: implications for drought-induced mortality. New Phytol. 203, 1028–1035. https://doi.org/10.1111/nph.12857

Peñuelas, J., Lloret, F., Montoya, R., 2001. Severe Drought Effects on Mediterranean Woody Flora in Spain. For. Sci. 47, 214–218. https://doi.org/10.1093/forestscience/47.2.214

Pinto-Correia, T., Azeda, C., 2017. Public policies creating tensions in Montado management models: Insights from farmers' representations. Land Use Policy 64, 76–82. https://doi.org/10.1016/j.landusepol.2017.02.029

Popa, I., Badea, O., Silaghi, D., 2017. Influence of climate on tree health evaluated by defoliation in the ICP level I network (Romania). IForest - Biogeosciences For. 10, 554. https://doi.org/10.3832/ifor2202-009

R Development Core Team, 2017. R: A language and environment for statistical computing. R Foundation for Statistical Computing, Vienna, Austria. 2016.

Redondo, M.Á., Pérez-Sierra, A., Abad-Campos, P., Torres, L., Solla, A., Reig-Armiñana, J., García-Breijo, F., 2015. Histology of *Quercus ilex* roots during infection by *Phytophthora cinnamomi*. Trees 29, 1943–1957. https://doi.org/10.1007/s00468-015-1275-3

Riffenburgh, R., 2012. Statistics in Medicine, 3rd ed. ed. Academic Press, San Diego, California, USA.

Romero de los Reyes, E., Navarro Cerrillo, R.M., García-Ferrer Porras, A., 2007. Aplicación de ortofotos para la estimación de pérdida de individuos en dehesas de encina: (*Quercus ilex* L. subps. *ballota* (Desf.) Samp.) afectadas por procesos de decaimiento. Bol. Sanid. Veg. Plagas 33, 121–134.

Romero, M.A., Sánchez, J.E., Jiménez, J.J., Belbahri, L., Trapero, A., Lefort, F., Sánchez, M.E., 2007. New *Pythium* Taxa Causing Root Rot on Mediterranean *Quercus* Species in South-west Spain and Portugal. J. Phytopathol. 155, 289–295. https://doi.org/10.1111/j.1439-0434.2007.01230.x

Ruiz-Gómez, F.J., Navarro-Cerrillo, R.M., Pérez-de-Luque, A., Oβwald, W., Vannini, A., Morales-Rodríguez, C., 2019a. Assessment of functional and structural changes of soil fungal and oomycete communities in holm oak declined dehesas through metabarcoding analysis. Sci. Rep. 9, 5315. https://doi.org/10.1038/s41598-019-41804-y

Ruiz-Gómez, F.J., Pérez-de-Luque, A., Navarro-Cerrillo, R.M., 2019b. The Involvement of *Phytophthora* Root Rot and Drought Stress in Holm Oak Decline: from Ecophysiology to Microbiome Influence. Curr. For. Rep. 5, 251–266. https://doi.org/10.1007/s40725-019-00105-3

Ruiz-Gómez, F.J., Navarro-Cerrillo, R.M., Sánchez-Cuesta, R., Pérez-de-Luque, A., 2015. Histopathology of Infection and Colonization of *Quercus Ilex* Fine Roots by *Phytophthora Cinnamomi*. Plant Pathol. 64, 605–616. *https://doi.org/10.1111/ppa.12310*

Ruiz-Gómez, F.J., Pérez-de-Luque, A., Sánchez-Cuesta, R., Quero, J.L., Navarro Cerrillo, R.M., 2018. Differences in the Response to Acute Drought and *Phytophthora cinnamomi* Rands Infection in *Quercus ilex* L. Seedlings. *Forests* 9, 634. https://doi.org/10.3390/f9100634

Sallé, A., Nageleisen, L.-M., Lieutier, F., 2014. Bark and wood boring insects involved in oak declines in Europe: Current knowledge and future prospects in a context of climate change. For. Ecol. Manag. 328, 79–93. https://doi.org/10.1016/j.foreco.2014.05.027

Sánchez, M.E., Caetano, P., Ferraz, J., Trapero, A., 2002. *Phytophthora* disease of *Quercus ilex* in south-western Spain. For. Pathol. 32, 5–18. https://doi.org/10.1046/j.1439-0329.2002.00261.x

Sánchez, M.E., Caetano, P., Romero, M.A., Navarro, R.M., Trapero, A., 2006. *Phytophthora* root rot as the main factor of oak decline in southern Spain, in: Proceedings of the Third International IUFRO Working Party S07.02.09. Presented at the Progress in research on *Phytophthora* diseases of forest trees, Forest Research, Freising (Germany).

Sánchez Peña, G., Torres Martínez, B., Prieto González, M., Revenga Fernández, G., 2010. Anuario de sanidad forestal, 2010. Servicio de Sanidad Forestal y Equilibrios Biológicos. Subdirección General de Política Forestal y Desertificación. Ministerio del Medio Ambiente y Medio Rural y Marino. Gobierno de España.

Sánchez-Cuesta, R., Navarro-Cerrillo, R.M., Quero, J.L., Ruiz-Gómez, F.J., 2020. Small-Scale Abiotic Factors Influencing the Spatial Distribution of *Phytophthora cinnamomi* under Declining *Quercus ilex* Trees. Forests 11, 375. https://doi.org/10.3390/f11040375

Sancho, R., Ávila, A., López-Carrasco, C., Santacruz, F., Espinosa, M., 2018. Caracterización de las masas de *Quercus* con decaimiento en Castilla-La Mancha y detección de podredumbre radical causada por *Phytophthora cinnamomi*., in: Detección y Diagnóstico, SEF. Presented at the XIX Congreso de la Sociedad Española de Fitopatología, Sociedad Española de Fitopatología, Toledo. Castilla-La Mancha, p. 239 (380).

Seidling, W., 2019. Forest monitoring: Substantiating cause-effect relationships. Sci. Total Environ. 687, 610–617. https://doi.org/10.1016/j.scitotenv.2019.06.048

Senf, C., Pflugmacher, D., Zhiqiang, Y., Sebald, J., Knorn, J., Neumann, M., Hostert, P., Seidl, R., 2018. Canopy mortality has doubled in Europe's temperate forests over the last three decades. Nat. Commun. 9, 4978. https://doi.org/10.1038/s41467-018-07539-6

Serrano, M.S., De Vita, P., Fernández-Rebollo, P., Sánchez-Hernández, M.E., 2012. Calcium fertilizers induce soil suppressiveness to *Phytophthora cinnamomi* root rot of *Quercus ilex*. Eur. J. Plant Pathol. 132, 271–279. https://doi.org/10.1007/s10658-011-9871-6

Simler-Williamson, A.B., Rizzo, D.M., Cobb, R.C., 2019. Interacting Effects of Global Change on Forest Pest and Pathogen Dynamics. Annu. Rev. Ecol. Evol. Syst. 50, 381–403. https://doi.org/10.1146/annurev-ecolsys-110218-024934

Team RStudio, 2016. RStudio: Integrated Development for R. Boston: RStudio Inc.

Thompson, S.E., Levin, S., Rodriguez-Iturbe, I., 2014. Rainfall and temperatures changes have confounding impacts on *Phytophthora cinnamomi* occurrence risk in the southwestern USA under climate change scenarios. Glob. Change Biol. 20, 1299–1312. https://doi.org/10.1111/gcb.12463

Tiberi, R., Branco, M., Bracalini, M., Croci, F., Panzavolta, T., 2016. Cork oak pests: a review of insect damage and management. Ann. For. Sci. 73, 219–232. https://doi.org/10.1007/s13595-015-0534-1

Trumbore, S., Brando, P., Hartmann, H., 2015. Forest health and global change. Science 349, 814–818. https://doi.org/10.1126/science.aac6759

Vicente-Serrano, S.M., Beguería, S., López-Moreno, J.I., 2010. A Multiscalar Drought Index Sensitive to Global Warming: The Standardized Precipitation Evapotranspiration Index. J. Clim. 23, 1696–1718. https://doi.org/10.1175/2009JCLI2909.1

Vinale, F., Sivasithamparam, K., Ghisalberti, E.L., Marra, R., Woo, S.L., Lorito, M., 2008. *Trichoderma*–plant–pathogen interactions. Soil Biol. Biochem. 40, 1–10. https://doi.org/10.1016/j.soilbio.2007.07.002

Wandresen, R.R., Netto, S.P., Koehler, H.S., Sanquetta, C.R., Behling, A., 2019. Nonparametric Method: Kernel Density Estimation applied to forestry data. FLORESTA 49, 561–570. https://doi.org/10.5380/rf.v49i3.60285

Capítulo 5

Estimación de la defoliación de la copa de la encina asociada a la podredumbre de la raíz, a nivel de árbol, mediante la integración de imágenes multiespectrales de alta resolución y datos LiDAR aéreos

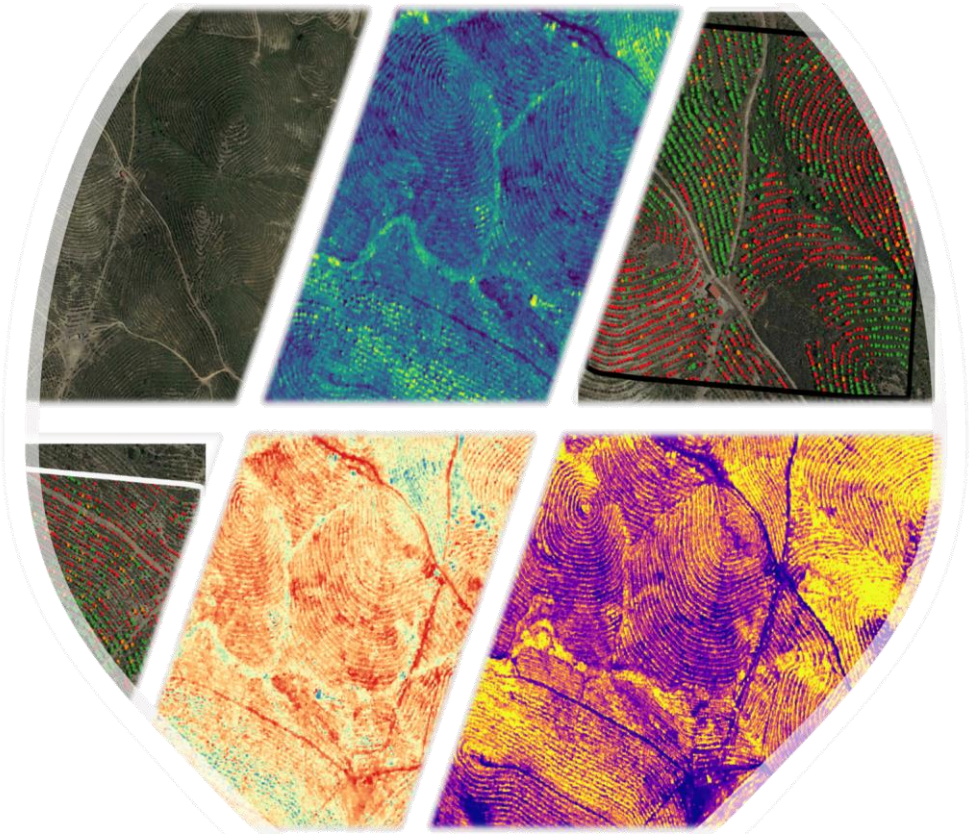

Forecasting crown defoliation of holm oak associated to root rot at tree level by integrating high-resolution multispectral imagery and airborne LiDAR data.

Resumen

Las plantaciones de encina (*Quercus ilex* L. subsp. *ballota* [Desf.] Samp.) han contribuido a crear beneficios ambientales que abarcan grandes áreas en condiciones ecológicas y de gestión dinámicas y complejas. Sin embargo, los oomicetos de la podredumbre de la raíz (*Phytophthora* y *Pythium*) producen procesos de decaimiento y mortalidad. En la actualidad, los sistemas basados en la teledetección son la mejor alternativa para la evaluación y el seguimiento de los ecosistemas forestales con gran precisión, sin requerir la participación directa del medio. El objetivo de esta investigación fue integrar los índices de vegetación de WorldView-2 y los datos LiDAR aéreos como entradas en modelos de aprendizaje automático para evaluar la defoliación de las copas de las plantaciones de encina-alcornoque, inducida por *Phytophthora cinnamomi* transmitida por el suelo, utilizando una metodología de clasificación semiautomatizada. Dos parcelas diferentes, establecidas en la plantación de *Quercus ilex-Q. suber* con condiciones de sitio contrastadas, fueron medidas (183 encinas y 246 alcornoques) para la evaluación mediante teledetección. Se midieron las posiciones de los árboles, las variables alométricas y la defoliación de las copas (en categorías de 5% de defoliación) de todos los árboles. Se adquirieron imágenes de satélite WorldView-2 (WV-2) y datos LiDAR aéreos, y se calcularon diecinueve índices de vegetación (VI). Para captar el componente estructural de la plantación de *Quercus*, se realizó una segmentación individual de los árboles y se extrajeron las métricas LiDAR. Las bandas medias y los valores de VI junto con las métricas LiDAR aerotransportadas se utilizaron como características de entrada para ejecutar modelos no paramétricos para producir resultados de mapeo de defoliación de árboles. El valor de reflectancia de las copas de los árboles mostró un considerable solapamiento entre las tres clases de defoliación, y las copas defoliadas fueron más permeables a los retornos LiDAR. BNDVI, MTVI1, NDVI y Elev.P_{70}, entre las bandas WV-2, los índices de vegetación y las métricas LiDAR, fueron los mejores predictores para los modelos de defoliación en *Q. ilex* y *Q. suber*. En general, los modelos no paramétricos de defoliación presentaron buenos índices de exactitud, excepto en el caso de la clase de defoliación intermedia (valores de exactitud global que oscilaron entre el 61,29% y el 71,43%, e índice Kappa entre 0,43 y 0,58). Por último, se obtuvo un mapa de predicción de la defoliación de los árboles basado en el modelo de clasificación de las redes neuronales que representaba los patrones espaciales del estado de defoliación asociados a los daños de la podredumbre de la raíz. Estos mapas representan la información espacial necesaria para planificar y llevar a cabo intervenciones preventivas y curativas en grandes regiones de robledales que han sido dañadas por la podredumbre de la raíz.

Abstract

Holm oak (*Quercus ilex* L. subsp. *ballota* [Desf.] Samp.) plantations have contributed to create environmental benefits covering large areas under dynamic and complex environmental and management conditions. However, root rot oomycetes (*Phytophthora* and *Pythium*) produce decline and mortality processes. Currently, systems based on remote sensing are the best alternative for the evaluation and monitoring of forest ecosystems with great precision, without requiring direct environmental involvement. The objective of this research was to integrate WorldView-2 vegetation indices and airborne LiDAR data as inputs in machine learning models to assess crown defoliation of holm-cork oak plantation induced by soil-borne *Phytophthora cinnamomi* using a semi-automated classification methodology. Two different plots, established at *Quercus ilex*-*Q. suber* plantation with contrasted site conditions, were measurements (183 holm oaks and 246 cork oaks) for remote sensing assessment. Tree positions, allometric variables and crown defoliation (in 5%-defoliation categories) of all trees were measured. A WorldView-2 (WV-2) satellite imagery and airborne LiDAR data were acquired, and nineteen vegetation indices (VI) were calculated. For capturing the structural component of *Quercus* plantation, an individual tree segmentation was conducted, and LiDAR metrics were extracted. Mean bands and VI values together with airborne LiDAR metrics were used as input features for running non-parametric models to produce tree defoliation mapping results. Reflectance value of the tree canopies showed considerably overlap between the three defoliation classes, and defoliated crowns were more porous to LiDAR returns. BNDVI, MTVI1, NDVI and Elev.P_{70}, among WV-2 bands, vegetation indices and LiDAR metrics, were the best predictors for defoliation models in *Q. ilex* and *Q. suber*. Overall, the non-parametric models of defoliation presented good accuracy rates, except in the case of the intermediate defoliation class (overall accuracy values ranging from 61.29% to 71.43%, and Kappa index from 0.43 to 0.58). Finally, a predicted tree-defoliation map based on the Neural Networks classification model was yielded representing the spatial patterns of defoliation status associated with root rot damages. These maps represent the spatial information needed to plan and carry out preventive and curative interventions in large regions of oak woodlands that have been damaged by root rot.

Keywords: Afforestation, Oak, decline, WorlView-2, LiDAR, defoliation models, spatial analysis.

1 Introduction

Dehesas, a Mediterranean savannah-like ecosystems, are an important element of the Iberian Peninsula's cultural legacy (including *montados* in Portugal), as they are associated with social and economic development of rural areas together with relevant environmental benefits. In these ecosystems, increase of biotic and abiotic stresses and, in general, forest decline, has been observed since the 1980s, frequently associated with severe mortality processes (Brasier et al., 1993; Tuset et al., 1996; Sánchez et al., 2006; Duque-Lazo et al., 2018). The European Economic Community promoted intensive afforestation of abandoned agricultural lands in Spain after 1993, planting a total of 232,858 ha of new forest plantations in Andalusia (1993-2006, Southwestern Spain), of which 82,755 ha were planted with holm oak (*Quercus ilex* L. subsp. *ballota* [Desf.] Samp.) and 1,393 ha with cork oak (*Quercus suber* L.) (Navarro Cerrillo et al., 2009). Those plantations were intended to create ecosystem services covering large areas under dynamic and complex environmental (i.e., climate, soil and topography) and management conditions (i.e., former agricultural and livestock uses, pest and diseases). Thus, this program contributed to increase the potential areas of *dehesa* forests. However, recent studies indicated that some of those plantations are severely affected by mortality processes related to oak decline (Jung et al., 2016; Sánchez-Cuesta et al., 2020).

Among the biotic factors related with this syndrome, the presence of root rot oomycetes (*Phytophthora* spp. and *Pythium* spp., Vettraino et al., 2002); and pests (*Cerambyx* spp., *Coroebus* spp. and *Prinobius* spp. predominantly, Carrasco Gotarredona et al., 2009) have been pointed out as major threats for *Q. ilex* and *Q. suber dehesas*. Decline and mortality processes produce some visible symptoms such as crown defoliation, leaf chlorosis, as well as the regressive death of branches and shoots (Corcobado et al., 2013). These symptoms have been generally evaluated by expert approach based on visual assessment (Nakajima et al., 2011) being necessary to standardize the methodology of crown visual assessment. Although time-consuming and labour-intensive, the ICP methodology is frequently utilized for this purpose.

Currently, systems based on remote sensing are the best alternative for the assessment and monitoring of forest ecosystems with great precision, and without requiring direct environmental intervention. Spectral signatures indicate changes in forest health parameters (Lausch et al., 2016), including

defoliation and crown status (e.g., pigment content, tree physiology, leaf area index) which can be quantified with good accuracy and efficiency using remote sensing techniques (Hall et al., 2016; Stone and Mohammed, 2017). There are different methods based on remote sensing to obtain maps of vegetation vigour (Kukunda et al., 2018). Previous works, using different spectral and spatial resolution imageries, have been successfully used to assess the tree health status of adult holm oaks *dehesas* (Navarro-Cerrillo et al., 2019) or describing previsual damages (Hernández-Clemente et al., 2019). Even so, spectral information allows to evaluate physiological tree respond, but it is limited to assess tridimensional tree structure. Light Detection and Ranging (LiDAR) data lay out highly accurate 3D information and it is considered the best approach to describe tree and canopy structural metrics (Vauhkonen et al., 2014). It is worth noting that the accessibility to different sensor and missions increases the possibilities for remote sensing data integration reducing uncertainty by combining multiple sensor types and utilizing their synergies and complementarities (Lausch et al., 2017). Therefore, new approaches to forest health assessment directly focus on the integration of different remote sensing products (Hall et al., 2016; Stone and Mohammed, 2017). Therefore, integration of remote sensing data may provide an accurate proxy of forest health indicators on *Quercus* plantations.

Assessment of holm and cork oak crown defoliation in regular plantations opens the possibility to describe the spatial dynamics of disease spread under homogeneous vegetation cover (Navarro-Cerrillo et al., 2019). The aim of this research was to integrate WorldView-2 vegetation indices and airborne Aerial Laser Scanning metrics as inputs in machine learning models to assess crown defoliation of holm-cork oak plantation induced by soil-borne *Phytophthora cinnamomi* using a semi-automated classification methodology. The specific objectives were: i) assessing the holm oak crown status, using Aerial Laser Scanning metrics and spectral vegetation indices derived from the multispectral WorldView-2 satellite sensor, ii) predicting the defoliation status of holm oaks at tree scale using non-parametric Machine Learning methods, and iii) obtaining robust cartographic information of crown defoliation of holm oaks plantations, which can be used for decision-making, implementation and management of projects of interest. These maps represent the spatial information needed to plan and carry out preventive and curative interventions in large regions of oak woodlands that have been damaged by root rot.

2 Material and Methods

2.1 Study area

The study area is located in a *Quercus ilex-Q. suber* plantation in south Spain (Puebla de Guzman (ETRS89, UTM29N: 650 000 m E, 4 160 000 m N, Huelva, Southwestern Spain, 190 m a.s.l., Figure 1). Plantation was established in 1995 under the EU afforestation program, and it has a current density of 208 trees ha^{-1} (82% *Q. ilex*, 18% *Q. suber*). The climate corresponds to a IV_2 class – genuine subtropical Mediterranean – (Allué, 1990), characterized by an average annual temperature of 16.8 ° C, and an average annual rainfall of 570 mm (UTM Zone 29 coordinate: 654 725.567 m E, 4 157 571.704 m N). The area has an undulating relief (with slopes less than 18%), with thin and acidic soils predominantly reddish-brown eutric regosols, with low organic matter content (2.53%) and sandy loam to loam texture. The study area is affected by root rot determined by the presence of oomycetes in the tree rhizosphere (including *Phytophthora cinnamomi* Rands.) identified by classical soil baiting techniques (Sánchez et al., 2002), and molecular analyses (Newbiotechnic S.A., NBT - Nº 41/04/PR/PSX), without the presence of other biotic or abiotic agents.

2.2 Field Data

Two different plots were stablished in the study area in 2008 (see Chapter 4), in contrasting site conditions (e.g., slope and aspect), crown condition (e.g., different level of defoliation) and species presence (e.g., *Quercus suber* and *Quercus ilex*) (Figure 1). Plot 1 (P_1) was located in the southern area of the afforestation and includes two subplots, one of *Q. ilex* trees south-exposed with high defoliation rates (P_1Qi) and another north-facing subplot of *Q. suber* with low defoliation rates (P_1Qs). The second plot (P_2) was located in the centre of the afforestation, including a subplots of *Q. ilex* (P_2Qi) and *Q. suber* (P_2Qs) facing north-west and north-east, respectively, being P_2Qi less defoliated than P_1Qi and P_2Qs slightly higher defoliated than P_1Qs (Figure 1; Table 1).

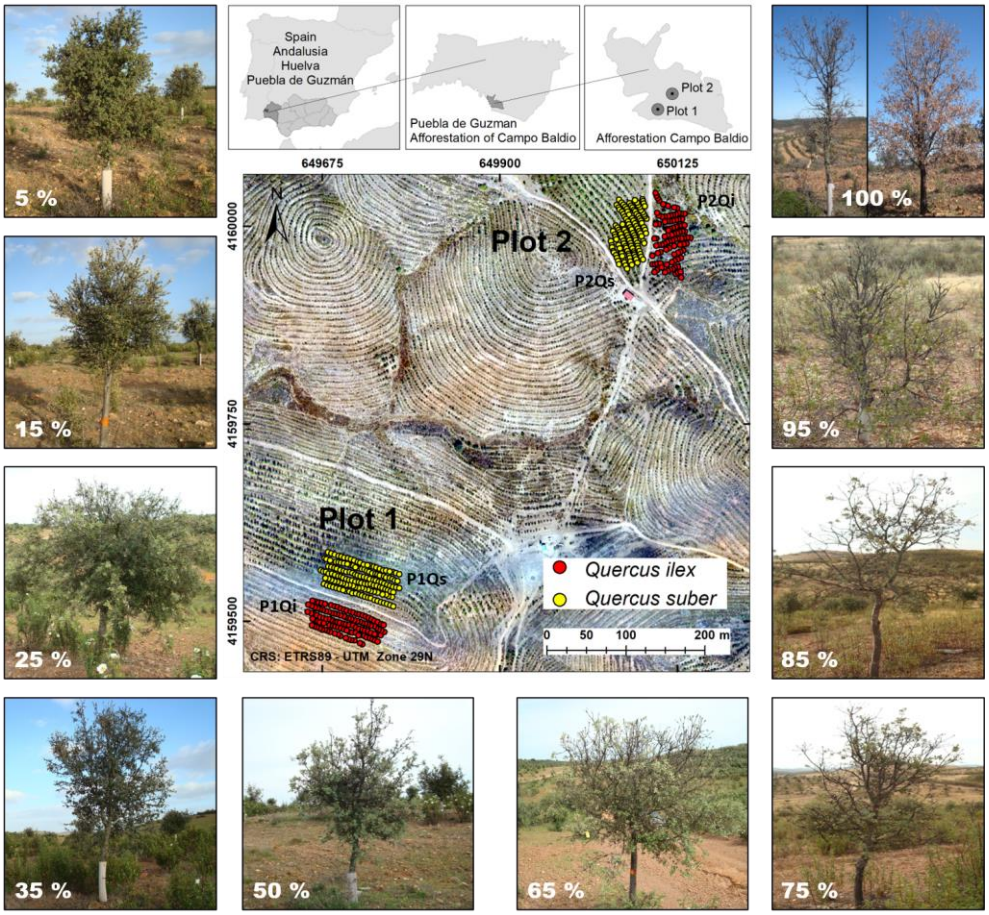

Figure 1. Location of holm oaks (red dots) and cork oaks (yellow dots) trees with crown defoliation assessment within study plots 1 and 2 (EU afforestation plan, Campo Baldío - Puebla de Guzmán - Huelva - Spain), according to the percentage of crown defoliation (ICP-Forest, Ferretti et al., 2016; Eichhorn et al., 2016).

In April 2018, field measurements were carried out on 429 trees (183 holm oaks and 246 cork oaks) for remote sensing assessment (Figure 1). Tree positions were recorded using a Manual Total Station (Leica FlexLine TS03) and tree density (N, tree ha^{-1}) was estimated. Allometric variables of all trees, such as diameter at breast height, were also measured (DBH, cm; 1.3 m above ground level - Haglöf Mantax caliper, Långsele, Sweden), mean crown projection diameter (Crown, m), and total height (H, m; Haglöf Vertex III). Crown defoliation was also estimated according to the methodological classification of the ICP Forests-European Network (Ferretti et al., 1994, 2016; Eichhorn et al., 2016), assessed visually, in situ, always by the same expert technician (http://icp-forests.net/page/icp-forests-manual) (Table 1). Crown defoliation was measured in 5%-defoliation categories (between 0 and 100%) and then trees were classified into three Defoliation Classes (DC): DC1 Low defoliation trees, with slight to moderate damage (<30% foliage loss), DC2 High defoliation trees, with moderate to severe damage (ranging from ≥30% to <90% foliage loss), and DC3 Dead trees (≥ 90% foliage loss) (Navarro-Cerrillo et al., 2019) (Table 1; Figure S5.1, Supplementary Material).

Table 1. Allometric variables (DBH = diameter at breast height), Crown = crown projection diameter, H = total height), defoliation (Def %) defoliation for each Defoliation Class (DC1, DC2, DC3 %) with the percentage of trees corresponding to each class (in square brackets). Data are presented for each plot and grouped by subplots and species. *n* = number of trees; P_i number of plot, Qi = *Quercus ilex,* Qs = *Q. suber*. Mean ± standard error.

Variable	All (*n*=429)	P_1Qi (*n*=95)	P_1Qs (*n*=141)	P_2Qi (*n*=88)	P_2Qs (*n*=105)	Qi (*n*=183)	Qs (*n*=246)
DBH (cm)	12.3±0.2	9.9±0.4	14.3±0.3	9.5±0.4	12.7±0.3	9.7±0.3	13.6±0.2
H (m)	3.8±0.05	2.49±0.09	4.45±0.07	3.30±0.09	3.48±0.06	2.96±0.07	4.19±0.05
Crown (m)	2.72±0.07	2.27±0.22	2.85±0.11	2.50±0.18	2.97±0.12	2.40±0.14	2.89±0.08
N (tree ha^{-1})	248	74	369	171	346	122	359
Def. (%)	54±1	88±2	33±2	70±3	40±2	79±2	36±1
DC1 (0-30)	16±1 [25]	20 [1]	16±1 [43]	13±2 [10]	17±1 [35]	14±2 [5]	16±1 [40]
DC2 (30-90)	50±1 [47]	57±4 [22]	44±1 [54]	56±3 [45]	50±2 [61]	57±2 [33]	47±1 [57]
DC3 (90-100)	97±0 [28]	97±0 [77]	96±2 [3]	96±1 [45]	95±0 [4]	97±0 [62]	96±1 [3]

2.3 WorldView-2 dataset and processing

Figure 2 depicts the methodological flow diagram for remote sensing modelling. Commercial multispectral and panchromatic World View-2 (WV-2) satellite imagery was chosen for evaluating tree spectral response according to previous studies (Navarro-Cerrillo et al., 2019). The image was acquired on 16 September 2017 (Table S5.1, Supplementary Material). The cloud cover was 0%, the GSD (Ground Sampling Distance) of the multispectral and panchromatic bands corresponds to 2.18 m and 0.54 m, respectively and an off-nadir angle of 28.8º. The image had a View Ready Standard 2A processing level, which implies a georeferencing to a map projection, in this case WGS84 UTM 29N, and radiometric correction. The FLAASH extension was used to convert radiance data into top of atmosphere reflectance in the first processing step (Fast Line-of-sight Atmosphere Analysis of Spectral Hypercubes) (Matthew et al., 2000). Subsequently, the multispectral and panchromatic bands were processed to fuse them into a pan-sharpening image and thus improve their spatial resolution (ENVI, 2006, Maurer, 2013, see Navarro-Cerrillo et al., 2019). Finally, the pan-sharpened multispectral image was co-register considering the LiDAR data (RMSE of 0.7 pixels on the 0.5 m WV-2 imagery; Navarro-Cerrillo et al., 2019).

Based on prior literature, 19 vegetation indices (VI) were generated, with a special focus on forest defoliation (Senf et al., 2017b; Table 2; Figure S5.2, Supplementary Material), to test its potential in forecasting and mapping defoliation evaluation (Zhu et al., 2018).

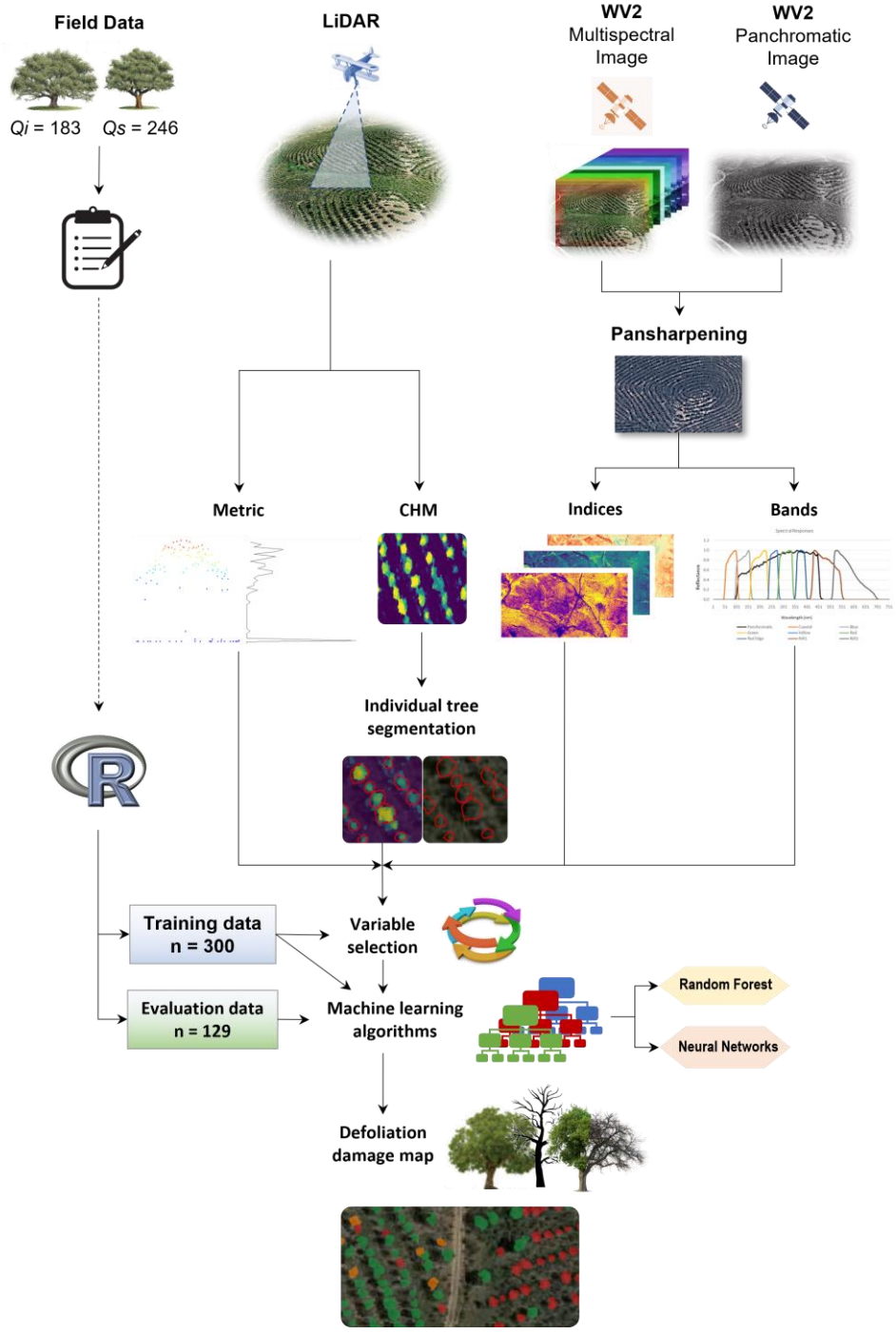

Figure 2. Workflow of remote sensing modelling for forecasting crown defoliation of holm-cork oak plantation associated to root rot at tree level by integrating high-resolution multispectral imagery and airborne LiDAR data.

Table 2. Remote sensing vegetation indices adapted to WorldView-2 imagen for forecasting crown defoliation of holm-cork oak crown defoliation (https://www.indexdatabase.de/db/r.php).

Abbreviation	Name	Formula
ARVI	Atmospherically resistance vegetation index	Band 8-(2*Band 5-Band 2)/Band 8+(2*Band 5-Band 2)
BNDVI	Blue Normalized Difference Vegetation Index	(Band 7-Band 2/Band 7-Band 2)
D800/550	Difference 800/550	Band 7-Band 3
D800/680	Difference 800/680	Band 7-Band 5
GLI	Green Leaf Index	(2Band 3-Band 5-Band 1)/(2Band 3+Band 5+Band 1)
ChlGREEN	Chlorophyll Green	$(\frac{Band\ 7}{Band\ 3})^{(-1)}$
GNDVI	Green Normalized Vegetation Index	(Band 7-Band 3)/(Band 7+Band 3)
GRNDVI	Green Red NDVI	(Band 8-(Band 3+Band 1))/(Band 8+(Band 3+Band 1))
RBNDVI	Red Blue NDVI	(Band 8-(Band 5+Band 1))/(Band 8+(Band 5+Band 1))
PSSRc1	Pigment Specific Simple Ratio C1	Band 7/Band 2
PNDVI	Pan NDVI	Band 8-(Band 3+Band 5+Band 1)/Band 8+(Band 3+Band 5+Band 1)
MTVI1	Modified Triangular Vegetation Index 1	1.2(1.2(Band 7-Band 3)-2.5(Band 5-Band 3))
EVI	Enhanced vegetation index	2.5*(Band 8-Band 5)/(Band 8+6*Band 5-7.5*Band 2+1)
MCARI1	Modified Chlorophyll Absorption in Reflectance Index 1	1.2(2.5(Band 7−Band 5)−1.3(Band 7−Band 3))
MCARI2	Modified Chlorophyll Absorption in Reflectance Index 2	$1.5\frac{2.5(Band\ 7-Band\ 5)-1.3(Band\ 7-Band\ 3)}{\sqrt{(2Band\ 7+1)^2-(6Band\ 7-5\sqrt{Band\ 5}-0.5}}$
NDVI	Normalized Difference Vegetation Index	(Band 7-Band 5)/(Band 7+Band 5)
SAVI	Soil Adjusted Vegetation Index	$\frac{Band\ 7-Band\ 5}{Band\ 7+Band\ 5+L}(1+L)$
SARVI	Soil and Atmospherically Resistant Vegetation Index	$(1+L)\frac{Band\ 7-(Band\ 5-\gamma(Band\ 2-Band\ 5)}{Band\ 7-(Band\ 5-\gamma(Band\ 2-Band\ 5)+L}$(1+L)
LIC2	Lichtenthaler indices 2	Band 1/Band 5

2.4 Aerial Laser Scanning data acquisition and processing

Airborne Laser Scanning (ALS) data were acquired on 6 April 2013 with a Leica ALS60 laser scanner mounted on a fixed-wing aircraft (Leica-Geosystems AG, Heerbrugg, Switzerland, Heliografics Fotogrametria S.L.-Alicante, Spain). An area of 310.7 ha was scanned from a flight altitude of 4442 fts at a speed of 105 knots, with a field of view (FOV) of 13 degrees, a scanning rate of 100 Hz and a pulse rate of 187.6 kHz. Pulses returned had an average density of 12 points m-2 (Table S5.1, Supplementary Material). For all echoes, the data was geo-referenced in the European Terrestrial Reference System 1989 coordinate system (ETRS89). The vertical and horizontal accuracy estimates were 0.07 and 0.12 meters, respectively. Changes in defoliation may have occurred as a result of the five-year time interval between ALS data gathering and field data collecting. Thus, ALS metrics were considered for contributing to the defoliation model through the structural tree component (size, cover, and crown projection). The influence of the difference adquistion date on tree structure can be considered low due to Q. ilex and Q. suber are slow-growing species (average diameter annual increment of 6.19 ± 0.43 mm year-1) (Martín et al., 2014). Bare earth points were retrieved from the total point cloud and then used for height normalization. Next, a pit-free Canopy Height Model (CHM) was computed using Khosravipour et al., (2014) algorithm in Lastools software (Isenburg, 2021).

2.5 Segmentation for crown delineation

For capturing the structural component of *Quercus* plantation, an individual tree segmentation was conducted. The previously computed pit-free algorithm was subjected to a region expanding segmentation algorithm (Erikson and Olofsson, 2005). Variance feature space, variance position space, and similarity threshold parameters, an anlysis was carried out by modifying their values until obtained the best fitted positions of the georreferenced trees in the field campaing was found, following methodology of Varo-Martínez & Navarro-Cerrillo, (2021). All processes were executed in SAGA (System for Automated Geoscientific Analyses) GIS (Conrad et al., 2015).

After obtaining tree canopy segments, mean values of the pixel data inside every delineated crown were computed for all the spectral bands (8) and vegetation indices (19 VI, Table 2). In addition, 43 LiDAR metrics were

extracted using *CloudMetrics* function from FUSION software (McGaughey, 2014) (Table S5.2, Supplementary Material).

2.6 Defoliation data modelling

Spectral bands and VI values together with ALS metrics were used as input features for running models to produce tree defoliation mapping results. Because the ALS data and VI may contain redundant information, a variance inflation factor (VIF) analysis was used to reduce the hight number of explanatory factors before tree defoliation classification (Akinwande et al., 2015). A VIF (treshold ≥10) was used to select the best explanatory variables, and collinear variables were eliminated from the study (Duque-Lazo et al., 2016; Kukunda et al., 2018). Raw data were separated into training and evaluation sets, covering 70% (300 trees) as training set and 30% (129 trees) as validation set of the input data. Because tree crown defoliation variable did not fit a normal distribution (Shapiro-Wilk test, $P < 0.05$), a matching learning non-parametric statistics (e.g., Random Forest and Neural Network methods) were used as modelling approaches.

For tuning Random Forest parameters, *randomForest* package (Liaw and Wiener, 2002) and *caret* package (Kuhn, 2008) were used in R environment (R Development Core Team, 2017). Number of classification trees (*ntree*) ranged between 500-2500 and the number of variables (*mtry*) ranged between 1-10. For decision making on the best Neural Network classification parameters, *decay* and *size* parameters were shifted from 0.1 to 0.4 and from 1 to 10, respectively, using *nnet* (Venables and Ripley, 2002) and *caret* packages. In both classification methods, best parameters were estimated by internal 5-times repeated 10-fold cross-validation and the external validation set (Belgiu and Drăguţ, 2016). The accuracy value and the Cohen's kappa index of the confusion matrix of the training and evaluation data were used to measure the statistical models' goodness of fit.

2.7 Defoliation mapping and site-specific responses

Finally, a map of canopy defoliation at individual tree scale was developed with the best model (highest classification accuracy and Kappa index with stable numbers between training and evaluation data) over the study area. It was used to evaluate a proxy of the site-specific sources of defoliation in *Quercus* species.

3 Results

3.1 Individual tree crown spectral and structural performance at different defoliation levels

The reflectance value of the tree canopies in each band showed that although defoliation classes 2 and 3 response was similar in the blue, green, red-edge and NIR-2 bands, defoliation class 3 had a different spectral response in the yellow, red and NIR-1 bands (Figure 3a). LiDAR data also showed that healthy trees were slightly higher than middle defoliated and heavily defoliated ones (Figure 3b). Furthermore, more returns were obtained at the tree upper layers in healthy trees (Elev.P80 and Elev.P90). On the other hand, most defoliated crowns (classes 2 and 3) had lower returns at the middle layers (Elev.P60 and Elev.P70, Figure 3b and Figure 4).

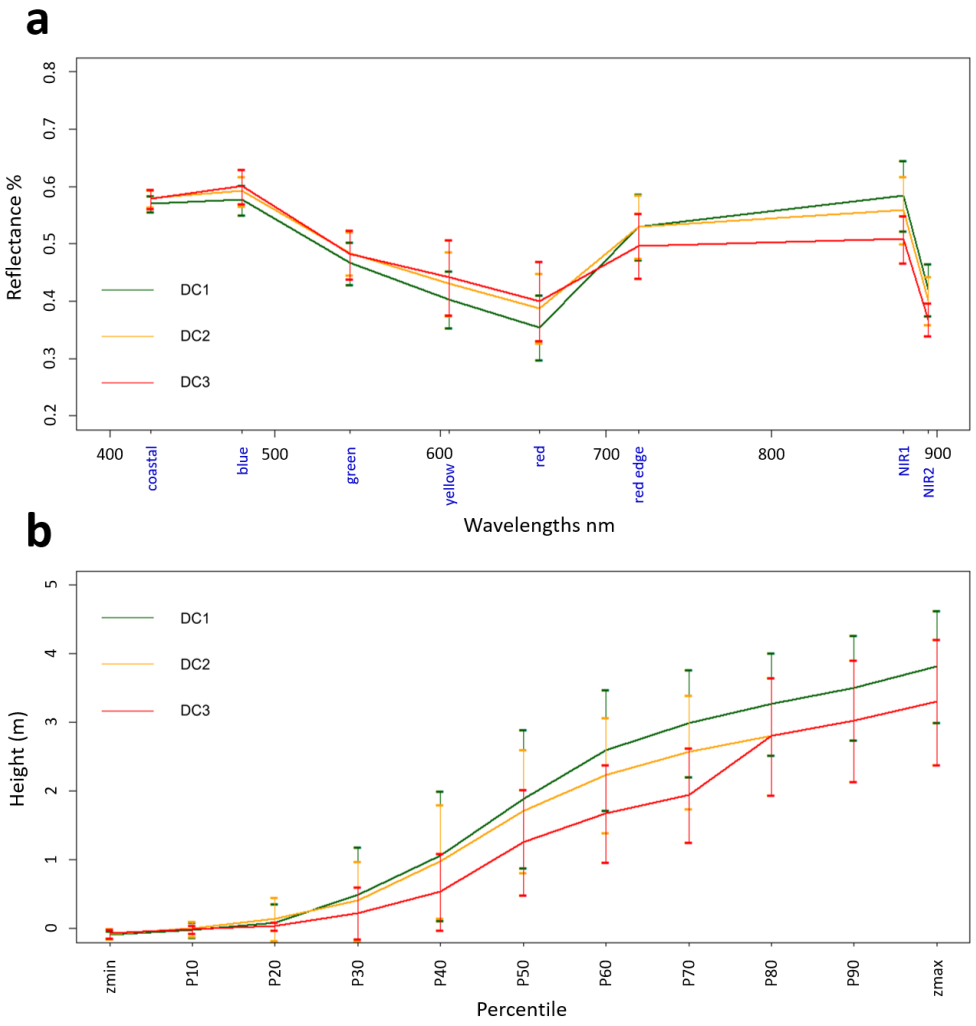

Figure 3. Distribution of remote sensing data considering defoliation classes. (a) Distribution of reflectance for mean pixel values of the 8 studied bands of Word View hyperspectral sensor. (b) Distribution of total tree heigh regarding LiDAR metrics (percentile value) of the point cloud.

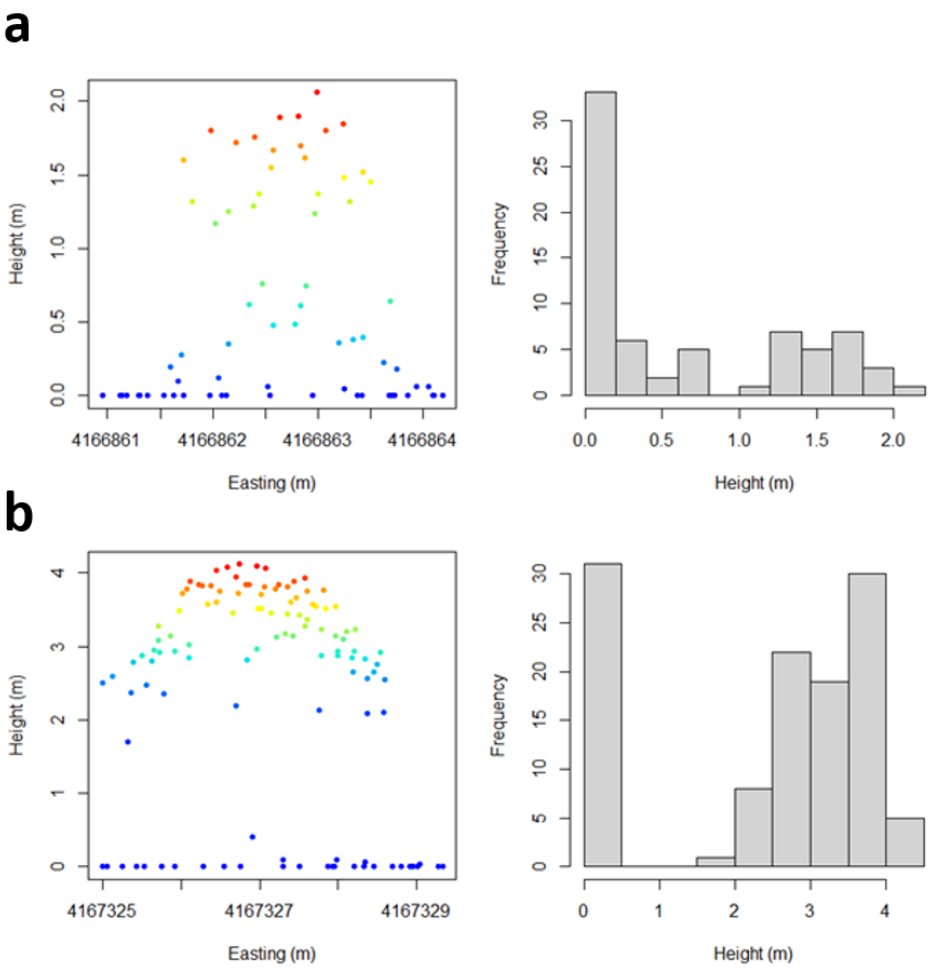

Figure 4. Point cloud distribution (left) and histogram of points frequency regarding height (right) of two trees with high differences in crown defoliation. (a) Tree from DC3 with 90% of defoliation. (b) Tree from DC1 with 5% of defoliation.

3.2 Random Forest models for defoliation assessment

From the all predictors, the VIF separated BNDVI, MTVI1, NDVI and Elev.P_{70} among WV-2 bands, vegetation indices and LiDAR metrics (Figure 5; Table S5.2, Supplementary Material) as predictors for defoliation models in *Q. ilex* and *Q. suber*. The variable selection for estimating defoliation was consistent for the different models.

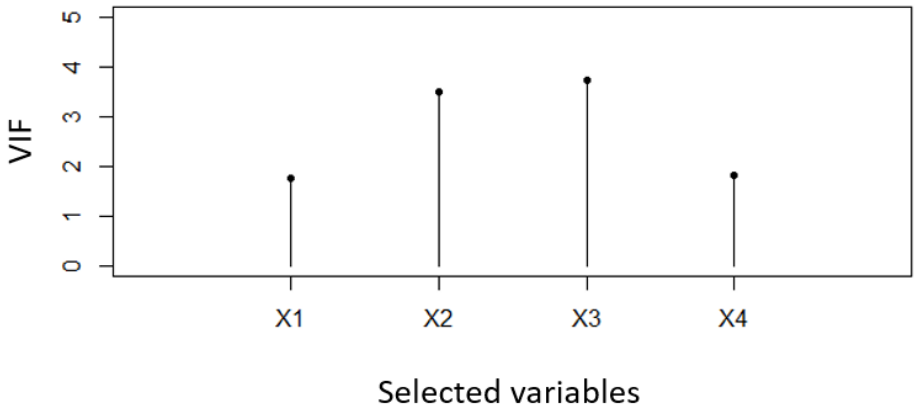

Figure 5. VIF values for the selected variables. X1: mean crown value for BNDVI, X2: mean crown value for MTVI1, X3: mean crown value for NDVI and X4: 70th percentile of normalized tree point cloud heights.

Non-parametric models of defoliation presented good accuracy rates, except in the case of the intermediate defoliation class (DC2) for the training group (Table 3). Random Forest had an overall accuracy values ranging of 61.29% (κ=0.43, for training data) to 71.43% (κ=0.58, for evaluation data). Neural Network model showed higher precision and kappa value in the training group (Accuracy=0.66% and κ=0.48), and the parameters were more stable when validation group was evaluated (Accuracy=0.64% and κ=0.49).

Table 3. Statistic for the classification models to estimate defoliation (%) of *Quercus ilex* and *Q. suber* in southwest Spain using multispectral vegetation indexes and LiDAR metrics.

Random forest. Training data

	Reference			
Prediction	DC1	DC2	DC3	User's accuracy
DC1	27.7	9	3.2	69.4
DC2	1.9	7.7	9.7	39.9
DC3	2.6	12.3	25.8	63.4
Producer's accuracy	86.0	26.6	66.7	

Accuracy (average): 61.29
Kappa: 0.439

Random forest. Evaluation data

	Reference			
Prediction	DC1	DC2	DC3	User's accuracy
DC1	35.7	7.1	0.0	83.3
DC2	0.0	14.3	0.0	100.0
DC3	0.0	21.4	21.4	50.0
Producer's accuracy	100.0	33.3	100.0	

Accuracy (average): 71.43
Kappa: 0.588

Neural Network. Training data

	Reference			
Prediction	DC1	DC2	DC3	User's accuracy
DC1	25.8	8.4	3.2	69.0
DC2	3.2	5.2	0	61.9
DC3	3.2	15.5	35.5	65.5
Producer's accuracy	80.1	17.9	91.7	

Accuracy (average): 66.45
Kappa: 0.487

Neural Network. Evaluation data

	Reference			
Prediction	DC1	DC2	DC3	User's accuracy
DC1	35.7	7.1	0.0	83.3
DC2	0.0	7.1	0.0	100.0
DC3	0.0	28.6	21.4	42.3
Producer's accuracy	100.0	16.7	100.0	

Accuracy (average): 64.29
Kappa: 0.4964

3.3 Defoliation mapping and site-specific responses

The Neural Networks classification model, which provided the highest overall accuracies and stability, was used to create a forecast tree-defoliation map. The map covers represent the spatial patterns of defoliation status associated with root rot damages (Figure 6). Overall, 62.28% of tree were classified as dead trees (DC3), 31.31% of trees as low defoliation class (DC1) and a short 6.41% of the trees were classified as heavy defoliated level (DC2). Defoliation appeared clustered, with large patches of dead trees in the most sun-exposed areas of *Q. ilex* stands. *Q. suber* trees were mostly classified in DC1 in northern exposure, with a few trees classified as DC2 or DC3, without a relevant aggregation pattern. It was observed that the most intense DC3 defoliations correspond to holm oak, while that DC1 and DC2 classes were predominate in cork oak. *Q. ilex* showed higher levels of defoliation in all aspects, while *Q. suber* showed lower defoliation in its targeted plantation sites, although there is a tendency to increase defoliation in areas with a lower slope and therefore more exposed to solar radiation.

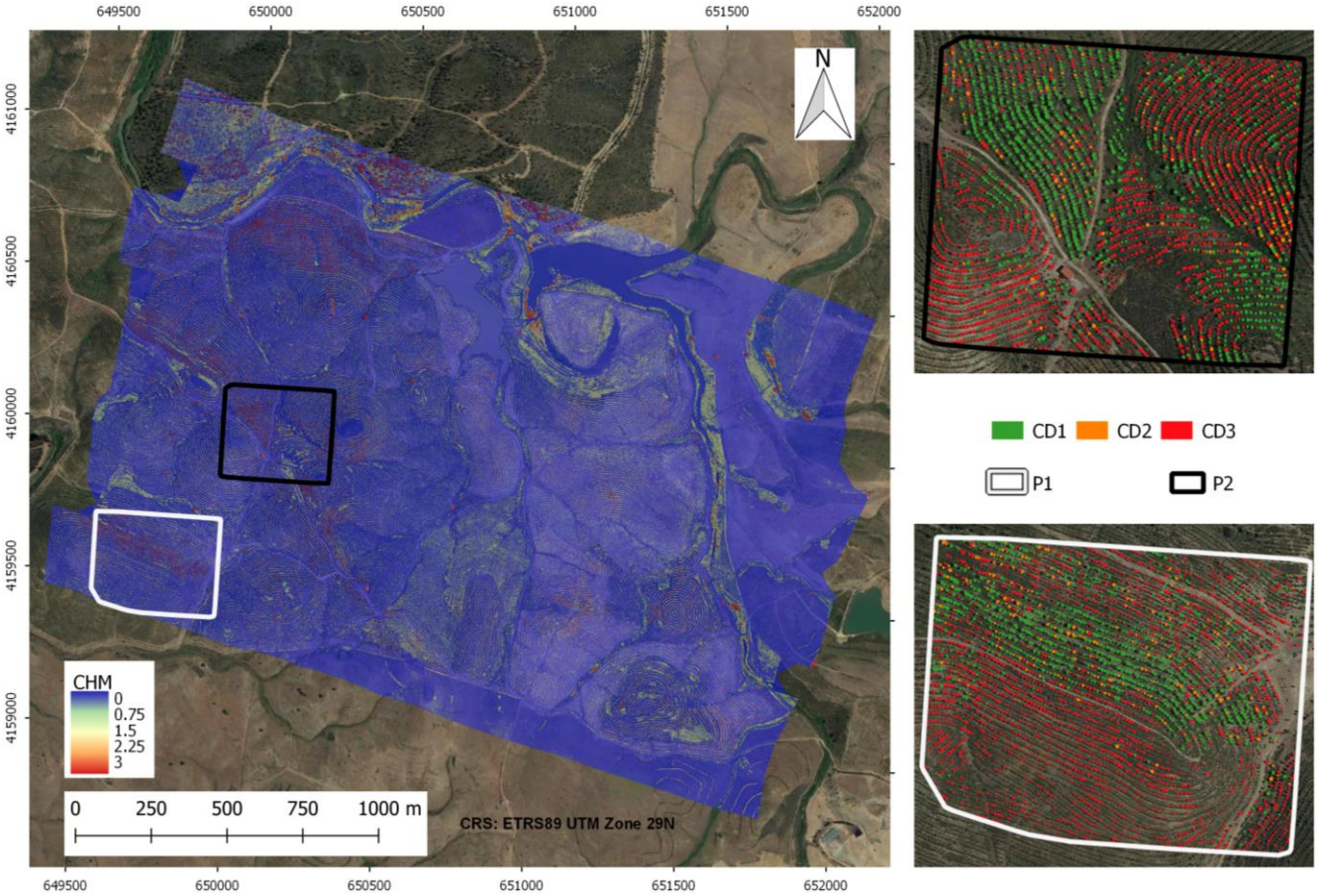

Figure 6. Tree defoliation map at 2 m resolution in a mixed *Q. ilex-Q. suber* plantation obtained using Canopy Height Segmentation Model (CHM) and Neural Networks classification model integrating vegetation indexes (WorldView-2) and airborne LiDAR metrics (Huelva, Southwest Spain). Green=low defoliated trees, orange=hight defoliated trees, red=dead trees.

4 Discussion

The expected increase of forest decline and mortality on Mediterranean oak forests demands an accurate diagnostic and spatial characterization of damages, which rely in high resolution canopy defoliation maps. Since 1990, holm oak natural forests and plantations have been badly impacted by root rot (Brasier, 1996), with positive identification of *P. cinnamomi, P. quercina*, and other oomycetes soilborne diseases (Ruiz-Gómez et al., 2019). Our results illustrate the efficacy of integrating vegetation indices (WorldView-2), and airborne ALS metrics to classify trees into different defoliation levels in an oak-dehesa type forest associated to root rot (*Phytophthora* spp. and *Pythium* spp. oomycetes). These results allow the generation of accurate tree-scale maps using remote sensing data, which can be used to improve the assessment and control of root rot infections, particularly under complex climate scenarios that may increase its expansion (Duque-Lazo et al., 2018), reducing labour and production costs (Hall et al., 2016; Meng et al., 2018). We also employed defoliation-derived cartography to demonstrate the presence of spatial patterns of defoliation linked to site factors.

4.1 Vegetation indices and ALS metrics related to tree defoliation

On this work, multispectral vegetation indices form a WorldView-2 imagery and ALS data were integrated to provide information about structural characteristics of oak trees defoliation associated to root rot at individual crown level. The best technique for detecting tree stress and mortality, according to several studies, is to combine ALS metric and optical satellite imaging (Holmgren et al., 2008; Lamonaca et al., 2008).

For oak tree segmentation, moderate density ALS data (12 points m^{-2}) was employed as a first step. Previous research has shown that ALS measurements can segment tree canopy in low-density forest species formations (savanna-type forests) (Shao et al., 2019), including holm and cork oak forest (Borlaf-Mena et al., 2019; Navarro-Cerrillo et al., 2019). These results show the usefulness of simple ALS metrics for detecting crown-scale defoliation. The quality of the segments (i.e., their approximation to real tree crowns) determines the success of an object-based classification; hence, high-density data from digital surface models improves the segmentation of tree crowns. In contrast to earlier investigations, our segmentation program was able to automatically delineate individual tree crowns using

intermediate density ALS (Li et al., 2012; Jakubowski et al., 2013). In term of crown defoliation model, the metric related to tree middle-height percentile (Elev.P_{70}) was chosen between the best predictors. The middle or upper-middle percentiles are often used in research that employ ALS data to assess defoliation (Meng et al., 2018), and is in concordance with previous defoliation models on *Q. ilex* stands affected by oak decline (Navarro-Cerrillo et al., 2019). Middle and low ALS percentiles have shown to be the best predictors for crown transparency detection due to the close link between the porosity of the tree crown since high defoliated trees show more points at these height positions (Meng et al., 2018; Kälin et al., 2019). However, other previous research assessing tree defoliation, due to other factors different from root rot, identified lower percentiles as the most predictive ones, ranging between Elev.P_{50} in eucalypt forests subjected to periodic flooding (Shendryk et al., 2016) to Elev.P_{40} and lower for stands affected by bark beetle (Stereńczak et al., 2019). In both cases defoliation affected all the canopy in a more homogeneous way; but defoliation produced by *Phytophthora cinnamomi*, on the other hand, follows an erratic pattern in oak decline, beginning with total defoliation of the top of the crown ("top tip drying") (de Sampaio e Paiva Camilo-Alves et al., 2013). Therefore, ALS point cloud percentile distribution has proven to be a good predictor of structural changes experienced by tree crown related to defoliation processes, being the middle-hight percentiles more adequate to assess irregular crown transparency such as the symptoms of *Phytophthora* root rot.

Because of their association with chlorophyll content and physiological status of vegetation, red edge and visible-near infrared single spectral indices (e.g., NDVI, EVI, OSAVI...) have been the indices most frequently utilized for mapping forest defoliation when examining multispectral images (Senf et al., 2017b). Other defoliation studies, on the other hand, imply that spectral indices (e.g., NDMI, MSI, NBR) that cover different shortwave-infrared or SWIR bands are more sensitive to plant water content (Otsu et al., 2018). The most relevant indicators for discriminating between defoliation levels in this study were the Modified Triangular Vegetation Index (MTVI1), NDVI, and Blue Normalized Digital Vegetation Index (BNDVI) which integrate the visible and the NIR-1 bands. Although the three defoliation classes showed overlapping in some bands, the mean spectral value of tree crown showed an inflection point in the red edge band, serving as turning point in which defoliation classes inverted the spectral trends. In the visible spectrum, defoliated trees

exhibited more reflectivity, while healthy vegetation had higher reflectivity in the infrared range. MTVI1 and BNDVI indexes have been reported to proposed for LAI estimation (Zou et al., 2018; Liang et al., 2020), thus the selection of those indexes is consistent with the ALS metric response. On the other hand, NDVI has been widely used to capture phenology (Cavender-Bares et al., 2020) the absorption of photosynthetically active radiation (FAPAR) and NDVI (Myneni and Williams, 1994).

Other bands of VI's associated with the leaf chlorophyll content were not included in the model to discriminate between the defoliation levels (Hunt et al., 2013, see Table 2), although the use of leaf pigment content indices in tree damage classification may reflect changes in canopy colour caused by physiological processes such as defoliation (Damm et al., 2018). The red-edge band, for example, has long been used to detect forest destruction (Adelabu et al., 2014; Bhattarai et al., 2020). Even though it is a crucial band for forecasting damage, it had not been very successful at the tree level until the development of a sensor with shorter wavelength detection and higher spatial resolution, such as the WV-2 (Oumar and Mutanga, 2013).

4.2 Machine learning models to predict tree defoliation

A Random Forest and Neural Network classification model were evaluated for estimating tree health status to forecast defoliation levels (Vitale et al., 2014; Adelabu et al., 2015). In this study, model using a categorical defoliation classification and integrating VI's and tree height metrics had the more stable classification scores in the cross-validation. It is remarkable that both Random Forest and Neural Network classification models mixes DC2 and DC3 as production error. That might be related to the subjectivity of the visual field defoliation estimation. However, because there are few previous research using remote sensing to map defoliation in holm oak forests it's difficult to put these findings into context, although they were similar to those founded by Navarro-Cerrillo et al (2019) and other analysing spectral signatures of defoliation with broadband multi-spectral sensors showing overall accuracy ranged from 0.46 to 0.77 (Waser et al., 2014; Senf et al., 2017b). In this regard, distinguishing between defoliation levels of holm oak trees is challenging due to several bias such as the precision of the GPS measuring equipment or the co-registration of the WV-2 and airborne ALS data. Misclassifications can also arise when crown parts from a nearby tree with a different level of damage are mixed. Despite these limitations, the overall accuracy of the classification

is equivalent to or better than previous tree defoliation classification efforts in other tree habitats (Barnes et al., 2017; Coleman et al., 2018).

4.3 Defoliation mapping and site-specific responses

A defoliation map for a holm oak plantation was eventually created in this study (between 74 to 369 trees ha^{-1}). This allowed for the detection of defoliation levels along a gradient of species (including cork oak in some places) and environmental conditions at landscape level. To assist forest managers in establishing effective *Phytophthora* damage mitigation strategies, the spatial distribution of tree defoliation was mapped. The maps obtained showed a high potential for assessing the magnitude of holm oak decline in the entire area affected by fungal pathogens, as they agreed with the presence of differences in environmental variables that consistently explain defoliation levels at tree scale, such as slope, elevation, temperature, solar radiation, aspect and soil composition (Cardillo et al., 2018; Sánchez-Cuesta et al., 2020; Sánchez-Cuesta et al., in press, Chapter 3). On this plantation, aspect was the main criterium to select oak species. Cork oak was established in NE-N-NW faced-slopes, predominating low defoliation levels (DC1), although there was found a trend to increase defoliation in sites at the lower part of the slope and in areas of low slope, as well as in areas of higher solar radiation (SE-S-SW aspect). On the other hand, *Q. ilex* showed higher levels of defoliation in all orientations, with areas with gentle slopes (Fernández-Habas et al., 2019; Sánchez-Cuesta et al., in press, Chapter 3).

The methodology proposed on this study can be easily translated at large scale to other locations using public low density airborne LiDAR data (e.g., PNOA data) and high-resolution multispectral imagery (e.g., Pleiades). Based on remote sensing data, the maps will aid in the production of tree size defoliation maps in holm and cork oak forests. Also, the distinction between different defoliation levels in oak plantations could also be addressed for future cartographic oriented to pest management (Meng et al., 2018). This study has filled a significant knowledge gap in crown-scale spectral and structural defoliation severity assessment, setting the groundwork for systematically mapping defoliation severity across different scales, which is vital for forest management and ecological research (McDowell et al., 2015; Senf et al., 2017a). Our research shows that combining VI's and LiDAR measurements can help scale remotely sensed defoliation severity

measurements from individual trees to inter-stand scales. More research is needed to determine how much crown-scale defoliation contributed to the change in spectral reflectance of broadband multi-spectral sensors like Sentinel-2A on a inter stand basis (Hawryło et al., 2018; Zarco-Tejada et al., 2018) or hyperspectral sensors (Hornero et al., 2021).

5 Conclusions

Using a semi-automated classification methodology, this study used WV-2 vegetation indicators and ALS metrics as inputs into machine learning models to analyse crown defoliation on holm-cork oak plantations caused by soil-borne *Phytophthora*. This method enables for the generation of tree-scale defoliation maps with a high spatial resolution (0.5 m), which can be used to identify decline and tree mortality processes, as well as the environmental causes that contribute to them. Based on reliable knowledge about the spatial distribution of tree defoliation, forest managers can develop effective measures to restrict or reduce the future consequences of *Phytophthora* damage. Producing satellite-based maps spanning huge areas with less processing effort and more spectral information, reducing field data collection costs, and improving accuracy and applicability for management activities would all help to achieve this efficacy. These maps represent the spatial information needed to plan and carry out preventive and curative root rot interventions in large regions of oak woodlands that have been damaged by root rot.

6 References

Adelabu, S., Mutanga, O., Adam, E., 2015. Testing the reliability and stability of the internal accuracy assessment of random forest for classifying tree defoliation levels using different validation methods. Geocarto Int. 30, 810–821. https://doi.org/10.1080/10106049.2014.997303

Adelabu, S., Mutanga, O., Adam, E., 2014. Evaluating the impact of red-edge band from Rapideye image for classifying insect defoliation levels. ISPRS J. Photogramm. Remote Sens. 95, 34–41. https://doi.org/10.1016/j.isprsjprs.2014.05.013

Akinwande, M.O., Dikko, H.G., Samson, A., 2015. Variance Inflation Factor: As a Condition for the Inclusion of Suppressor Variable(s) in Regression Analysis. Open J. Stat. 05, 754. https://doi.org/10.4236/ojs.2015.57075

Allué, J.L., 1990. Atlas fitoclimático de España: taxonomías. Ministerio de Agricultura, Pesca y Alimentación, Instituto Nacional de Investigaciones Agrarias.

Barnes, C., Balzter, H., Barrett, K., Eddy, J., Milner, S., Suárez, J.C., 2017. Airborne laser scanning and tree crown fragmentation metrics for the assessment of *Phytophthora ramorum*

infected larch forest stands. For. Ecol. Manag. 404, 294–305. https://doi.org/10.1016/j.foreco.2017.08.052

Belgiu, M., Drăguţ, L., 2016. Random forest in remote sensing: A review of applications and future directions. ISPRS J. Photogramm. Remote Sens. 114, 24–31. https://doi.org/10.1016/j.isprsjprs.2016.01.011

Bhattarai, R., Rahimzadeh-Bajgiran, P., Weiskittel, A., MacLean, D.A., 2020. Sentinel-2 based prediction of spruce budworm defoliation using red-edge spectral vegetation indices. Remote Sens. Lett. 11, 777–786. https://doi.org/10.1080/2150704X.2020.1767824

Borlaf-Mena, I., Tanase, M.A., Gómez-Sal, A., 2019. Methods for tree cover extraction from high resolution orthophotos and airborne LiDAR scanning in Spanish dehesas. Rev. Teledetec. 17–32. https://doi.org/10.4995/raet.2019.11320

Brasier, C.M., 1996. *Phytophthora cinnamomi* and oak decline in southern Europe. Environmental constraints including climate change. Ann. Sci. For. 53, 347–358. https://doi.org/10.1051/forest:19960217

Brasier, C.M., Robredo, F., Ferraz, J.F.P., 1993. Evidence for *Phytophthora cinnamomi* involvement in Iberian oak decline. Plant Pathol. 42, 140–145. https://doi.org/10.1111/j.1365-3059.1993.tb01482.x

Cardillo, E., Acedo, A., Abad, E., 2018. Topographic effects on dispersal patterns of *Phytophthora cinnamomi* at a stand scale in a Spanish heathland. PLoS ONE 13. https://doi.org/10.1371/journal.pone.0195060

Carrasco Gotarredona, Á., Fernández Cancio, Á., Trapero Casas, A., López Pantoja, G., Sánchez Osorio, I., Ruiz Navarro, J.M., Jiménez Molina, J.J., Domínguez Nevado, L., Romero Martín, M. de los Á., Carbonero Muñoz, M.D., Sánchez Hernández, M.E., Lucas Caetano, P.C., Gil Hernández, P., Fernández Rebollo, P., Navarro Cerrillo, R.M., Sánchez de la Cuesta, R., Raposo Llobet, R., Rodríguez Reviriego, S., 2009. Procesos de Decaimiento Forestal (la Seca): Situación del Conocimiento, 1ª edición. ed. Consejería de Medio Ambiente, Córdoba, España.

Cavender-Bares, J., Gamon, J.A., Townsend, P.A. (Eds.), 2020. Remote Sensing of Plant Biodiversity. Springer Nature. https://doi.org/10.1007/978-3-030-33157-3

Coleman, T.W., Graves, A.D., Heath, Z., Flowers, R.W., Hanavan, R.P., Cluck, D.R., Ryerson, D., 2018. Accuracy of aerial detection surveys for mapping insect and disease disturbances in the United States. For. Ecol. Manag. 430, 321–336. https://doi.org/10.1016/j.foreco.2018.08.020

Conrad, O., Bechtel, B., Bock, M., Dietrich, H., Fischer, E., Gerlitz, L., Wehberg, J., Wichmann, V., Böhner, J., 2015. System for Automated Geoscientific Analyses (SAGA) v. 2.1.4. Geosci. Model Dev. 8, 1991–2007. https://doi.org/10.5194/gmd-8-1991-2015

Corcobado, T., Solla, A., Madeira, M.A., Moreno, G., 2013. Combined effects of soil properties and *Phytophthora cinnamomi* infections on *Quercus ilex* decline. Plant Soil 373, 403–413. https://doi.org/10.1007/s11104-013-1804-z

Damm, A., Paul-Limoges, E., Haghighi, E., Simmer, C., Morsdorf, F., Schneider, F.D., van der Tol, C., Migliavacca, M., Rascher, U., 2018. Remote sensing of plant-water relations: An overview and future perspectives. J. Plant Physiol., From aquaporin to ecosystem: Plants in the water cycle 227, 3–19. https://doi.org/10.1016/j.jplph.2018.04.012

de Sampaio e Paiva Camilo-Alves, C., da Clara, M.I.E., de Almeida Ribeiro, N.M.C., 2013. Decline of Mediterranean oak trees and its association with *Phytophthora cinnamomi*: a review. Eur. J. For. Res. 132, 411–432. https://doi.org/10.1007/s10342-013-0688-z

Duque-Lazo, J., Navarro-Cerrillo, R.M., van Gils, H., Groen, T.A., 2018. Forecasting oak decline caused by *Phytophthora cinnamomi* in Andalusia: Identification of priority areas for intervention. For. Ecol. Manag. 417, 122–136. https://doi.org/10.1016/j.foreco.2018.02.045

Duque-Lazo, J., van Gils, H., Groen, T.A., Navarro-Cerrillo, R.M., 2016. Transferability of species distribution models: The case of *Phytophthora cinnamomi* in Southwest Spain and Southwest Australia. Ecol. Model. 320, 62–70. https://doi.org/10.1016/j.ecolmodel.2015.09.019

Eichhorn, J., Roskams, P., Ferretti, M., Mues, V., Szepesi, A., 2016. Visual assessment of crown condition and damaging agents. Manual Part IV, in: Manual on Methods and Criteria for Harmonized Sampling, Assessment, Monitoring and Analysis of the Effects of Air Pollution on Forests. UNECE ICP Forests Programme Co-ordinating Centre, Eberswalde, Germany, p. 49.

Erikson, M., Olofsson, K., 2005. Comparison of three individual tree crown detection methods. Mach. Vis. Appl. 16, 258–265. https://doi.org/10.1007/s00138-005-0180-y

Fernández-Habas, J., Fernández-Rebollo, P., Casado, M.R., García Moreno, A.M., Abellanas, B., 2019. Spatio-temporal analysis of oak decline process in open woodlands: A case study in SW Spain. J. Environ. Manage. 248, 109308. https://doi.org/10.1016/j.jenvman.2019.109308

Ferretti, M., König, N., Granke, O., 2016. Quality assurance within the ICP forests monitoring programme. Manual Part III, in: Manual on Methods and Criteria for Harmonized Sampling, Assessment, Monitoring and Analysis of the Effects of Air Pollution on Forests. UNECE ICP Forests Programme Co-ordinating Centre, Eberswalde, Germany, p. 10.

Ferretti, M., Sánchez Peña, G., Economou, A., Beccu, E., Canu, G., Cocco, S., Bussotti, F., Cenni, E., Cozzi, A., Conceição Andrada, M., 1994. Especies forestales mediterráneas: guía para la evalución de las copas, CEC-UN/ECE. ed. LINNAEA ambiente Srl, Bruselas, Ginebra.

Hall, R.J., Castilla, G., White, J.C., Cooke, B.J., Skakun, R.S., 2016. Remote sensing of forest pest damage: a review and lessons learned from a Canadian perspective. Can. Entomol. 148, S296–S356. https://doi.org/10.4039/tce.2016.11

Hawryło, P., Bednarz, B., Wężyk, P., Szostak, M., 2018. Estimating defoliation of Scots pine stands using machine learning methods and vegetation indices of Sentinel-2. Eur. J. Remote Sens. 51, 194–204. https://doi.org/10.1080/22797254.2017.1417745

Hernández-Clemente, R., Hornero, A., Mottus, M., Penuelas, J., González-Dugo, V., Jiménez, J.C., Suárez, L., Alonso, L., Zarco-Tejada, P.J., 2019. Early Diagnosis of Vegetation Health From High-Resolution Hyperspectral and Thermal Imagery: Lessons Learned From Empirical Relationships and Radiative Transfer Modelling. Curr. For. Rep. 5, 169–183. https://doi.org/10.1007/s40725-019-00096-1

Holmgren, J., Persson, Å., Söderman, U., 2008. Species identification of individual trees by combining high resolution LiDAR data with multi-spectral images. Int. J. Remote Sens. 29, 1537–1552. https://doi.org/10.1080/01431160701736471

Hornero, A., Zarco-Tejada, P.J., Quero, J.L., North, P.R.J., Ruiz-Gómez, F.J., Sánchez-Cuesta, R., Hernandez-Clemente, R., 2021. Modelling hyperspectral- and thermal-based plant traits for the early detection of *Phytophthora*-induced symptoms in oak decline. Remote Sens. Environ. 263, 112570. https://doi.org/10.1016/j.rse.2021.112570

Hunt, E.R., Doraiswamy, P.C., McMurtrey, J.E., Daughtry, C.S.T., Perry, E.M., Akhmedov, B., 2013. A visible band index for remote sensing leaf chlorophyll content at the canopy scale. Int. J. Appl. Earth Obs. Geoinformation 21, 103–112. https://doi.org/10.1016/j.jag.2012.07.020

Isenburg, M., 2021. LAStools: efficient LiDAR processing software. LAStools.

Jakubowski, M.K., Li, W., Guo, Q., Kelly, M., 2013. Delineating Individual Trees from Lidar Data: A Comparison of Vector- and Raster-based Segmentation Approaches. Remote Sens. 5, 4163–4186. https://doi.org/10.3390/rs5094163

Jung, T., Orlikowski, L., Henricot, B., Abad-Campos, P., Aday, A.G., Casal, O.A., Bakonyi, J., Cacciola, S.O., Cech, T., Chavarriaga, D., Corcobado, T., Cravador, A., Decourcelle, T., Denton, G., Diamandis, S., Doğmuş-Lehtijärvi, H.T., Franceschini, A., Ginetti, B., Green, S., Glavendekić, M., Hantula, J., Hartmann, G., Herrero, M., Ivic, D., Jung, M.H., Lilja, A., Keca, N., Kramarets,

V., Lyubenova, A., Machado, H., Lio, G.M. di S., Vázquez, P.J.M., Marçais, B., Matsiakh, I., Milenkovic, I., Moricca, S., Nagy, Z.Á., Nechwatal, J., Olsson, C., Oszako, T., Pane, A., Paplomatas, E.J., Varela, C.P., Prospero, S., Martínez, C.R., Rigling, D., Robin, C., Rytkönen, A., Sánchez, M.E., Ros, A.V.S., Scanu, B., Schlenzig, A., Schumacher, J., Slavov, S., Solla, A., Sousa, E., Stenlid, J., Talgø, V., Tomic, Z., Tsopelas, P., Vannini, A., Vettraino, A.M., Wenneker, M., Woodward, S., Peréz-Sierra, A., 2016. Widespread *Phytophthora* infestations in European nurseries put forest, semi-natural and horticultural ecosystems at high risk of Phytophthora diseases. For. Pathol. 46, 134–163. https://doi.org/10.1111/efp.12239

Kälin, U., Lang, N., Hug, C., Gessler, A., Wegner, J.D., 2019. Defoliation estimation of forest trees from ground-level images. Remote Sens. Environ. 223, 143–153. https://doi.org/10.1016/j.rse.2018.12.021

Khosravipour, A., Skidmore, A.K., Isenburg, M., Wang, T., Hussin, Y.A., 2014. Generating Pit-free Canopy Height Models from Airborne Lidar. Photogramm. Eng. Remote Sens. 80, 863–872. https://doi.org/10.14358/PERS.80.9.863

Kuhn, M., 2008. Building Predictive Models in R Using the caret Package. J. Stat. Softw. 28, 1–26. https://doi.org/10.18637/jss.v028.i05

Kukunda, C.B., Duque-Lazo, J., González-Ferreiro, E., Thaden, H., Kleinn, C., 2018. Ensemble classification of individual *Pinus* crowns from multispectral satellite imagery and airborne LiDAR. Int. J. Appl. Earth Obs. Geoinformation 65, 12–23. https://doi.org/10.1016/j.jag.2017.09.016

Lamonaca, A., Corona, P., Barbati, A., 2008. Exploring forest structural complexity by multi-scale segmentation of VHR imagery. Remote Sens. Environ. 112, 2839–2849. https://doi.org/10.1016/j.rse.2008.01.017

Lausch, A., Erasmi, S., King, D.J., Magdon, P., Heurich, M., 2017. Understanding Forest Health with Remote Sensing-Part II—A Review of Approaches and Data Models. Remote Sens. 9, 129. https://doi.org/10.3390/rs9020129

Lausch, A., Erasmi, S., King, D.J., Magdon, P., Heurich, M., 2016. Understanding Forest Health with Remote Sensing -Part I—A Review of Spectral Traits, Processes and Remote-Sensing Characteristics. Remote Sens. 8, 1029. https://doi.org/10.3390/rs8121029

Li, W., Guo, Q., Jakubowski, M.K., Kelly, M., 2012. A New Method for Segmenting Individual Trees from the Lidar Point Cloud. Photogramm. Eng. Remote Sens. 78, 75–84. https://doi.org/10.14358/PERS.78.1.75

Liang, L., Huang, T., Di, L., Geng, D., Yan, J., Wang, S., Wang, L., Li, L., Chen, B., Kang, J., 2020. Influence of Different Bandwidths on LAI Estimation Using Vegetation Indices. IEEE J. Sel. Top. Appl. Earth Obs. Remote Sens. 13, 1494–1502. https://doi.org/10.1109/JSTARS.2020.2984608

Liaw, A., Wiener, M., 2002. Classification and Regression by RandomForest. R News 2/3, 18–22.

Martín, D., Vázquez-Piqué, J., Fernández, M., Alejano, R., 2014. Effect of ecological factors on intra-annual stem girth increment of holm oak. Trees 28, 1367–1381. https://doi.org/10.1007/s00468-014-1041-y

Matthew, M.W., Adler-Golden, S.M., Berk, A., Richtsmeier, S.C., Levine, R.Y., Bernstein, L.S., Acharya, P.K., Anderson, G.P., Felde, G.W., Hoke, M.L., Ratkowski, A.J., Burke, H.K., Kaiser, R.D., Miller, D.P., 2000. Status of atmospheric correction using a MODTRAN4-based algorithm, in: Algorithms for Multispectral, Hyperspectral, and Ultraspectral Imagery VI. Presented at the Algorithms for Multispectral, Hyperspectral, and Ultraspectral Imagery VI, SPIE, pp. 199–207. https://doi.org/10.1117/12.410341

McDowell, N.G., Coops, N.C., Beck, P.S.A., Chambers, J.Q., Gangodagamage, C., Hicke, J.A., Huang, C., Kennedy, R., Krofcheck, D.J., Litvak, M., Meddens, A.J.H., Muss, J., Negrón-Juarez, R., Peng, C., Schwantes, A.M., Swenson, J.J., Vernon, L.J., Williams, A.P., Xu, C., Zhao, M.,

Running, S.W., Allen, C.D., 2015. Global satellite monitoring of climate-induced vegetation disturbances. Trends Plant Sci. 20, 114–123. https://doi.org/10.1016/j.tplants.2014.10.008

McGaughey, R.J., 2014. FUSION/LDV: Software for LiDAR Data Analysis and Visualization. Washington: USDA, Forest Service, Pacific Northwest Research Station.

Meng, R., Dennison, P.E., Zhao, F., Shendryk, I., Rickert, A., Hanavan, R.P., Cook, B.D., Serbin, S.P., 2018. Mapping canopy defoliation by herbivorous insects at the individual tree level using bi-temporal airborne imaging spectroscopy and LiDAR measurements. Remote Sens. Environ. 215, 170–183. https://doi.org/10.1016/j.rse.2018.06.008

Myneni, R.B., Williams, D.L., 1994. On the relationship between FAPAR and NDVI. Remote Sens. Environ. 49, 200–211. https://doi.org/10.1016/0034-4257(94)90016-7

Nakajima, H., Kume, A., Ishida, M., Ohmiya, T., Mizoue, N., 2011. Evaluation of estimates of crown condition in forest monitoring: comparison between visual estimation and automated crown image analysis. Ann. For. Sci. 68, 1333–1340. https://doi.org/10.1007/s13595-011-0132-9

Navarro Cerrillo, R.M., Pemán García, J., del Campo García, A.D., Moreno Sánchez, J., Lara Gómez, M.A., Díaz Hernández, J.L., Pousa Salvador, F., Piñón Castillo, F.M., 2009. Manual de especies para la forestación de tierras agrarias en Andalucía. Junta de Andalucía. Consejería de Agricultura y Pesca, Sevilla (Spain).

Navarro-Cerrillo, R.M., Varo-Martínez, M.Á., Acosta, C., Palacios Rodriguez, G., Sánchez-Cuesta, R., Ruiz Gómez, F.J., 2019. Integration of WorldView-2 and airborne laser scanning data to classify defoliation levels in *Quercus ilex* L. Dehesas affected by root rot mortality: Management implications. For. Ecol. Manag. 451, 117564. https://doi.org/10.1016/j.foreco.2019.117564

Otsu, K., Pla, M., Vayreda, J., Brotons, L., 2018. Calibrating the Severity of Forest Defoliation by Pine Processionary Moth with Landsat and UAV Imagery. Sensors 18, 3278. https://doi.org/10.3390/s18103278

Oumar, Z., Mutanga, O., 2013. Using WorldView-2 bands and indices to predict bronze bug (*Thaumastocoris peregrinus*) damage in plantation forests. Int. J. Remote Sens. 34, 2236–2249. https://doi.org/10.1080/01431161.2012.743694

R Development Core Team, 2017. R: A language and environment for statistical computing. R Foundation for Statistical Computing, Vienna, Austria. 2016.

Ruiz-Gómez, F.J., Navarro-Cerrillo, R.M., Pérez-de-Luque, A., Oβwald, W., Vannini, A., Morales-Rodríguez, C., 2019. Assessment of functional and structural changes of soil fungal and oomycete communities in holm oak declined dehesas through metabarcoding analysis. Sci. Rep. 9, 5315. https://doi.org/10.1038/s41598-019-41804-y

Sánchez, M.E., Caetano, P., Ferraz, J., Trapero, A., 2002. *Phytophthora* disease of *Quercus ilex* in south-western Spain. For. Pathol. 32, 5–18. https://doi.org/10.1046/j.1439-0329.2002.00261.x

Sánchez, M.E., Caetano, P., Romero, M.A., Navarro, R.M., Trapero, A., 2006. *Phytophthora* root rot as the main factor of oak decline in southern Spain, in: Proceedings of the Third International IUFRO Working Party S07.02.09. Presented at the Progress in research on Phytophthora diseases of forest trees, Forest Research, Freising (Germany).

Sánchez-Cuesta, R., Navarro-Cerrillo, R.M., Quero, J.L., Ruiz-Gómez, F.J., 2020. Small-Scale Abiotic Factors Influencing the Spatial Distribution of *Phytophthora cinnamomi* under Declining Quercus ilex Trees. Forests 11, 375. https://doi.org/10.3390/f11040375

Senf, C., Campbell, E.M., Pflugmacher, D., Wulder, M.A., Hostert, P., 2017a. A multi-scale analysis of western spruce budworm outbreak dynamics. Landsc. Ecol. 32, 501–514. https://doi.org/10.1007/s10980-016-0460-0

Senf, C., Seidl, R., Hostert, P., 2017b. Remote sensing of forest insect disturbances: Current state and future directions. Int. J. Appl. Earth Obs. Geoinformation 60, 49–60. https://doi.org/10.1016/j.jag.2017.04.004

Shao, Gang, Shao, Guofan, Fei, S., 2019. Delineation of individual deciduous trees in plantations with low-density LiDAR data. Int. J. Remote Sens. 40, 346–363. https://doi.org/10.1080/01431161.2018.1513664

Shendryk, I., Broich, M., Tulbure, M.G., McGrath, A., Keith, D., Alexandrov, S.V., 2016. Mapping individual tree health using full-waveform airborne laser scans and imaging spectroscopy: A case study for a floodplain eucalypt forest. Remote Sens. Environ. 187, 202–217. https://doi.org/10.1016/j.rse.2016.10.014

Stereńczak, K., Mielcarek, M., Modzelewska, A., Kraszewski, B., Fassnacht, F.E., Hilszczański, J., 2019. Intra-annual *Ips typographus* outbreak monitoring using a multi-temporal GIS analysis based on hyperspectral and ALS data in the Białowieża Forests. For. Ecol. Manag. 442, 105–116. https://doi.org/10.1016/j.foreco.2019.03.064

Stone, C., Mohammed, C., 2017. Application of Remote Sensing Technologies for Assessing Planted Forests Damaged by Insect Pests and Fungal Pathogens: a Review. Curr. For. Rep. 3, 75–92. https://doi.org/10.1007/s40725-017-0056-1

Tuominen, J., Lipping, T., Kuosmanen, V., Haapanen, R., 2009. Remote sensing of forest health, in: Ho, P.G. (Ed.), Geoscience and Remote Sensing. IntechOpen, Zagreb (Croatia), pp. 29–52.

Tuset, J.J., Hinarejos, C., Mira, J.L., Cobos, J.M., 1996. Implicación de *Phytophthora cinnamomi* Rands en la enfermedad de la "seca" de encinas y alcornoques. Bol. Sanid. Veg. Plagas 22, 491–499.

Varo-Martínez, M.Á., Navarro-Cerrillo, R.M., 2021. Stand Delineation of *Pinus sylvestris* L. Plantations Suffering Decline Processes Based on Biophysical Tree Crown Variables: A Necessary Tool for Adaptive Silviculture. Remote Sens. 13, 436. https://doi.org/10.3390/rs13030436

Vauhkonen, J., Maltamo, M., McRoberts, R.E., Næsset, E., 2014. Introduction to Forestry Applications of Airborne Laser Scanning, in: Maltamo, M., Næsset, E., Vauhkonen, J. (Eds.), Forestry Applications of Airborne Laser Scanning: Concepts and Case Studies, Managing Forest Ecosystems. Springer Netherlands, Dordrecht, pp. 1–16. https://doi.org/10.1007/978-94-017-8663-8_1

Venables, W.N., Ripley, B.D., 2002. Modern Applied Statistics with S, Fourth. ed, Statistics and Computing. Springer, New York.

Vettraino, A.M., Barzanti, G.P., Bianco, M.C., Ragazzi, A., Capretti, P., Paoletti, E., Luisi, N., Anselmi, N., Vannini, A., 2002. Occurrence of *Phytophthora* species in oak stands in Italy and their association with declining oak trees. For. Pathol. 32, 19–28. https://doi.org/10.1046/j.1439-0329.2002.00264.x

Vitale, M., Proietti, C., Cionni, I., Fischer, R., De Marco, A., 2014. Random Forests Analysis: a Useful Tool for Defining the Relative Importance of Environmental Conditions on Crown Defoliation. Water. Air. Soil Pollut. 225, 1992. https://doi.org/10.1007/s11270-014-1992-z

Waser, L.T., Küchler, M., Jütte, K., Stampfer, T., 2014. Evaluating the Potential of WorldView-2 Data to Classify Tree Species and Different Levels of Ash Mortality. Remote Sens. 6, 4515–4545. https://doi.org/10.3390/rs6054515

Zarco-Tejada, P.J., Hornero, A., Hernández-Clemente, R., Beck, P.S.A., 2018. Understanding the temporal dimension of the red-edge spectral region for forest decline detection using high-resolution hyperspectral and Sentinel-2a imagery. ISPRS J. Photogramm. Remote Sens. 137, 134–148. https://doi.org/10.1016/j.isprsjprs.2018.01.017

Zhu, C., Zhang, X., Zhang, N., Hassan, M.A., Zhao, L., 2018. Assessing the Defoliation of Pine Forests in a Long Time-Series and Spatiotemporal Prediction of the Defoliation Using Landsat Data. Remote Sens. 10, 360. https://doi.org/10.3390/rs10030360

Zou, X., Haikarainen, I., Haikarainen, I.P., Mäkelä, P., Mõttus, M., Pellikka, P., 2018. Effects of Crop Leaf Angle on LAI-Sensitive Narrow-Band Vegetation Indices Derived from Imaging Spectroscopy. Appl. Sci. 8, 1435. https://doi.org/10.3390/app8091435

Capítulo 6

Discusión general

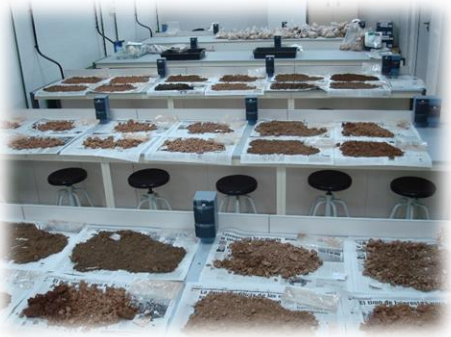

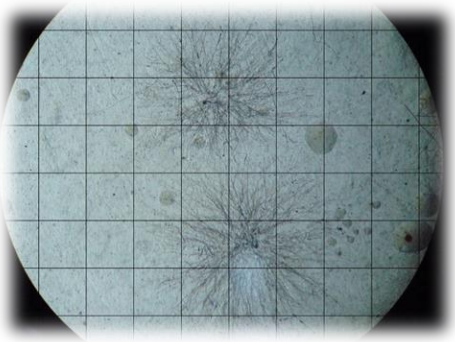

1 Discusión general

La gestión de los sistemas forestales afectados por procesos de decaimiento se ha convertido en uno de los grandes retos del siglo XXI, principalmente por la heterogeneidad de los factores implicados y la complejidad de su influencia en la dinámica y evolución del arbolado, lo que a su vez, condiciona el aprovechamiento y la sostenibilidad económica en el ecosistema (Trumbore et al., 2015; Simler-Williamson et al., 2019). Este proceso de decaimiento es especialmente relevante en los sistemas forestales mediterráneos, y más concretamente en los sistemas de dehesa de *Quercus* del sur de la Península Ibérica. En ellos no sólo interactúan factores como el cambio climático, la degradación de suelos o la introducción de especies invasoras o patógenos, factores que afectan a los sistemas forestales a nivel global, sino que, de una manera especial, lo hace el manejo histórico, de forma cada vez más pronunciada (Carrasco Gotarredona et al., 2009; Gea-Izquierdo et al., 2013; Duque-Lazo et al., 2018b).

Desde que se dio a conocer, en los años 80, el problema de *la Seca* en las dehesas de Andalucía, han sido muchos los esfuerzos realizados en el ámbito de la investigación, las prácticas culturales, las técnicas de gestión y, en definitiva, del manejo integral de la enfermedad, así como en el diagnóstico y control de los procesos de decaimiento, las plagas y las enfermedades asociadas, junto con el resto de los factores bióticos y abióticos involucrados. Entre otros aspectos, se ha profundizado en el estudio de los factores contribuyentes y desencadenantes, identificando al oomiceto de podredumbre de raíz *Phytophthora cinnamomi*, como causante de los episodios más graves de mortalidad del arbolado (Brasier, 1996; Sánchez et al., 2002). A pesar de la implicación que existe en los procesos de podredumbre de la raíz de la encina y el alcornoque, de otros oomicetos de los géneros *Phytophthora* spp. y *Pythium* spp. (Corcobado et al., 2010; Pérez-Sierra et al., 2013; Ruiz-Gómez et al., 2019a), y de que su proceso de dispersión e infección es muy parecido entre estos patógenos (Oßwald et al., 2014), *P. cinnamomi* está considerado como el patógeno que provoca los daños más graves en el sistema radicular absorbente de sus huéspedes (Sánchez et al., 2005; Moralejo et al., 2009) y es, por tanto, el organismo sobre el que se han focalizado las principales investigaciones en el conocimiento del decaimiento de la encina y el alcornoque. Así por ejemplo se ha avanzado en el estudio de la interacción entre el oomiceto y el huésped – *Q. ilex* y *Q. suber* – (Cahill, 1989; Ruiz-Gómez et al., 2015) y con otros agentes

presentes en el entorno (Corcobado et al., 2014; Ruiz-Gómez et al., 2019a), profundizando en la ecofisiología de la interacción (Ruiz-Gómez et al., 2018) o en los tratamientos de control de la podredumbre (Serrano et al., 2012; Ríos et al., 2017).

Estos trabajos han ido ofreciendo información sobre la forma en que los factores bióticos y abióticos influyen sobre el patógeno y condicionan sus patrones de distribución espacial en el suelo, a diferentes escalas espaciotemporales y, por tanto, mostrando su relevancia en el estado de salud del arbolado, constituyendo la base general de la presente Tesis Doctoral. En esta, se muestra cómo la ocurrencia del oomiceto en el suelo depende, a escala de árbol, de rodal, o de región, de factores abióticos (ej., las propiedades fisicoquímicas del suelo, la topografía del terreno, la humedad del suelo, la radiación solar, y de los eventos climáticos) y factores bióticos (ej., la presencia y el estado fitosanitario de sus huéspedes, y la vegetación) condicionando la distribución espacial del patógeno en la zona de influencia de sus huéspedes.

2 Influencia de los factores abióticos edáficos y topográficos en la distribución espacial de *P. cinnamomi*

2.1 Características fisicoquímicas del suelo

La variabilidad de las características fisicoquímicas y del contenido de humedad de los suelos puede condicionar la presencia o ausencia de oomicetos patógenos de podredumbre radical (*Phytophthora* spp., y *Pythium* spp.), así como alterar sus ciclos biológicos y su nivel de patogenicidad pasando de estado latente a infectivo (Oßwald et al., 2014). De esta forma, tanto a pequeña escala bajo la influencia de la proyección de la copa individual de encinas jóvenes de 15 años de edad (***Capítulo 2***), como a escala de una forestación de encinas y alcornoques, en el mismo área de estudio (***Capítulo 3***), usando técnicas de Análisis Espacial mediante Índices de Distancias (SADIE), Modelos Lineales Generalizados Mixtos (GLMMs) y Modelos de Ecuaciones Estructurales (SEM), se observó una correlación entre los patrones de distribución espacial de algunas propiedades y nutrientes del suelo (texturas finas, P, N, pH, K, la materia orgánica y la humedad). Estas características pueden ser a su vez influenciadas por la presencia y estructura del dosel arbóreo (Gallardo, 2003; Gea-Izquierdo et al., 2010; Simón et al., 2013; Andivia et al., 2015). En cualquier caso, la presencia agregada en la rizosfera de las unidades formadoras de colonia (ufc), a nivel de árbol (Figura 1a) y de forestación (Figura 1b) de estos

patógenos de podredumbre radical coincidió con agregaciones de estos factores, confirmando en particular algunas observaciones previas sobre el comportamiento del inóculo ante el cambio de determinadas características evaluadas de forma individual (Sánchez et al., 2002; Gómez-Aparicio et al., 2012).

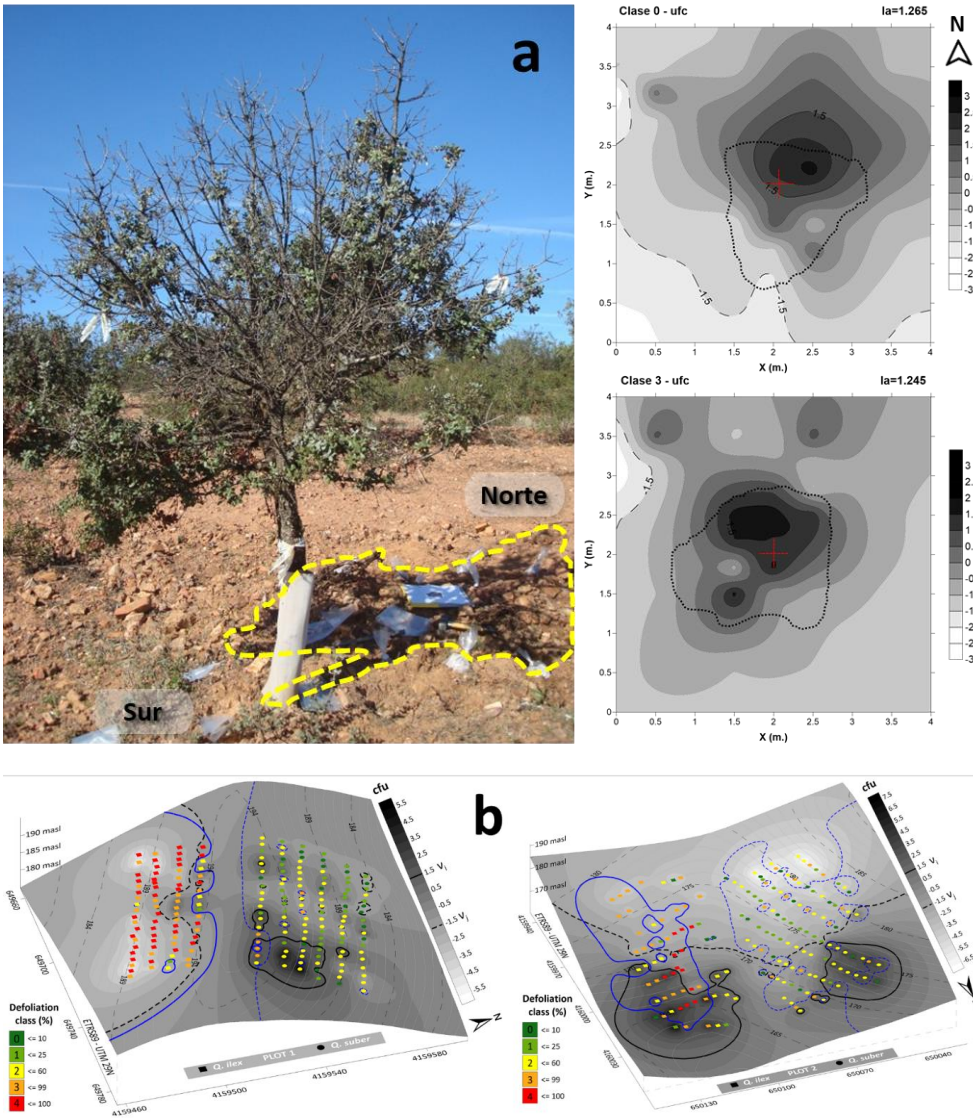

Figura 1. Condiciones favorables de micrositio para *P. cinnamomi* en las orientaciones norte, (a) bajo la influencia de la encina (*Capítulo 2*) y (b) en la forestación (*Capítulo 3*).

La agregación de ciertos nutrientes en el suelo, como el N, el P y el K, o la presencia de materia orgánica en el área de influencia de los árboles y su sistema radical, es el resultado de la actividad biológica de las raíces, las micorrizas, el agua y del resto de microorganismos del suelo, a través de los procesos biológicos y fisicoquímicos del suelo y la mineralización de dichos elementos, así como el efecto de lixiviación que se produce desde las copas de los árboles hasta el suelo (Gallardo, 2003; Shen et al., 2011; Delgado-Baquerizo et al., 2013; Sardans y Peñuelas, 2013; Satyaprakash et al., 2017), generando un microambiente en el área de influencia de la proyección de la copa de los árboles y su sistema radical, que permita a los oomicetos completar su ciclo biológico e infectivo en dicho área. De este modo, las interacciones entre los diferentes elementos del patosistema modelan el entorno propiciando mayores intensidades del efecto del patógeno sobre los huéspedes (Figura 2).

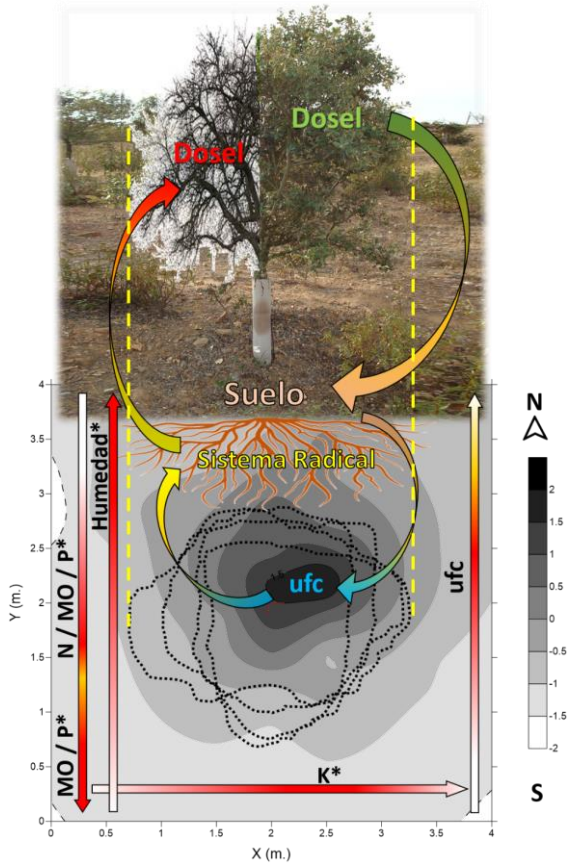

Figura 2. Esquema general de las interacciones, a nivel de árbol, en el patosistema *P. cinnamomi* – *Q. ilex* – ambiente. Flechas curvas: sentido de la influencia entre los componentes del sistema. Flechas rectas: sentido y zona de concentración (rojo) de la variable (* diferencias significativas entre dentro y fuera de la proyección de la copa [líneas discontinuas]).

Por otro lado, a partir del estudio de las parcelas de *Quercus* spp. de la Red SEDA con presencia de *P. cinnamomi* (***Capítulo 4***), se observó que las parcelas con mayor contenido de materia orgánica presentaron mayor mortalidad de árboles que aquellas no infestadas (Figura 3). Esto concuerda con la relación encontrada en los anteriores capítulos (*capítulo 2* y *capítulo 3*), donde los patrones de agregación de la materia orgánica se relacionaban con los de abundancia de ufc de oomicetos en el suelo.

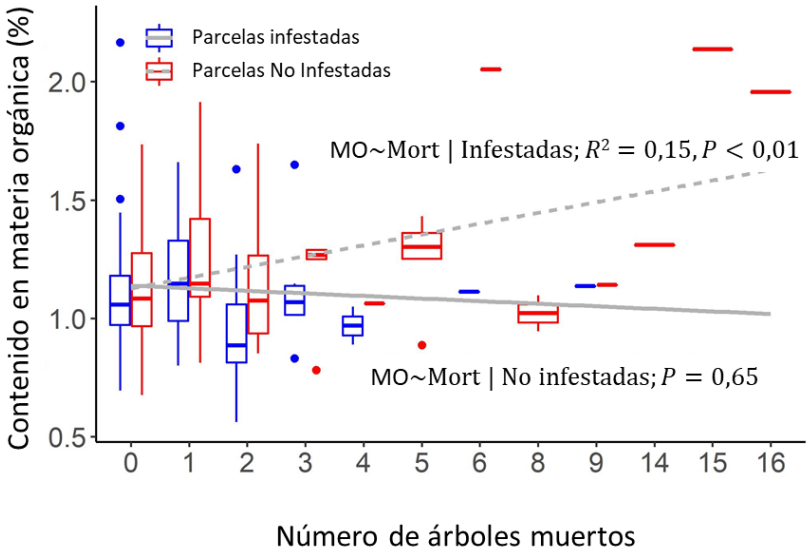

Figura 3. Distribución en Diagrama de cajas del contenido de Materia Orgánica en parcelas con y sin infestación y eventos de mortalidad acumulada en cada parcela durante el periodo de estudio (2001-2016) de las parcelas de la Red SEDA en Andalucía.

Estudios previos han mostrado que los suelos con mayor contenido en materia orgánica tienen tendencia a ser más ácidos, y con mayor capacidad de retención de humedad, condiciones que favorecen a *P. cinnamomi* y su capacidad infectiva (Serrano et al., 2012; Corcobado et al., 2013; de Sampaio e Paiva Camilo-Alves et al., 2013). Así mismo, en años con mayor precipitación, las parcelas infestadas mostraron mayores niveles de defoliación que las no infestadas, lo que favorece las condiciones para que el patógeno aumente la probabilidad de esporulación y dispersión infestando un mayor número de raíces finas y causando daños más graves al arbolado (Hardham, 2005). Los modelos a escala regional confirmaron estas hipótesis, coincidiendo los patrones de defoliación y mortalidad en el área de distribución de la dehesa con gradientes claros en estas dos características, entre otras (Figura 4).

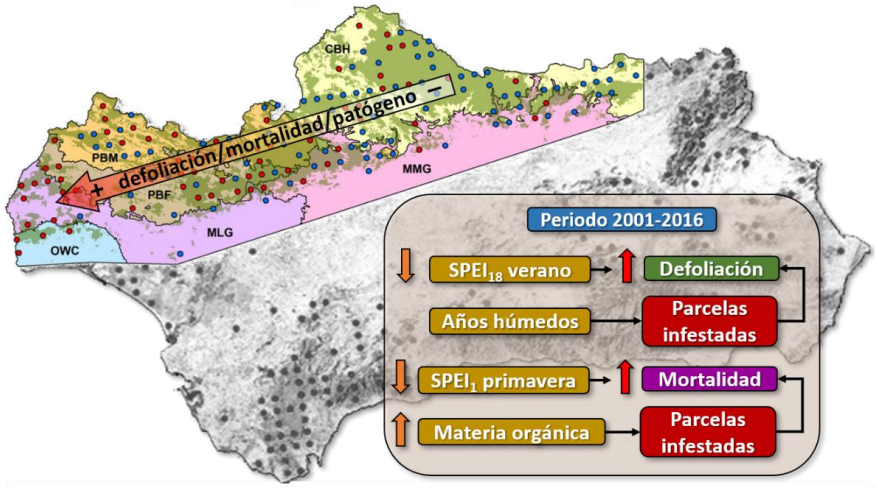

Figura 4. Tendencias regionales de los principales drivers asociados a mortalidad y defoliación del arbolado en las dehesas andaluzas.

2.2 Influencia de la topografía

Las variaciones altitudinales y de exposición del paisaje conforman relieves muy heterogéneos en unidades ecológicas y administrativas a escala de rodal, bosque, masa forestal, plantación o explotación. Los cambios de desnivel, exposición o de pendiente en el terreno, dan lugar a variaciones topográficas que condicionan la radiación solar y el régimen hídrico a escala de micrositio. Esto, unido a la composición fisicoquímica del suelo, conforma la presencia de microcuencas con capacidades de retención de agua diferentes y condiciones edáficas diferenciadoras que modulan tanto el comportamiento de *P. cinnamomi* como la fisiología de las masas forestales frente a la disponibilidad del agua y de los nutrientes del suelo, y por tanto su influencia en la idoneidad del ecosistema hacia el patógeno (Moreira y Martins, 2005; Cardillo et al., 2018; Sena et al., 2018; Fernández-Habas et al., 2019). A este respecto, las zonas con elevada concentración de ufc de patógenos de podredumbre radical en las parcelas de la forestación de encinas y alcornoques de la finca de Campo Baldío (***Capítulo 3***), se caracterizaron por estar situadas en zonas con menor pendiente, exposición norte y menores niveles de radiación solar, condiciones que están en consonancia con los resultados obtenidos a nivel de microescala de árbol (***Capítulo 2***), donde la tendencia a presentar mayor concentración de ufc bajo la copa de las encinas fue en la zona norte de influencia del árbol, con menor incidencia solar y condiciones micro climáticas más favorables (Figura 5).

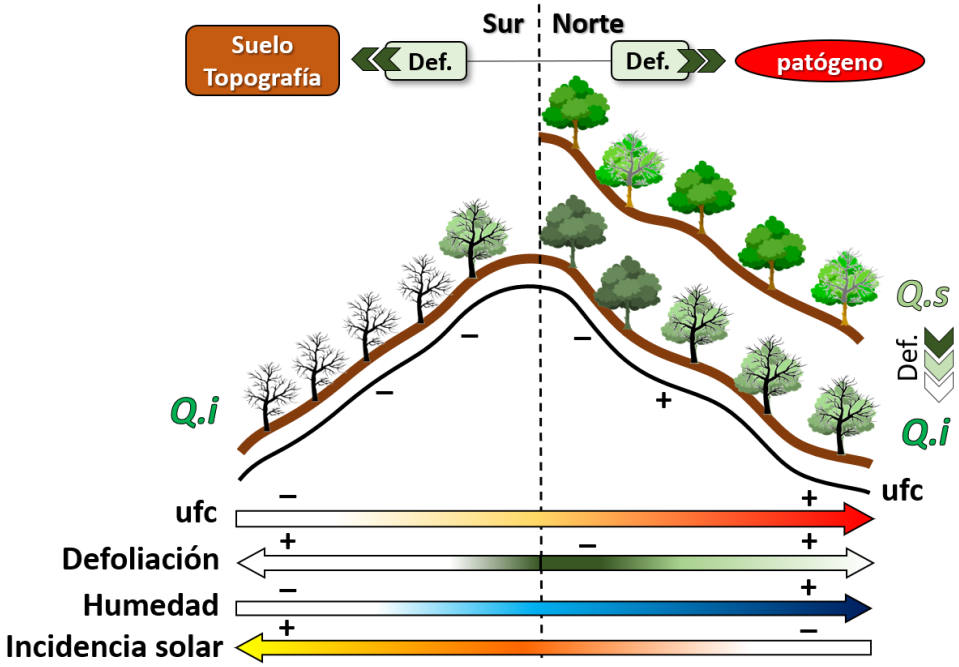

Figura 5. Distribución espacial de las unidades formadoras de colonia (cfu), la defoliación y las variables abióticas más destacadas, según el relieve y la topografía en la reforestación de encinas y alcornoques de Campo Baldío (Puebla de Guzmán – Huelva). Las flechas indican sentido y zona de concentración de las variables a lo largo del perfil.

Estos resultados son consistentes con el efecto de agregación del patógeno bajo la copa de encinas y alcornoques observado en los *Capítulos 2* y *3* (Figura 1), así como en otros trabajos (Gallardo, 2003; Gea-Izquierdo et al., 2010; Andivia et al., 2015).

La defoliación y la mortalidad de las encinas situadas en orientación sur (P_1Qi) dentro de la forestación (***Capítulo 3***), parecen estar relacionadas con un efecto acumulativo de la escasa capacidad de retención de agua del terreno y la mayor incidencia solar, pero con menor presencia del patógeno en el suelo que en el resto de las subparcelas, en el momento del muestreo. Por el contrario, en las áreas de orientación norte, con mayor compensación hídrica, los valores de defoliación y de mortalidad se relacionaron con una mayor agregación del patógeno, asociada a la menor incidencia solar y a la mayor humedad del suelo. Estos datos concuerdan con los diferentes niveles de defoliación observados a escala de forestación (***Capítulo 5***), donde los patrones de daños siguen las mismas tendencias, condicionadas por la topografía del terreno (Figura 6).

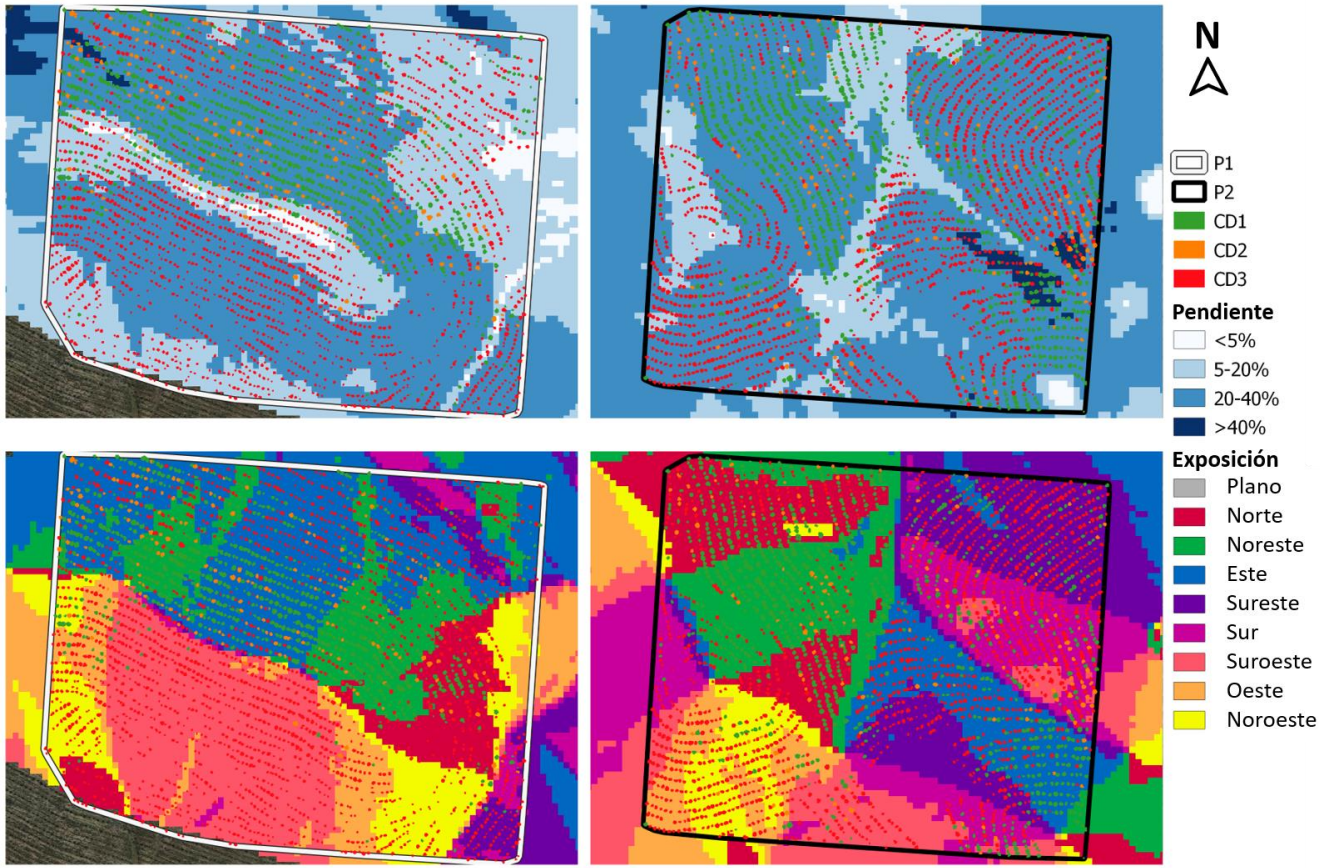

Figura 6. Mapa de pendientes y orientaciones de la forestación de Campo Baldío (Puebla de Guzmán - Huelva), con la clasificación de defoliación (CD) del arbolado (*Q. ilex – Q. suber*)

3 Influencia de la presencia de huéspedes en la densidad de ufc en suelo

La presencia de especies vegetales, su fisiológica y susceptibilidad a un determinado patógeno de raíces, suponen una cierta garantía para que el parásito sobreviva y se propague completando su ciclo biológico. Esto, a su vez, viene modulado por la plasticidad de otros rasgos ecológicos clave del patógeno, como el rango de hospedadores, la estrategia de dispersión, la capacidad saprofítica y de latencia en periodos y condiciones desfavorables, la cantidad de "sustrato huésped" susceptible (raíces finas), la presencia y actividad de los antagonistas y los requisitos climáticos y ecológicos (temperatura, humedad y pH) necesarios para su crecimiento y supervivencia en el medio en el que habita (Termorshuizen, 2014; Ruiz-Gómez et al., 2019a). La escasa biodiversidad vegetal y microbiana que albergan las forestaciones monoespecíficas de tierras agrarias, y la limitada fertilidad y de materia orgánica de sus suelos, pueden actuar como un potenciador de los daños ocasionados por la podredumbre radical sobre las especies vegetales susceptibles, aumentando su nivel de defoliación (Pollastrini et al., 2016).

En el caso de estudio de esta Tesis (***Capítulos 2, 3 y 5***), se han seleccionado forestaciones de encina y alcornoque, con presencia dispersa de cobertura arbustiva de jara pringosa (*Cistus ladanifer* L.), susceptible al patógeno, (Moreira y Martins, 2005). Este estrato vegetal supone un reservorio y medio de propagación de la enfermedad por toda la plantación, a través del entramado de raíces finas que alberga la rizosfera, más allá de la propia área de influencia de la proyección de copa de los árboles. Cuando el efecto del patógeno de podredumbre radical, en combinación con las condiciones ecológicas limitantes que se observan en muchas forestaciones de tierras agrarias, afectan de forma genérica a las especies forestales, se puede provocar el colapso de gran parte del sistema arbóreo debido a la pudrición generalizada del sistema secundario de raíces, limitando su acceso a los recursos hídricos y nutricionales, y generando un incremento en la defoliación de las copas y en la radiación solar directa sobre el suelo bajo la proyección de las mismas, generando, en muchas ocasiones, la muerte de los árboles (***Capítulo 3 y 5***). Este proceso altera la interacción patógeno-huésped, dificultando las condiciones de vida y la abundancia tanto de los patógenos como del resto de microorganismos del suelo (Gómez-Aparicio et al., 2012), tal y como parece ocurrir en las zonas

orientadas al sur o fuertemente expuestas a la radiación solar, y de escasa pendiente dentro del área de estudio (Figura 6, Figura 7).

Figura 7. Aspecto general (arriba) e individual (abajo) de encinas defoliadas, y con presencia de líquenes, en áreas de exposición sur y elevadas (alta incidencia solar) dentro de la forestación.

Los resultados del estudio a nivel de árbol individual (***Capítulo 2***), muestran el efecto de la copa de los árboles sobre el suelo y su influencia directa en la abundancia y en los patrones de agregación de las ufc del patógeno (Figura 1a y Figura 2), concentrándose estas en el lado norte del árbol, relacionado, probablemente, con el microclima que genera la sombra del árbol sobre el suelo y la mayor humedad bajo el dosel, carácter fundamental para que el oomiceto complete su ciclo biológico e infectivo (Jeon et al., 2016; Tecon y Or, 2017).

4 Estado fitosanitario del arbolado en presencia de oomicetos de podredumbre radical

Por lo general, la capacidad que tienen los patógenos de podredumbre de raíz para dispersarse en el suelo es escasa, del orden de metros por año, por lo que su transporte a mayores distancias viene promovido por factores de origen antropogénico, como el movimiento de inóculo a través de maquinaria o aperos, o por el traslado de materiales vegetales infectados de los viveros o de suelo infestado (Termorshuizen, 2014). Este último factor ha sido apuntado como altamente relevante para el caso del género *Phytophthora* spp., asociado a los procesos de mortalidad de forestaciones y restauraciones tanto a nivel europeo como de forma global, y, de forma más cercana, en el caso de estudio del suroeste de la Península Ibérica (Pérez-Sierra y Jung, 2013; Bienapfl y Balci, 2014; Parke et al., 2014; Prigigallo et al., 2015; Jung et al., 2016; Junker et al., 2016; Garbelotto et al., 2018; Simamora et al., 2018; Rooney-Latham et al., 2019; Frankel et al., 2020).

La defoliación, pese a ser un parámetro frecuentemente utilizado en la evaluación del estado de salud de los árboles en relación con la incidencia por podredumbre de la raíz (Navarro-Cerrillo et al., 2019; Ruiz-Gómez et al., 2019a; Ruiz-Gómez y Miguel-Rojas, 2021), en ocasiones no es un indicador fiable de la abundancia de patógeno en el suelo y del daño ocasionado, pues esta sintomatología puede tener su origen en otros factores abióticos y bióticos, asociados o combinados entre ellos, como la defoliación por efecto de la sequía o por el déficit de nutrientes (Ruiz-Gómez et al., 2019b), la presencia de insectos defoliadores, o la influencia de los factores ambientales como el cambio climático (Natalini et al., 2016; Encinas-Valero et al., 2021; Gea-Izquierdo et al., 2020), por lo que la evaluación de salud del arbolado a través de la defoliación requiere de un amplio muestreo de individuos, a nivel local (Navarro-Cerrillo et al., 2019; Pollastrini et al., 2016), para correlacionar los daños aéreos del árbol con la densidad de oomicetos patógenos en el suelo (***Capítulos 3 y 5***). En nuestros trabajos dentro de la forestación de encinas y alcornoques (***Capítulos 3 y 5***), *Q. ilex* mostró niveles de defoliación y mortalidad más elevados que *Q. suber* (Figura 8a), sin diferencias en las densidades medias de ufc en el suelo entre especies.

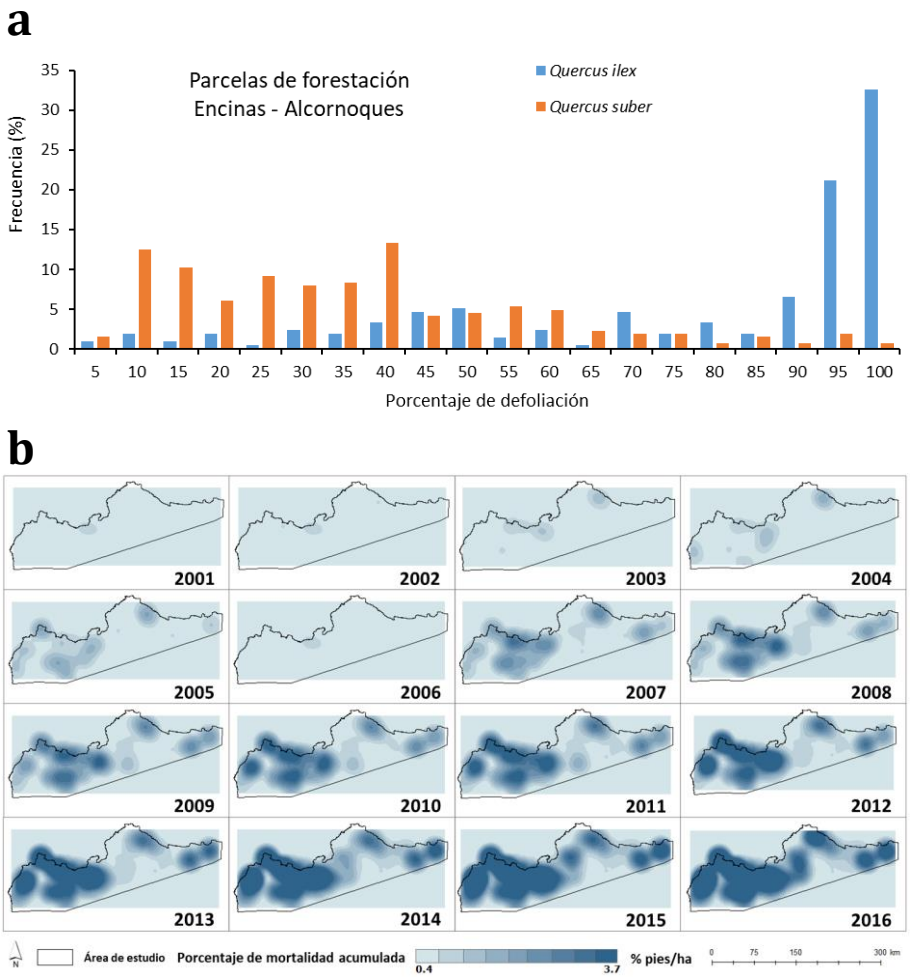

Figura 8. (a) Distribución de frecuencias de encinas y alcornoques (%) en relación con los porcentajes de defoliación por especies en la forestación de Campo Baldío. (b) Porcentaje de mortalidad acumulada de *Quercus* spp., a nivel regional de Andalucía.

Los resultados confirman las hipótesis de otros estudios que indican una mayor susceptibilidad de *Q. ilex* frente a *P. cinnamomi* y la podredumbre radical que origina, respecto a otras especies de *Quercus* mediterráneos (*Q. suber, Q. canariensis, Q. faginea, Q. pubescens y Q. pyrenaica*) (Moralejo et al., 2009). A escala regional (***Capítulo 4***) la defoliación media y la mortalidad no fueron tan elevados como en otros estudios con una intensidad de muestreo mayor sobre zonas muy afectadas (Natalini et al., 2016), al igual que sucedió en el *Capítulo 3*, pero sí progresivamente crecientes y continuas en el tiempo (Figura 8b) (Carnicer et al., 2011; Duque-Lazo y Navarro-Cerrillo, 2017; Sucena-Paiva et al.,

2022). Las redes de muestreo tienen ventajas y desventajas, entre ellas, la imposibilidad de analizar fenómenos locales relevantes. Sin embargo, entre sus principales ventajas se encuentra la capacidad de capturar dinámicas espaciales y regionales imposibles de evaluar a nivel local (Navarro-Cerrillo y Ruiz-Gómez, 2020). En nuestro caso, se identificó la importancia de los impulsores climáticos (SPEI, temperatura y precipitación) en estos procesos (Sánchez-Cuesta et al., 2021), que podría alterar la dinámica del progresivo declive tanto de las forestaciones como de las dehesas de *Quercus* spp. en los próximos años, de cumplirse alguna de las predicciones de los diferentes escenarios de cambio climático (Gil-Pelegrín et al., 2017; Duque-Lazo et al., 2018a, 2018b; Hernández-Lambraño et al., 2018).

5 Principales resultados y aplicaciones derivadas de la Tesis Doctoral

Capítulo 2. Este estudio ha permitido aumentar la eficacia de los muestreos de campo para llevar a cabo el diagnóstico de *P. cinnamomi*, orientando los muestreos de suelo hacia las zonas con mayor probabilidad de ocurrencia del patógeno bajo el árbol en lugar de plantear elevadas densidades de muestreo distribuidas uniformemente bajo copa, lo que permitirá muestrear un mayor número de árboles. Esta metodología se ha aplicado con éxito en un trabajo recientemente publicado (Ruiz-Gómez y Miguel-Rojas, 2021).

Capítulo 3. El análisis espacial de los factores bióticos y abióticos que promueven o limitan la podredumbre radical, es una herramienta eficaz de gestión en la selección de las zonas más favorables para el establecimiento de nuevas forestaciones. Nuestro resultado pone de manifiesto la importancia de las condiciones edáficas y topográficas, a nivel local, que condicionan la abundancia y dispersión espacial del patógeno. Este conocimiento permitirá desarrollar y adaptar estrategias preventivas que reduzcan el riesgo de fracaso de las forestaciones y llevar a cabo una gestión integral del territorio.

Capítulo 4. Las Redes de Sanidad Forestal como la Red SEDA en Andalucía, constituyen una fuente de datos de gran valor, que muestran la dinámica y evolución de las masas forestales, actuando como herramienta de alerta temprana frente a los procesos de decaimiento, permitiendo llevar a cabo programas de gestión integral y adaptativa frente a cada problemática ambiental (plagas y enfermedades, cambio climático, etc.), favoreciendo la vitalidad de los bosques y dehesas de *Quercus* spp. mediante prácticas silvícolas,

eco-hidrológicas, preventivas y de control de patógenos de podredumbre radical. Nuestros resultados han permitido evidenciar la influencia de factores escasamente estudiados hasta la fecha (Tablas 1 y 2, Capítulo 4) como responsables de los procesos de defoliación del arbolado a nivel regional, más allá de la presencia de un patógeno determinado. Esta evidencia es de aplicación al establecimiento de las políticas de gestión ambiental a nivel regional.

Capítulo 5. El modelado del estado fitosanitario de los árboles de la forestación, mediante imágenes LiDAR y satélite, permite planificar una gestión integral agrosilvopastoral del territorio en función del grado de decaimiento. Se han puesto a punto herramientas de análisis espacial que pueden ser aplicadas en otros contextos ofreciendo cartografías de daños de alto nivel de detalle, como soporte a la toma de decisión en la gestión del territorio afectado por el decaimiento de la dehesa.

6 Nuevas líneas de trabajo e investigación sobre los drivers ambientales del decaimiento

6.1 Relación de la defoliación con *P. cinnamomi*

Los trabajos científicos derivados de esta Tesis han mostrado la dificultad asociada al análisis de los procesos de defoliación del arbolado relacionados con la podredumbre radical. Las principales dificultades se basan en asociar la defoliación y la mortalidad del arbolado a un único factor principal (*P. cinnamomi*) dada la gran cantidad de factores bióticos y abióticos que interactúan en el proceso de decaimiento, tanto a nivel de patógeno como de huésped. La defoliación suele ser el principal factor evaluado cuando se estudia el estado sanitario del arbolado en relación con patógenos del suelo (González et al., 2017; Navarro-Cerrillo et al., 2019), siguiendo la metodología de clasificación de la defoliación de las copas del ICP-Forests (Eichhorn et al., 2016). Sin embargo, varios de los resultados de esta investigación han puesto en evidencia la dificultad de asociar el nivel de defoliación o la mortalidad de cada árbol a un único factor principal, en nuestro caso *P. cinnamomi*, dada la gran cantidad de factores bióticos y abióticos y la complejidad de sus interacciones, que pueden influir en el decaimiento del arbolado.

La medición de la defoliación en porcentajes es muy útil por su facilidad de aplicación y no requiere de ningún instrumental para su asignación,

únicamente entrenamiento visual. Por este motivo se utiliza muy a menudo. Sin embargo, tiene cierto grado de subjetividad dependiendo de la experiencia del operario que realice la medición y, entre otras, de la superficie o número de copas a estimar, que va a determinar la necesidad o no de varios operarios realizando mediciones, lo que conlleva un intercalibrado entre ellos, que no siempre va a ser perfecto.

El correcto uso de la variable de defoliación respecto a la podredumbre de raíz causada por *P. cinnamomi*, pasa por 2 dificultades sobre las que se debe seguir trabajando, la primera de ellas la capacidad de asociar esta medida a otras medidas más relacionadas con la fisiología del arbolado y su estructura, y la segunda a una capacidad de diagnóstico del patógeno más precisa y con un elevado componente de análisis espacial. Los avances pasan por integrar técnicas de teledetección en la detección previsual de daños (Hernández-Clemente et al., 2017; Hornero et al., 2021) que incluyan parámetros de estructura del arbolado, que también pueden relacionarse con la defoliación, como es el caso de la tecnología LiDAR o Radar (Gonzalez-Cascon et al., 2018; Navarro-Cerrillo et al., 2019), y otros que necesitan de un soporte de campo, como la cuantificación de pigmentos en copa, que ha demostrado una alta capacidad de discriminación en pies afectados por la podredumbre de raíz (Hernández-Clemente et al., 2012, 2017; Hornero et al., 2021).

6.2 Avances en el diagnóstico y la distribución del inóculo

El uso de unidades formadoras de colonia (ufc g^{-1} suelo seco) aisladas en un medio selectivo se usa como aproximación a la densidad de inóculo, pero presenta algunos problemas a la hora de asociar dichas densidades con los daños al arbolado. El uso de ufc como medida de la abundancia del patógeno en suelo, no siempre es un buen indicador del nivel de daño asociado al huésped que parasita, debido a factores como la temporalidad y las condiciones climáticas en las que se realiza el muestreo, que influyen directamente en el éxito de la técnica, al estar influida por la fenología del patógeno. Es decir, en un suelo recogido en condiciones óptimas, varios días después de abundantes lluvias, se encontrarán muchas más estructuras infectivas del patógeno, debido a su gran capacidad de completar el ciclo asexual de manera rápida, mientras que, en otras ocasiones, o debido a condiciones micro ambientales más desfavorables, el inóculo permanecerá latente, dando lugar a una menor intensidad de proliferación de ufc, sin conllevar ello una menor amenaza para el huésped. Por tanto, son necesarios muestreos dirigidos, repetidos en el

tiempo, y masivos para caracterizar y estimar la carga de patógenos que soporta una determinada zona del suelo mediante esta técnica.

Por otro lado, la técnica de muestreo de ufc presenta un alto grado de subjetividad si no se encuentra apoyada por otras técnicas de determinación. En un muestreo de muy pocos puntos, con varias repeticiones, el número de placas a evaluar se eleva a cientos, y el número de colonias por placa puede llegar a cifras de la misma magnitud, por lo que es un trabajo intenso, que requiere de personal altamente cualificado para ser una técnica repetible y confiable. Una alternativa sería el apoyo de estos muestreos con técnicas de determinación molecular de ADN, que permitirían de forma muy precisa identificar las especies originadas a partir de las ufc en las placas de medio selectivo. De hecho, las técnicas de PCR cuantitativa (qPCR) y metagenómica (Català et al., 2017; Ruiz-Gómez et al., 2019a), podrían ser una mejor alternativa de diagnóstico si la tendencia a la mejora de la técnica y el abaratamiento de los costes continúa.

6.3 Implicaciones del diseño experimental

Los trabajos de campo están frecuentemente limitados por la dificultad de establecer diseños experimentales adecuados, ya sea por el número de unidades experimentales (ej., árboles), o por el número de repeticiones para poder disponer de datos estadísticamente robustos para variables de alta variación espacial (defoliación y mortalidad, densidad de ufc en el suelo). Esto supone, en algunos casos, un elevado esfuerzo de muestreo, y un metódico procesado de muestras para un correcto diagnóstico, lo que reduce significativamente el número de pies, las especies o las condiciones de sitio que se pueden abordar.

En el caso de los estudios regionales, las Redes de seguimiento de daños en sistemas forestales (Red SEDA), presentan un diseño con una baja intensidad de muestreo, lo que provoca un sesgo en los datos de inventario (baja representatividad de la realidad). Así mismo, se producen errores numéricos sistemáticos debido a la interpretación de los factores bióticos/abióticos y sus niveles de daño y abundancia por parte del observador y errores aleatorios asociados a la variabilidad de las condiciones de campo y de la digitalización de los datos de inventario volcados a la base de datos.

Por otro lado, la cuantificación de variables biofísicas no se realiza de forma directa a partir de la relación empírica entre los datos recogidos con

sensores remotos y las observaciones realizadas en campo. Esto se debe a que la variación de factores geométricos y de iluminación asociada a cada sitio y momento del año, afecta a la señal espectral y con ello a su relación directa con los datos observados en campo. Una de las metodologías que se ha propuesto para cuantificar parámetros biofísicos es la del uso de modelos de transferencia radiativa que permite realizar una cuantificación biofísica de la vegetación.

En cualquier caso, la mejora en el aspecto del muestreo y el establecimiento de diseños experimentales más intensivos y eficientes, pasa por la evolución de las técnicas de teledetección, diagnóstico y monitorización del entorno, aplicando nuevos sensores tanto remotos como próximos (TLS, Tree-Talkers, picosatélites, radar…) que faciliten el estudio del ecosistema a diferentes niveles de detalle y su escalado.

6.4 ¿Cómo continuar?

De forma resumida, estas podrían ser algunas de las futuras líneas de investigación que derivan del trabajo realizado en la presente Tesis Doctoral, para seguir avanzando en la creación de herramientas útiles para el manejo de los ecosistemas de dehesa y las reforestaciones afectadas por el decaimiento asociado a la podredumbre de raíz:

1. Estudio de los patrones de distribución espacial de patógenos de podredumbre radical a través de técnicas moleculares masivas.
2. Comparar los resultados obtenidos a nivel de árbol, con análisis similares en encinas adultas sometidas a procesos de decaimiento.
3. Crear una red de parcelas permanentes en forestaciones de encina y alcornoque, similares a las parcelas de la Red SEDA de Andalucía, que permitan realizar un seguimiento temporal de su evolución, para poder evaluar las medidas de gestión más apropiadas en estas masas y asegurar así su conversión a futuras dehesas y bosques de *Quercus* spp.
4. Estudiar los patrones de distribución en forestaciones mixtas de *Quercus* spp. con otras especies (algarrobo, pinos y acebuches) incluyendo otros aspectos como la funcionalidad ecosistémica o la influencia de la biodiversidad sobre el componente biológico del suelo.
5. Continuar apoyando el seguimiento de la salud de las masas forestales a través del análisis de los datos de la Red SEDA, en el caso del decaimiento de las masas de *Quercus* en Andalucía, incorporando a las campañas de

seguimiento el análisis de patógenos de podredumbre radical mediante diagnóstico molecular periódico.

6. Ampliar la cartografía de daños al resto de forestaciones de encinas y alcornoques, por provincias, en Andalucía.

7 Referencias

Andivia, E., Fernández, M., Alejano, R., Vázquez-Piqué, J., 2015. Tree patch distribution drives spatial heterogeneity of soil traits in cork oak woodlands. Ann. For. Sci. 72, 549–559. https://doi.org/10.1007/s13595-015-0475-8

Bienapfl, J.C., Balci, Y., 2014. Movement of *Phytophthora* spp. in Maryland's Nursery Trade. Plant Dis. 98, 134–144. https://doi.org/10.1094/PDIS-06-13-0662-RE

Brasier, C.M., 1996. *Phytophthora cinnamomi* and oak decline in southern Europe. Environmental constraints including climate change. Ann. Sci. For. 53, 347–358. https://doi.org/10.1051/forest:19960217

Cahill, D., 1989. Cellular and Histological Changes Induced by *Phytophthora cinnamomi* in a Group of Plant Species Ranging from Fully Susceptible to Fully Resistant. Phytopathology 79, 417. https://doi.org/10.1094/Phyto-79-417

Cardillo, E., Acedo, A., Abad, E., 2018. Topographic effects on dispersal patterns of *Phytophthora cinnamomi* at a stand scale in a Spanish heathland. PLoS ONE 13. https://doi.org/10.1371/journal.pone.0195060

Carnicer, J., Coll, M., Ninyerola, M., Pons, X., Sánchez, G., Peñuelas, J., 2011. Widespread crown condition decline, food web disruption, and amplified tree mortality with increased climate change-type drought. Proc. Natl. Acad. Sci. 201010070. https://doi.org/10.1073/pnas.1010070108

Carrasco Gotarredona, Á., Fernández Cancio, Á., Trapero Casas, A., López Pantoja, G., Sánchez Osorio, I., Ruiz Navarro, J.M., Jiménez Molina, J.J., Domínguez Nevado, L., Romero Martín, M. de los Á., Carbonero Muñoz, M.D., Sánchez Hernández, M.E., Lucas Caetano, P.C., Gil Hernández, P., Fernández Rebollo, P., Navarro Cerrillo, R.M., Sánchez de la Cuesta, R., Raposo Llobet, R., Rodríguez Reviriego, S., 2009. Procesos de Decaimiento Forestal (la Seca): Situación del Conocimiento, 1ª edición. ed. Consejería de Medio Ambiente, Córdoba, España.

Català, S., Berbegal, M., Pérez-Sierra, A., Abad-Campos, P., 2017. Metabarcoding and development of new real-time specific assays reveal *Phytophthora* species diversity in holm oak forests in eastern Spain. Plant Pathol. 66, 115–123. https://doi.org/10.1111/ppa.12541

Corcobado, T., Cubera, E., Pérez-Sierra, A., Jung, T., Solla, A., 2010. First report of *Phytophthora gonapodyides* involved in the decline of *Quercus ilex* in xeric conditions in Spain. New Dis. Rep. 22, 33. https://doi.org/10.5197/j.2044-0588.2010.022.033

Corcobado, T., Solla, A., Madeira, M.A., Moreno, G., 2013. Combined effects of soil properties and *Phytophthora cinnamomi* infections on *Quercus ilex* decline. Plant Soil 373, 403–413. https://doi.org/10.1007/s11104-013-1804-z

Corcobado, T., Vivas, M., Moreno, G., Solla, A., 2014. Ectomycorrhizal symbiosis in declining and non-declining *Quercus ilex* trees infected with or free of *Phytophthora cinnamomi*. For. Ecol. Manag. 324, 72–80. https://doi.org/10.1016/j.foreco.2014.03.040

de Sampaio e Paiva Camilo-Alves, C., da Clara, M.I.E., de Almeida Ribeiro, N.M.C., 2013. Decline of Mediterranean oak trees and its association with *Phytophthora cinnamomi*: a review. Eur. J. For. Res. 132, 411–432. https://doi.org/10.1007/s10342-013-0688-z

Delgado-Baquerizo, M., Maestre, F.T., Gallardo, A., Bowker, M.A., Wallenstein, M.D., Quero, J.L., Ochoa, V., Gozalo, B., García-Gómez, M., Soliveres, S., García-Palacios, P., Berdugo, M., Valencia, E., Escolar, C., Arredondo, T., Barraza-Zepeda, C., Bran, D., Carreira, J.A., Chaieb, M., Conceição, A.A., Derak, M., Eldridge, D.J., Escudero, A., Espinosa, C.I., Gaitán, J., Gatica, M.G., Gómez-González, S., Guzman, E., Gutiérrez, J.R., Florentino, A., Hepper, E., Hernández, R.M., Huber-Sannwald, E., Jankju, M., Liu, J., Mau, R.L., Miriti, M., Monerris, J., Naseri, K., Noumi, Z., Polo, V., Prina, A., Pucheta, E., Ramírez, E., Ramírez-Collantes, D.A., Romão, R., Tighe, M., Torres, D., Torres-Díaz, C., Ungar, E.D., Val, J., Wamiti, W., Wang, D., Zaady, E., 2013. Decoupling of soil nutrient cycles as a function of aridity in global drylands. Nature 502, 672–676. https://doi.org/10.1038/nature12670

Duque-Lazo, J., Navarro-Cerrillo, R.M., 2017. What to save, the host or the pest? The spatial distribution of xylophage insects within the Mediterranean oak woodlands of Southwestern Spain. For. Ecol. Manag. 392, 90–104. https://doi.org/10.1016/j.foreco.2017.02.047

Duque-Lazo, J., Navarro-Cerrillo, R.M., Ruíz-Gómez, F.J., 2018a. Assessment of the future stability of cork oak (*Quercus suber* L.) afforestation under climate change scenarios in Southwest Spain. For. Ecol. Manag. 409, 444–456. https://doi.org/10.1016/j.foreco.2017.11.042

Duque-Lazo, J., Navarro-Cerrillo, R.M., van Gils, H., Groen, T.A., 2018b. Forecasting oak decline caused by *Phytophthora cinnamomi* in Andalusia: Identification of priority areas for intervention. For. Ecol. Manag. 417, 122–136. https://doi.org/10.1016/j.foreco.2018.02.045

Eichhorn, J., Roskams, P., Ferretti, M., Mues, V., Szepesi, A., 2016. Visual assessment of crown condition and damaging agents. Manual Part IV, in: Manual on Methods and Criteria for Harmonized Sampling, Assessment, Monitoring and Analysis of the Effects of Air Pollution on Forests. UNECE ICP Forests Programme Co-ordinating Centre, Eberswalde, Germany, p. 49.

Encinas-Valero, M., Esteban, R., Hereş, A.-M., Becerril, J.M., García-Plazaola, J.I., Artexe, U., Vivas, M., Solla, A., Moreno, G., Curiel Yuste, J., 2021. Photoprotective compounds as early markers to predict holm oak crown defoliation in declining Mediterranean savannahs. Tree Physiol. tpab006. https://doi.org/10.1093/treephys/tpab006

Fernández-Habas, J., Fernández-Rebollo, P., Casado, M.R., García Moreno, A.M., Abellanas, B., 2019. Spatio-temporal analysis of oak decline process in open woodlands: A case study in SW Spain. J. Environ. Manage. 248, 109308. https://doi.org/10.1016/j.jenvman.2019.109308

Frankel, S.J., Conforti, C., Hillman, J., Ingolia, M., Shor, A., Benner, D., Alexander, J.M., Bernhardt, E., Swiecki, T.J., 2020. *Phytophthora* Introductions in Restoration Areas: Responding to Protect California Native Flora from Human-Assisted Pathogen Spread. Forests 11, 1291. https://doi.org/10.3390/f11121291

Gallardo, A., 2003. Effect of tree canopy on the spatial distribution of soil nutrients in a Mediterranean Dehesa. Pedobiologia 47, 117–125. https://doi.org/10.1078/0031-4056-00175

Garbelotto, M., Frankel, S.J., Scanu, B., 2018. Soil- and waterborne *Phytophthora* species linked to recent outbreaks in Northern California restoration sites. Calif. Agric. 724 208-216 72, 208–216. https://doi.org/10.3733/ca.2018a0033

Gea-Izquierdo, G., Allen-Díaz, B., San Miguel, A., Canellas, I., 2010. How do trees affect spatio-temporal heterogeneity of nutrient cycling in mediterranean annual grasslands? Ann. For. Sci. 67, 112.

Gea-Izquierdo, G., Fernández-de-Uña, L., Cañellas, I., 2013. Growth projections reveal local vulnerability of Mediterranean oaks with rising temperatures. For. Ecol. Manag. 305, 282–293. https://doi.org/10.1016/j.foreco.2013.05.058

Gea-Izquierdo, G., Natalini, F., Cardillo, E., 2020. Holm oak death is accelerated but not sudden and expresses drought legacies. Sci. Total Environ. 141793. https://doi.org/10.1016/j.scitotenv.2020.141793

Gil-Pelegrín, E., Peguero-Pina, J.J., Sancho-Knapik, D., 2017. Oaks and People: A Long Journey Together, in: Gil-Pelegrín, E., Peguero-Pina, J.J., Sancho-Knapik, D. (Eds.), Oaks Physiological Ecology. Exploring the Functional Diversity of Genus *Quercus* L., Tree Physiology. Springer International Publishing, Cham, pp. 1–11. https://doi.org/10.1007/978-3-319-69099-5_1

Gómez-Aparicio, L., Ibáñez, B., Serrano, M.S., De Vita, P., Ávila, J.M., Pérez-Ramos, I.M., García, L.V., Esperanza Sánchez, M., Marañón, T., 2012. Spatial patterns of soil pathogens in declining Mediterranean forests: implications for tree species regeneration. New Phytol. 194, 1014–1024. https://doi.org/10.1111/j.1469-8137.2012.04108.x

González, M., Romero, M., Ramo, C., Serrano, M.S., Sánchez, M.E., 2017. Control of *Phytophthora* root rot on Mediteranean *Quercus* spp. Using fosetyl-Al trunk injections. M. https://doi.org/10.13039/501100011011

Gonzalez-Cascon, R., Pacheco-Labrador, J., Moreno, G., Migliavacca, M., Martín, M.P., 2018. Estimating Leaf and Canopy Biochemistry Variables in Mediterranean Holm oak (*Quercus ilex*) from Proximal and Airborne Hyperspectral Data, in: IGARSS 2018 - 2018 IEEE International Geoscience and Remote Sensing Symposium. Presented at the IGARSS 2018 - 2018 IEEE International Geoscience and Remote Sensing Symposium, pp. 8992–8995. https://doi.org/10.1109/IGARSS.2018.8517383

Hardham, A.R., 2005. *Phytophthora cinnamomi*. Mol. Plant Pathol. 6, 589–604. https://doi.org/10.1111/j.1364-3703.2005.00308.x

Hernández-Clemente, R., Navarro-Cerrillo, R.M., Zarco-Tejada, P.J., 2012. Carotenoid content estimation in a heterogeneous conifer forest using narrow-band indices and PROSPECT+DART simulations. https://doi.org/10.1016/j.rse.2012.09.014

Hernández-Clemente, R., North, P.R.J., Hornero, A., Zarco-Tejada, P.J., 2017. Assessing the effects of forest health on sun-induced chlorophyll fluorescence using the FluorFLIGHT 3-D radiative transfer model to account for forest structure. Remote Sens. Environ. 193, 165–179. https://doi.org/10.1016/j.rse.2017.02.012

Hernández-Lambraño, R.E., González-Moreno, P., Sánchez-Agudo, J.Á., 2018. Environmental factors associated with the spatial distribution of invasive plant pathogens in the Iberian Peninsula: The case of *Phytophthora cinnamomi* Rands. For. Ecol. Manag. 419–420, 101–109. https://doi.org/10.1016/j.foreco.2018.03.026

Hornero, A., Zarco-Tejada, P.J., Quero, J.L., North, P.R.J., Ruiz-Gómez, F.J., Sánchez-Cuesta, R., Hernandez-Clemente, R., 2021. Modelling hyperspectral- and thermal-based plant traits for the early detection of Phytophthora-induced symptoms in oak decline. Remote Sens. Environ. 263, 112570. https://doi.org/10.1016/j.rse.2021.112570

Jeon, S., Krasnow, C.S., Kirby, C.K., Granke, L.L., Hausbeck, M.K., Zhang, W., 2016. Transport and Retention of *Phytophthora capsici* Zoospores in Saturated Porous Media. Environ. Sci. Technol. 50, 9270–9278. https://doi.org/10.1021/acs.est.6b01784

Jung, T., Orlikowski, L., Henricot, B., Abad-Campos, P., Aday, A.G., Casal, O.A., Bakonyi, J., Cacciola, S.O., Cech, T., Chavarriaga, D., Corcobado, T., Cravador, A., Decourcelle, T., Denton, G., Diamandis, S., Doğmuş-Lehtijärvi, H.T., Franceschini, A., Ginetti, B., Green, S., Glavendekić, M., Hantula, J., Hartmann, G., Herrero, M., Ivic, D., Jung, M.H., Lilja, A., Keca, N., Kramarets, V., Lyubenova, A., Machado, H., Lio, G.M. di S., Vázquez, P.J.M., Marçais, B., Matsiakh, I., Milenkovic, I., Moricca, S., Nagy, Z.Á., Nechwatal, J., Olsson, C., Oszako, T., Pane, A., Paplomatas, E.J., Varela, C.P., Prospero, S., Martínez, C.R., Rigling, D., Robin, C., Rytkönen, A., Sánchez, M.E., Ros, A.V.S., Scanu, B., Schlenzig, A., Schumacher, J., Slavov, S., Solla, A., Sousa, E., Stenlid, J., Talgø, V., Tomic, Z., Tsopelas, P., Vannini, A., Vettraino, A.M., Wenneker, M., Woodward, S., Peréz-Sierra, A., 2016. Widespread *Phytophthora* infestations in European

nurseries put forest, semi-natural and horticultural ecosystems at high risk of *Phytophthora* diseases. For. Pathol. 46, 134–163. https://doi.org/10.1111/efp.12239

Junker, C., Goff, P., Wagner, S., Werres, S., 2016. Occurrence of *Phytophthora* Species in Commercial Nursery Production. Plant Health Prog. 17, 64–75. https://doi.org/10.1094/PHP-RS-15-0045

Moralejo, E., García-Muñoz, J.A., Descals, E., 2009. Susceptibility of Iberian trees to *Phytophthora ramorum* and *P. cinnamomi*. Plant Pathol. 58, 271–283. https://doi.org/10.1111/j.1365-3059.2008.01956.x

Moreira, A.C., Martins, J.M.S., 2005. Influence of site factors on the impact of *Phytophthora cinnamomi* in cork oak stands in Portugal. For. Pathol. 35, 145–162. https://doi.org/10.1111/j.1439-0329.2005.00397.x

Natalini, F., Alejano, R., Vázquez-Piqué, J., Cañellas, I., Gea-Izquierdo, G., 2016. The role of climate change in the widespread mortality of holm oak in open woodlands of Southwestern Spain. Dendrochronologia 38, 51–60. https://doi.org/10.1016/j.dendro.2016.03.003

Navarro-Cerrillo, R., Ruiz-Gómez, F., 2020. Seguimiento de plagas y enfermedades forestales en Andalucía: interpretación a diferentes escalas. Cuad. Soc. Esp. Cienc. For. 46, 33-56Ruiz Gómez.

Navarro-Cerrillo, R.M., Varo-Martínez, M.Á., Acosta, C., Palacios Rodriguez, G., Sánchez-Cuesta, R., Ruiz Gómez, F.J., 2019. Integration of WorldView-2 and airborne laser scanning data to classify defoliation levels in *Quercus ilex* L. Dehesas affected by root rot mortality: Management implications. For. Ecol. Manag. 451, 117564. https://doi.org/10.1016/j.foreco.2019.117564

Oßwald, W., Fleischmann, F., Rigling, D., Coelho, A.C., Cravador, A., Diez, J., Dalio, R.J., Horta Jung, M., Pfanz, H., Robin, C., Sipos, G., Solla, A., Cech, T., Chambery, A., Diamandis, S., Hansen, E., Jung, T., Orlikowski, L.B., Parke, J., Prospero, S., Werres, S., 2014. Strategies of attack and defence in woody plant–Phytophthora interactions. For. Pathol. 44, 169–190. https://doi.org/10.1111/efp.12096

Parke, J.L., Knaus, B.J., Fieland, V.J., Lewis, C., Grünwald, N.J., 2014. *Phytophthora* Community Structure Analyses in Oregon Nurseries Inform Systems Approaches to Disease Management. Phytopathology® 104, 1052–1062. https://doi.org/10.1094/PHYTO-01-14-0014-R

Pérez-Sierra, A., Jung, T., 2013. *Phytophthora* in woody ornamental nurseries, in: *Phytophthora*: A Global Perspective. CABI, pp. 166–177.

Pérez-Sierra, A., López-García, C., León, M., García-Jiménez, J., Abad-Campos, P., Jung, T., 2013. Previously unrecorded low-temperature *Phytophthora* species associated with *Quercus* decline in a Mediterranean forest in eastern Spain. For. Pathol. 43, 331–339. https://doi.org/10.1111/efp.12037

Pollastrini, M., Feducci, M., Bonal, D., Fotelli, M., Gessler, A., Grossiord, C., Guyot, V., Jactel, H., Nguyen, D., Radoglou, K., Bussotti, F., 2016. Physiological significance of forest tree defoliation: Results from a survey in a mixed forest in Tuscany (central Italy). For. Ecol. Manag. 361, 170–178. https://doi.org/10.1016/j.foreco.2015.11.018

Prigigallo, M.I., Mosca, S., Cacciola, S.O., Cooke, D.E.L., Schena, L., 2015. Molecular analysis of *Phytophthora* diversity in nursery-grown ornamental and fruit plants. Plant Pathol. 64, 1308–1319. https://doi.org/10.1111/ppa.12362

Ríos, P., González, M., Obregón, S., Carbonero, M.-D., LEAL, J.-R., Fernandez, P., De-Haro, A., Sánchez, M.-E., 2017. Brassica-based seedmeal biofumigation to control *Phytophthora cinnamomi* in the Spanish "dehesa" oak trees. Phytopathol. Mediterr. 56, 392–399.

Rooney-Latham, S., Blomquist, C.L., Kosta, K.L., Gou, Y.Y., Woods, P.W., 2019. *Phytophthora* Species Are Common on Nursery Stock Grown for Restoration and Revegetation Purposes in California. Plant Dis. 103, 448–455. https://doi.org/10.1094/PDIS-01-18-0167-RE

Ruiz-Gómez, F.J., Miguel-Rojas, C., 2021. Antagonistic Potential of Native *Trichoderma* spp. against *Phytophthora cinnamomi* in the Control of Holm Oak Decline in Dehesas Ecosystems. Forests 12, 945. https://doi.org/10.3390/f12070945

Ruiz-Gómez, F.J., Navarro-Cerrillo, R.M., Pérez-de-Luque, A., Oβwald, W., Vannini, A., Morales-Rodríguez, C., 2019a. Assessment of functional and structural changes of soil fungal and oomycete communities in holm oak declined dehesas through metabarcoding analysis. Sci. Rep. 9, 5315. https://doi.org/10.1038/s41598-019-41804-y

Ruiz-Gómez, F.J., Navarro-Cerrillo, R.M., Sánchez-Cuesta, R., Pérez-de-Luque, A., 2015. Histopathology of Infection and Colonization of *Quercus Ilex* Fine Roots by *Phytophthora cinnamomi*. Plant Pathol. 64, 605–616. https://doi.org/10.1111/ppa.12310

Ruiz-Gómez, F.J., Pérez-de-Luque, A., Navarro-Cerrillo, R.M., 2019b. The Involvement of *Phytophthora* Root Rot and Drought Stress in Holm Oak Decline: from Ecophysiology to Microbiome Influence. Curr. For. Rep. 5, 251–266. https://doi.org/10.1007/s40725-019-00105-3

Ruiz-Gómez, F.J., Pérez-de-Luque, A., Sánchez-Cuesta, R., Quero, J.L., Navarro Cerrillo, R.M., 2018. Differences in the Response to Acute Drought and *Phytophthora cinnamomi* Rands Infection in *Quercus ilex* L. Seedlings. Forests 9, 634. https://doi.org/10.3390/f9100634

Sánchez, M.E., Andicoberry, S., Trapero, A., 2005. Pathogenicity of three *Phytophthora* spp. causing late seedling rot of *Quercus ilex* ssp. ballota. For. Pathol. 35, 115–125. https://doi.org/10.1111/j.1439-0329.2004.00392.x

Sánchez, M.E., Caetano, P., Ferraz, J., Trapero, A., 2002. *Phytophthora* disease of *Quercus ilex* in south-western Spain. For. Pathol. 32, 5–18. https://doi.org/10.1046/j.1439-0329.2002.00261.x

Sánchez-Cuesta, R., Ruiz-Gómez, F.J., Duque-Lazo, J., González-Moreno, P., Navarro-Cerrillo, R.M., 2021. The environmental drivers influencing spatio-temporal dynamics of oak defoliation and mortality in dehesas of Southern Spain. For. Ecol. Manag. 485, 118946. https://doi.org/10.1016/j.foreco.2021.118946

Sardans, J., Peñuelas, J., 2013. Plant-soil interactions in Mediterranean forest and shrublands: impacts of climatic change. Plant Soil 365, 1–33. https://doi.org/10.1007/s11104-013-1591-6

Satyaprakash, M., Nikitha, T., Reddi, E.U.B., Sadhana, B., Vani, S.S., 2017. Phosphorous and phosphate solubilising bacteria and their role in plant nutrition. Int J Curr Microbiol App Sci 6, 2133–2144.

Sena, K., Crocker, E., Vincelli, P., Barton, C., 2018. *Phytophthora cinnamomi* as a driver of forest change: Implications for conservation and management. For. Ecol. Manag. 409, 799–807. https://doi.org/10.1016/j.foreco.2017.12.022

Serrano, M.S., De Vita, P., Fernández-Rebollo, P., Sánchez-Hernández, M.E., 2012. Calcium fertilizers induce soil suppressiveness to *Phytophthora cinnamomi* root rot of *Quercus ilex*. Eur. J. Plant Pathol. 132, 271–279. https://doi.org/10.1007/s10658-011-9871-6

Shen, J., Yuan, L., Zhang, J., Li, H., Bai, Z., Chen, X., Zhang, W., Zhang, F., 2011. Phosphorus Dynamics: From Soil to Plant. Plant Physiol. 156, 997–1005. https://doi.org/10.1104/pp.111.175232

Simamora, A.V., Paap, T., Howard, K., Stukely, M.J.C., Hardy, G.E.St.J., Burgess, T.I., 2018. *Phytophthora* Contamination in a Nursery and Its Potential Dispersal into the Natural Environment. Plant Dis. 102, 132–139. https://doi.org/10.1094/PDIS-05-17-0689-RE

Simler-Williamson, A.B., Rizzo, D.M., Cobb, R.C., 2019. Interacting Effects of Global Change on Forest Pest and Pathogen Dynamics. Annu. Rev. Ecol. Evol. Syst. 50, 381–403. https://doi.org/10.1146/annurev-ecolsys-110218-024934

Simón, N., Montes, F., Díaz-Pinés, E., Benavides, R., Roig, S., Rubio, A., 2013. Spatial distribution of the soil organic carbon pool in a Holm oak dehesa in Spain. Plant Soil 366, 537–549. https://doi.org/10.1007/s11104-012-1443-9

Sucena-Paiva, L., Correia, O., Rosário, L., Chozas, S., 2022. Holm oak wood pastures in SE Portugal: a spatial and temporal multiscale approach. Agrofor. Syst. https://doi.org/10.1007/s10457-021-00714-7

Tecon, R., Or, D., 2017. Biophysical processes supporting the diversity of microbial life in soil. FEMS Microbiol. Rev. 41, 599–623. https://doi.org/10.1093/femsre/fux039

Termorshuizen, A.J., 2014. Root Pathogens, in: Dighton, J., Krumins, J.A. (Eds.), Interactions in Soil: Promoting Plant Growth, Biodiversity, Community and Ecosystems. Springer Netherlands, Dordrecht, pp. 119–137. https://doi.org/10.1007/978-94-017-8890-8_6

Trumbore, S., Brando, P., Hartmann, H., 2015. Forest health and global change. Science 349, 814–818. https://doi.org/10.1126/science.aac6759

Capítulo 7

Conclusiones

Conclusiones

1. La distribución espacial de *Phytophthora cinnamomi*, en la rizosfera de la encina, se ha relacionado con patrones de agregación de nutrientes, materia orgánica y humedad del suelo bajo la proyección de la copa. La presencia agregada en la rizosfera de las unidades formadoras de colonias (ufc), tanto a nivel de árbol como de forestación, coincidió con la agregación de estos factores, confirmando observaciones previas sobre el comportamiento del inóculo ante la concentración de materia orgánica del suelo, la textura y la humedad, y revelando nuevas asociaciones como la influencia de los macronutrientes (nitrógeno, fósforo y potasio).
2. El microambiente creado por la proyección de la copa de los árboles y su sistema radical modula las interacciones entre los diferentes elementos del ecosistema a microescala, favoreciendo una mayor concentración de inóculo en las áreas más sombreadas, generalmente al norte, relacionado con la mayor humedad del suelo en estas zonas.
3. Se ha evaluado el estado fitosanitario de las dos principales especies afectadas por podredumbre de raíz en las dehesas andaluzas, en parcelas de campo infestadas por *P. cinnamomi,* bajo condiciones ecológicas y climáticas homogéneas. *Q. ilex* mostró niveles de defoliación y mortalidad más elevados que *Q. suber*, sin diferencias en las densidades medias de ufc en el suelo, confirmando la mayor susceptibilidad de la encina a la podredumbre de raíz causada por *P. cinnamomi*.
4. El contenido en materia orgánica del suelo se ha mostrado como un factor de gran relevancia en los procesos de decaimiento de las dehesas. Junto con su influencia sobre la agregación de inóculo a nivel de árbol (bajo copa) y a nivel de forestación, el estudio del patrón espaciotemporal de afección del arbolado en dehesas reveló su relación con la mortalidad en parcelas de la Red SEDA con presencia de *P. cinnamomi*. Estos resultados destacan la importancia de la materia orgánica en la etiología de la podredumbre de la raíz y la necesidad de seguir profundizando en su estudio.
5. En las plantaciones de encina y alcornoque, las zonas con menor pendiente, de exposición norte y con menores niveles de radiación solar, presentaron una mayor concentración de ufc de patógenos de podredumbre radical, en consonancia con los resultados obtenidos a nivel de microescala de árbol.

6. La defoliación y la mortalidad de las plantaciones de encina situadas en orientación sur presentaron un patrón acumulativo relacionado con la escasa capacidad de retención de agua del suelo y la mayor incidencia solar, pero con menor presencia del patógeno que en el resto de las subparcelas. Por el contrario, en las áreas de orientación norte, con mayor compensación hídrica, los valores de defoliación y de mortalidad se relacionan con una menor incidencia solar y una mayor humedad del suelo.
7. En función de lo anterior, la influencia de los factores bióticos y abióticos en el decaimiento está modulada por la topografía, destacando los factores abióticos en las situaciones más limitantes (exposición sur, baja humedad del suelo), mientras que los factores bióticos (presencia del patógeno, ufc) condicionan el estado fitosanitario, en mayor grado, en las situaciones más favorables (exposición norte o menor incidencia solar, mayor contenido de agua en el suelo y capacidad de retención).

8. Se ha evidenciado la importancia de los detonantes climáticos (SPEI, temperatura y precipitación) en los procesos de defoliación y mortalidad de *Q. ilex* y *Q. suber*, que podrían alterar la dinámica del progresivo declive tanto de las forestaciones como de las dehesas de *Quercus* spp. en los próximos años, de cumplirse alguna de las predicciones de los diferentes escenarios de cambio climático.

9. Se han puesto a punto herramientas de análisis espacial basadas en teledetección que se pueden aplicar en la evaluación de procesos de decaimiento y mortalidad en otros contextos, y que permiten generar cartografía de daños de alto nivel de detalle, como soporte a la toma de decisión en la gestión del territorio afectado por el decaimiento de la dehesa. La cartografía a escala de árbol del estado fitosanitario, elaborada a partir de datos LiDAR e imágenes satélite, identifica patrones de decaimiento en forestaciones, y facilita la planificación de la gestión integral agrosilvopastoral en explotaciones y plantaciones de encina y alcornoque.

Anexos

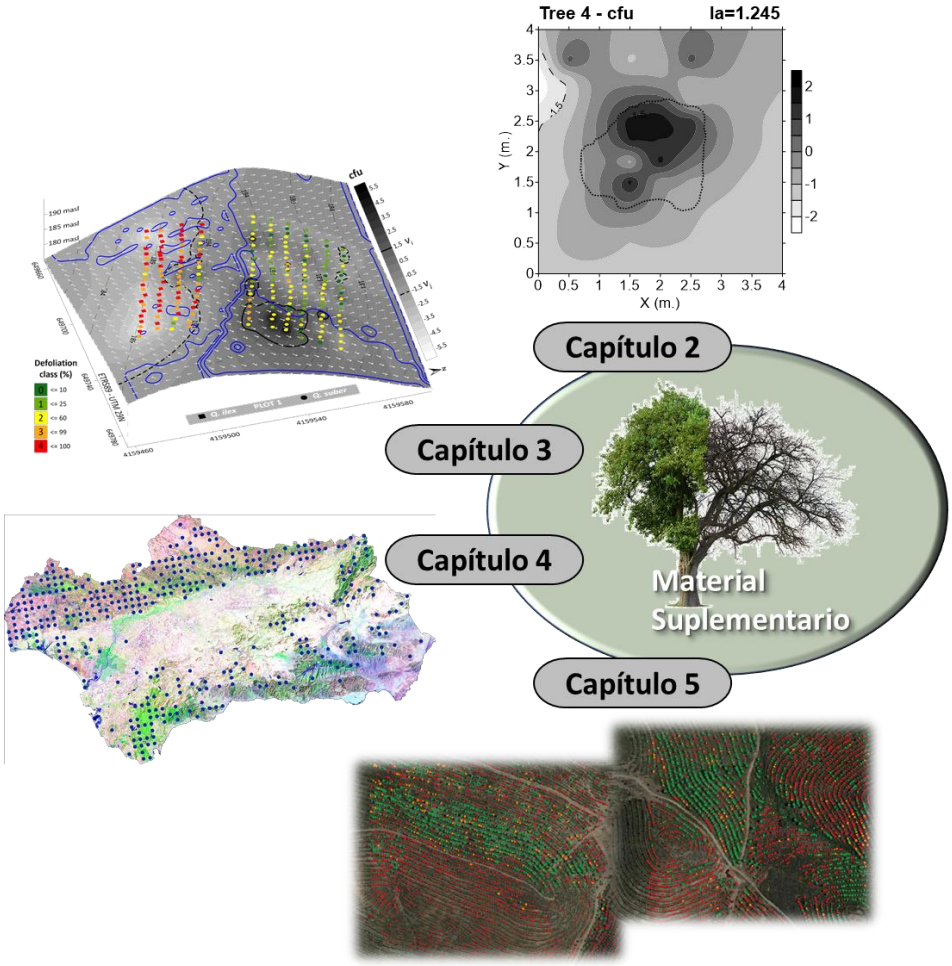
Tree 4 - cfu
Ia=1.245
Y (m.)
X (m.)
cfu
Defoliation class (%)
Capítulo 2
Capítulo 3
Capítulo 4
Capítulo 5
Material Suplementario

Supplementary Material - CAPÍTULO 2

Table S2.1. Visual symptomatology and morphological parameters of the four trees selected for this study.

Appearance		
Height (m)	2.65	2.40
Diameter (cm)	10.5	9
Defoliation (%)	15	25
Slope (%)	6	5
Appearance		
Height (m)	2.70	2.35
Diameter (cm)	10	8.5
Defoliation (%)	35	70
Slope (%)	5	10

Table S2.2. Soil Physicochemical parameters and analytical technique used.

VARIABLE	TECHNIQUE	UNITS	REFERENCE VALUES
Physical properties (Granulometry)			
Texture **Clay - Silt - Sand**	Densimetría Bauyoucos	%	N/A
Chemical properties			
***pH**	Potentiometry	upH	6,5–7,5
Potentiometry (titration)			
Total **Organic Matter (OM)**	Walkley-Black	%	2,00–3,00
Organic **Nitrogen (N)**	Kjeldahl	%	0,1–0,15
Carbon/Nitrogen ratio (**C/N)**	Relation	N/A	9,00–11,00
Spectrophotometry U.V./VIS			
Assimilable **Phosphorus (P)**	Olsen method	Mg/Kg	20,0–70,0
Atomic absorption spectroscopy			
Calcium change (**Ca**)	Atomic absorption spectrometry	meq/100g	2,00–12,0
Potassium change (**K**)	Atomic absorption spectrometry	meq/100g	0,25–0,80

Parameters marked with an asterisk (*) are accredited by ENAC (National Accreditation Entity) nº 1000/LE 1975.

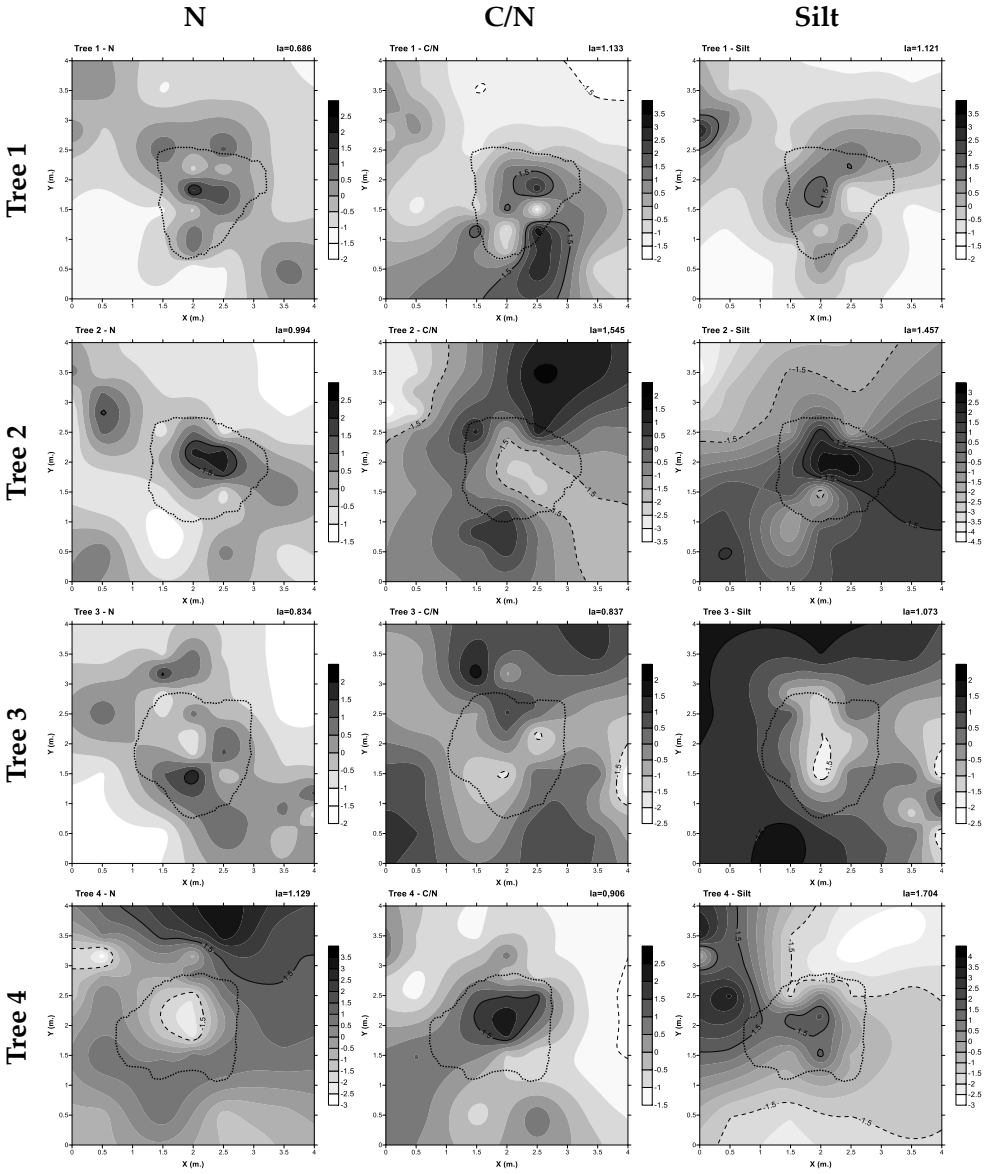

Figure S2.1. Maps of clustering indices (ν) of the edaphic variables. By columns: N (nitrogen), C/N (carbon/nitrogen ratio), silt, sand, pH, Ca (calcium) and moisture. By rows, trees 1 to 4 (projected to 4x4 meters surface). Dark areas show clustering spots of edaphic variables (ν > 1.5) are delimited by a continuous line, and the light areas show edaphic variables clustering gaps (ν < -1.5) are delimited by a discontinuous line. The dotted line represents the crown projection of each tree. In the upper right corner of each sampling unit, the general aggregation pattern (I_a) is indicated. Legends are unitless.

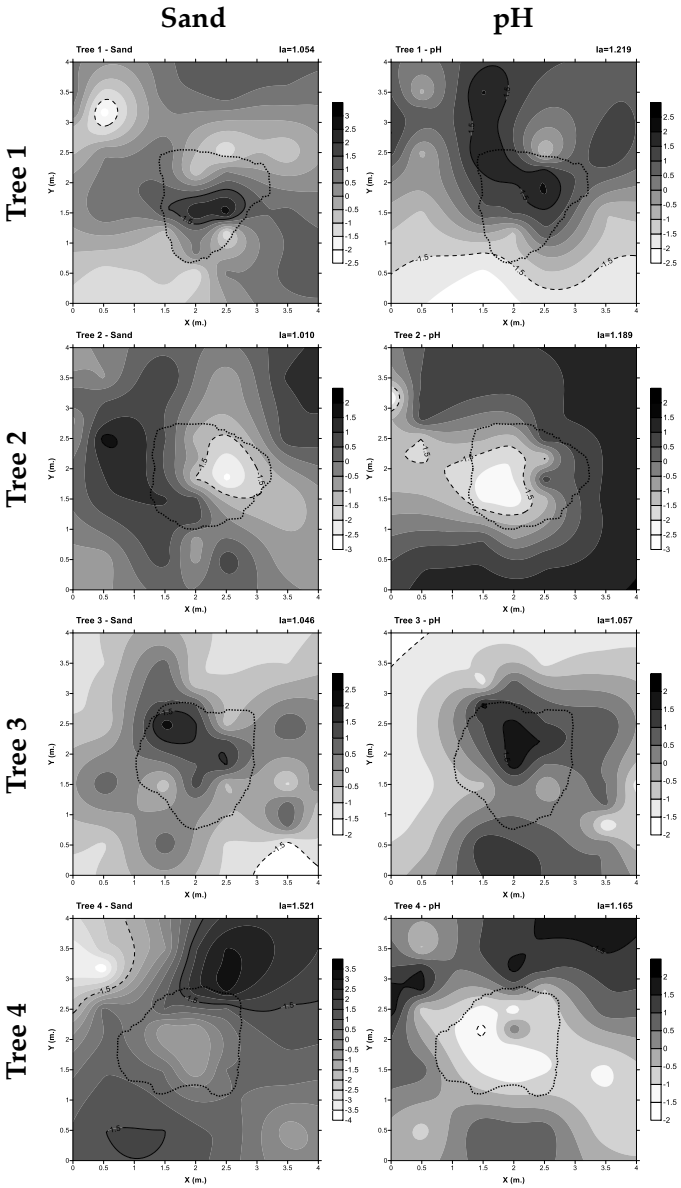

Figure S2.1. Continued.

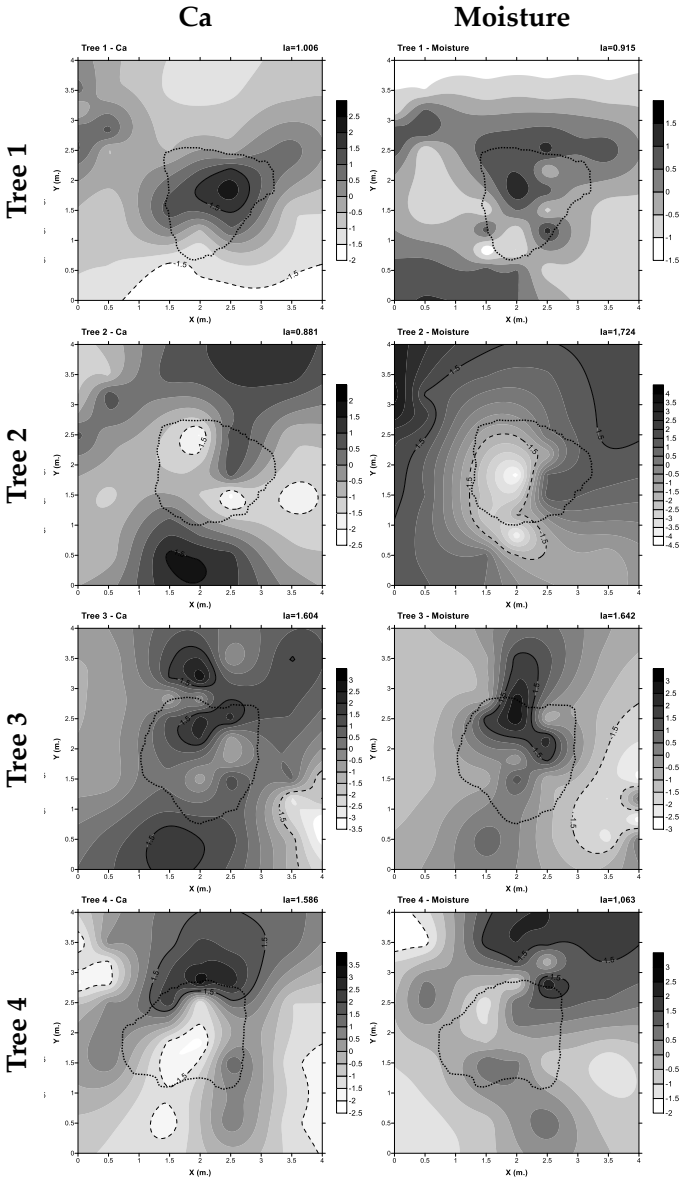

Figure S2.1. Continued.

Supplementary Material - CAPÍTULO 3

Table S3.1. Variables used in the study of spatial distribution patterns and modelling the decay process in *Quercus* spp. afforestation in Huelva (Spain). The group names between brackets ( ) correspond to the code used for SEM modelling process. • The variable does not adjust to the normal distribution.

VARIABLES	CODE	UNITS	REFERENCE VALUES*
Dasometry			
Diameter Breast Height Tree Measure (n = year)	DBH_n	cm	
Tree height (n = year)	H_n	m	
Phytosanitary		m	
Percentage of tree defoliation (n = year) •	Def_n	%	
Soil biotics			
Colony forming units of *Phytophthora cinnamomi* •	cfu	cfu/g	
Soil physical & texture (Physical)			
Apparent density of fines ^	Fden	g/cm^3	
Total apparent soil density ^	Tden	g/cm^3	
Percentage of gravel in the soil (sieve nº 4; >4.75 mm) ^	Grav	%	
Percentage of fines in the soil (sieve nº 200; <0.075 mm) ^	Fine	%	
Percentage of clay *	Clay	%	
Percentage of sand *	Sand	%	
Percentage of silt *	Silt	%	
Percentage of roots per volume of soil	Root	%	
Soil macro and micro-nutrient content (Nutrients)			
Organic Nitrogen *	N	%	0.1 – 0.15
Assimilable Phosphorus *	P	ppm	20 – 70
Interchangeable Potassium *	K	meq/100g	0.25 – 0.80
Interchangeable Sodium *	Na	meq/100g	0.02 – 0.25
Interchangeable Magnesium *	Mg	meq/100g	1.5 – 3.0
Interchangeable Calcium • *	Ca	meq/100g	2 – 12
Cupper (micronutrient) ^	Cu	mg/kg	10 – 20
Zinc (micronutrient) ^	Zn	mg/kg	20 – 50
Iron (micronutrient) ^	Fe	mg/kg	40 – 200
Manganese (micronutrient) ^	Mn	mg/kg	30 – 100
Soil chemical characteristics (Chemical)			
Cation exchange capacity *	CEC	meq/100g	20 – 35
Carbon/Nitrogen ratio • *	C/N	-	9 – 11
Soil organic Carbon *	SOC	Kg/m^2	7.6 #
Soil organic matter *	OM	%	2 – 3
Soil pH ^	pH	-	6.5 – 7.5
Volumetric soil water content (Moisture)			
Moisture in (m = month) •	M_5-M_7-M_{12}	%	12 / 22 / 34 +
Topographic characteristics (Topographic)			
Digital Elevation Model •	DEM	m.a.s.l.	
Slope	Slope	%	
Orientation •	Orien	Degrees (360 º)	
Annual solar incidence •	Solar	h/year	

* Agri-food laboratory of Córdoba (Spain). ^ University of Córdoba soil science laboratory (Córdoba. Spain).
# Mean value of the variable "SOC" for peninsular Spain (Rovira et al., 2007).
+ Water content in loamy soils: permanent wilting point / available water / field capacity

Table S3.2. Dasometric mean values of trees between 2010-2018 (DBH – H, mean ± standard error), grouped by subplots and species. Different lowercase letters in superscripts indicate significant differences between treatments (Bonferroni Test, $P < 0.0083$ for subplots comparison and Student's *t*-Test, $P < 0.05$ for species comparison).

Variable	All (n=359)	P_1Qi (n=78)	P_1Qs (n=119)	P_2Qi (n=61)	P_2Qs (n=101)	Qi (n=139)	Qs (n=220)
DBH_{10}	11.80±0.25	10.55±0.55^{a}	14.51±0.41^{b}	8.39±0.44^{a}	10.73±0.31^{a}	9.35±0.36^{a}	12.77±0.29^{b}
DBH_{18}	12.22±0.21	10.06±0.46^{a}	14.21±0.32^{b}	9.88±0.51^{a}	11.82±0.32^{a}	9.96±0.35^{a}	13.11±0.24^{b}
H_{10}	2.93±0.07	2.32±0.10^{a}	2.90±0.20^{ab}	2.83±0.12^{ab}	3.25±0.09^{b}	2.58±0.09^{a}	3.20±0.08^{b}
H_{18}	3.55±0.09	2.53±0.12^{a}	4.52±0.37^{b}	3.48±0.15^{c}	3.86±0.09^{cb}	3.01±0.12^{a}	3.95±0.10^{b}

Table S3.3. Results of manifests standardized influence over latent variables in SEM models. Estimate represents the standardized level of influence for each exogenous variable (manifest) over their correspondent latent variable. R-square represents the variability of the exogenous variable explained by the model (fraction of 1).

MODEL	Latent	Manifest	Estimate	Z-value	P	R-Square
All plots	*Topographic*	DEM	0.808	29.704	<0.001	0.653
		Orien	0.527	14.750	<0.001	0.277
		Solar	0.395	7.623	<0.001	0.156
	Chemical	CEC	0.838	23.468	<0.001	0.702
		pH	0.785	24.636	<0.001	0.616
		C/N	0.645	19.920	<0.001	0.416
		SOC	0.708	20.249	<0.001	0.501
	Nutrients	Ca	0.893	28.208	<0.001	0.797
		P	-0.611	-13.399	<0.001	0.374
		Cu	0.965	37.249	<0.001	0.931
		Mn	0.852	26.739	<0.001	0.725
		N	0.834	23.197	<0.001	0.695
	Physical	Fden	0.718	17.041	<0.001	0.515
		Fine	0.834	26.598	<0.001	0.696
		Sand	-0.866	-29.384	<0.001	0.749
		Silt	0.915	25.211	<0.001	0.836
	Moisture	M_5	0.278	5.017	<0.001	0.126
		M_7	0.837	6.318	<0.001	0.020
***Q. ilex* subplots**	*Topographic*	Orien	0.594	8.539	<0.001	0.352
		Solar	0.915	36.842	<0.001	0.838
	Chemical	CEC	0.980	22.954	<0.001	0.961
		OM	0.829	15.541	<0.001	0.687
		SOC	0.949	20.862	<0.001	0.901
		pH	0.760	11.381	<0.001	0.577
	Moisture	M_7	0.558	12.723	<0.001	1.000
***Q. suber* subplots**	*Topographic*	DEM	0.780	9.377	<0.001	1.000
	Physical	Fine	0.824	19.739	<0.001	0.679
		Tden	0.740	13.633	<0.001	0.548
		Sand	-0.849	-22.068	<0.001	0.721
	Nutrients	Ca	0.921	29.171	<0.001	0.849
		Cu	0.978	38.316	<0.001	0.956
		Fe	-0.639	-9.552	<0.001	0.409
		Mn	0.840	21.903	<0.001	0.706
	Moisture	M_5	0.484	4.272	<0.001	1.000

Table S3.4. Soil and topographic mean values (mean ± standard error) at the sampling points (*n*) respect to subplots and species. Different superscripts indicate significant differences between treatments (ANOVA – Bonferroni test, $P < 0.0083$ and Tamhane test, $P < 0.05$ for subplots comparison and Student's *t* & Welch test, $P < 0.05$ for species comparison, under normal conditions of the variables; Kruskal-Wallis, $P < 0.05$, and Mann-Whitney U test – Bonferroni correction, $P < 0.0083$, for non-normal distributed variables '•').

		Subplots				Species	
Variable	All *n*=98	P_1Qi *n*=21	P_1Qs *n*=28	P_2Qi *n*=21	P_2Qs *n*=28	Qi *n*=42	Qs *n*=56
Root	0.005±0.001	0.002±0.000^{a}	0.003±0.000^{a}	0.009±0.002^{b}	0.006±0.001^{b}	0.006±0.001^{a}	0.004±0.001^{a}
Fden	1.05±0.02	0.98±0.03^{a}	0.94±0.03^{a}	1.06±0.04^{ab}	1.21±0.04^{b}	1.02±0.03^{a}	1.07±0.03^{a}
Tden	1.35±0.02	1.36±0.03^{ab}	1.27±0.02^{a}	1.34±0.04^{ab}	1.44±0.03^{b}	1.35±0.03^{a}	1.35±0.02^{a}
Grav	36.81±1.14	44.19±1.51^{a}	39.91±2.56^{ab}	35.33±2.29^{bc}	29.30±1.25^{c}	39.76±1.52^{a}	34.61±1.58^{b}
Fine	63.19±1.14	55.81±1.51^{a}	60.09±2.56^{ab}	64.67±2.29^{bc}	70.70±1.25^{c}	60.24±1.52^{a}	65.39±1.58^{b}
Clay	20.85±0.65	16.03±0.47^{a}	21.51±1.47^{b}	19.83±1.29^{b}	24.56±0.93^{c}	17.93±0.74^{a}	23.03±0.89^{b}
Sand	36.73±0.74	43.60±0.67^{a}	37.67±1.53^{b}	37.44±1.24^{b}	30.09±0.72^{c}	40.52±0.84^{a}	33.88±0.98^{b}
Silt	42.43±0.32	40.37±0.42^{a}	40.82±0.44^{a}	42.73±0.58^{a}	45.36±0.53^{b}	41.55±0.40^{a}	43.09±0.46^{b}
N ↔	0.12±0.00	0.10±0.00^{a}	0.12±0.00^{b}	0.12±0.01^{bc}	0.14±0.00^{c}	0.11±0.00^{a}	0.13±0.00^{b}
P ↓	3.32±0.10	4.14±0.24^{a}	3.07±0.16^{bc}	3.72±0.14^{ab}	2.65±0.12^{c}	3.93±0.14^{a}	2.86±0.10^{b}
K ←	0.25±0.01	0.24±0.01^{bc}	0.26±0.01^{ab}	0.30±0.02^{a}	0.22±0.01^{c}	0.27±0.01^{a}	0.24±0.01^{b}
Na ↑	0.33±0.00	0.34±0.01^{a}	0.33±0.00^{a}	0.31±0.01^{b}	0.34±0.01^{a}	0.32±0.01^{a}	0.34±0.00^{b}
Mg ↔	2.55±0.06	2.64±0.11^{ab}	2.80±0.11^{a}	2.19±0.07^{b}	2.51±0.10^{ab}	2.41±0.07^{a}	2.66±0.08^{b}
Ca • ←	3.22±0.12	2.23±0.14^{a}	2.86±0.14^{a}	2.94±0.22^{a}	4.54±0.14^{b}	2.58±0.14^{a}	3.70±0.15^{b}
CEC ↓	9.61±0.17	7.33±0.17^{a}	9.35±0.22^{b}	10.12±0.26^{b}	11.19±0.17^{c}	8.72±0.27^{a}	10.27±0.19^{b}
C/N • ↓	0.81±0.01	0.77±0.01^{a}	0.80±0.01^{ab}	0.82±0.02^{b}	0.84±0.01^{b}	0.79±0.01^{a}	0.82±0.01^{b}
SOC ↓	1.22±0.05	0.90±0.03^{a}	1.02±0.05^{a}	1.56±0.13^{b}	1.41±0.07^{b}	1.23±0.08^{a}	1.21±0.05^{a}
OM ↔	2.53±0.07	2.26±0.11^{a}	2.62±0.16^{ab}	2.87±0.15^{b}	2.37±0.11^{ab}	2.56±0.10^{a}	2.50±0.10^{a}
Cu ↓	0.79±0.03	0.56±0.02^{a}	0.61±0.02^{a}	0.85±0.05^{b}	1.11±0.03^{c}	0.71±0.03^{a}	0.86±0.04^{b}
Zn ↓	0.62±0.04	0.51±0.06^{a}	0.57±0.05^{a}	0.82±0.13^{a}	0.61±0.05^{a}	0.66±0.07^{a}	0.59±0.04^{a}
Fe ↓	3.59±0.13	3.58±0.27^{ab}	3.95±0.30^{ab}	4.00±0.22^{a}	2.93±0.12^{b}	3.79±0.18^{a}	3.44±0.18^{a}
Mn ↓	4.33±0.17	2.90±0.27^{a}	3.75±0.19^{ab}	4.68±0.39^{bc}	5.73±0.22^{c}	3.79±0.27^{a}	4.74±0.20^{b}
pH ↓	5.85±0.04	5.64±0.05^{a}	5.61±0.06^{a}	5.92±0.06^{b}	6.19±0.03^{c}	5.78±0.05^{a}	5.90±0.05^{a}
M_5 •	9.17±0.06	9.11±0.10^{ab}	9.48±0.15^{a}	9.15±0.13^{ab}	8.91±0.08^{b}	9.13±0.08^{a}	9.19±0.09^{a}
M_7 •	1.13±0.11	1.76±0.27^{a}	1.80±0.22^{a}	0.30±0.06^{b}	0.62±0.08^{b}	1.03±0.18^{a}	1.21±0.14^{a}
M_{12} •	18.18±0.70	13.39±0.76^{a}	16.46±1.41^{a}	17.82±1.29^{a}	23.75±0.97^{b}	15.60±0.82^{a}	20.11±0.98^{b}
DEM •	182.19±0.99	191.43±0.36^{a}	191.27±0.50^{a}	170.20±0.79^{b}	175.18±0.67^{c}	180.81±1.71^{a}	183.23±1.16^{a}
Slope	12.44±0.29	11.33±0.27^{a}	11.83±0.68^{a}	10.75±0.31^{a}	15.14±0.29^{b}	11.04±0.21^{a}	13.49±0.43^{b}
Orien •	93.50±9.74	209.14±2.10^{a}	56.89±18.72^{b}	73.67±25.47^{b}	58.25±1.39^{c}	141.40±16.47^{a}	57.57±9.30^{b}
Solar •	1936.1±17.4	2232.6±6.5^{a}	1792.3±15.4^{b}	1860.6±14.7^{bc}	1913.9±6.5^{c}	2046.6±30.1^{a}	1853.1±11.6^{b}

↔ ← ↓ ↑ The mean value is "between", "near the lower limit", "below", "above" the reference values, respectively.

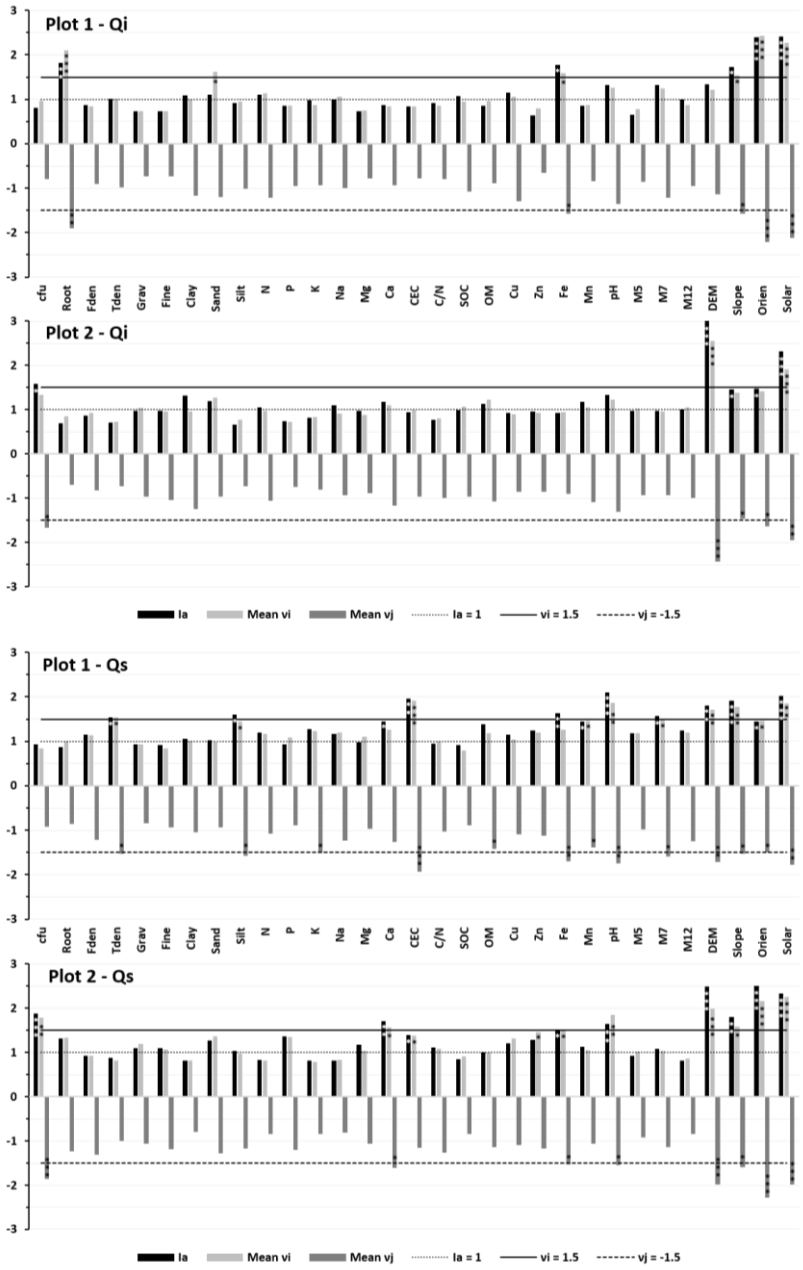

Figure S3.1. Aggregation indices (I_a) and clustering indices (ν) for the study of 31 soil variables in the subplots P_1Qi-P_1Qs and P2Qi-P2Qs. The horizontal dotted line I_a = 1 indicates the limit of the type of distribution pattern of the variable (I_a > 1 aggregated, I_a < 1 regular and I_a = 1 random). The horizontal continuous line (mean $\nu_i \geq 1.5$) indicates the limit for which the index ν is grouped into patches, i.e., higher values of a given variable. The horizontal discontinuous line (mean $\nu_j \leq -1.5$) indicates the limit for which the index ν is grouped into gaps, i.e., lower values of a given variable. * - $P < 0.05$; ** - $P < 0.01$; *** - $P < 0.001$.

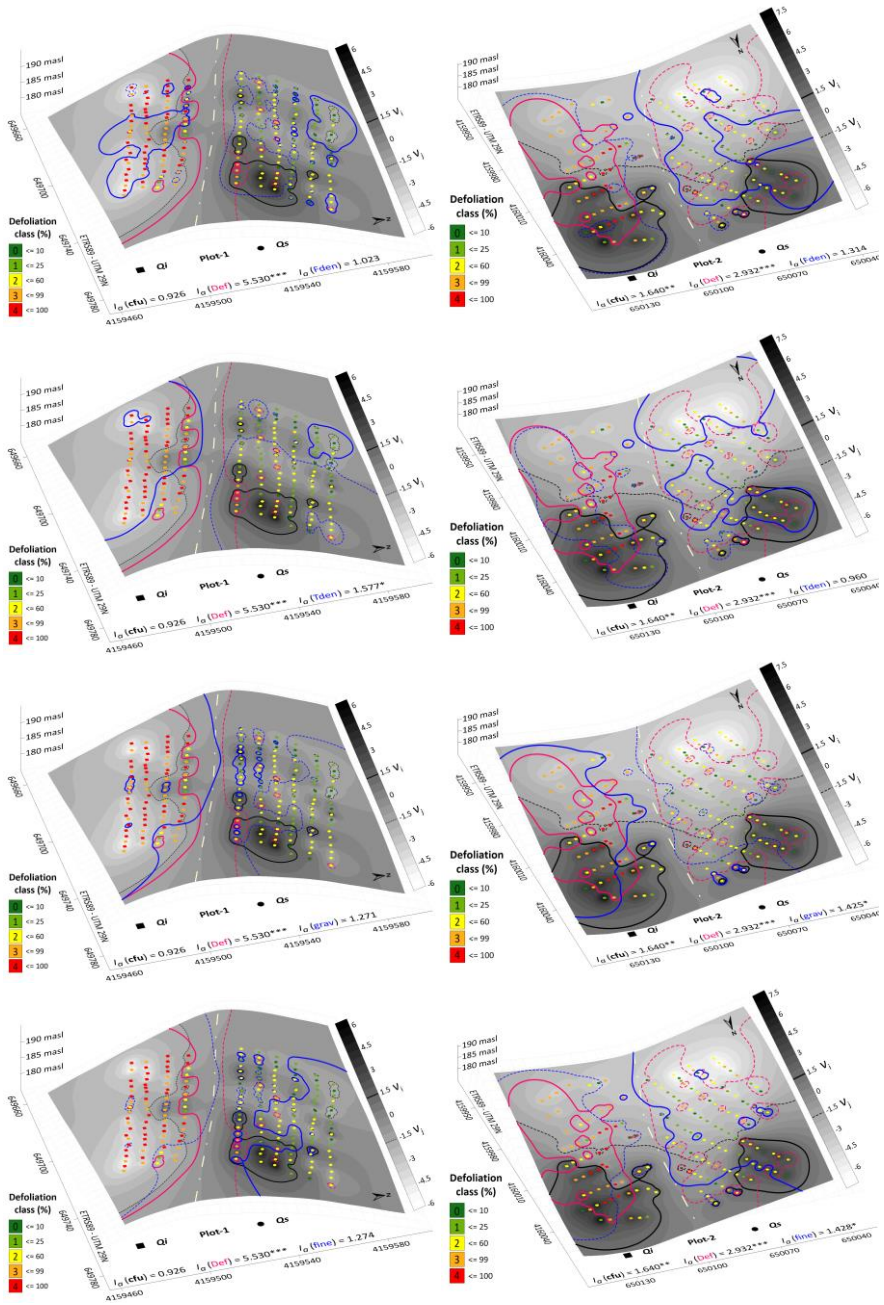

Figure S3.2. 3D maps of clustering indices (ν) of the edaphic and topographical. By columns: P_1 (left) and P_2 (right). Map background shows trees with percentage of crown defoliation in 2018 (Def) represented by dots coloured for the 4 defoliation classes. (0-4) (square – holm oak; circle – cork oak), and colony forming units (cfu) with patches and gaps. Patches (ν > 1.5) are represented with continuous line and gaps (ν < -1.5) with a dashed line, in black for cfu, red for Def and blue for the considered variable. Each variable is indicated in each figure legend (Figure continues the next page).

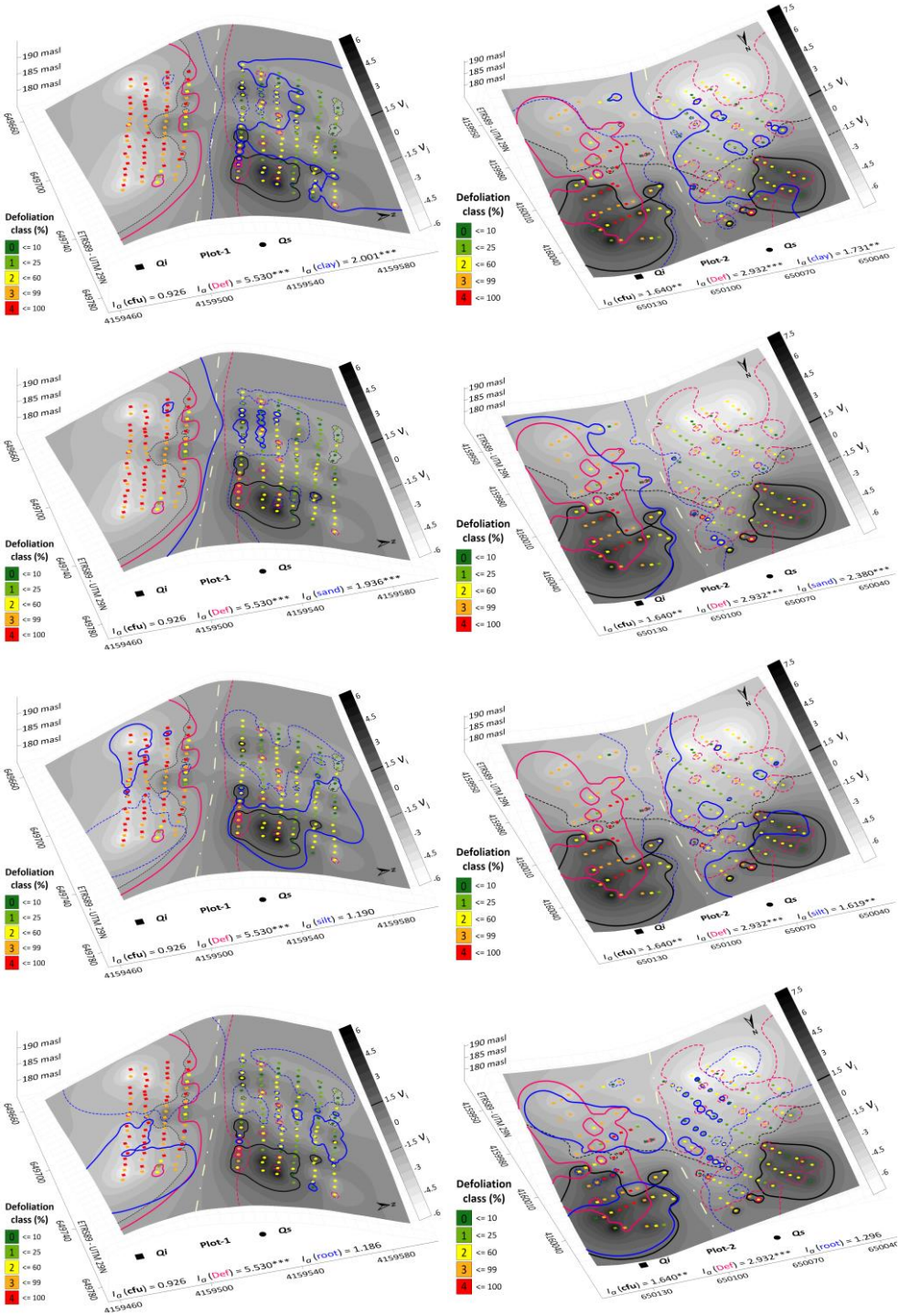

Figure S3.2. (continuation).

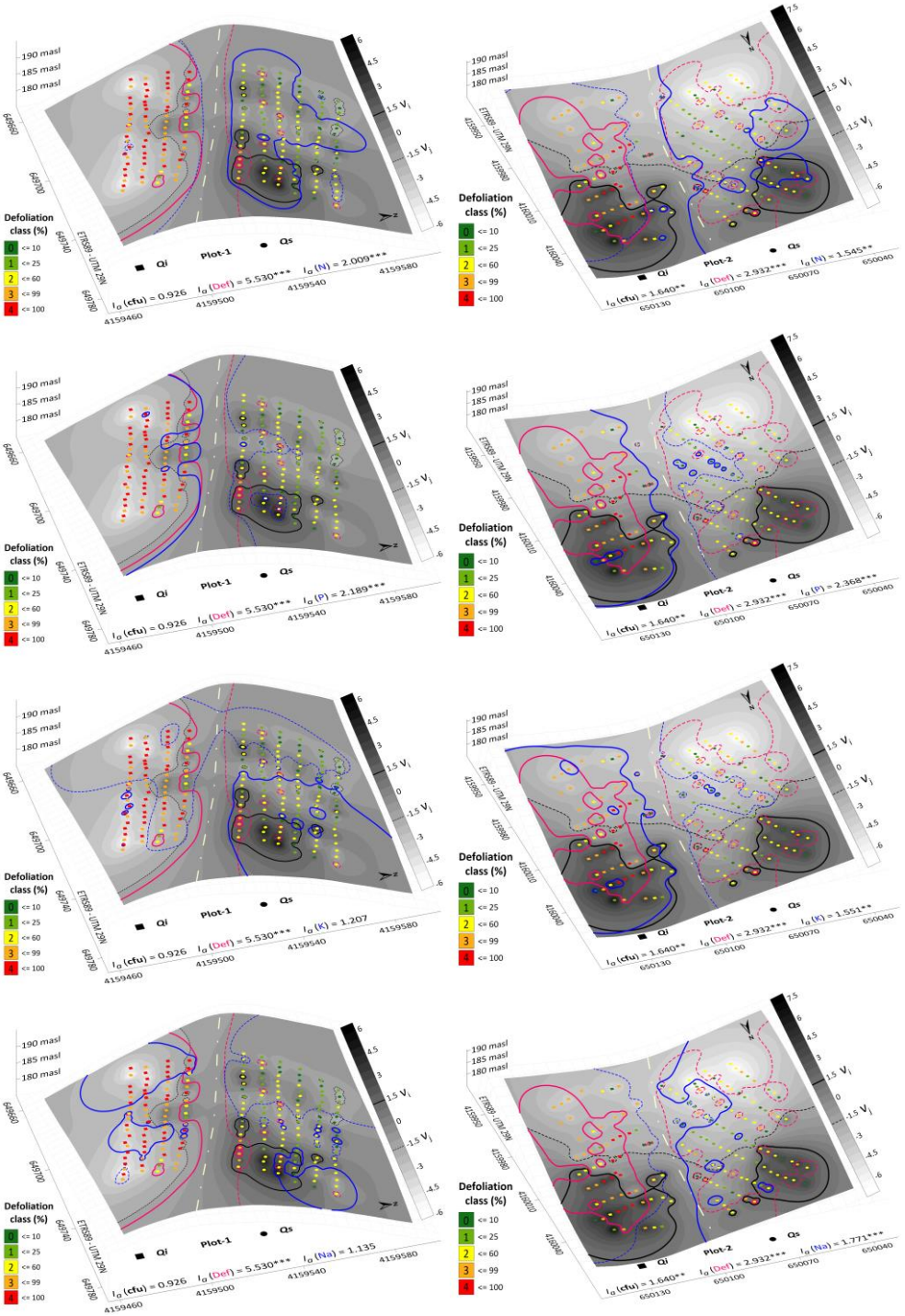

Figure S3.2. (continuation).

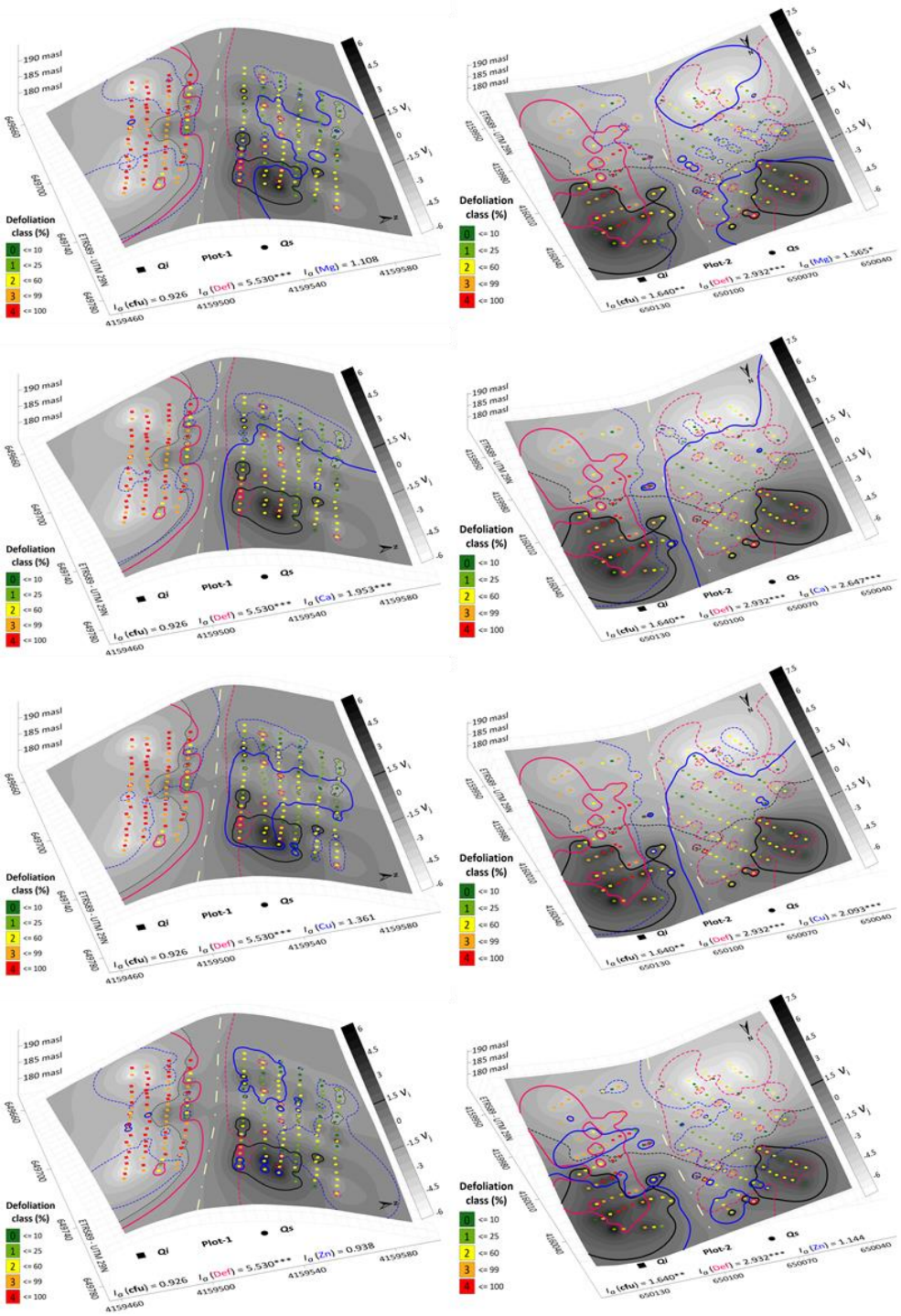

Figure S3.2. (continuation).

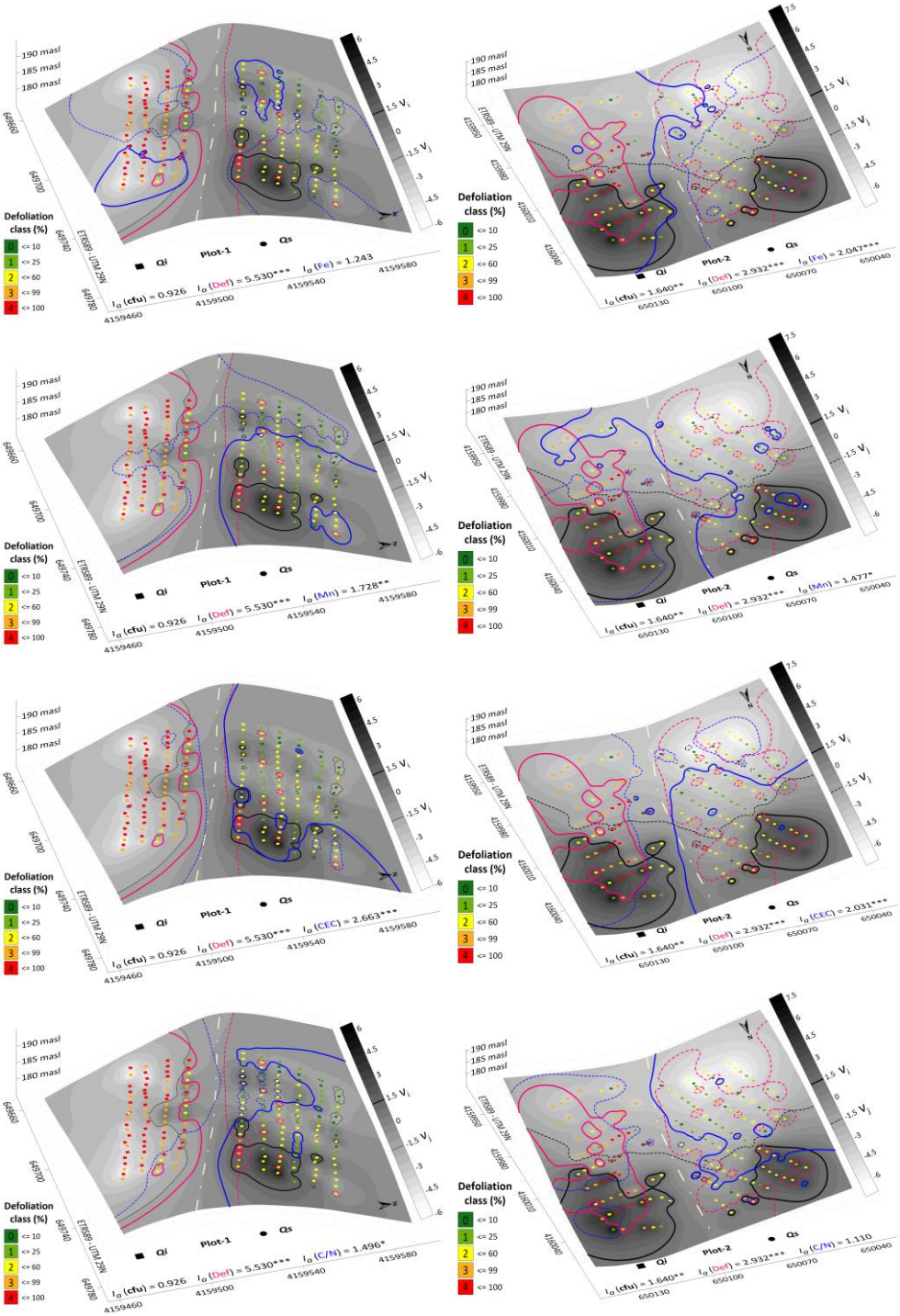

Figure S3.2. (continuation).

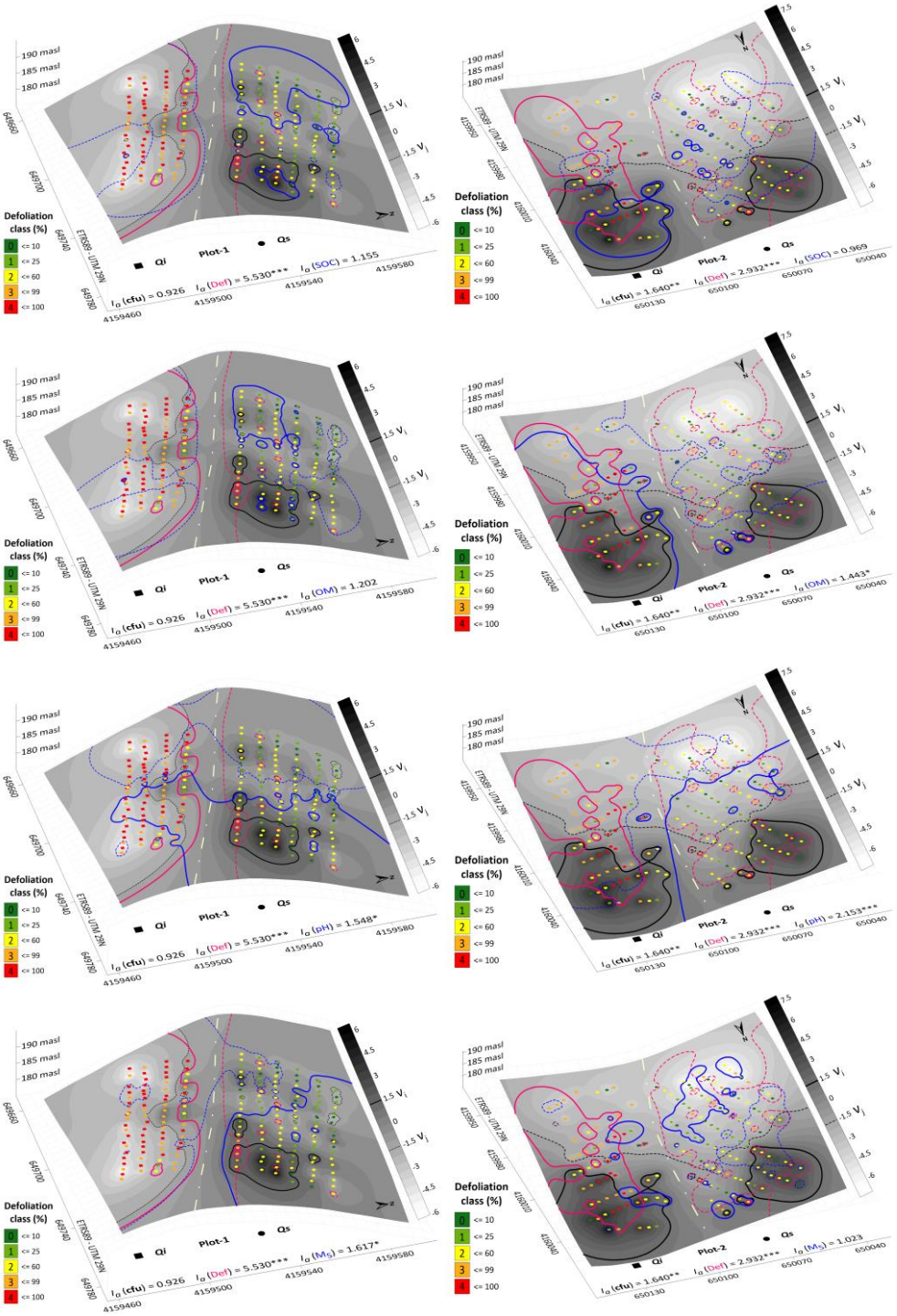

Figure S3.2. (continuation).

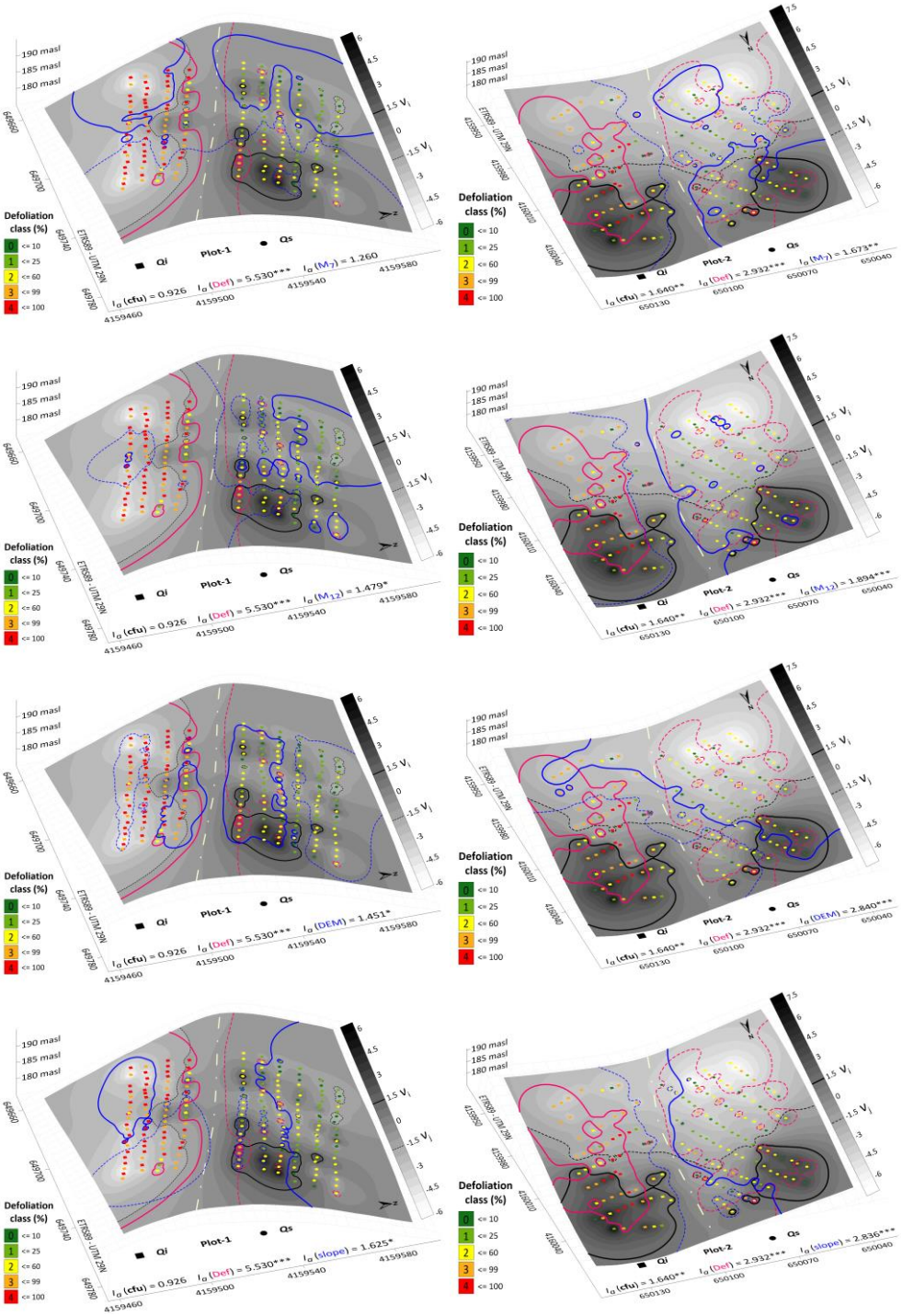

Figure S3.2. (continuation).

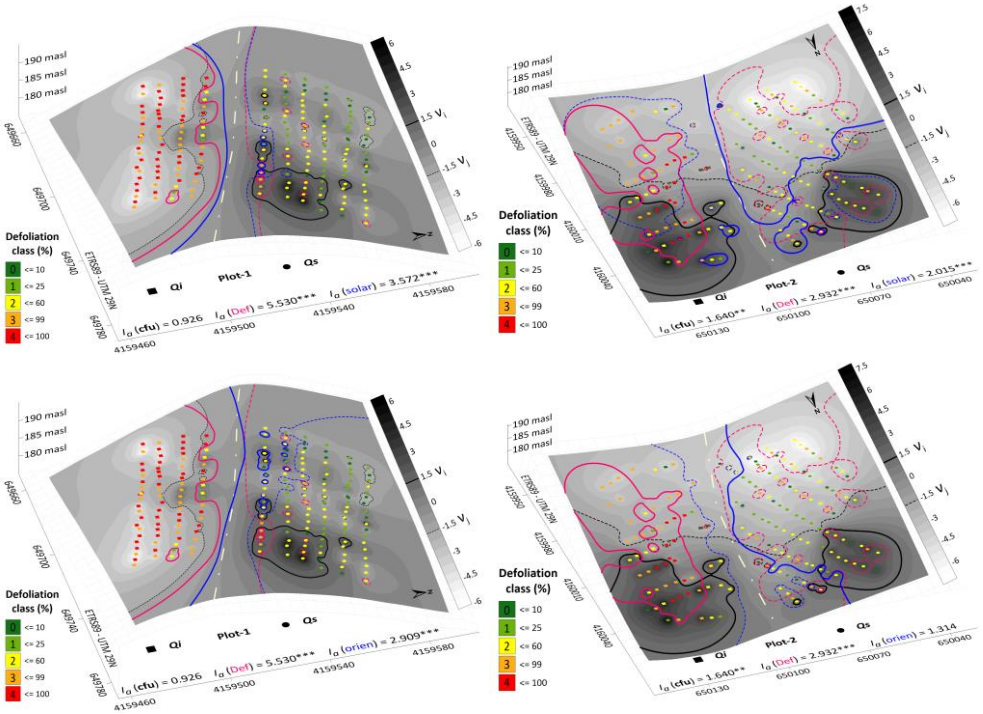

Figure S3.2. (continuation).

Supplementary Material - CAPÍTULO 4

Table S4.1. Summary of plots classified according to three different root rot oomycete diagnosis types. Infested plots = 66. Non-infested plot = 86. Total plots = 152.

	1. SEDA - papers	2. Laboratory isolation	3. Symptomatology
1. SEDA - papers	42	12	0
2. Laboratory isolation	12	13	0
3. Symptomatology	0	0	23

Table S4.2. Characterization of root rot oomycete occurrence per plot according to the three methods. 1 indicates occurrence (infested) and 0 absence (non-infested). The infestation column indicates that at least one method is positive. Coordinate reference system: ETRS89 UTM zone 30N.

PLOT	UTM_X	UTM_Y	Infestation (0: - ; 1: +)	Bibliographic source	Lab. isolation	Symptomatology
CO1004	313548	4276464	1	1	0	0
CO1013	330568	4271091	1	1	0	0
CO1014	338466	4272340	0	0	0	0
CO1020	316022	4260643	0	0	0	0
CO1022	331868	4263193	1	0	0	1
CO1023	339741	4264392	1	1	0	0
CO1024	347614	4265667	0	0	0	0
CO1025	355536	4266917	0	0	0	0
CO1029	301451	4250271	1	1	0	0
CO1030	309374	4251521	0	0	0	0
CO1032	325220	4253995	0	0	0	0
CO1035	348913	4257794	0	0	0	0
CO1036	356786	4259044	0	0	0	0
CO1043	326419	4246097	1	1	0	0
CO1047	358061	4251121	0	0	0	0
CO1049	280228	4230733	0	0	0	0
CO1050	288179	4231976	0	0	0	0
CO1051	296077	4233176	0	0	0	0
CO1052	303925	4234475	0	0	0	0

PLOT	UTM_X	UTM_Y	Infestation (0: - ; 1: +)	Bibliographic source	Lab. isolation	Symptomatology
CO1053	311885	4235720	0	0	0	0
CO1054	319796	4236950	0	0	0	0
CO1055	327694	4238224	1	1	1	0
CO1056	335592	4239424	0	0	0	0
CO1057	343515	4240699	1	1	0	0
CO1058	351388	4241923	0	0	0	0
CO1060	367208	4244448	1	1	0	0
CO1061	375106	4245672	0	0	0	0
CO1062	383029	4246947	0	0	0	0
CO1065	297336	4225274	0	0	0	0
CO1066	305262	4226595	1	0	0	1
CO1067	313174	4227800	1	1	0	0
CO1069	328954	4230305	0	0	0	0
CO1071	344513	4233122	0	0	0	0
CO1073	360515	4235340	0	0	0	0
CO1075	376371	4237794	0	0	0	0
CO1077	392151	4240274	0	0	0	0
CO1082	314396	4219905	1	1	0	0
CO1083	322271	4221167	0	0	0	0
CO1087	353872	4226157	0	0	0	0
CO1093	284022	4207005	1	1	0	0
CO1097	315642	4212017	0	0	0	0
CO1101	347254	4217003	1	0	1	0
CO1107	394642	4224523	0	0	0	0
CO1108	293208	4200340	0	0	0	0
CO1109	301134	4201661	1	1	0	0
CO1110	308983	4202844	0	0	0	0
CO1111	316869	4204109	0	0	0	0
CO1113	332701	4206619	0	0	0	0
CO1121	294529	4192414	1	1	1	0
CO1122	302290	4193735	0	0	0	0
CO1124	318139	4196219	0	0	0	0
CO1125	326043	4197461	0	0	0	0
CO1126	333961	4198732	0	0	0	0
CO1128	349738	4201225	1	1	0	0
CO1130	365546	4203728	0	0	0	0

PLOT	UTM_X	UTM_Y	Infestation (0: - ; 1: +)	Bibliographic source	Lab. isolation	Symptomatology
CO1136	319387	4188297	0	0	0	0
HU1001	159238	4227729	1	1	0	0
HU1004	160519	4219850	1	1	0	0
HU1006	176311	4222316	0	0	0	0
HU1007	130122	4206909	1	1	1	0
HU1009	145945	4209440	0	0	0	0
HU1010	153825	4210689	0	0	0	0
HU1011	161801	4211938	1	0	0	1
HU1012	169680	4213155	0	0	0	0
HU1013	177560	4214404	1	0	0	1
HU1019	155106	4202777	0	0	0	0
HU1020	163018	4204026	0	0	0	0
HU1021	170898	4205307	1	1	0	0
HU1023	186712	4207768	1	0	0	1
HU1025	202588	4210264	1	1	1	0
HU1027	124740	4189836	1	1	1	0
HU1028	132652	4191150	1	1	0	0
HU1033	172157	4197411	0	0	0	0
HU1034	180055	4198659	0	0	0	0
HU1035	187961	4199894	0	0	0	0
HU1039	219581	4204905	0	0	0	0
HU1040	110198	4179458	1	1	1	0
HU1041	118078	4180739	1	1	0	0
HU1042	125989	4181989	1	0	0	1
HU1043	133922	4183204	1	0	0	1
HU1052	205011	4194513	1	1	1	0
HU1053	212912	4195772	1	0	0	1
HU1054	220813	4196907	1	1	0	0
HU1056	111435	4171551	1	0	0	1
HU1059	135151	4175340	1	0	0	1
HU1060	143033	4176569	1	1	1	0
HU1067	198381	4185352	0	0	0	0
HU1068	206215	4186514	1	1	0	0
HU1069	214215	4187820	1	1	1	0
HU1079	175959	4173692	0	0	0	0
HU1082	113946	4155755	1	1	0	0

PLOT	UTM_X	UTM_Y	Infestation (0: - ; 1: +)	Bibliographic source	Lab. isolation	Symptomatology
HU1084	129698	4158334	1	0	0	1
HU1085	145496	4160836	0	0	0	0
HU1089	177144	4165749	1	0	0	1
HU1092	107306	4146619	1	0	0	1
HU1094	123107	4149092	1	1	0	0
HU1096	138927	4151764	1	1	1	0
HU1104	108582	4138625	1	0	0	1
JA1001	390902	4248222	0	0	0	0
JA1003	407956	4242809	1	1	0	0
JA1009	455368	4250344	0	0	0	0
JA1011	471178	4252828	0	0	0	0
JA1016	401304	4233671	0	0	0	0
JA1017	409179	4234934	0	0	0	0
JA1019	424989	4237459	0	0	0	0
JA1020	432884	4238681	0	0	0	0
JA1022	448715	4241206	0	0	0	0
JA1023	456610	4242428	0	0	0	0
JA1024	464505	4243671	0	0	0	0
JA1026	480316	4246175	0	0	0	0
JA1035	410450	4227066	0	0	0	0
JA1037	426234	4229529	1	1	0	0
JA1041	457888	4234515	0	0	0	0
JA1042	465755	4235782	0	0	0	0
JA1052	395910	4216621	0	0	0	0
JA1053	403947	4217875	0	0	0	0
JA1055	419629	4220376	1	1	0	0
JA1056	427515	4221621	0	0	0	0
JA1058	443288	4224151	0	0	0	0
SE1002	256555	4226762	0	0	0	0
SE1003	264474	4228215	0	0	0	0
SE1005	257837	4219069	1	1	1	0
SE1007	227470	4206134	1	0	0	1
SE1008	235287	4207420	0	0	0	0
SE1011	259092	4211189	0	0	0	0
SE1015	236679	4199516	1	1	0	0
SE1017	252421	4201991	1	0	0	1

PLOT	UTM_X	UTM_Y	Infestation (0: - ; 1: +)	Bibliographic source	Lab. isolation	Symptomatology
SE1018	260336	4203241	1	1	0	0
SE1019	268231	4204472	0	0	0	0
SE1023	245769	4192810	0	0	0	0
SE1024	253659	4194150	1	1	0	0
SE1027	277361	4197878	0	0	0	0
SE1032	207525	4178693	1	0	0	1
SE1033	215451	4179939	0	0	0	0
SE1035	231196	4182445	1	0	0	1
SE1036	239165	4183747	0	0	0	0
SE1037	247028	4184945	1	1	0	0
SE1038	254927	4186193	1	1	0	0
SE1039	262774	4187446	0	0	0	0
SE1040	270746	4188715	1	0	0	1
SE1042	286602	4191258	0	0	0	0
SE1045	216597	4172073	1	0	0	1
SE1046	224566	4173362	1	0	0	1
SE1048	240366	4175736	1	1	1	0
SE1049	248293	4177057	1	0	0	1
SE1050	256188	4178282	1	1	0	0
SE1052	272019	4180771	0	0	0	0
SE1053	279913	4181973	1	0	0	1
SE1055	202128	4161649	0	0	0	0
SE1058	225793	4165298	0	0	0	0
SE1062	257378	4170427	0	0	0	0
SE1094	205875	4137928	0	0	0	0

Table S4.3. Environmental data used to model defoliation and mortality processes in dehesas of *Quercus* spp. in North Andalusia (Spain).

VARIABLES	CODE	UNITS
Climatic – Mean climate		
Duration of drought	ddro	Months
Annual precipitation	ptt	mm
Mean annual temperature for all the time series	ta	ºC
Mean temperature of the hottest month for all the time series	tmh	ºC
Climatic – Annual temperature		
Mean temperature for current year	temp	ºC
Mean temperature from *n* years ago	temp_*n*lag	ºC
Mean temperature in Spring per year	t_mean_spr	ºC
Mean temperature in Spring of previous year	t_mean_summ_1lag	ºC
Mean temperature in Summer per year	t_mean_summ	ºC
Mean temperature in Winter per year	t_mean_wint	ºC
Climatic – Annual precipitation		
Precipitation from *n* natural years ago	prec_*n*lag	mm
Precipitation for current natural year	prec	mm
Precipitation accumulated for last *n* natural years	prec_*n*sum	mm
Precipitation from *n* hydrological years ago	prech_*n*lag	mm
Precipitation for current hydrological year	prec_hid	mm
Precipitation accumulated for last *n* hydrological years	prech_*n*sum	mm
Climatic – Annual Drought index		-
SPEI in Spring with *n*-month scale	$spei_n$_spr	-
SPEI from last Summer with 1-month scale	spei1_summ_1lag	-
SPEI in Summer with *n*-month scale	$spei_n$_summ	-
Edaphic		
Average clay content	Clay	%
Mean silt content	Silt	%
Mean organic matter in the soil profile	OM	%
Soil pH	pH	-
Limestone	Ca	%
Cation exchange capacity	CEC	meq/100g
Soil depth	Sd	cm
Topographic		
Aspect	Orien	Degrees
Slope	Slp	%
Biotic agents		
Occurrence of root rot oomycetes	Oom	

n – Time unit of the data record (years or months)

Table S4.4. Results of the log-rank test for the Kaplan-Meier estimates climatic regions. OWC: Oceanic Mediterranean climate of the windward coast; MLG: Semi-oceanic Mediterranean climate of the lower Guadalquivir; PBF: semi-oceanic (subhumid-humid) Mediterranean climate of the western peribetic foothills; PBM: semi-oceanic (sub-humid-humid) Mediterranean climate of the western peribetic mountains; MMG: Semi-continental (dry-subhumid) Mediterranean climate of the Middle Guadalquivir; CBH: continental (dry-sub-humid) Mediterranean climate of eastern circumbetic ranges and hills.

Zone	Events	Obs.	Expect.	(O-E)^2/E	(O-E)^2/V
OWC	92	0	6.32	6.32	6.55
MLG	241	26	15.75	6.67	7.22
MMG	433	27	29.04	0.14	0.17
PBF	571	67	37.11	24.08	29.05
PBM	682	59	44.68	4.59	5.77
CBH	1328	44	90.09	23.58	39.79

χ^2 = 65.8; df = 5; critical χ^2 =11.7; $P < 0.001$

Table S4.5. Results of the log-rank test for the Kaplan-Meier estimates considering presence of root rot oomycetes and climatic regions as factors. MLG: Semi-oceanic Mediterranean climate of the lower Guadalquivir; PBF: semi-oceanic (subhumid-humid) Mediterranean climate of the western peribetic foothills; PBM: semi-oceanic (sub-humid-humid) Mediterranean climate of the western peribetic mountains; MMG: Semi-continental (dry-subhumid) Mediterranean climate of the Middle Guadalquivir; CBH: continental (dry-sub-humid) Mediterranean climate of eastern circumbetic ranges and hills. χ^2_1 : comparison statistic for pairs of climatic regions.

8

							χ^2_1 (df=1; critical χ^2=3.84)			
Plots	**Zone**	**Events**	**Obs.**	**Expect.**	**(O-E)^2/E**	**(O-E)^2/V**	MMG	PBF	PBM	CBH
Non-infested	MLG	56	7	3.69	2.97	3.04	3.76	3.28	13.93	27.51
	MMG	293	24	20.03	0.79	0.87	--	1.10	11.74	25.32
	PBF	137	11	9.30	0.31	0.33	--	--	11.27	24.85
	PBM	347	8	24.33	10.96	12.37	--	--	--	35.49
	CBH	993	28	69.21	24.54	35.79	--	--	--	--
Infested	MLG	185	19	12.52	3.36	3.58	8.13	28.80	43.10	5.76
	MMG	140	3	9.86	4.77	5.02	--	30.22	44.51	7.17
	PBF	434	56	28.89	25.45	29.40	--	--	65.19	27.85
	PBM	335	51	21.66	39.74	44.28	--	--	--	42.14
	CBH	335	16	23.51	2.40	2.70	--	--	--	--

χ^2 = 116; df = 9; critical χ^2 =16.92; $P < 0.001$

Table S4.6. Significance values (*P*) of the Pairwise test results (with Bonferroni's correction) for average defoliation grouped by climatic zones.

	OWC	CBH	MLG	MMG	PBF
CBH	0.21	-	-	-	-
MLG	0.99	<0.001	-	-	-
MMG	0.23	0.99	<0.001	-	-
PBF	0.99	<0.001	0.99	<0.001	-
PBM	0.53	0.99	<0.001	0.99	<0.001

Table S4.7. Goodness of fit (AICc and weight) of univariate models explaining defoliation levels for temperature, SPEI and precipitation variables. For each group, variables are ranked in relative importance (lower AICc). In bold, variables selected for final model.

Temperature

variable	coefficient	df	logLik	AICc	delta	weight
ta	0.026	4	281.877	-555.7	0	0.589
t_mean_spr	0.008	4	281.421	-554.8	0.91	0.374
temp	0.009	4	278.82	-549.6	6.11	0.028
t_mean_summ_1lag	-0.006	4	277.463	-546.9	8.83	0.007
t_mean_wint	0.005	4	275.525	-543	12.7	0.001
t_mean_summ	0.004	4	275.074	-542.1	13.61	0.001
null		3	272.944	-539.9	15.86	0
temp_2lag	-0.003	4	273.567	-539.1	16.62	0
temp_1lag	0.002	4	273.14	-538.3	17.47	0
temp_3lag	0.000	4	272.951	-537.9	17.85	0

SPEI

variable	coefficient	df	logLik	AICc	delta	weight
$spei_{18}$_summ	-0.010	4	301.815	-595.6	0	0.602
$spei_{24}$_summ	-0.010	4	300.773	-593.5	2.08	0.212
$spei_{24}$_spr	-0.010	4	300.308	-592.6	3.01	0.133
$spei_{18}$_spr	-0.010	4	299.361	-590.7	4.91	0.052
$spei_{12}$_spr	-0.009	4	294.722	-581.4	14.18	0.001
$spei_{12}$_summ	-0.008	4	291.124	-574.2	21.38	0
$spei_{6}$_spr	-0.008	4	288.659	-569.3	26.31	0
$spei_{3}$_summ	-0.007	4	286.602	-565.2	30.42	0
$spei_{6}$_summ	-0.006	4	281.140	-554.3	41.35	0
$spei_{1}$_summ	-0.005	4	280.244	-552.5	43.14	0
$spei_{3}$_spr	-0.005	4	280.027	-552	43.58	0
$spei_{1}$_spr	-0.005	4	279.237	-550.5	45.16	0
Null		3	272.944	-539.9	55.73	0
$spei_{1}$_summ_1lag	0.001	4	272.994	-538	57.64	0

Precipitation

variable	coefficient	df	logLik	AICc	delta	weight
prech_2sum	-0.012	4	298.144	-588.3	0	0.995
prec_1lag	-0.010	4	292.718	-577.4	10.85	0.004
prec_2sum	-0.010	4	290.149	-572.3	15.99	0
prec_hid	-0.009	4	289.101	-570.2	18.09	0
prec_3sum	-0.010	4	284.699	-561.4	26.89	0
prech_3sum	-0.010	4	283.780	-559.5	28.73	0
prech_1lag	-0.006	4	280.032	-552	36.23	0
prech_2lag	0.004	4	277.228	-546.4	41.83	0
prech_3lag	0.003	4	275.048	-542.1	46.19	0
prec_3lag	0.003	4	274.476	-540.9	47.34	0
prec	-0.003	4	274.455	-540.9	47.38	0
null		3	272.944	-539.9	48.39	0
prech_5sum	0.003	4	273.772	-539.5	48.75	0
prec_2lag	0.000	4	272.990	-538	50.31	0
prec_5sum	-0.001	4	272.967	-537.9	50.35	0

Table S4.8. Goodness of fit (AICc and weight) of univariate models explaining mortality levels for temperature, SPEI and precipitation variables. For each group, variables are ranked in relative importance (lower AICc). In bold, variables selected for final model.

Temperature

variable	coefficient	df	logLik	AICc	delta	weight
ta	0.513	3	-543.023	1092.1	0	0.769
temp	0.368	3	-545.263	1096.5	4.48	0.082
t_mean_spr	0.336	3	-545.283	1096.6	4.52	0.08
temp_2lag	0.320	3	-545.998	1098	5.95	0.039
temp_3lag	0.299	3	-546.502	1099	6.96	0.024
temp_1lag	0.170	3	-549.216	1104.4	12.39	0.002
t_mean_summ	0.159	3	-549.259	1104.5	12.47	0.002
null		2	-550.36	1104.7	12.67	0.001
tmc*	0.033	3	-550.333	1106.7	14.62	0.001
t_mean_wint	0.027	3	-550.334	1106.7	14.62	0.001
t_mean_summ_1lag	0.013	3	-550.349	1106.7	14.65	0.001

Precipitation

variable	coefficient	df	logLik	AICc	delta	weight
prec_1lag	-0.189	3	-548.512	1103	0	0.194
prec_2sum	-0.160	3	-549.182	1104.4	1.34	0.1
null		2	-550.36	1104.7	1.69	0.083
prech_2lag	0.000	3	-549.474	1105	1.92	0.074
prec_3lag	0.119	3	-549.525	1105.1	2.03	0.071
prech_2sum	-0.128	3	-549.58	1105.2	2.14	0.067
prec_2lag	0.114	3	-549.598	1105.2	2.17	0.066
prec_hid	-0.113	3	-549.652	1105.3	2.28	0.062
prech_3lag	0.000	3	-549.813	1105.6	2.6	0.053
prech_1lag	-0.053	3	-550.197	1106.4	3.37	0.036
prec_3sum	-0.059	3	-550.214	1106.4	3.4	0.035
prec_5sum	0.052	3	-550.262	1106.5	3.5	0.034
prec	-0.029	3	-550.313	1106.6	3.6	0.032
prech_3sum	-0.022	3	-550.341	1106.7	3.66	0.031
prech_5sum	0.011	3	-550.356	1106.7	3.69	0.031
ptt	-0.008	3	-550.359	1106.7	3.69	0.031

SPEI

variable	coefficient	df	logLik	AICc	delta	weight
$spei_{1}$_spr	-0.228	3	-546.791	1099.6	0	0.427
$spei_{18}$_summ	-0.182	3	-548.185	1102.4	2.79	0.106
$spei_{3}$_summ	-0.163	3	-548.565	1103.1	3.55	0.072
$spei_{24}$_summ	-0.164	3	-548.568	1103.1	3.55	0.072
$spei_{12}$_summ	-0.163	3	-548.593	1103.2	3.6	0.07
$spei_{18}$_spr	-0.155	3	-548.775	1103.6	3.97	0.059
$spei_{24}$_spr	-0.134	3	-549.178	1104.4	4.77	0.039
$spei_{12}$_spr	-0.129	3	-549.277	1104.6	4.97	0.036
null		2	-550.36	1104.7	5.13	0.033
$spei_{6}$_summ	-0.112	3	-549.497	1105	5.41	0.029
$spei_{6}$_spr	-0.078	3	-549.952	1105.9	6.32	0.018
$spei_{3}$_spr	-0.048	3	-550.204	1106.4	6.83	0.014
$spei_{1}$_summ_1lag	0.076	3	-550.23	1106.5	6.88	0.014
$spei_{1}$_summ	0.008	3	-550.356	1106.7	7.13	0.012

***** Identified as relevant in the mean climate selection.

Table S4.9. Partial least square results for time trends of core drivers. AdjR²: Adjusted R Squared. F^P: Comparison statistic and model significance. A^P: Adjustment of residual to the normal distribution (Anderson-Darling statistic) and test significance. Defol: Mean average defoliation of plot (%). AnnMort: Mortality events in one plot at year. P values: n/s: Not significant; *: $P < 0.05$; **: $P < 0.01$; ***: $P < 0.001$.

Formula	Intercept	Slope	AdjR^2	F^P	Residual freq	A^P
spei18_summ~Year	0.29	-0.018	0.01	22.44***	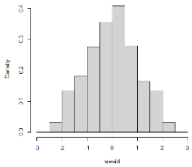	2.51***
spei18_summ~Defol	0.434	-0.013	0.02	27.49***	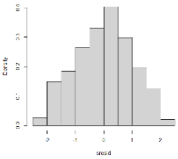	4.06***
spei1_spr~Year	0.207	-0.008	0.01	13.20***	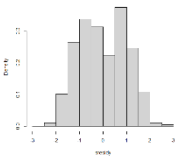	19.4***
spei1_spr~AnnMort	0.135	-0.051	0.001	3.95*	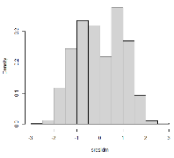	20.6***

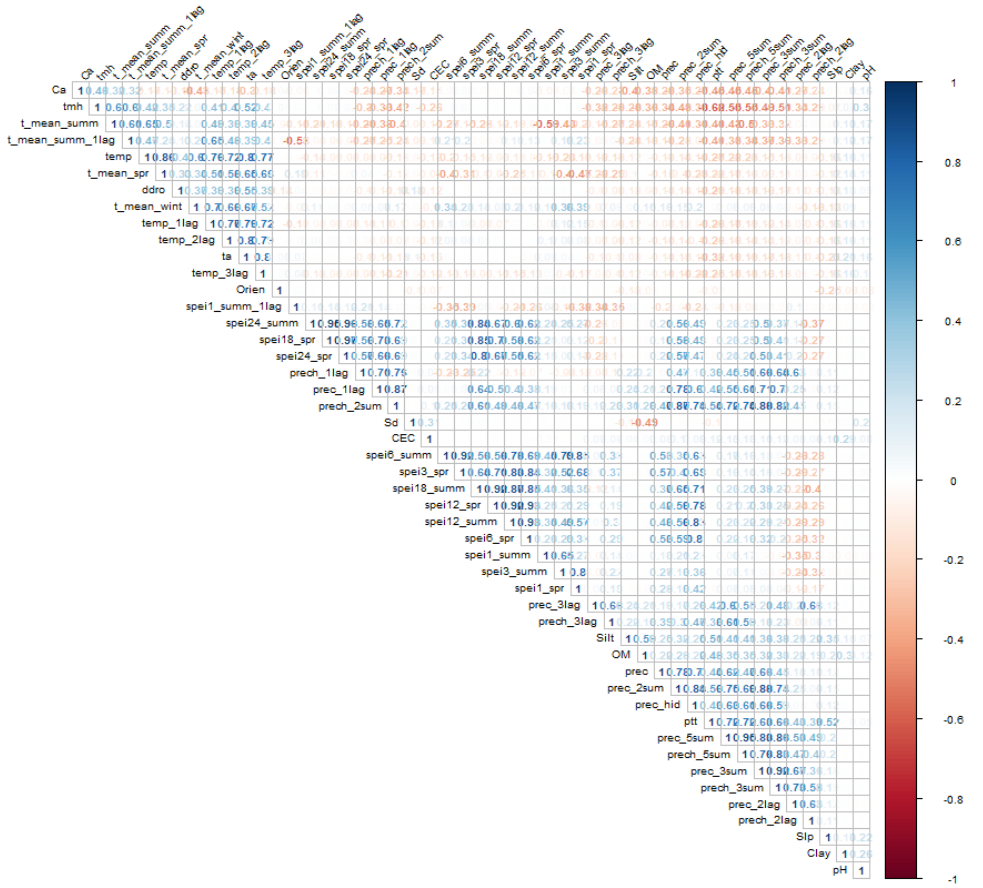

Figure S4.1. Correlation plot for all variables considered in the study. Values correspond to Pearson's correlation coefficient. Variables are sorted according to the clustering method using complete linkage.

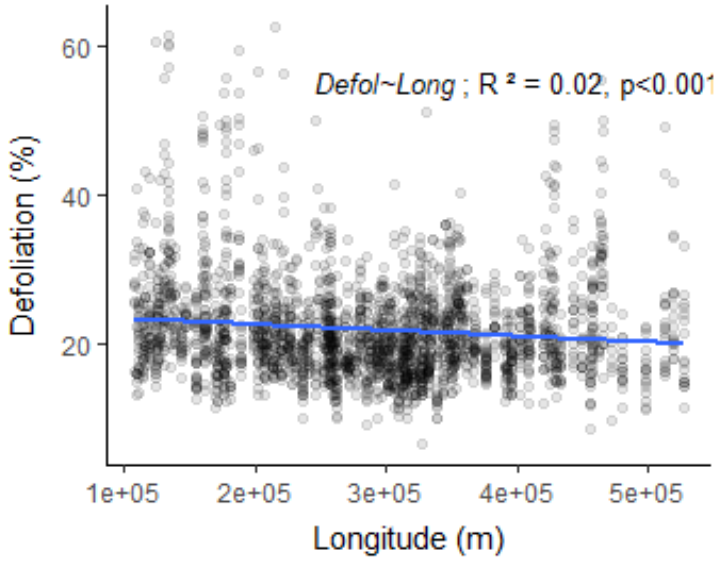

Figure S4.2. Scatterplot of defoliation values by geographical distribution (longitude) from West to East. X axis represents geographical projected coordinates (ETRS89 UTM/Zone 30N).

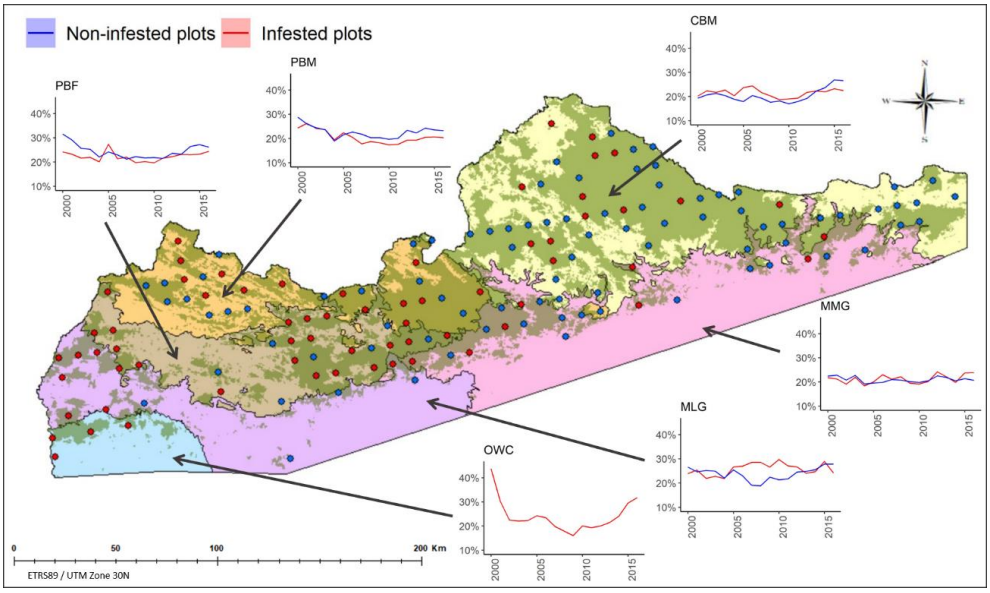

Figure S4.3. Average defoliation per year for each bioclimatic region and infested / non-infested plots.

Supplementary Material - CAPÍTULO 5

Table S5.1. Technical specifications of the WorldView-2 image and the LiDAR data.

Characteristic	Value
World View-2	
Acquisition date	16 September 2017
Scan direction	Forward
Mean satellite elevation	58º
Mean satellite azimuth	248º
Mean off nadir view angle	28.2º
LiDAR	
Acquisition date	6 April 2013
Laser scanning system	Leica ALS60
Wavelength	1064 nm
Average flying altitude over sea level	4500 fts
Maximum scan angle	26°
Average point density	12.09 points/m^2
Accuracy of the point cloud (RMSEz)	≤0.07 m

Table S5.2. Calculated LiDAR-derived structural metrics from 2013 aerial LiDAR data collections used in this study.

Index acronym	LiDAR-derive structural metrics	Interpretation
CHM	Canopy height model	Mean vegetation crown height
COV	Canopy cover	Number of first returns above the cover cutoff (2 m) divided by the number of all first returns and output as a percentage
DNS	Canopy density	Number of all points above the cover cutoff (2 m) divided by the number of all returns
QAV	Mean quadratic height	Mean of the quadratic height ($\sum i=1nhi2/n$), h_i is the height of a return point and n is the number of all points
SKE	Skewness	The skewness of return points
KUR	Kurtosis	The kurtosis of return points
$\mathbf{P_{nth}}$	nth percentile height	nth (i.e., 10, 20, 30, 40, 50, 60, 70, 80, and 90) percentile height value of return points between the ground and the maximum height

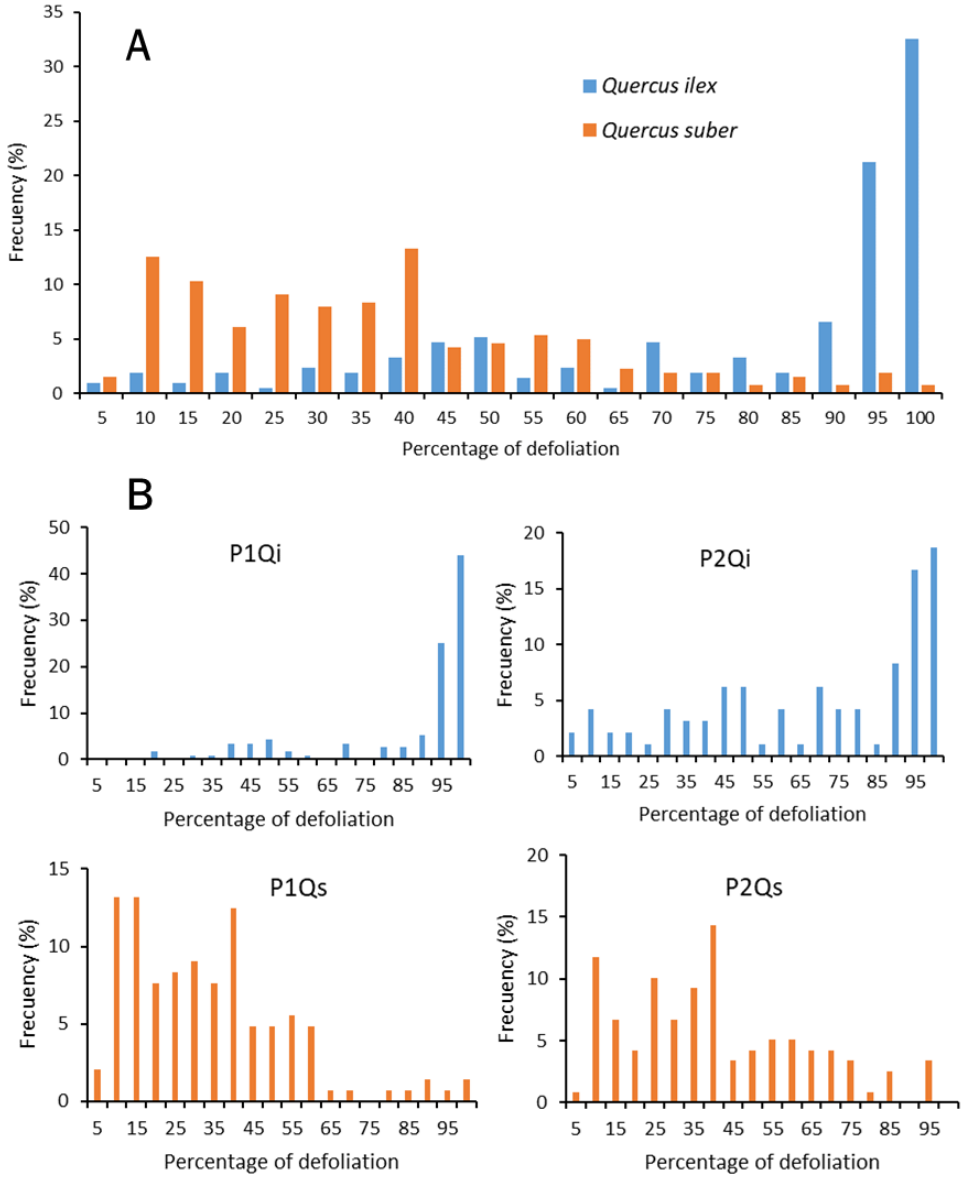

Figure S5.1. Histogram of frequencies (%), according to the percentages of defoliation of holm oak (*Quercus ilex*) and cork oak (*Quercus suber*) crowns, at species level (A) and subplot level (B).

Figure S5.2. Correlation plot for all variables considered in the study. Values correspond to Pearson's correlation coefficient. Variables are sorted according to the clustering method using complete linkage.